HEPATIC TOXICITY AND POLYCHLORINATED BIPHENYLS: TOXICOGENOMIC EXAMINATION OF SINGLE CONGENER AND MIXTURE EFFECTS IN C57BL/6 MICE

By

Anna Katarzyna Kopec

A DISSERTATION

Submitted to
Michigan State University
in partial fulfillment of the requirements
for the degree of

DOCTOR OF PHILOSOPHY

Biochemistry and Molecular Biology - Environmental Toxicology

2010

ABSTRACT

HEPATIC TOXICITY AND POLYCHLORINATED BIPHENYLS: TOXICOGENOMIC EXAMINATION OF SINGLE CONGENER AND MIXTURE EFFECTS IN C57BL/6 MICE

By

Anna Katarzyna Kopec

Human exposures to persistent organic pollutants rarely occur in isolation but rather as complex mixtures. Interactions between environmental contaminants, such as 2,3,7,8-tetrachlorodibenzo-*p*-dioxin (TCDD) and polychlorinated biphenyls (PCBs), can produce additive, synergistic or antagonistic interactions, which may influence risk assessment. Therefore, scientifically based risk and health hazard evaluation requires toxicological data from chemical mixture studies, in addition to traditional studies involving single chemical exposure.

Dioxins and PCBs are ubiquitous toxicants that persist in the environment due to their lipophilicity and propensity to bioaccumulate in biological tissues. These chemicals elicit tissue- and species-specific effects including hepatotoxicity, immune suppression, endocrine disruption, and carcinogenicity. Structural similarity to the most toxic coplanar dioxin, TCDD, determines the dioxin-like effects of individual PCBs and the spectrum of aryl hydrocarbon receptor (AhR)-mediated biochemical and toxic responses. In contrast, non-coplanar PCB congeners are more abundant in the environment and elicit responses that are unique and non-AhR-mediated. The main objective of this research was to evaluate how mixture interactions between these

structurally different, dioxin and non-dioxin-like chemicals affect the gene expression responses underlying the hepatic toxicity in the immature C57BL/6 mouse model.

Comprehensive time course and dose-response hepatic gene expression analyses were performed for dioxin-like 3,3',4,4',5-pentachlorobiphenyl (PCB126) and non-dioxin-like 2,2',4,4',5,5'-hexachlorobiphenyl (PCB153) relative to TCDD, and differentially expressed genes were phenotypically anchored to changes in physiological endpoints to establish a quantitative baseline of toxic responses. Assessment of the toxic effects exerted by a mixture of TCDD and PCB153 was performed using a 1 to 10,000 ratio, respectively, to reflect relative environmental concentrations of each of the chemicals and to compare obtained results to previous literature reports examining non-additive AhR interactions.

In summary, the single chemical studies demonstrated that each compound elicited a complex and unique temporal and dose-dependent gene expression profile that could be linked to the physiological outcomes. In the mixture studies, microarray profiling and statistical dose-response modeling identified a small subset of non-additive, synergistically induced gene expression responses, which were consistent with effects on relative liver weights, histopathology, hepatocellular lipid accumulation and tissue level pharmacokinetics.

To my family

ACKNOWLEDGMENTS

It is my great pleasure and honor to thank all those who supported me throughout the doctoral program at Michigan State University. Without you, I could not have completed this journey.

I first wish to thank my advisor Dr. Tim Zacharewski for accepting me into his laboratory as an undergraduate student, and later as a graduate assistant. I am very thankful for his patience, faith in my abilities and all the extraordinary opportunities he provided that allowed me to develop scientifically and professionally. I could not have asked for a better mentor. I also wish to extend my gratitude to Jana Zacharewski, the warmest and sweetest person who always cared for all the Zacharewski lab students with the greatest passion and love. Thank you for always looking out for me.

I would like to express my gratitude to my Committee Members, Drs. Dave Dewitt, Eric Hegg, Norb Kaminski and John Wang for your guidance, support and insightful comments during our meetings that provided me with a broader perspective on my research.

I also wish to acknowledge the Department of Biochemistry & Molecular Biology and the Environmental and Integrative Toxicological Science program at the Center for Integrative Toxicology for the invaluable training and funding that facilitated my travel to scientific meetings. I extend special thanks to Amy Swagart, Carol Chvojka, Teresa Vollmer, Jessica Lawrence and Lesley Reed for their fantastic support during my graduate years.

Next, I wish to think all the members of the Zacharewski lab for their friendship, advice and support. I owe my deepest gratitude to Darrell Boverhof who introduced me to the area of toxicogenomics, provided answers to every single question and was the best project supervisor

every new student could ever wish for. I would also like to thank Lyle Burgoon who gave me an invaluable insight into the bioinformatic world and offered priceless management advice. Next, I extend my gratitude to Josh Kwekel, the “cave king” for his support, patience and a great ear to listen. I am extremely grateful to Qi Ding and Suntae Kim for all the conversions on life and culture inside and outside of science. Without Ed Dere (the *Kuler* Color Guru), I would have never gained the appreciation for color and finesse for graphical representation of the data. I would also like to thank Michelle Angrish and Agnes Forgacs for their amazing friendship, shopping, gym trips, and endless conversations and for always having my back! Big thanks to the past lab members, including Bryan Mets, May Tan, Naisha Shah, Sharon Dubois, Andrea Lee, and Michelle (Little Michelle) D’Souza for their invaluable support in and outside of the lab.

I would also like to give a shout-out to my loving Polish friends, especially Marta Szumko, Magda Kedzierska, Dominika Bijos, Jakub Olszowiec, Anna Behrendt, and Michal Migalski. Thank you for your friendship, constant support, advice and for always being there for me when I needed you. Also, I cannot forget about my darling friend from Michigan and a fellow graduate student – Dorothy Tappenden – thank you for making me feel like a part of your family, you and your girls will always be dear to my heart. Dr. Matthews thank you for all the crazy love and support!

Finally, I wish to thank my family for their love and support, my mom Elzbieta, my dad Stanislaw, my sweet little brother Mateusz and my grandparents. Thank you for pushing me in the right direction and always supporting my choices. If it was not for you, I would not be here. I hope to repay you one day for everything you have taught me.

TABLE OF CONTENTS

LIST OF TABLES

LIST OF FIGURES

LIST OF ABBREVIATIONS

1,2,3,4-TCDD	1,2,3,4-Tetrachlorodibenzo-*p*-dioxin
1,2,3,4-TCDF	1,2,3,4-Tetrachlorodibenzofuran
AhR	Aryl hydrocarbon receptor
ALT	Alanine aminotransferase
ANOVA	Analysis of variance
ARNT	Aryl hydrocarbon receptor nuclear translocator
bHLH	Basic-helix-loop-helix
BHT	2,6-di-tert-butyl-4-methylphenol
BW	Body weight
CAR	Constitutive androstane receptor
CARE	Constitutive androstane receptor response element
cDNA	Complementary deoxyribonucleic acid
CHOL	Cholesterol
CV	Central vein
dNTP	Deoxynucleotide triphosphate
DRE	Dioxin response element
DTT	Dithiothreitol
ED_{50}	Effective dose 50
EDTA	Ethylene-di-amine-tetra-acetic acid
EROD	Ethoxyresorufin-O-deethylase

FAME	Fatty acid methyl ester
GC-MS	Gas chromatography-mass spectrometry
GLU	Glucose
HEPES	4-(2-hydroxyethyl)-1-piperazineethanesulfonic acid
HRGC-HRMS	High resolution gas chromatography-high resolution mass spectrometry
IU	International unit
Min	Minutes
MSS	Matrix similarity score
MUFA	Monounsaturated fatty acid
N/A	Not available
NC	No change
NADPH	Nicotinamide adenine dinucleotide phosphate
NEFA	Non-esterified fatty acids
NTP	National Toxicology program
ORO	Oil red O
PAS	Per-Arnt-Sim
PCA	Principal component analysis
PCAH	Polycyclic aromatic hydrocarbon
PCB	Polychlorinated biphenyl
PCB111	2,3,3',5,5'-Pentachlorobiphenyl
PCB126	3,3',4,4',5-Pentachlorobiphenyl
PCB153	2,2',4,4',5,5'-Hexachlorobiphenyl
PCDD	Polychlorinated dibenzo-*p*-dioxin

PCDF	Polychlorinated dibenzofurans
PND	Postnatal day
POP	Persistent organic pollutant
PPT	Parts per trillion
PUFA	Polyunsaturated fatty acid
PV	Portal vein
PWM	Position weight matrix
PXR	Pregnane X receptor
PXRE	Pregnane X receptor response element
QRTPCR	Quantitative real time polymerase chain reaction
REP	Relative potency
RLW	Relative liver weight
RNA	Ribonucleic acid
RT	Room temperature
RXR	Retinoid X receptor
SD	Standard deviation
SE	Standard error
Sec	Seconds
SFA	Saturated fatty acid
T	2,3,7,8-Tetrachlorodibenzo-*p*-dioxin
TCDD	2,3,7,8-Tetrachlorodibenzo-*p*-dioxin
TCDF	2,3,7,8-Tetrachlorodibenzofuran
TEF	Toxic equivalency factor

TEQ	Toxic equivalents
TG	Triglycerides
TLC	Thin layer chromatography
TSS	Transcriptional start site
UTR	Untranslated region
V	Vehicle
VEH	Vehicle
WHO	World Health Organization

CHAPTER 1

CHAPTER 1

REVIEW OF THE LITERATURE: PERSISTENT ORGANIC POLLUTANTS, HUMAN EXPOSURE, SINGLE CONGENER AND MIXTURE TOXICITY

INTRODUCTION

Persistent organic pollutants (POPs) have become widespread environmental contaminants and currently represent a global toxicological threat. The Stockholm Convention coordinated by the United Nations Environment Programme has been convened to protect human health and the environment from POPs [1]. In implementing the Convention, over 150 participating countries (including Poland and the United States) are required to take appropriate measures to eliminate or significantly reduce the production and use of these persistent chemicals. More specifically, the Convention identified an initial list of 12 POPs (the so called "dirty dozen"), including polychlorinated biphenyls (PCBs), polychlorinated dibenzo-*p*-dioxins (PCDDs), and polychlorinated dibenzofurans (PCDFs) as a significant hazard to human and wildlife health on a global scale [2, 3]. The toxicity and environmental persistence of POPs is enhanced by their lipophilic properties and capability of long-range, transboundary atmospheric transport and deposition. POPs are resistant to degradation through chemical and biological processes, allowing them to bioaccumulate in the fatty tissues of animals and humans and biomagnify through the food chain, having potentially detrimental impact on the environment and human health [4].

Human exposure to POPs, and potential interactions between the individual chemicals, can significantly influence the spectrum of elicited toxic responses, including effects on the liver, as one of the major target organs of PCB and PCDD toxicity. Comprehensive transcriptomic and phenotypic level examination of hepatic effects elicited by individual chemicals and their mixtures using an *in vivo* model can significantly expand current understanding of the toxic mode of action and may have major implications for human risk assessment.

POLYCHLORINATED BIPHENYLS AND DIOXINS: PRODUCTION, USE AND HUMAN EXPOSURE

PCBs represent a class of oily liquid or solid man-made chemicals that are colorless to light yellow, have no smell or taste, and do not naturally occur in the environment. PCBs were commonly found as commercial Aroclor mixtures of individual chlorinated biphenyl components (congeners) with varying number and position of chlorine substituents [5]. PCBs were manufactured for use predominantly as coolants, lubricants, insulating fluids for transformers and capacitors, lighting ballasts, surface coatings (paints, carbonless copy paper, flame retardants), inks and plasticizers (gasket sealers, caulking), due to their general chemical inertness and thermal stability [6, 7]. In the United States the manufacture of PCBs continued for about 50 years until it was banned in 1977, however in Poland, PCBs were still produced until 1981 [8-10]. Unlike the deliberate manufacture and use of PCBs, the continuous release of PCDDs and PCDFs into the environment occurs as by-products of municipal waste and sewage sludge incineration, herbicide production, pulp and paper bleaching, and other industrial processes [11-14].

Industrial regulations have led to a significant decrease in PCB and dioxin levels over the years [15, 16]. However, these POPs still enter the environment from poorly maintained

hazardous waste sites, accidental spills and leaks, and from illegal or improper disposal of wastes, where incomplete combustion or heating of PCBs can lead to formation of PCDFs [9, 17-19]. Exposure can also occur from ambient inhalation of lighter congeners present in the atmosphere or from natural weathering of the caulking used around windows and expansion joints resulting in elevated levels of PCBs in the soil surrounding the deteriorating buildings [20-23]. In addition, backyard barrel burning of household waste has risen dramatically over the years, becoming the primary source of dioxin emissions [16]. For the general population, however, the main source of PCB, PCDD and PCDF exposures continues to be the consumption of contaminated food, such as fish, meat and dairy products [8, 9]. Breast-fed infants of mothers who have diets high in contaminated fish are at particularly high risk due to significant PCB and dioxin accumulation via lactational transfer [24-26].

Direct exposure to PCBs has been well documented in the two large-scale food poisoning cases, in Japan (1968) and Taiwan (1979), where a PCB mixture used as a heat-transfer medium leaked into rice oil during the manufacturing process [27-30]. It was later found that the cooking oil was also contaminated with PCDFs [31]. The illnesses, commonly referred to as “Yusho” (oil disease in Japanese) and “Yu-Cheng” (oil disease in Chinese), were characterized by a syndrome of persistent events presented as general malaise, eye discharge, neuropathy, hyperpigmentation, severe chloracne, as well as hepatic toxicity, including elevated levels of serum alanine aminotransferase, indicative of liver damage [27, 30]. Follow-up reports indicated a 2.7-fold increase in mortality due to chronic liver disease and cirrhosis compared to the general population [32].

Of more recent and local relevance is contamination of the Great Lakes and the Saginaw and Tittabawassee rivers that have been significantly impacted by historical industrial activities

[33]. Recent studies reported that consumption of fish from Lake Michigan correlated with PCB levels detected in human serum and maternal milk [34]. In addition, although PCB, PCDD and PCDFs concentrations in several Lake Michigan fish have declined, reproductive effects have persisted in aquatic birds, representing an ongoing environmental concern [35].

Human exposure to one of the most toxic PCDDs, 2,3,7,8-tetrachlorodibenzo-*p*-dioxin (TCDD), was reported after an accidental contamination of Agent Orange used as a herbicide and defoliant during the Vietnam War [36, 37]. It is estimated that between 1961 and 1971, approximately 360 kg of dioxin was sprayed multiple times over 2.6 million acres, resulting in an estimated 4.8 million exposed or potentially exposed Vietnam residents and war veterans [36]. Similar mass dioxin poisoning occurred in Seveso, Italy (1976), where a residential population was exposed to high levels of TCDD as a result of an industrial accident in a chemical plant manufacturing pesticides and herbicides [38]. The most recent and well known case of TCDD exposure in humans is that of Victor Yushchenko, a candidate for the presidential election in Ukraine, poisoned with dioxin in 2004. Analysis of Yushchenko's blood revealed 108,000 pg/g lipid weight of TCDD, exceeding background dioxin levels in general population by at least 50,000 fold [39]. The documented acute and long term toxic effects following human exposure to TCDD include chloracne, general fatigue and weakness, nausea, hepatic toxicity, neurotoxicity, lymphoid atrophy, birth defects, miscarriages, type 2 diabetes and increased incidences of cancer [37, 38, 40-44].

The significant overlap of the endocrine-disrupting and toxic effects observed in response to PCBs and dioxins further emphasizes that human exposure to environmental POPs rarely occurs in isolation and that some chemicals contribute to the observed toxicity more than others.

Structural similarity to the most toxic dioxin, TCDD (Figure 1A-D), has been used as a criterion for toxicity and mode of action classification for PCBs and other POPs and is discussed below.

DIOXIN-LIKE PCBS: TOXICITY AND MODE OF ACTION

PCBs represent a family of theoretically 209 possible congeners, consisting of two benzene rings with up to ten possible chlorine substitutions [5]. Commercial PCB mixtures typically consist of a smaller number of congeners, but only about half are considered environmentally relevant [9, 45]. Naturally occurring PCB mixtures often do not match any of the known commercial formulations, because they have been subjected to chemical and biological transformation, including reductive dechlorination by anaerobic bacteria [46-48]. In this process, chlorine is removed from the biphenyl ring and replaced by hydrogen, resulting in a product mixture with diminished number of chlorines. Chlorines substituted in the *meta* and *para* positions are preferentially removed by this process, but *ortho* chlorines are rarely removed [47]. Reductive dechlorination also helps to convert highly chlorinated (and highly persistent) congeners into forms that are more amenable to aerobic degradation [49].

PCB congeners' potencies for several distinct toxic effects vary according to structures and chlorine substitution on the biphenyl rings. PCBs with chlorine substituents at the *meta* and *para* positions are the most toxic because structurally they resemble TCDD, assuming a coplanar configuration. Hence, the coplanar PCBs are termed dioxin-like and elicit a spectrum of TCDD-like toxic responses, including dermal toxicity, tumor promotion, immune suppression and hepatotoxicity [50]. 3,3',4,4',5-Pentachlorobiphenyl (PCB126) is the most potent PCB congener and accounts for 40-60% of the total toxic potency of all dioxin-like PCBs [17].

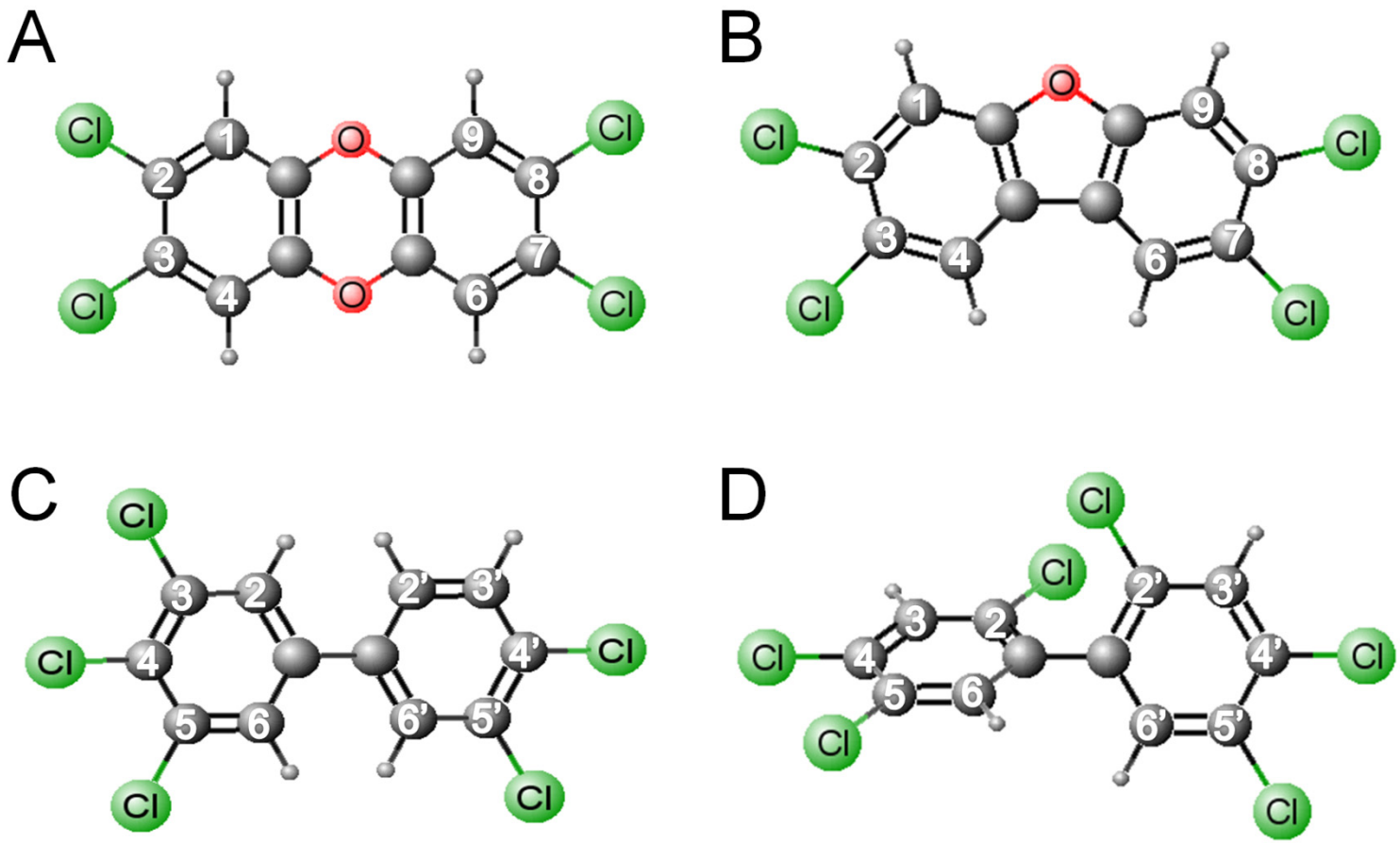

Figure 1. Structural comparisons between dioxin and non-dioxin-like chemicals.

For interpretation of the references to color in this and all other figures, the reader is referred to the electronic version of this dissertation. (A) TCDD and (B) TCDF assume coplanar conformation. (C) PCB126 has chlorine substitutions in *meta* (3,5,5') and *para* (4,4') positions and also assumes a coplanar configuration. (D) PCB153 has two *ortho* (2,2') substitutions resulting in steric hindrance and repulsion between the rings leading to its non-coplanar conformation.

To date, numerous studies have suggested that many, if not all, of the toxic effects elicited by TCDD, PCB126 and other dioxin-like chemicals are mediated by the aryl hydrocarbon receptor (AhR), a ligand-dependent basic-helix-loop-helix PER-ARNT-SIM (bHLH-PAS) domain transcription factor (Figure 2) [19, 51, 52]. Multiple studies have demonstrated that the AhR is present in multiple tissues and different species and that it shares functional and structural characteristics with members of the nuclear receptor superfamily. However, the primary structure of the AhR and the lack of the zinc-finger domain, typical of steroid receptors, prevented its classification into the nuclear receptor family [53, 54].

The AhR resides in the cytoplasm complexed with a dimer of heat shock proteins 90 (Hsp90), aryl hydrocarbon receptor interacting protein (AIP also known as ARA9 or XAP2) and prostaglandin E synthase 3 (p23) [55]. Upon binding of a dioxin-like ligand, the chaperone proteins dissociate and the AhR translocates to the nucleus and heterodimerizes with the AhR nuclear translocator (ARNT), another member of the bHLH-PAS family of transcription factors. The activated AhR-ARNT heterodimer binds to the 5'-GCGTG-3' core sequences termed dioxin response elements (DREs) in the regulatory regions of target genes to drive transcriptional events, which ultimately lead to observed toxic and biochemical responses [56, 57]. Some of the well-characterized AhR target genes belonging to the "AhR gene battery" include phase I and II enzyme families involved in xenobiotic metabolism, principally Cyp1a1, Cyp1a2, Tiparp, Nqo1, Aldh3a1 and Ugt1a6 [58, 59]. In addition to classic AhR ligands like TCDD or dioxin-like chemicals, the AhR is also known to be activated by a wide range of natural and synthetic compounds, including indolo-[3,2-*b*]-carbazole, UV photoproducts of tryptophan, bilirubin, and flavonols such as quercetin [60, 61].

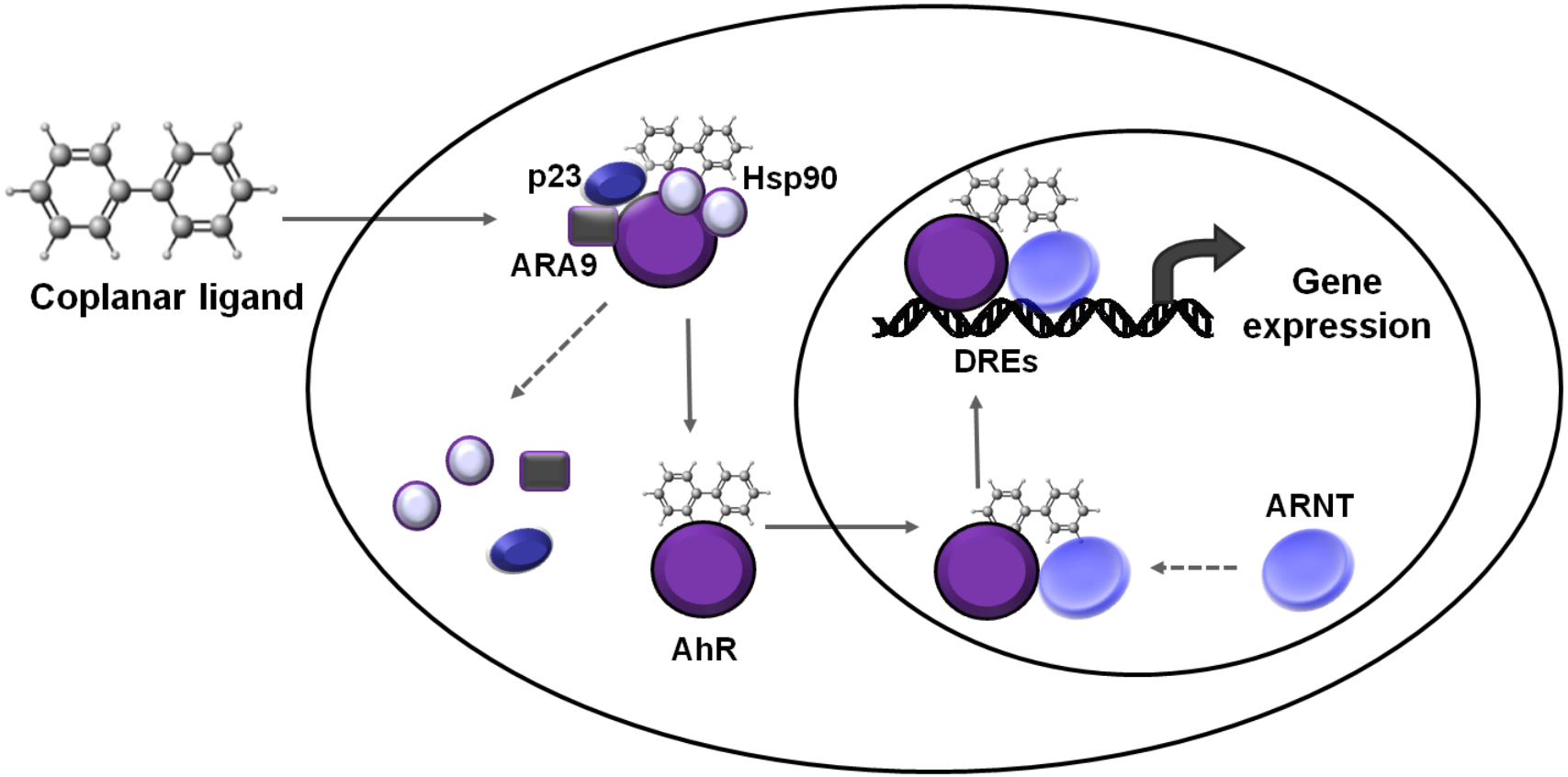

Figure 2. Aryl hydrocarbon receptor-mediated signaling.
In the absence of the ligand, the aryl hydrocarbon receptor (AhR) is bound by chaperone proteins (Hps90 dimer, ARA9 and p23). Following binding of the coplanar ligand (e.g. TCDD, PCB126 or TCDF), the chaperone proteins dissociate and the ligand-bound receptor translocates to the nucleus where it heterodimerizes with the AhR nuclear translocator (ARNT). The AhR/ARNT heterodimer binds specific DNA response elements called dioxin response elements (DREs) in the promoter of target genes, leading to changes in gene expression.

Multiple reports have demonstrated the obligatory involvement of the AhR in mediating dioxin-like toxicity. For example, mice with low-affinity AhR alleles are less susceptible to TCDD's toxic effects, while complete lack of the AhR abolishes inducible expression of Cyp1a1 and Cyp1a2 and leads to an overall resistance to toxic and teratogenic effects of TCDD [62-65]. The AhR-null mice, however, exhibit significantly reduced growth rates in the first three weeks of life, and also reveal defects in liver development and the immune system compared to wild type animals [63, 66]. It has also been reported that AhR-null female mice have difficulty maintaining conception, lactation and rearing pups to weaning [67].

Data from a significant number of reports clearly illustrate the necessary requirement for the AhR signaling in mediating toxic effects of TCDD and dioxin-like compounds. Few reports, however, comment on the involvement of an alternative pathway, which does not involve the AhR or ARNT. For example, the inflammatory action of TCDD has been proposed to act through a rapid increase in intracellular calcium concentration, enzymatic activation of phospholipase A2 (cPLA2) and Cox-2, as artificial suppression of these enzymes leads to a significant reduction of TCDD-elicited wasting syndrome and hydronephrosis [68-70]. In addition, AhR-null mice treated with 2000 μg/kg TCDD revealed occasional hepatocyte necrosis with moderate portal fibrosis, blood vessel proliferation and mild oval cell hyperplasia [62]. The same treatment elicited a significant increase in lymphocyte and macrophage infiltrates in the lung of AhR-deficient mice, suggesting that at very high doses, TCDD-exerted effects on lung tissue are apparently AhR-independent [62]. Although published results support the existence of the alternative pathway, there is an overall lack of acceptance of this proposed mode of action, probably to due insufficient amount of experimental evidence and the overwhelming dominance of the classical model based on the AhR activation of target genes [68].

TOXIC EQUIVALENCY FACTORS

Risk assessment of dioxin-like chemicals uses a toxic equivalency factor (TEF) approach established by the World Health Organization (WHO), relating the potency of the individual dioxin-like compounds to that of TCDD, the most toxic congener [71-76]. The TEF method is based on a congener's structural similarity to TCDD, binding and activation of the AhR-mediated biochemical and toxic responses, and persistence and bioaccumulation potential in the food chain [76]. Among 75, 135 and 209 possible PCDD, PCDF and PCB chemicals, respectively, only 7 PCDDs, 10 PCDFs and 12 PCBs are considered dioxin-like and have TEF values ranging from 0.00003 to 1, where 1 is the maximum possible TEF value [76]. Table 1 summarizes 2005 WHO TEF values for the dioxin-like chemicals [76]. For example, PCB126 and 2,3,7,8-tetrachlorodibenzofuran (TCDF) have a TEF of 0.1, indicating that when compared to TCDD, a 10-fold higher dose of PCB126 or TCDF is required to elicit comparable toxic effects [75, 76].

TEFs are single point potency estimates that are derived from a wide range of relative potency values using different biological endpoints and species, and are therefore considered estimates than can vary by a half-log unit [7, 19, 74, 76-79]. TEFs are used to calculate toxic equivalents (TEQs) defined by the sum of the products of the concentration of each dioxin-like chemical multiplied by its TEF to estimate the total TCDD-like activity of a mixture [76].

The development of the TEF/TEQ concept was largely based on the structure-activity relationships and bioassays that suggested that at the submaximal doses, the contributions of individual congeners are additive and that TEFs are independent of dose, time and tissue [7, 19, 78]. Environmental mixtures change over time and contain relatively low concentrations of dioxin-like chemicals, compared to the high levels of di-*ortho*-substituted, non-coplanar PCBs,

Table 1. Summary of WHO 2005 TEF values.

Dioxin-like compounds	WHO 2005 TEF
PCDDs	
2,3,7,8-Tetrachlorodibenzo-*p*-dioxin (TCDD)	1
1,2,3,7,8-Pentachlorodibenzo-*p*-dioxin	1
1,2,3,4,7,8-Hexachlorodibenzo-*p*-dioxin	0.1
1,2,3,6,7,8-Hexachlorodibenzo-*p*-dioxin	0.1
1,2,3,7,8,9-Hexachlorodibenzo-*p*-dioxin	0.1
1,2,3,4,6,7,8-Heptachlorodibenzo-*p*-dioxin	0.01
Octachlorodibenzo-*p*-dioxin (OCDD)	0.0003
PCDFs	
2,3,7,8-Tetrachlorodibenzo-*p*-furan (TCDF)	0.1
1,2,3,7,8-Pentachlorodibenzo-*p*-furan	0.03
2,3,4,7,8-Pentachlorodibenzo-*p*-furan	0.3
1,2,3,4,7,8-Hexachlorodibenzo-*p*-furan	0.1
1,2,3,6,7,8-Hexachlorodibenzo-*p*-furan	0.1
1,2,3,7,8,9-Hexachlorodibenzo-*p*-furan	0.1
2,3,4,7,8,9-Hexachlorodibenzo-*p*-furan	0.1
1,2,3,4,6,7,8-Heptachlorodibenzo-*p*-furan	0.01
1,2,3,4,7,8,9-Heptachlorodibenzo-*p*-furan	0.01
Octachlorodibenzo-*p*-furan (OCDF)	0.0003
Non-*ortho*-substituted PCBs	
3,3',4,4'-Tetrachlorobiphenyl (PCB77)	0.0001
3,4,4',5-Tetrachlorobiphenyl (PCB81)	0.0003
3,3',4,4',5-Pentachlorobiphenyl (PCB126)	0.1
3,3',4,4',5,5'-Hexachlorobiphenyl (PCB169)	0.03
Mono-*ortho*-substituted PCBs	
2,3,3',4,4'-Pentachlorobiphenyl (PCB105)	0.00003
2,3,4,4',5-Pentachlorobiphenyl (PCB114)	0.00003
2,3',4,4',5-Pentachlorobiphenyl (PCB118)	0.00003
2',3,4,4',5-Pentachlorobiphenyl (PCB123)	0.00003
2,3,3',4,4',5-Hexachlorobiphenyl (PCB156)	0.00003
2,3,3',4,4',5'-Hexachlorobiphenyl (PCB157)	0.00003
2,3',4,4',5,5'-Hexachlorobiphenyl (PCB167)	0.00003
2,3,3',4,4',5,5'-Heptachlorobiphenyl (PCB189)	0.00003

which do not have TEF values and do not activate AhR, and this can profoundly complicate mixture risk assessment [78, 80]. There are also pharmacokinetic and distributional differences between the congeners resulting from the hepatic sequestration of dioxin-like chemicals that may affect their relative potencies, additional aspects which are not accounted for in the TEF method [81-85].

NON-DIOXIN-LIKE PCBS: TOXICITY AND MODE OF ACTION

Research into the PCB toxic mode of action has focused mainly on the AhR and the coplanar, non-*ortho*-substituted, dioxin-like congeners. However, it has become more evident that certain non-coplanar PCBs with low affinity for the AhR also exhibit important biological activities. Originally thought to be inactive, current evidence suggests that these non-dioxin-like congeners show evidence of toxic effects, including neurotoxicity, carcinogenicity and endocrine disruption [45, 86-90]. Non-dioxin-like PCBs are primarily found in blood and other tissues of humans, wildlife and fish exposed via the food chain. Due to their high abundance, prevalence and distribution in the environment, non-dioxin-like congeners are also termed "indicator PCBs" [91]. Compared to dioxin-like PCBs, which use TEFs for toxicity evaluation, no unifying method currently exists for the risk assessment of non-dioxin-like PCBs, even though humans are exposed to significantly higher levels of non-coplanar PCBs. Recent reports, however, suggest the use of alternative biomarkers, like thyroid hormone levels for the generation of a new and dynamic TEF scheme that would be applicable to non-dioxin-like PCBs and other structurally related chemicals. Ideally, the new TEF would parallel the WHO TEF for dioxin-like chemicals and become a useful tool for non-dioxin-like PCBs in risk assessment to address the endocrine-disrupting and the potentially neurotoxic effects of PCBs [45].

The 2,2',4,4',5,5'-hexachlorobiphenyl (PCB153) is the most abundant PCB congener and is found at the highest concentrations in humans and in the environment on a molar basis [92, 93]. The di-*ortho*-substitution on the biphenyl ring leads to steric hindrance and the non-coplanar conformation of PCB153, resulting in its minimal structural resemblance to TCDD. Consequently, PCB153 has very low binding affinity for the AhR, is not assigned a TEF value and exerts its toxic effects via a mechanism independent of the Ah receptor activation [76, 94, 95]. Based on a structural similarity to phenobarbital, the mode of action for PCB153 has been proposed to be mediated via members of the nuclear receptor family, the constitutive androstane and pregnane X receptors (CAR and PXR) (Figure 3) [96-100].

CAR and PXR share a lot of structural and functional similarities and both belong to the type I family of nuclear receptors that also includes the vitamin D receptor [97, 101, 102]. Following ligand binding, these receptors dissociate from their co-chaperone partners, including cytoplasmic CAR retention protein (Ccrp) and Hsp90, and translocate to the nucleus to heterodimerize with the retinoid X receptor (RXR) [101, 103]. Similar to the AhR signaling, the CAR/RXR or PXR/RXR heterodimers bind to CAR and PXR response elements in the promoter regions of target genes, recruiting co-activators and leading to transcriptional changes, including expression of cytochrome P450 genes from the 2b and 3a families (e.g. Cyp2b10, Cyp3a11) [97, 101, 103-107]. It has also been shown that the DNA binding domains of CAR and PXR are similar in amino acid composition and therefore bind similar DNA motifs. However, similarities between the ligand binding domains of human and rodent CAR and PXR are significantly lower, suggesting that ligand-specificity may differ drastically between species [97]. Some of the most well characterized and potent CAR agonists include phenobarbital and TCPOBOP, while

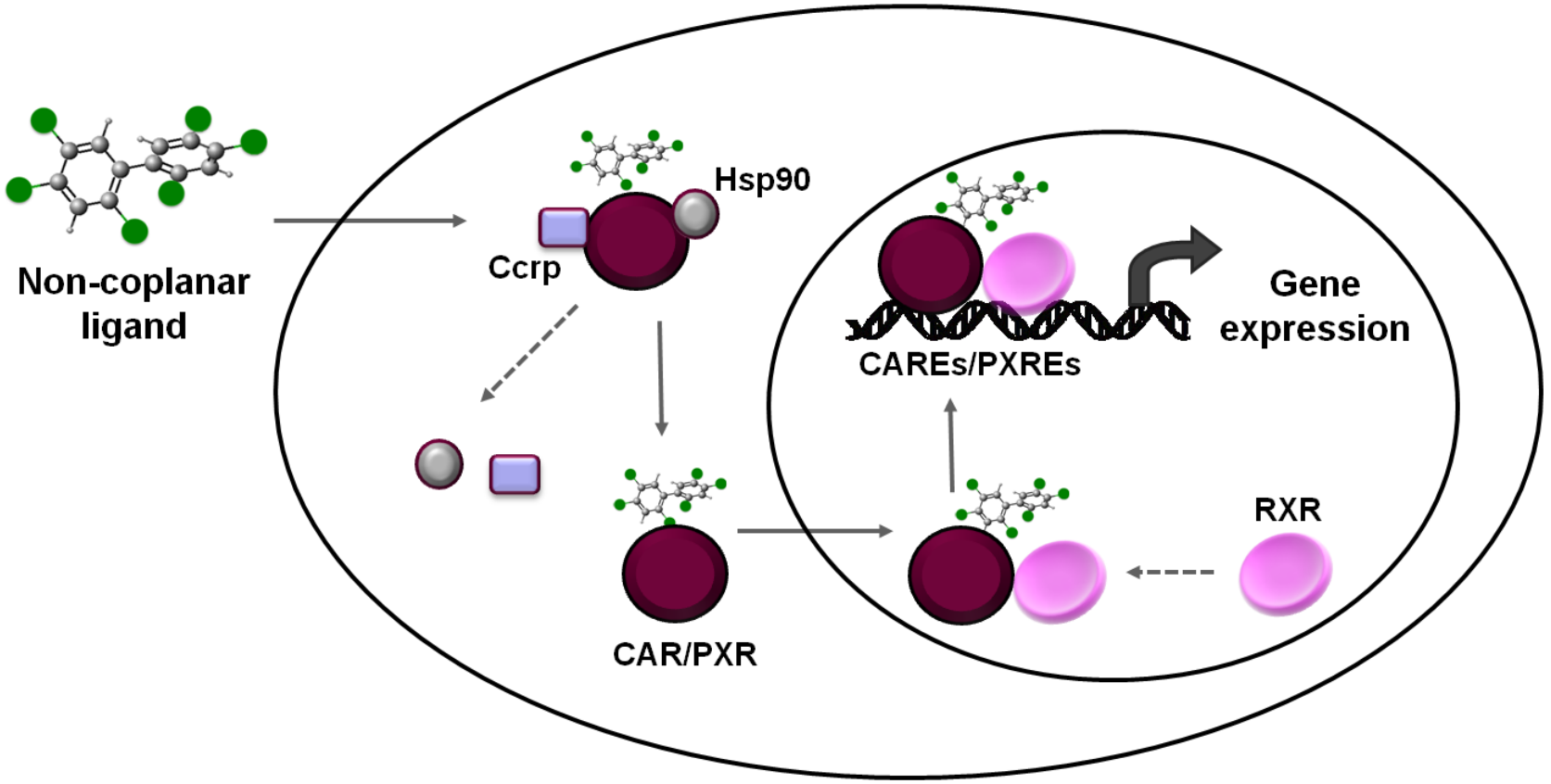

Figure 3. Constitutive androstane/pregnane X receptor-mediated signaling.
In the absence of ligand, the constitutive androstane or pregnane X receptors (CAR/PXR) are bound by chaperone proteins (Hsp90 and Ccrp). Following binding of a non-coplanar ligand (e.g. PCB153), the chaperone proteins dissociate and the ligand-bound receptors translocate to the nucleus, where they heterodimerize with the retinoid X receptor (RXR). The CAR/RXR or PXR/RXR heterodimers bind to specific DNA response elements, the CAR or PXR response elements (CAREs/PXREs), in the promoter region of target genes, leading to changes in gene expression.

pregnanes (e.g. PCN) and glucocorticoids (e.g. dexamethasone) have been shown to activate the PXR [97].

MIXTURE EFFECTS

Understanding the interactions between the dioxin and non-dioxin-like chemicals is of importance because environmental extracts usually contain lower levels of dioxin-like chemicals and relatively high concentration of non-coplanar chemicals, confounding the risk assessment of a mixture. Two or more chemicals can exert an additive effect, represented as the arithmetic sum of effects elicited by individual chemicals, or the resulting effect can be non-additive. The non-additive interactions include synergism, where the mixture has a total effect that is greater than the additive effect, or antagonism, where the mixture interactions lead to a lower effect than the one based on additivity [108]. In addition, different types of interactions can be observed at the receptor level. Full receptor agonists are capable of eliciting a maximum response, whereas partial agonists are unable to elicit a full response even when they are present at very high concentrations or doses [109]. On the contrary, inverse agonists bind the same receptor site as full or partial agonists, but they exert the opposite effects through reversal of ligand-induced constitutive activity [110].

Several groups have investigated non-additive interactions between non-coplanar PCB153 and AhR agonists, like PCB126 or TCDD. PCB153 has been shown to antagonize TCDD- and PCB126-mediated cleft palate and immunotoxicity, as well as suppress hepatic microsomal ethoxyresorufin-O-deethylase (EROD) induction in C57BL/6 mice [111, 112]. At low doses of AhR agonists, PCB153 significantly antagonized TCDD- and PCB126-induced relative Cyp1a1 mRNA expression in CH12.LX B cells [113]. Co-treatment studies in chick embryos revealed that PCB153 significantly reduced PCB126-induced embryo malformations,

edema and liver lesions [114]. Other studies reported synergistic interactions between dioxin and non-dioxin-like ligands. For example, treatment with PCB153 markedly enhanced the TCDD-induced hepatic porphyrin levels in Sprague-Dawley rats [115], while PCB126 and PCB153 co-treatment synergistically altered hepatocellular foci development and expression of γ-glutamyltranspeptidase [116]. Co-treatment of PCB153 and TCDD resulted in a significant synergistic induction of hepatic EROD and aryl hydrocarbon hydroxylase activity compared to TCDD treatment alone [117]. In addition, immunohistochemistry of rat livers following co-treatment with PCB126 and PCB153 showed differential induction of Cyp1a1 compared to PCB126 alone [118]. Consequently, a more thorough examination of PCB153 in mixtures with dioxin-like ligands is warranted in order to further elucidate the mechanisms involved in these non-additive activities.

CONCLUSIONS

Exposure to dioxin and non-dioxin-like chemicals occurs due to their environmental persistence, lipophilicity and bioaccumulation in the food chain and results in a spectrum of tissue and species-specific responses, including immune suppression, endocrine disruption, and hepatotoxicity. Understanding the toxicity of individual chemicals is necessary to establish a quantitative baseline of toxic responses, but it is not completely adequate for risk assessment since human and animal exposure to these chemicals rarely occurs in isolation. Dose addition is currently the underlying assumption behind the TEF approach, implying that the exposures or the responses to the mixture components are additive, even though multiple studies report on the non-additive interactions in mixtures of dioxin and non-dioxin-like chemicals at varying concentrations and doses. In practice, however, the risk assessment of these chemical mixtures is frequently inhibited by the lack of desirable dose-response evaluation of the individual

components and their mixtures [119, 120]. Mathematical formulas allow for the determination of predicted and observed responses of chemical mixtures and enable statistical assessment of the non-additive effects [120]. Comprehensive dose-response and time course evaluation of single congener and mixture effects on gene expression and physiological endpoints will increase our understanding of the hepatotoxic mode of action and address limitations with current approaches to human and wildlife mixture risk assessment.

REFERENCES

REFERENCES

1. Fisher, B.E., *Most unwanted.* Environ Health Perspect, 1999. **107**(1): p. A18-23.

2. Mansour, S.A., *Persistent organic pollutants (POPs) in Africa: Egyptian scenario.* Hum Exp Toxicol, 2009. **28**(9): p. 531-66.

3. Kaiser, J. and M. Enserink, *Environmental toxicology. Treaty takes a POP at the dirty dozen.* Science, 2000. **290**(5499): p. 2053.

4. Schecter, A., et al., *Chlorinated dioxins and dibenzofurans in human tissue from general populations: a selective review.* Environ Health Perspect, 1994. **102 Suppl 1**: p. 159-71.

5. Mullin, M.D., et al., *High-resolution PCB analysis: synthesis and chromatographic properties of all 209 PCB congeners.* Environ. Set Technol., 1984. **18**: p. 468-476.

6. *Guidelines for the identification of PCBs and materials containing PCBs.* United Nations Environment Programme, 1999(First Issue): p. 1-40.

7. Safe, S., *Polychlorinated biphenyls (PCBs), dibenzo-p-dioxins (PCDDs), dibenzofurans (PCDFs), and related compounds: environmental and mechanistic considerations which support the development of toxic equivalency factors (TEFs).* Crit Rev Toxicol, 1990. **21**(1): p. 51-88.

8. *Toxicological profile for polychlorinated biphenyls (PCBs).* U.S. DEPARTMENT OF HEALTH AND HUMAN SERVICES, Public Health Service, Agency for Toxic Substances and Disease Registry, 2000: p. 1-948.

9. Kimbrough, R.D., *Polychlorinated biphenyls (PCBs) and human health: an update.* Crit Rev Toxicol, 1995. **25**(2): p. 133-63.

10. *Dolnośląska Fundacja Ekorozwoju: Program PCB Stop*. Available from: http://www.pcb.pl/pcb_ministerstwo.shtml.

11. Mason, G. and S. Safe, *Synthesis, biologic and toxic effects of the major 2,3,7,8-tetrachlorodibenzo-p-dioxin metabolites in the rat.* Toxicology, 1986. **41**(2): p. 153-9.

12. Poland, A. and E. Glover, *Studies on the mechanism of toxicity of the chlorinated dibenzo-p-dioxins.* Environ Health Perspect, 1973. **5**: p. 245-51.

13. Commoner, B., K. Shapiro, and T. Webster, *The Origin and Health Risks of PCDD and PCDF.* Waste Management & Research, 1987. **5**: p. 327-346.

14. Safe, S., et al., *Halogenated biphenyls: molecular toxicology.* Can J Physiol Pharmacol, 1982. **60**(7): p. 1057-64.

15. Rappolder, M., et al., *Temporal trends and spatial distribution of PCDD, PCDF, and PCB in pine and spruce shoots.* Chemosphere, 2007. **67**(9): p. 1887-1896.

16. *The Chlorine Chemistry Division of the American Chemistry Council: Trends in Dioxin Emissions and Exposure in the United States*. Available from: http://www.dioxinfacts.org/sources_trends/trends_emissions.html.

17. NTP, *NTP toxicology and carcinogenesis studies of 3,3',4,4',5-pentachlorobiphenyl (PCB 126) (CAS No. 57465-28-8) in female Harlan Sprague-Dawley rats (Gavage Studies).* NTP Technical Report, 2006(520): p. 4-246.

18. Hopf, N.B., A.M. Ruder, and P. Succop, *Background levels of polychlorinated biphenyls in the U.S. population.* Sci Total Environ, 2009.

19. Poland, A. and J.C. Knutson, *2,3,7,8-tetrachlorodibenzo-p-dioxin and related halogenated aromatic hydrocarbons: examination of the mechanism of toxicity.* Annu Rev Pharmacol Toxicol, 1982. **22**: p. 517-54.

20. Herrick, R.F., D.J. Lefkowitz, and G.A. Weymouth, *Soil contamination from PCB-containing buildings.* Environ Health Perspect, 2007. **115**(2): p. 173-5.

21. Harrad, S.J., et al., *Polychlorinated biphenyls (PCBs) in the British environment: sinks, sources and temporal trends.* Environ Pollut, 1994. **85**(2): p. 131-46.

22. Hu, D., A. Martinez, and K.C. Hornbuckle, *Discovery of non-aroclor PCB (3,3'-dichlorobiphenyl) in Chicago air.* Environ Sci Technol, 2008. **42**(21): p. 7873-7.

23. Zuccato, E., et al., *PCB concentrations in some foods from four European countries.* Food Chem Toxicol, 2008. **46**(3): p. 1062-7.

24. Gallenberg, L.A. and M.J. Vodicnik, *Potential mechanisms for redistribution of polychlorinated biphenyls during pregnancy and lactation.* Xenobiotica, 1987. **17**(3): p. 299-310.

25. Schecter, A., et al., *Comparison of dibenzodioxin levels in blood and milk in agricultural workers and others following pentachlorophenol exposure in China.* Chemosphere, 1994. **29**(9-11): p. 2371-80.

26. Vodicnik, M.J. and J.J. Lech, *The transfer of 2,4,5,2',4',5'-hexachlorobiphenyl to fetuses and nursing offspring. I. Disposition in pregnant and lactating mice and accumulation in young.* Toxicol Appl Pharmacol, 1980. **54**(2): p. 293-300.

27. Lung, S.C., Y.L. Guo, and H.Y. Chang, *Serum concentrations and profiles of polychlorinated biphenyls in Taiwan Yu-cheng victims twenty years after the incident.* Environ Pollut, 2005. **136**(1): p. 71-9.

28. Ryan, J.J., et al., *Blood serum levels of PCDFs and PCBs in Yu-Cheng children peri-natally exposed to a toxic rice oil.* Chemosphere, 1994. **29**(6): p. 1263-78.

29. Masuda, Y., *Health status of Japanese and Taiwanese after exposure to contaminated rice oil.* Environ Health Perspect, 1985. **60**: p. 321-5.

30. Yoshimura, T., *Yusho in Japan.* Ind Health, 2003. **41**(3): p. 139-48.

31. Nagayama, J., M. Kuratsune, and Y. Masuda, *Determination of chlorinated dibenzofurans in kanechlors and "yusho oil".* Bull Environ Contam Toxicol, 1976. **15**(1): p. 9-13.

32. Yu, M.L., et al., *Increased mortality from chronic liver disease and cirrhosis 13 years after the Taiwan "yucheng" ("oil disease") incident.* Am J Ind Med, 1997. **31**(2): p. 172-5.

33. Wan, Y., et al., *Bioaccumulation of polychlorinated dibenzo-p-dioxins, dibenzofurans, and dioxin-like polychlorinated biphenyls in fishes from the Tittabawassee and Saginaw Rivers, Michigan, USA.* Sci Total Environ, 2010. **408**(11): p. 2394-401.

34. Tryphonas, H., *Immunotoxicity of PCBs (Aroclors) in relation to Great Lakes.* Environ Health Perspect, 1995. **103 Suppl 9**: p. 35-46.

35. Giesy, J.P., et al., *Contaminants in fishes from Great Lakes-influenced sections and above dams of three Michigan rivers. I: Concentrations of organo chlorine insecticides, polychlorinated biphenyls, dioxin equivalents, and mercury.* Arch Environ Contam Toxicol, 1994. **27**(2): p. 202-12.

36. Ngo, A.D., et al., *Association between Agent Orange and birth defects: systematic review and meta-analysis.* Int J Epidemiol, 2006. **35**(5): p. 1220-30.

37. Frumkin, H., *Agent Orange and cancer: an overview for clinicians.* CA Cancer J Clin, 2003. **53**(4): p. 245-55.

38. Bertazzi, P.A., et al., *The Seveso studies on early and long-term effects of dioxin exposure: a review.* Environ Health Perspect, 1998. **106 Suppl 2**: p. 625-33.

39. Sorg, O., et al., *2,3,7,8-tetrachlorodibenzo-p-dioxin (TCDD) poisoning in Victor Yushchenko: identification and measurement of TCDD metabolites.* Lancet, 2009. **374**(9696): p. 1179-85.

40. Birnbaum, L.S. and J. Tuomisto, *Non-carcinogenic effects of TCDD in animals.* Food Addit Contam, 2000. **17**(4): p. 275-88.

41. Sweeney, M.H. and P. Mocarelli, *Human health effects after exposure to 2,3,7,8-TCDD.* Food Addit Contam, 2000. **17**(4): p. 303-16.

42. Hobson, L.B., *Human effects of TCDD exposure.* Bull Environ Contam Toxicol, 1984. **33**(6): p. 696-701.

43. Consonni, D., et al., *Mortality in a population exposed to dioxin after the Seveso, Italy, accident in 1976: 25 years of follow-up.* Am J Epidemiol, 2008. **167**(7): p. 847-58.

44. Michalek, J.E. and M. Pavuk, *Diabetes and cancer in veterans of Operation Ranch Hand after adjustment for calendar period, days of spraying, and time spent in Southeast Asia.* J Occup Environ Med, 2008. **50**(3): p. 330-40.

45. Yang, J.M., A.G. Salmon, and M.A. Marty, *Development of TEFs for PCB congeners by using an alternative biomarker - Thyroid hormone levels.* Regul Toxicol Pharmacol, 2010. **56**(2): p. 225-36.

46. Quensen, J.F., S.A. Boyd, and J.M. Tiedje, *Dechlorination of Four Commercial Polychlorinated Biphenyl Mixtures (Aroclors) by Anaerobic Microorganisms from Sediments.* Appl Environ Microbiol, 1990. **56**(8): p. 2360-2369.

47. Ganey, P.E. and S.A. Boyd, *An approach to evaluation of the effect of bioremediation on biological activity of environmental contaminants: dechlorination of polychlorinated biphenyls.* Environ Health Perspect, 2005. **113**(2): p. 180-5.

48. Wu, Q., K.R. Sowers, and H.D. May, *Microbial Reductive Dechlorination of Aroclor 1260 in Anaerobic Slurries of Estuarine Sediments.* Appl Environ Microbiol, 1998. **64**(3): p. 1052-1058.

49. Bedard, D.L., et al., *Rapid assay for screening and characterizing microorganisms for the ability to degrade polychlorinated biphenyls.* Appl Environ Microbiol, 1986. **51**(4): p. 761-8.

50. Denison, M.S. and S. Heath-Pagliuso, *The Ah receptor: a regulator of the biochemical and toxicological actions of structurally diverse chemicals.* Bull Environ Contam Toxicol, 1998. **61**(5): p. 557-68.

51. Poland, A., E. Glover, and A.S. Kende, *Stereospecific, high affinity binding of 2,3,7,8-tetrachlorodibenzo-p-dioxin by hepatic cytosol. Evidence that the binding species is receptor for induction of aryl hydrocarbon hydroxylase.* J Biol Chem, 1976. **251**(16): p. 4936-46.

52. Swanson, H.I. and C.A. Bradfield, *The AH-receptor: genetics, structure and function.* Pharmacogenetics, 1993. **3**(5): p. 213-30.

53. Evans, R.M., *The steroid and thyroid hormone receptor superfamily.* Science, 1988. **240**(4854): p. 889-95.

54. Okey, A.B., *An aryl hydrocarbon receptor odyssey to the shores of toxicology: the Deichmann Lecture, International Congress of Toxicology-XI.* Toxicol Sci, 2007. **98**(1): p. 5-38.

55. Patel, R.D., et al., *Aryl-hydrocarbon receptor activation regulates constitutive androstane receptor levels in murine and human liver.* Hepatology, 2007. **46**(1): p. 209-18.

56. Hankinson, O., *The aryl hydrocarbon receptor complex.* Annu Rev Pharmacol Toxicol, 1995. **35**: p. 307-40.

57. Swanson, H.I., W.K. Chan, and C.A. Bradfield, *DNA binding specificities and pairing rules of the Ah receptor, ARNT, and SIM proteins.* J Biol Chem, 1995. **270**(44): p. 26292-302.

58. Nebert, D.W., et al., *Role of the aromatic hydrocarbon receptor and [Ah] gene battery in the oxidative stress response, cell cycle control, and apoptosis.* Biochem Pharmacol, 2000. **59**(1): p. 65-85.

59. Boutros, P.C., et al., *Dioxin-dependent and dioxin-independent gene batteries: comparison of liver and kidney in AHR-null mice.* Toxicol Sci, 2009. **112**(1): p. 245-56.

60. Flaveny, C.A., I.A. Murray, and G.H. Perdew, *Differential gene regulation by the human and mouse aryl hydrocarbon receptor.* Toxicol Sci, 2010. **114**(2): p. 217-25.

61. Denison, M.S., et al., *Ligand binding and activation of the Ah receptor.* Chem Biol Interact, 2002. **141**(1-2): p. 3-24.

62. Fernandez-Salguero, P.M., et al., *Aryl-hydrocarbon receptor-deficient mice are resistant to 2,3,7,8-tetrachlorodibenzo-p-dioxin-induced toxicity.* Toxicol Appl Pharmacol, 1996. **140**(1): p. 173-9.

63. Schmidt, J.V., et al., *Characterization of a murine Ahr null allele: involvement of the Ah receptor in hepatic growth and development.* Proc Natl Acad Sci U S A, 1996. **93**(13): p. 6731-6.

64. Mimura, J., et al., *Loss of teratogenic response to 2,3,7,8-tetrachlorodibenzo-p-dioxin (TCDD) in mice lacking the Ah (dioxin) receptor.* Genes Cells, 1997. **2**(10): p. 645-54.

65. Okey, A.B., L.M. Vella, and P.A. Harper, *Detection and characterization of a low affinity form of cytosolic Ah receptor in livers of mice nonresponsive to induction of cytochrome P1-450 by 3-methylcholanthrene.* Mol Pharmacol, 1989. **35**(6): p. 823-30.

66. Mimura, J. and Y. Fujii-Kuriyama, *Functional role of AhR in the expression of toxic effects by TCDD.* Biochim Biophys Acta, 2003. **1619**(3): p. 263-8.

67. Abbott, B.D., et al., *Adverse reproductive outcomes in the transgenic Ah receptor-deficient mouse.* Toxicol Appl Pharmacol, 1999. **155**(1): p. 62-70.

68. Matsumura, F., *The significance of the nongenomic pathway in mediating inflammatory signaling of the dioxin-activated Ah receptor to cause toxic effects.* Biochem Pharmacol, 2009. **77**(4): p. 608-26.

69. Dong, B. and F. Matsumura, *Roles of cytosolic phospholipase A2 and Src kinase in the early action of 2,3,7,8-tetrachlorodibenzo-p-dioxin through a nongenomic pathway in MCF10A cells.* Mol Pharmacol, 2008. **74**(1): p. 255-63.

70. Puga, A., D.W. Nebert, and F. Carrier, *Dioxin induces expression of c-fos and c-jun proto-oncogenes and a large increase in transcription factor AP-1.* DNA Cell Biol, 1992. **11**(4): p. 269-81.

71. Ahlborg, U.G., *Human health risk assessment and risk perception related to the Baltic Sea.* Arch Toxicol Suppl, 1994. **16**: p. 53-9.

72. Barnes, D.G., *Toxicity equivalents and EPA's risk assessment of 2,3,7,8-TCDD.* Sci Total Environ, 1991. **104**(1-2): p. 73-86.

73. Birnbaum, L.S. and M.J. DeVito, *Use of toxic equivalency factors for risk assessment for dioxins and related compounds.* Toxicology, 1995. **105**(2-3): p. 391-401.

74. Haws, L.C., et al., *Development of a refined database of mammalian relative potency estimates for dioxin-like compounds.* Toxicol Sci, 2006. **89**(1): p. 4-30.

75. Van den Berg, M., et al., *Toxic equivalency factors (TEFs) for PCBs, PCDDs, PCDFs for humans and wildlife.* Environ Health Perspect, 1998. **106**(12): p. 775-92.

76. Van den Berg, M., et al., *The 2005 World Health Organization reevaluation of human and Mammalian toxic equivalency factors for dioxins and dioxin-like compounds.* Toxicol Sci, 2006. **93**(2): p. 223-41.

77. Starr, T.B., et al., *The trouble with TEFs.* Environ Health Perspect, 1999. **107**(10): p. A492-3.

78. Safe, S., *Limitations of the toxic equivalency factor approach for risk assessment of TCDD and related compounds.* Teratog Carcinog Mutagen, 1997. **17**(4-5): p. 285-304.

79. Harris, M., T. Zacharewski, and S. Safe, *Comparative potencies of Aroclors 1232, 1242, 1248, 1254, and 1260 in male Wistar rats--assessment of the toxic equivalency factor (TEF) approach for polychlorinated biphenyls (PCBs).* Fundam Appl Toxicol, 1993. **20**(4): p. 456-63.

80. Wolfle, D., *Interactions between 2,3,7,8-TCDD and PCBs as tumor promoters: limitations of TEFs.* Teratog Carcinog Mutagen, 1997. **17**(4-5): p. 217-24.

81. Budinsky, R.A., et al., *Recommended relative potency factors for 2,3,4,7,8-pentachlorodibenzofuran: the impact of different dose metrics.* Toxicol Sci, 2006. **91**(1): p. 275-85.

82. DeVito, M.J., et al., *Dose-response relationships for polyhalogenated dioxins and dibenzofurans following subchronic treatment in mice. I. CYP1A1 and CYP1A2 enzyme activity in liver, lung, and skin.* Toxicol Appl Pharmacol, 1997. **147**(2): p. 267-80.

83. DeVito, M.J., et al., *Dose-response relationships for disposition and hepatic sequestration of polyhalogenated dibenzo-p-dioxins, dibenzofurans, and biphenyls following subchronic treatment in mice.* Toxicol Sci, 1998. **46**(2): p. 223-34.

84. Diliberto, J.J., et al., *Subchronic Exposure of [3H]- 2,3,7,8-tetrachlorodibenzo-p-dioxin (TCDD) in female B6C3F1 mice: relationship of steady-state levels to disposition and metabolism.* Toxicol Sci, 2001. **61**(2): p. 241-55.

85. Safe, S.H., *Modulation of gene expression and endocrine response pathways by 2,3,7,8-tetrachlorodibenzo-p-dioxin and related compounds.* Pharmacol Ther, 1995. **67**(2): p. 247-81.

86. Fischer, L.J., et al., *Symposium overview: toxicity of non-coplanar PCBs.* Toxicol Sci, 1998. **41**(1): p. 49-61.

87. Seegal, R.F., *Epidemiological and laboratory evidence of PCB-induced neurotoxicity.* Crit Rev Toxicol, 1996. **26**(6): p. 709-37.

88. Shain, W., B. Bush, and R. Seegal, *Neurotoxicity of polychlorinated biphenyls: structure-activity relationship of individual congeners.* Toxicol Appl Pharmacol, 1991. **111**(1): p. 33-42.

89. Crofton, K.M., et al., *Thyroid-hormone-disrupting chemicals: evidence for dose-dependent additivity or synergism.* Environ Health Perspect, 2005. **113**(11): p. 1549-54.

90. Knerr, S. and D. Schrenk, *Carcinogenicity of "non-dioxinlike" polychlorinated biphenyls.* Crit Rev Toxicol, 2006. **36**(9): p. 663-94.

91. Kim, M., et al., *Comparison of seven indicator PCBs and three coplanar PCBs in beef, pork, and chicken fat.* Chemosphere, 2004. **54**(10): p. 1533-1538.

92. Schecter, A., et al., *Polychlorinated biphenyl levels in the tissues of exposed and nonexposed humans.* Environ Health Perspect, 1994. **102 Suppl 1**: p. 149-58.

93. NTP, *NTP technical report on the toxicology and carcinogenesis studies of 2,2',4,4',5,5'-hexachlorobiphenyl (PCB 153) (CAS No. 35065-27-1) in female Harlan Sprague-Dawley rats (Gavage studies).* Natl Toxicol Program Tech Rep Ser, 2006(529): p. 4-168.

94. Sipka, S., et al., *Oral administration of PCBs induces proinflammatory and prometastatic responses.* Environ Toxicol Pharmacol, 2008. **25**(2): p. 251-259.

95. Kafafi, S.A., et al., *Binding of polychlorinated biphenyls to the aryl hydrocarbon receptor.* Environ Health Perspect, 1993. **101**(5): p. 422-8.

96. Craft, E.S., M.J. DeVito, and K.M. Crofton, *Comparative responsiveness of hypothyroxinemia and hepatic enzyme induction in Long-Evans rats versus C57BL/6J mice exposed to TCDD-like and phenobarbital-like polychlorinated biphenyl congeners.* Toxicol Sci, 2002. **68**(2): p. 372-80.

97. Honkakoski, P., T. Sueyoshi, and M. Negishi, *Drug-activated nuclear receptors CAR and PXR.* Ann Med, 2003. **35**(3): p. 172-82.

98. Pascussi, J.M., et al., *The Tangle of Nuclear Receptors that Controls Xenobiotic Metabolism and Transport: Crosstalk and Consequences.* Annu Rev Pharmacol Toxicol, 2007.

99. Strathmann, J., et al., *PCB 153, a non-dioxin-like tumor promoter, selects for beta-catenin (Catnb)-mutated mouse liver tumors.* Toxicol Sci, 2006. **93**(1): p. 34-40.

100. Tabb, M.M., et al., *Highly chlorinated PCBs inhibit the human xenobiotic response mediated by the steroid and xenobiotic receptor (SXR).* Environ Health Perspect, 2004. **112**(2): p. 163-9.

101. Timsit, Y.E. and M. Negishi, *CAR and PXR: the xenobiotic-sensing receptors.* Steroids, 2007. **72**(3): p. 231-46.

102. Moore, J.T., et al., *Functional and structural comparison of PXR and CAR.* Biochim Biophys Acta, 2003. **1619**(3): p. 235-8.

103. Squires, E.J., T. Sueyoshi, and M. Negishi, *Cytoplasmic localization of pregnane X receptor and ligand-dependent nuclear translocation in mouse liver.* J Biol Chem, 2004. **279**(47): p. 49307-14.

104. Lemaire, G., et al., *Discovery of a highly active ligand of human pregnane x receptor: a case study from pharmacophore modeling and virtual screening to "in vivo" biological activity.* Mol Pharmacol, 2007. **72**(3): p. 572-81.

105. Blumberg, B. and R.M. Evans, *Orphan nuclear receptors--new ligands and new possibilities.* Genes Dev, 1998. **12**(20): p. 3149-55.

106. Masahiko, N. and P. Honkakoski, *Induction of drug metabolism by nuclear receptor CAR: molecular mechanisms and implications for drug research.* Eur J Pharm Sci, 2000. **11**(4): p. 259-64.

107. Honkakoski, P., et al., *The nuclear orphan receptor CAR-retinoid X receptor heterodimer activates the phenobarbital-responsive enhancer module of the CYP2B gene.* Mol Cell Biol, 1998. **18**(10): p. 5652-8.

108. Staal, Y.C., et al., *Binary PAH mixtures cause additive or antagonistic effects on gene expression but synergistic effects on DNA adduct formation.* Carcinogenesis, 2007. **28**(12): p. 2632-40.

109. Zhu, B.T., *Mechanistic explanation for the unique pharmacologic properties of receptor partial agonists.* Biomed Pharmacother, 2005. **59**(3): p. 76-89.

110. Kenakin, T., *Principles: receptor theory in pharmacology.* Trends Pharmacol Sci, 2004. **25**(4): p. 186-92.

111. Biegel, L., et al., *2,2',4,4',5,5'-hexachlorobiphenyl as a 2,3,7,8-tetrachlorodibenzo-p-dioxin antagonist in C57BL/6J mice.* Toxicol Appl Pharmacol, 1989. **97**(3): p. 561-71.

112. Zhao, F., et al., *Inhibition of 3,3',4,4',5-pentachlorobiphenyl-induced fetal cleft palate and immunotoxicity in C57BL/6 mice by 2,2',4,4',5,5'-hexachlorobiphenyl.* Chemosphere, 1997. **34**(5-7): p. 1605-13.

113. Suh, J., et al., *Antagonism of aryl hydrocarbon receptor-dependent induction of CYP1A1 and inhibition of IgM expression by di-ortho-substituted polychlorinated biphenyls.* Toxicol Appl Pharmacol, 2003. **187**(1): p. 11-21.

114. Zhao, F., et al., *Inhibition of 3,3',4,4',5-pentachlorobiphenyl-induced chicken embryotoxicity by 2,2',4,4',5,5'-hexachlorobiphenyl.* Fundam Appl Toxicol, 1997. **35**(1): p. 1-8.

115. van Birgelen, A.P., et al., *Synergistic effect of 2,2',4,4',5,5'-hexachlorobiphenyl and 2,3,7,8-tetrachlorodibenzo-p-dioxin on hepatic porphyrin levels in the rat.* Environ Health Perspect, 1996. **104**(5): p. 550-7.

116. Bager, Y., et al., *Interaction of 3,4,5,3',4'-pentachlorobiphenyl and 2,4,5,2',4',5'-hexachlorobiphenyl in promotion of altered hepatic foci in rats.* Pharmacol Toxicol, 1995. **77**(2): p. 149-54.

117. Bannister, R. and S. Safe, *Synergistic interactions of 2,3,7,8-TCDD and 2,2',4,4',5,5'-hexachlorobiphenyl in C57BL/6J and DBA/2J mice: role of the Ah receptor.* Toxicology, 1987. **44**(2): p. 159-69.

118. Chubb, L.S., et al., *Regional induction of CYP1A1 in rat liver following treatment with mixtures of PCB 126 and PCB 153.* Toxicol Pathol, 2004. **32**(4): p. 467-73.

119. Borgert, C.J., et al., *Evaluating chemical interaction studies for mixture risk assessment.* Human and Ecological Risk Assessment, 2001. **7**(2): p. 259-305.

120. Hertzberg, R.C. and L.K. Teuschler, *Evaluating quantitative formulas for dose-response assessment of chemical mixtures.* Environ Health Perspect, 2002. **110 Suppl 6**: p. 965-70.

CHAPTER 2

CHAPTER 2

RATIONALE, HYPOTHESIS AND SPECIFIC AIMS

RATIONALE

Human exposure to toxicants typically occurs as complex mixtures of environmental chemicals with varying potencies and toxicities. The more toxic, dioxin-like chemicals, including 2,3,7,8-tetrachlorodibenzo-*p*-dioxin (TCDD) and 3,3',4,4',5-pentachlorobiphenyl (PCB126), elicit their toxicity through the AhR-mediated pathway, while the more abundant, non-dioxin-like congeners like 2,2',4,4',5,5'-hexachlorobiphenyl (PCB153) elicit toxic effects through unique, non-AhR-mediated mechanisms. Interactions between these chemicals can lead to responses that deviate from the dose-additive assumption underlying mixture risk assessment approaches. Comprehensive mixture dose-response and time course evaluation, in addition to single chemical, single time point or single dose studies, is required for scientifically based risk and health hazard assessment. The systematic transcriptomic and phenotypic examination of single congener and mixture toxicity will provide valuable insight into elucidation of potential non-additive effects occurring at both molecular and physiological levels. These comprehensive studies have the potential of significantly improving quantitative risk assessment of human exposures to ubiquitously persistent environmental toxicants.

HYPOTHESIS

The binary mixture of TCDD and PCB153 elicits non-additive hepatic gene expression and phenotypic effects compared to single chemical exposure.

SPECIFIC AIMS

To address this hypothesis, the following specific aims with the application of genome-wide transcript profiling and phenotypic anchoring of the gene expression responses will be used:

1. Establish baseline quantitative temporal and dose-dependent data on the hepatic effects elicited by dioxin-like PCB126 in comparison to TCDD in a mouse model.
2. Establish baseline quantitative temporal and dose-dependent data on the hepatic effects elicited by non-dioxin-like PCB153 in a mouse model.
3. Characterize the effects of a reconstituted binary mixture of TCDD and PCB153 on eliciting hepatic toxicity in a mouse model.

CHAPTER 3

Kopec AK, Boverhof DR, Burgoon LD, Ibrahim-Aibo D, Harkema JR, Tashiro C, Chittim B, Zacharewski TR: **Comparative Toxicogenomic Examination of the Hepatic Effects of PCB126 and TCDD in Immature, Ovariectomized C57BL/6 Mice.** *Toxicol Sci* 2008, **102:**61-75.

CHAPTER 3

COMPARATIVE TOXICOGENOMIC EXAMINATION OF THE HEPATIC EFFECTS OF PCB126 AND TCDD IN IMMATURE, OVARIECTOMIZED C57BL/6 MICE

ABSTRACT

Polychlorinated biphenyls are persistent environmental pollutants that elicit a wide range of effects in humans and wildlife, mediated by the aryl hydrocarbon receptor. 3,3',4,4',5-pentachlorobiphenyl (PCB126) is the most potent congener with relative effect potencies (REPs) ranging from 0.0026 to 0.857, and a toxic equivalency factor (TEF) of 0.1 set by an expert panel of the World Health Organization. In this study, the hepatic effects elicited by 300 μg/kg PCB126 were compared with 30 μg/kg 2,3,7,8-tetrachlorodibenzo-*p*-dioxin (TCDD) in immature, ovariectomized female C57BL/6 mice. Comprehensive hepatic gene expression analyses with complementary histopathology, high-resolution gas chromatograph/high resolution mass spectrometer tissue analysis, and clinical chemistry were examined. For temporal analysis, mice were orally gavaged with PCB126 or sesame oil vehicle and sacrificed after 2, 4, 8, 12, 18, 24, 72, 120, or 168 h. In the dose-response study, mice were gavaged with 0.3, 1, 3, 10, 30, 100, 300, 1000 μg/kg PCB126, 30 or 100 μg/kg TCDD and sacrificed after 72 h. 251 and 367 genes were differentially expressed by PCB126 at one or more time points or doses, respectively, significantly less than elicited by TCDD. In addition, there was less vacuolization and necrosis, and no immune cell infiltration, despite comparable or higher TEF-adjusted hepatic PCB126

levels. The functional annotation of differentially expressed genes was consistent with the observed histopathology. Collectively, the data indicate that 300 μg/kg PCB126 elicited a subset of weaker effects compared with 30 μg/kg TCDD in immature, ovariectomized C57BL/6 mice.

INTRODUCTION

Polychlorinated biphenyls (PCBs) are ubiquitous environmental contaminants that are found as mixtures of individual congeners. There are 209 possible PCB congeners with different degrees of chlorination [1]. Many commercial PCB mixtures are known by their industrial name Aroclor, followed by a number designating the number of carbon atoms and the percent chlorine by weight. PCBs were produced between 1930 and 1977 for use as coolants, lubricants, and dielectric insulating fluids for capacitors and transformers, due to their chemical inertness and stability [1]. Even though production has ceased, they are still released into the environment through the improper use and disposal of PCB containing products [2]. Once released, PCB mixtures are continuously altered through volatilization, partitioning and biochemical transformations [3, 4]. 3,3',4,4',5-pentachlorobiphenyl (PCB126) is the most potent PCB congener and accounts for 40-60% of the total toxic potency of all dioxin-like PCBs [2].

Dioxin and related compounds elicit a broad spectrum of species- and tissue-specific biochemical and toxic effects including wasting syndrome, dermal toxicity, tumor promotion, teratogenicity, immunotoxicity, and hepatotoxicity [5]. Many, if not all, of these toxic responses are mediated through the activation of the aryl hydrocarbon receptor (AhR), a basic-helix-loop-helix-PAS (bHLH-PAS) protein [6]. Dioxin and related compounds bind to the cytoplasmic AhR, which then translocates to the nucleus to form a heterodimer with the AhR nuclear translocator (ARNT), another member of the bHLH-PAS family [7]. The activated AhR/ARNT complex interacts with dioxin response elements (DREs) located in the regulatory region of

target genes, leading to changes in gene expression [8]. The involvement of AhR/ARNT signaling pathway in mediating these responses is supported by several complementary lines of evidence including studies with low affinity AhR allele mice [9], structure activity studies [10], and AhR-null mice [11].

The toxic equivalency factor (TEF)/toxic equivalents (TEQ) approach is used to assess the potential risks associated with exposure to mixtures of polychlorinated dibenzo-*p*-dioxins (PCDDS), polychlorinated dibenzofurans (PCDFs), and PCBs. It assumes that PCDDS, PCDFs and PCBs structurally similar to 2,3,7,8-tetrachlorobidenzo-*p*-dioxin (TCDD) elicit their toxicity through the AhR. The relative effect potency (REP) for a specific endpoint is determined for individual congeners relative to TCDD, the most potent of the dioxin-like chemicals [12]. REPs were used by an expert panel convened by the World Health Organization (WHO) to establish a TEF point estimate with the understanding that it may vary by a half-log unit. The potential toxicity of a mixture could then be represented by the sum of the concentrations of individual congeners multiplied by their corresponding TEFs to obtain an estimated toxicity relative to TCDD. This approach assumes that at submaximal doses, the contributions of individual components are essentially additive [10] and that TEFs are independent of dose, time point, and tissue [13, 14].

To facilitate the creation of TEFs, the expert panel used the REP2004 Database, a comprehensive listing of REP values for all known dioxins and dioxin-like compounds [15, 16]. *In vitro* data were only considered when there were insufficient *in vivo* data. For PCB126 there were 318 separate *in vivo* REPs, from 33 different peer-reviewed publications, a thesis, or government technical report for PCB126. The 2005 WHO expert panel excluded 64 mouse studies due to discrepancies between mouse and rat enzyme activity assay data. Although the

official list of studies considered is not available, the Committee stated that they used the REP2004 Database criteria for inclusion and exclusion. The rat studies that were considered included a range of endpoints from short-term enzyme induction to hepatocellular adenomas following chronic exposures (1-2 years). Although the tight range of REPs for PCB126 in rat studies supports a TEF of 0.1, information from mouse and some human studies, especially for enzyme induction, suggests it may have been too high [16]. The 2005 WHO expert panel concluded that there was insufficient information to change the PCB126 TEF of 0.1, but called for further studies.

In this study, comprehensive time course and dose-response gene expression analyses were conducted with complementary histopathology, clinical chemistry, and high-resolution gas chromatograph/high resolution mass spectrometer (HRGC-HRMS) tissue level analyses to compare the hepatic effects of 300 μg/kg PCB126 (TEF=0.1) to 30 μg/kg TCCD (TEF=1) in the immature, ovariectomized female C57BL/6 mice. Comparisons were also made to a previously published TCDD study that used the same animal species, experimental design, cDNA microarray platform, and analysis methods [17]. Collectively, and consistently, 300 μg/kg PCB126 elicited weaker responses and only a subset of effects induced by 30 μg/kg TCDD. However, more comprehensive time optimized dose-response studies are required for each endpoint of interest in order to provide REP data that could be used, in the context of all other available data, when considering the TEF for PCB126.

MATERIALS & METHODS

ANIMAL HANDLING

Female C57BL/6 mice, ovariectomized by the supplier on postnatal day (PND) 20, with body weights (BW) within 19% of the average, were obtained from Charles Rivers Laboratories

(Wilmington, MA) on PND 25. Animals were housed in polycarbonate cages containing cellulose fiber chips (Aspen Chip Laboratory Bedding, Northeastern Products, Warrensberg, NY) with 30-40% humidity and a 12-h light/dark cycle (07:00 A.M. – 7:00 P.M.). Mice had free access to deionized water and Harlan Teklad 22/5 Rodent Diet 8640 (Madison, WI). Animals were acclimatized prior to being dosed on PND 28. The immature ovariectomized mouse was used to facilitate comparisons with other data sets obtained in the same model [17]. The comparisons of the hepatotoxic potency of PCB126 were made to either 'internal' TCDD-treated group of mice or to an independent, previously published comprehensive TCDD time course study by Boverhof *et al*. that used the same animal model [17]. All procedures were carried out with the approval of the Michigan State University All-University Committee on Animal Use and Care.

TIME COURSE AND DOSE-RESPONSE STUDIES

A stock solution of PCB126 (99.7% purity, AccuStandard, New Haven, CT) was prepared by first dissolving it in acetone (J.T. Baker), then diluting it with sesame oil (Sigma, St. Louis, MO), and evaporating the acetone under a mild stream of nitrogen gas. The PCB126 stock solution was further diluted in sesame oil to achieve the desired dose. For the time course study, mice (n=5 per group) were orally gavaged with either 300 μg/kg PCB126, 30 μg/kg TCDD (gift from the Dow Chemical Company, Midland, MI), or sesame oil vehicle. PCB126 and vehicle-treated animals were sacrificed at 2, 4, 8, 12, 18, 24, 72, 120, or 168 h post exposure, whereas TCDD animals were sacrificed at 72 h. 30 μg/kg TCDD was initially selected to study because it elicited maximum induction of Cyp1a1 and 1a2 mRNA levels while not inducing significant changes in BW gain [17]. It was used again in the present study to facilitate comparisons between studies that employed the same model species, experimental design, cDNA platform,

and analysis methods. A concentration of 300 μg/kg PCB126 was used to examine the hypothesis that it would elicit hepatic effects comparable to 30 μg/kg TCDD, based on the PCB126 TEF of 0.1. The vehicle groups were not the same between the current PCB126 study and Boverhof *et al.* study, but the same vehicle controls were used for the internal TCDD-treated mice in the current PCB126 study.

For the dose-response study, mice were gavaged with a single dose of 0.3, 1, 3, 10, 30, 100, 300, or 1000 μg/kg of PCB126, 30 or 100 μg/kg TCDD, or vehicle and sacrificed 72 h following treatment. All mice were sacrificed by cervical dislocation and tissue samples were removed, weighed, flash frozen in liquid nitrogen, and stored at –80°C. For both the time course and dose-response studies, the right lobe of the liver was fixed in 10% neutral buffered formalin (Sigma) for histological analysis.

CLINICAL CHEMISTRY AND HISTOLOGICAL ANALYSIS

Blood samples were collected by submandibular vein puncture and blood was allowed to clot in the Microtainer Serum Separator Tubes (VWR International, Batavia, IL). Serum was separated by spinning at 10,000 × g for 5 min, after which the samples were stored at –80°C. Serum triglycerides (TG), non-esterified fatty acids (NEFA), cholesterol (CHOL), alanine aminotransferase (ALT), and glucose (GLU) were measured using an Olympus AU640 Automated Chemistry Analyzer (Olympus America Inc., Melville, NY) by the Michigan State University Clinical Pathology Laboratory (http://cvm.msu.edu/clinpath/new.htm).

Fixed liver tissues were sectioned and processed in ethanol, xylene, and paraffin using a Thermo Electron Excelsior tissue processor (Waltham, MA). Tissues were then embedded in paraffin with Miles Tissue Tek II embedding center, after which paraffin blocks were sectioned at 5 μm with a rotary microtome. Sections were placed on glass microscope slides, dried, and

stained with the standard hematoxylin and eosin stain. All histological processing was performed at the Michigan State University Histology Laboratory (http://humanpathology.msu.edu/histology/index.html).

THIN LAYER CHROMATOGRAPHY

Liver samples were first homogenized (Polytron PT2100, Kinematica AG, Luzern, CH) in 1% methanol and acidified with concentrated HCl. Lipids were extracted with chloroform: methanol (2:1) containing 1 mM 2,6-di-tert-butyl-4-methylphenol (BHT; Sigma). The protein and aqueous phases were re-extracted with chloroform and the organic phases were pooled, dried under nitrogen gas, and resuspended in chloroform with 1 mM BHT, and stored at –80°C in glass vials with PTFE caps (VWR International). Lipid extracts were then fractionated by thin layer chromatography on silica gel adsorption plates (TLC; LK6D Silica G 60A; Whatman Inc., Florham Park, NJ) with hexane:diethyl ether:acetic acid (90:30:1) and developed with iodine (Sigma). Lipid migrations were compared to triacylglycerol, diacylglycerol and cholesterol ester standards (Nu-Chek Prep, Elysian, MN).

QUANTIFICATION OF HEPATIC PCB126 AND TCDD LEVELS

Liver samples were processed in parallel with laboratory blanks and a reference or background sample at Wellington Laboratories Inc. (Guelph, ON, Canada). Samples were weighed, spiked with $^{13}C_{12}$-2,3,7,8-TCDD or $^{13}C_{12}$ -PCB126 surrogate, digested with sulfuric acid, and extracted. Extracts were cleaned, concentrated, and spiked with $^{13}C_{12}$-1,2,3,4-TCDD or $^{13}C_{12}$-PCB111 as injection standards. Analysis was performed on a high-resolution gas chromatograph/high resolution mass spectrometer (HRGC-HRMS) using a Hewlett Packard 5890 Series II GC interfaced to a VG 70SE HRMS. The HRMS was operated in the electron

ionization/selective ion recording mode (EI/SIR) at 10,000 resolution. A 60-m DB5 column (J&W Scientific, Folsom, CA) with an internal diameter of 0.25 mm and film thickness of 0.25 μm was employed. Injection volumes were 2 μl and a splitless injection was used.

RNA ISOLATION

Frozen liver samples (on average ~100 mg) were retrieved from –80°C storage and immediately transferred to 1 ml of TRIzol (Invitrogen, Carlsbad, CA) and homogenized using a Mixer Mill 300 tissue homogenizer (Retsch, Germany). Total RNA was isolated according to the manufacturer's protocol with an additional acid phenol:chloroform extraction. Isolated RNA was resuspended in RNA storage solution (Ambion Inc., Austin, TX), quantified (A_{260}), and quality was assessed by determining the A_{260}/A_{280} ratio and by visual inspection of 2 μg on a denaturing gel.

cDNA MICROARRAY EXPERIMENTAL DESIGN AND PROTOCOLS

In the time course study, PCB126-treated samples were co-hybridized with time-matched vehicles controls using an independent reference design [18]. Dose-dependent changes in gene expression were analyzed using a common reference design, where PCB126 samples were compared to a common vehicle control. cDNA microarrays were also performed for the 'internal' TCDD-treated group of mice, which used the same vehicle controls as in the PCB126 microarray design. In the Boverhof *et al*. study, independent groups of the TCDD-treated and vehicle control mice were used. All experiments were performed with three biological replicates with two independent labelings of each sample (dye swap) for each time point or dose group, using custom mouse cDNA microarrays containing 13,361 features representing 8,516 unique genes (UniGene build 152).

Detailed protocols for microarray preparation, labeling of the cDNA probe, sample hybridization, and washing can be found at http://dbzach.fst.msu.edu/interfaces/microarray.html. Microarrays were printed at the Michigan State University Research Technology Support Facility (http://www.genomics.msu.edu/). Briefly, PCR amplified mouse cDNAs were robotically arrayed onto epoxy-coated glass slides (Schott-Nexterion, Duryea, PA) using an Omnigrid arrayer (GeneMachines, San Carlos, CA) equipped with 48 (4×12) Chipmaker 2 pins (TeleChem, Sunnyvale, CA). Total RNA (30 μg) was reverse transcribed in the presence of Cy3- or Cy5-dUTP (Amersham, Piscataway, NJ) to create fluor-labeled cDNA which was purified using a Qiagen PCR purification kit (Qiagen, Valencia, CA). Cy3 and Cy5 samples were mixed, vacuum dried, and resuspended in 48 μl of hybridization buffer (40% formamide, 4× sodium chloride sodium citrate, 1% sodium dodecyl sulfate) with 20 μg polydA and 20 μg of mouse COT-1 DNA (Invitrogen) as competitor. This probe mixture was heated at 95°C for 3 min and hybridized on the array under a 22 × 60 mm lifterslip (Erie Scientific Company, Portsmouth, NH) for 18-24 h in a 42°C water bath. Slides were then washed, dried by centrifugation, and scanned at 635 nm (Cy5) and 532 nm (Cy3) on a GenePix 4100A scanner (Molecular Devices, Union City, CA). Images were analyzed for feature and background intensities using GenePix Pro 6.0 (Molecular Devices).

cDNA Microarray Data Normalization and Analysis and Feature-to-Gene Filtering Criteria

All microarray data used within this study passed the laboratory quality assurance protocol [19]. Microarray data were normalized using a semiparametric approach [20], and the posterior probabilities were calculated using an empirical Bayes analysis on a per gene and time point or dose basis [21]. Gene expression data were ranked and prioritized using a P1(t) cut-off

≥0.9999 and |fold change|≥1.5 to identify treatment active genes and to obtain an initial subset of differentially regulated genes for further investigation and data interpretation. Relaxed filtering criteria (from P1(t)≥0.9999 and |fold change|≥1.5 to P1(t)≥0.99 and |fold change|≥1.2) were also used to examine overlapping, differentially regulated genes to minimize classifying genes as PCB126 or TCDD specific as a result of using hard cut-offs. Active genes were analyzed by agglomerative hierarchical clustering using a standard correlation distance metric implemented in GeneSpring 6.0 (Agilent Technologies; Santa Clara, CA).

Multiple features spotted on our cDNA microarray may represent the same gene (e.g. Cyp1a1). To obtain the number of unique genes, the features were first screened by their corresponding Entrez Gene IDs. If several features had the same Entrez Gene ID, they were all considered to be representative of the same gene and counted as one gene. Due to this redundancy, and because of the changes to the mouse genome annotation, the 13,361 features spotted on our cDNA microarray correspond to 8,516 unique genes based on the annotation provided by UniGene build 152.

QUANTITATIVE REAL-TIME PCR

Quantitative real-time PCR (QRTPCR) verification of microarray responses was performed as described [17]. Briefly, 1 μg of total RNA was reverse transcribed by SuperScript II (Invitrogen) using an anchored oligo-dT primer as described by the manufacturer. The cDNA (1.0 μl) was used as a template in a 30 μl PCR reaction containing 0.1 μM of forward and reverse gene-specific primers, 3 mM $MgCl_2$, 1 mM dNTPs, 0.025 IU AmpliTaq Gold, and 1× SYBR Green PCR buffer (Applied Biosystems, Foster City, CA). PCR amplification was conducted on an Applied Biosystems PRISM 7500 Sequence Detection System. cDNAs were quantified using a standard curve approach and the copy number of each sample was standardized to 3

housekeeping genes (ActB, Gapdh, Hprt) to control for the differences in RNA loading, quality, and cDNA synthesis [22]. For graphing purposes, the relative expression levels were scaled such that the expression level of the time-matched control group was equal to one.

DOSE-RESPONSE MODELING

A Java application was developed to identify the best-fit dose-response model, by minimizing the Euclidean distance, for differential gene expression responses in the dose-response study. The algorithm uses particle swarm optimization [23] to identify the best-fit model (i.e., the model with the parameter set that best fits the experimental data) within each of five classes (sigmoidal, exponential, linear, Gaussian, parametric), termed the best in-class model. The algorithm then chooses the best-fit of the five best in-class models. The best-fit model is used to calculate model-specific end points, such as the ED_{50}, ED_{99}, ED_{01}, probabilistic point of departure, and the benchmark dose.

FUNCTIONAL GENE ANNOTATION AND STATISTICAL ANALYSIS

Annotation and functional categorization of differentially regulated genes was performed using a Database for Annotation, Visualization and Integrated Discovery (DAVID) [24]. All statistical analyses were performed with SAS 8.02 (SAS Institute, Cary, NC). Data were analyzed by analysis of variance followed by Tukey's and Dunnett's *post hoc* tests. Differences between treatment groups were considered significant when $p<0.05$.

RESULTS

ORGAN AND BODY WEIGHTS

Increases in liver weight and decreases in BW gain are hallmark, dose-dependent toxic responses following treatment with TCDD and related compounds including PCB126 [5].

Significant ($p<0.05$) increases in relative liver weights (RLW) were seen with 30 μg/kg TCDD at 72 h and 300 μg/kg PCB126 at 168 h in the time course study (Table 2). In the dose-response study, PCB126 elicited modest increases in RLW that were not significant due to the greater response variance (Table 3). However, TCDD at doses of 30 and 100 μg/kg significantly ($p<0.05$) increased RLW at 72 h (Table 3). No other significant treatment-related changes in BW or BW gain were observed at any time point or dose, consistent with a comparable published TCDD study [17], indicating that neither a single dose of 30 μg/kg TCDD nor 300 μg/kg PCB126 elicits a 'wasting syndrome' response within 168 h.

HEPATIC PCB126 AND TCDD TISSUE LEVELS

Absolute hepatic PCB126 and TCDD levels per wet weight of three individual liver samples were determined at each time point and dose level. In order to facilitate comparisons between the two compounds, PCB126 TEQs were calculated by multiplying the tissue concentration by the TEF value of 0.1 [16]. In the time course study, PCB126 levels continued to increase throughout the study, achieving the highest concentrations at 120 and 168 h (Figure 4A). In contrast, TCDD levels significantly decreased after 72 h [17] and approached vehicle control levels by 24 weeks (Boverhof *et al.*, manuscript in preparation). Moreover, PCB126 TEQs increased ($p<0.05$) in a dose-dependent manner (Figure 4B) at 72 h with 30 and 100 μg/kg TCDD achieving similar levels.

Hepatic concentrations of PCB126 in this study are comparable with reports in rats using similar exposure regimens. For example, a single bolus dose of 275 μg/kg to male rats resulted in 3,300,000 pg/g of PCB126 in the liver after 7 days [25], similar to the 3,000,000 pg/g in this study at 168 h. The National Toxicology Program study on PCB126 in female rats reported that

Table 2. Temporal effects of 300 µg/kg PCB126 or 30 µg/kg TCDD on terminal body, whole liver, and RLW.

Sacrifice time (h)	Treatment	BW (g)	Liver weight (g)	RLW
2	Vehicle	12.62 ± 0.44	0.702 ± 0.037	0.056 ± 0.004
	PCB126	12.00 ± 0.80	0.563 ± 0.323	0.058 ± 0.004
4	Vehicle	12.26 ± 0.65	0.689 ± 0.080	0.056 ± 0.004
	PCB126	12.12 ± 0.99	0.651 ± 0.077	0.054 ± 0.003
8	Vehicle	12.08 ± 1.65	0.613 ± 0.084	0.051 ± 0.001
	PCB126	12.08 ± 0.89	0.617 ± 0.074	0.051 ± 0.003
12	Vehicle	12.92 ± 0.89	0.694 ± 0.058	0.054 ± 0.002
	PCB126	12.82 ± 0.82	0.687 ± 0.073	0.053 ± 0.003
18	Vehicle	13.38 ± 1.03	0.750 ± 0.106	0.056 ± 0.005
	PCB126	12.82 ± 1.31	0.779 ± 0.063	0.061 ± 0.003
24	Vehicle	12.68 ± 1.16	0.709 ± 0.090	0.056 ± 0.004
	PCB126	12.86 ± 1.21	0.814 ± 0.094	0.063 ± 0.002
72	Vehicle	14.32 ± 2.37	0.822 ± 0.131	0.057 ± 0.002
	PCB126	13.88 ± 0.92	0.889 ± 0.127	0.064 ± 0.007
	TCDD	16.54 ± 1.59	1.008 ± 0.163	0.069 ± 0.004*
120	Vehicle	15.86 ± 0.72	0.885 ± 0.066	0.056 ± 0.002
	PCB126	15.46 ± 1.42	0.973 ± 0.134	0.063 ± 0.004
168	Vehicle	17.46 ± 0.69	0.997 ± 0.043	0.057 ± 0.001
	PCB126	16.54 ± 1.59	1.087 ± 0.088	0.066 ± 0.003*

Note. Values represent averages ± SD (n=5).
Asterisk (*) indicates $p<0.05$ (PCB126 vs. vehicle and TCDD vs. vehicle).

Table 3. Dose-dependent effects of PCB126 on terminal body, whole liver, and RLW at 72 h.

Dose (µg/kg)	Treatment	BW (g)	Liver weight (g)	RLW
0	Vehicle	15.37 ± 0.87	0.843 ± 0.095	0.055 ± 0.005
0.3	PCB126	15.42 ± 1.39	0.885 ± 0.113	0.057 ± 0.003
1	PCB126	15.62 ± 0.79	0.890 ± 0.058	0.057 ± 0.003
3	PCB126	16.22 ± 1.41	0.975 ± 0.153	0.060 ± 0.006
10	PCB126	15.99 ± 0.82	0.912 ± 0.077	0.057 ± 0.002
30	PCB126	15.17 ± 1.31	0.817 ± 0.117	0.054 ± 0.005
100	PCB126	15.78 ± 0.26	0.967 ± 0.086	0.061 ± 0.005
300	PCB126	15.34 ± 0.56	0.912 ± 0.125	0.059 ± 0.008
1000	PCB126	14.66 ± 0.72	0.906 ± 0.188	0.061 ± 0.011
30	TCDD	14.78 ± 1.08	0.944 ± 0.050	0.064 ± 0.004*
100	TCDD	15.20 ± 2.31	1.058 ± 0.205	0.069 ± 0.005*

Note. Values represent averages ± SD (n=5). Asterisk (*) indicates $p<0.05$ (PCB126 vs. vehicle and TCDD vs. vehicle).

Figure 4. Hepatic PCB126 and TCDD levels.
Hepatic tissue levels from the (A) time course and (B) dose-response studies measured using HRGC-HRMS. The results are displayed as the mean ± standard error of at least three independent samples. Tissue levels (per liver wet weight) were multiplied by the corresponding TEF value for each compound to facilitate comparisons. Animals were dosed with 300 μg/kg PCB126 and 30 μg/kg TCDD in the time course study. Doses used in the dose-response study are represented in the graph. Dose-response data are displayed on a log scale to visualize tissue concentrations at all doses. An asterisk (*) indicates a significant ($p<0.05$) difference between the treated samples and vehicle controls. (C) Comparison of PCB126 tissue levels to published TCDD levels [17]. An asterisk (*) indicates significant ($p<0.05$) difference between PCB126 and TCDD TEQ hepatic levels at 168 h. Results are displayed as the mean ± standard error of three independent replicates.

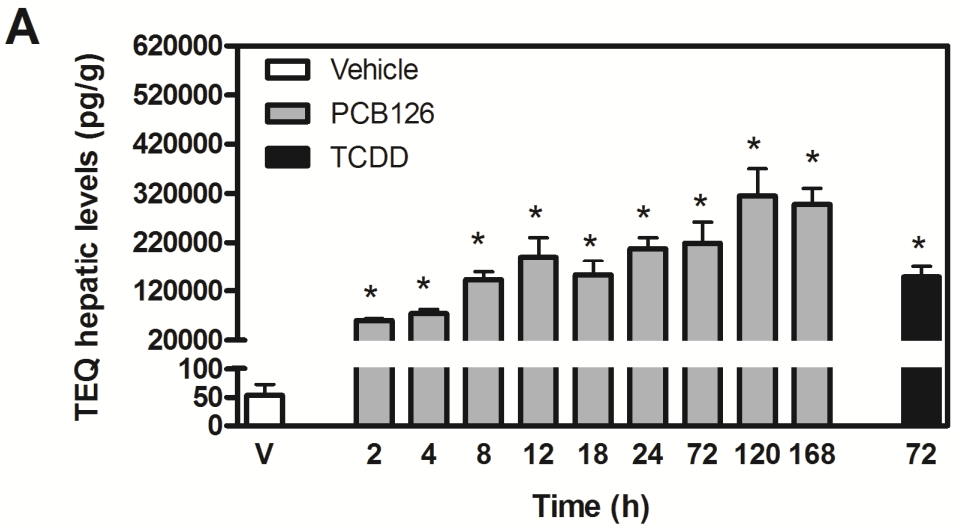
A
TEQ hepatic levels (pg/g)
620000
520000
420000
320000
220000
120000
20000
100
50
0
Vehicle
PCB126
TCDD
V
2
4
8
12
18
24
72
120
168
72
Time (h)

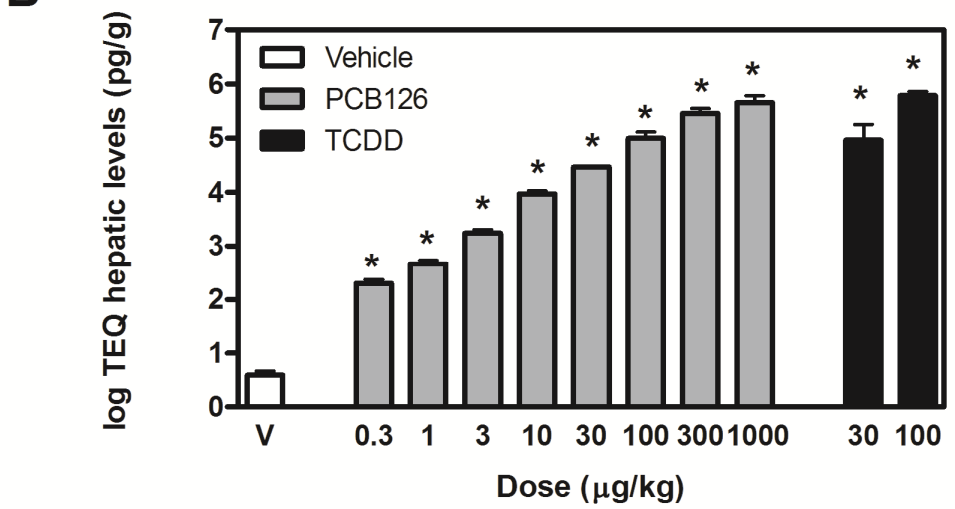
B
log TEQ hepatic levels (pg/g)
7
6
5
4
3
2
1
0
Vehicle
PCB126
TCDD
V
0.3
1
3
10
30
100
300
1000
30
100
Dose (µg/kg)

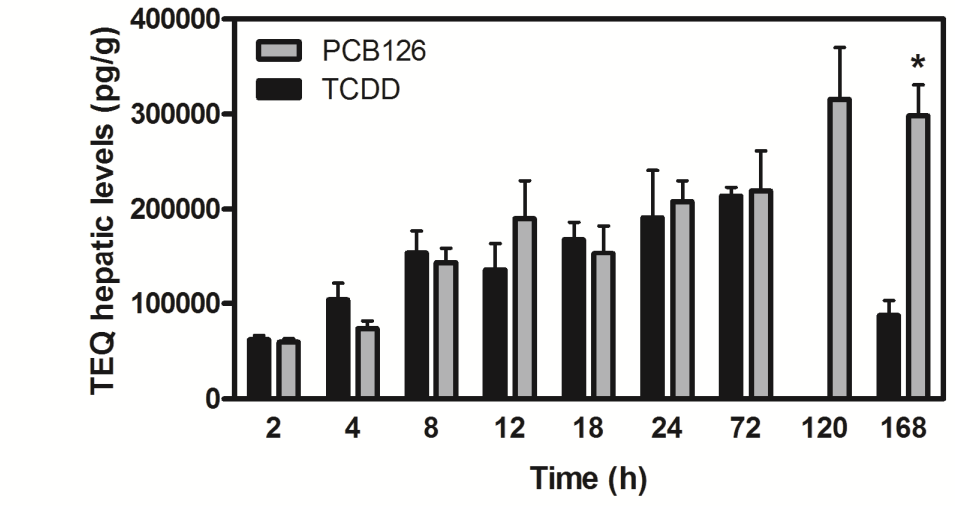
C
TEQ hepatic levels (pg/g)
400000
300000
200000
100000
0
PCB126
TCDD
2
4
8
12
18
24
72
120
168
Time (h)

the highest concentrations of PCB126 were discovered in the liver, followed by fat, with the lowest concentrations in blood [2].

Comparison of hepatic PCB126 to published TCDD levels indicates that the TEQ levels are comparable at every time point except for 168 h, where a significant decrease in TCDD hepatic concentration was observed [17] (Figure 4C). This single-dose finding is similar to a chronic exposure study (5 days/week over 13 weeks), where PCB126 was found to be sequestered within the liver to a greater extent than TCDD, which was in part mediated by binding to inducible Cyp1a2 [26].

PATHOLOGY

Hepatocellular vacuolization was observed in vehicle, PCB126- and TCDD-treated livers, mainly in the periportal and midzonal regions and frequently extended into the centrilobular region in more severely affected animals. Affected hepatocytes were characterized by perinuclear and/or midcellular cytoplasmic loss and replacement by poorly delineated clear vacuoles (Figure 5A-F). At 72 h, TCDD-treated animals also exhibited mixed cell infiltration (neutrophils and mononuclear cells) (Figure 5F). In the PCB126 time course, vacuolization was present in both treated and control animals. However, TCDD-elicited increases in vacuole formation were significantly greater than the changes in vehicles and PCB126-treated livers at all time points and doses. PCB126 elicited a pronounced dose-dependent increase in vacuolization, (Figure 5B and 5C), however, microscopic changes (vacuolization and mixed cell infiltration) elicited by TCDD were in any case more severe (Table 4, Figure 5D and 5E) [17]. Furthermore, PCB126 did not induce necrosis in the time course and dose-response study, whereas TCDD induced necrosis in the time course and dose-response studies (Table 5 and 6). Together, these

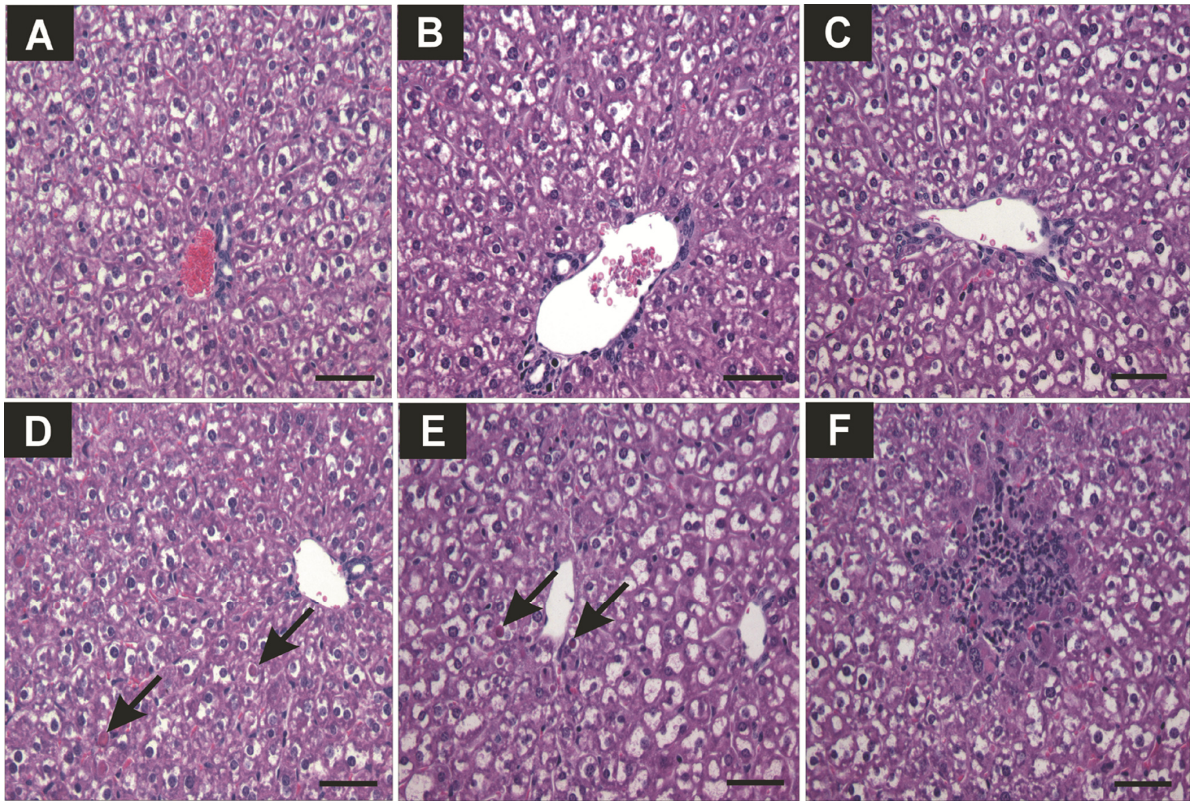

Figure 5. Representative histopathology results from vehicle, PCB126 and TCDD treated mice at 72 h.

Liver sections from (A) vehicle showed minimal vacuolization most likely due to free access to chow. (B) 300 μg/kg PCB126 elicited slight/moderate hepatocellular vacuolization, which exhibited (C) dose-dependent increase at 1000 μg/kg PCB126. (D) 30 μg/kg TCDD elicited marked vacuolization and minimal/slight necrosis, with (E) more pronounced vacuolization and (F) mixed cell infiltration at 100 μg/kg TCDD. Arrows indicate necrotic hepatocytes. Bars = 50μm.

Table 4. Comparison of temporal incidence and severity of liver microscopic changes in PCB126 and TCDD experiments [17].

	Time (h) and treatment																	
	18				24				72				120		168			
	V	P	V	T	V	P	V	T	V	P	V	T	V	P	V	P	V	T
Hepatocellular vacuolization:																		
Average severity	1.6	1.0	1.3	3.0	1.4	2.4	2.3	4.0	2.0	1.8	1.3	3.3	1.4	1.4	1.6	1.4	1.3	3.0
Hepatocellular necrosis:																		
Average severity	0	0	0	0	0	0	0	0	0	0	0	0.8	0	0	0	0	0	1.5
Mixed cell infiltration:																		
Average severity	0	0	0	0	0	0	0	0	0	0	0	1	0	0	0	1	0	1.3

Note. The average severity scores are reported as a weighted average of minimal (grade of 1), slight (grade of 2), moderate (grade of 3), and/or marked (grade of 4) responses divided by the total number of examined animals. V, vehicle; P, PCB126; T, TCDD.

Table 5. Temporal incidence and severity of liver microscopic changes in the vehicle-, PCB126- and TCDD-treated mice.

	Time (h) and treatment																		
	2		**4**		**8**		**12**		**18**		**24**		**72**		**120**		**168**		**72**
	V	P	V	P	V	P	V	P	V	P	V	P	V	P	V	P	V	P	T
Hepatocellular vacuolization: Average severity	0.4	0	0.4	0.6	0	0.2	0.4	0.2	1.6	1	1.4	2.4	2	1.8	1.4	1.4	1.6	1.4	2.4
Hepatocellular necrosis: Average severity	0	0	0	0	0	0	0	0	0	0	0	0	0	0	0	0	0	0	0.8
Mixed cell infiltration: Average severity	0	0	0	0	0	0	0	0	0	0	0	0	0	0	0	0	0	1	0.2

Note. The average severity scores are reported as a weighted average of minimal (grade of 1), slight (grade of 2), moderate (grade of 3), and/or marked (grade of 4) responses divided by the total number of examined animals. V, vehicle; P, PCB126; T, TCDD.

Table 6. Dose-dependent incidence and severity of liver microscopic changes in the vehicle-, PCB126- and TCDD-treated mice at 72 h.

	Treatment and dose (µg/kg)										
	Vehicle		PCB126							TCDD	
	0	0.3	1	3	10	30	100	300	1000	30	100
Hepatocellular vacuolization: Average severity	0.6	1	0.8	1.2	1.2	1.4	1.8	1.8	2.2	2	3
Hepatocellular necrosis: Average severity	0	0	0	0	0	0	0	0	0	0.4	1
Mixed cell infiltration: Average severity	0	0	0	0	0	0	0	0	0	0	0.6

Note. The average severity scores are reported as a weighted average of minimal (grade of 1), slight (grade of 2), moderate (grade of 3), and/or marked (grade of 4) responses divided by the total number of examined animals.

data indicate that 300 μg/kg PCB126 is not equivalent to 30 μg/kg TCDD at inducing histopathological changes.

Analysis of liver lipid extracts by TLC revealed increases in TG in TCDD- and PCB126-treated animals at 72 and 168 h, respectively (Figure 6), consistent with the increases in RLW, suggesting that fatty accumulation may contribute to increases in liver weight. These findings are consistent with general hallmarks of liver toxicity due to dioxin and PCB exposure [27, 28].

Serum samples from vehicle and PCB126-treated animals were examined for changes in TG, NEFA, CHOL, GLU, and ALT levels at 12, 24, 72, 120, and 168 h. Unlike TCDD, which significantly increased serum TG, NEFA, and ALT, and decreased CHOL levels [17], PCB126 only increased ($p<0.05$) ALT levels at 168 h, indicative of slight liver injury.

TEMPORAL GENE EXPRESSION CHANGES

Hepatic gene expression was examined using custom mouse cDNA microarrays with 13,361 features representing 8,516 unique genes. In the PCB126 time course, 294 features corresponding to 251 unique genes were differentially regulated ($P1(t)\geq 0.9999$ and $|\text{fold change}|\geq 1.5$) at one or more time points relative to the time-matched vehicle controls (Figure 7A). Application of the same filtering criteria for the internal TCDD data set at 72 h identified 221 differentially regulated features, corresponding to 182 unique genes, representing approximately twice as many dysregulated genes than PCB126 (Figure 7A).

Fifty-eight genes regulated by 30 μg/kg TCDD and 300 μg/kg PCB126 at 72 h were identified. TCDD-specific differential expression correlated with the emergence of inflammatory cell aggregates associated with degenerative and necrotic hepatocytes. Examples include lymphocyte antigen 6 complex, locus A (Ly6a) and complement component 1, s subcomponent (C1s) which were down-regulated by TCDD, but unaffected following PCB126 treatment.

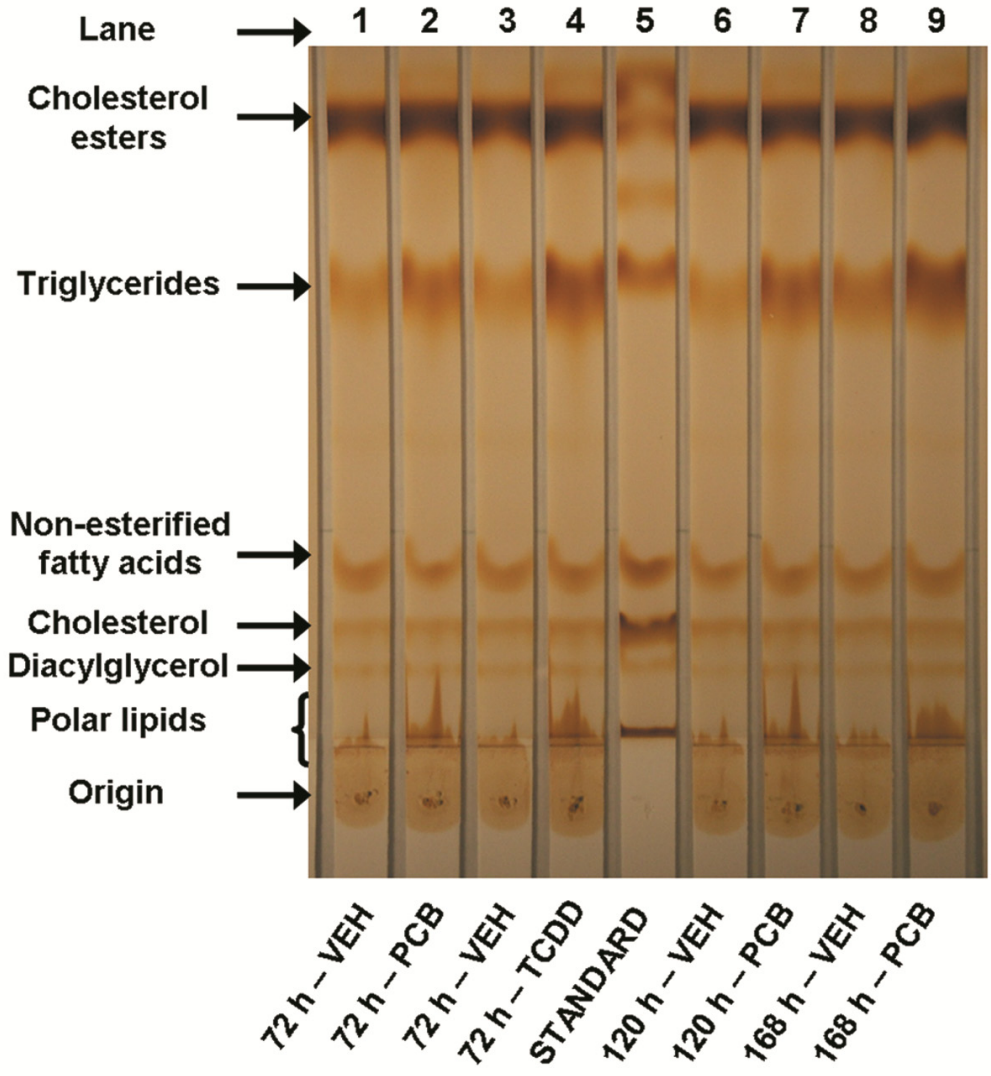

Figure 6. Thin layer chromatograph of hepatic lipid extracts from vehicle-, PCB126-, and TCDD- treated samples in the time course study.

Lipids from homogenized liver samples were extracted using chloroform:methanol. The extracts were spotted on TLC plates, fractionated with hexane:diethyl ether:acetic acid mixture (90:30:1) and developed with iodine. Lanes 1-4 represent vehicle, PCB126, vehicle and TCDD at 72 h, respectively. Lane 5 represents the standard, while lanes 6-9 correspond to vehicle and PCB126 at 120 h and vehicle and PCB126 at 168 h, respectively. Increasing amounts of TG could be observed in the treated samples when compared to the time-matched vehicle controls.

Responses specific to PCB126 typically included marginal differential expression that were selected due to the hard statistical cut-offs. When the selection criteria were relaxed (P1(t)≥0.99 and |fold change|≥1.2), the number of overlapping genes dramatically increased. Consequently, the majority of genes differentially expressed following PCB126 treatment simply missed the cut-offs or were regulated at time points other than 72 h. In contrast, TCDD elicited robust gene expression responses associated with inflammatory cell infiltration and necrosis, consistent with the histopathology assessment.

Clustering of microarray data provides a general view of the similarity of the temporal profiles between the two compounds. Agglomerative hierarchical clustering of temporal gene expression data by time point resulted in three main branches: early (2 and 4 h), mid (8-24 h), and late (72-168 h) time points (Figure 8A). The clustering of 72 h TCDD with larger clustered group of 8 + 12 h PCB126 and 18 + 24 h PCB126 indicates that the two chemicals are most similar at these time points relative to the other time points, despite the differences in intensity and gene expression patterns (Figure 8A).

DOSE-RESPONSE GENE EXPRESSION CHANGES

Analysis of the dose-response data at 72 h identified 436 microarray features representing 367 unique annotated genes, which were differentially expressed (P1(t)≥0.9999 and |fold change|≥1.5) relative to vehicle controls, at one or more doses (Figure 7B). Among the 244 genes regulated by two TCDD doses and 265 genes regulated by 1000 μg/kg PCB126, 137 genes were commonly regulated by both compounds. 249 of the 436 differentially expressed features, corresponding to 214 unique genes, exhibited a sigmoidal dose-response profile as determined by the particle swarm optimization [23] Java application. This tool first examines the dose-

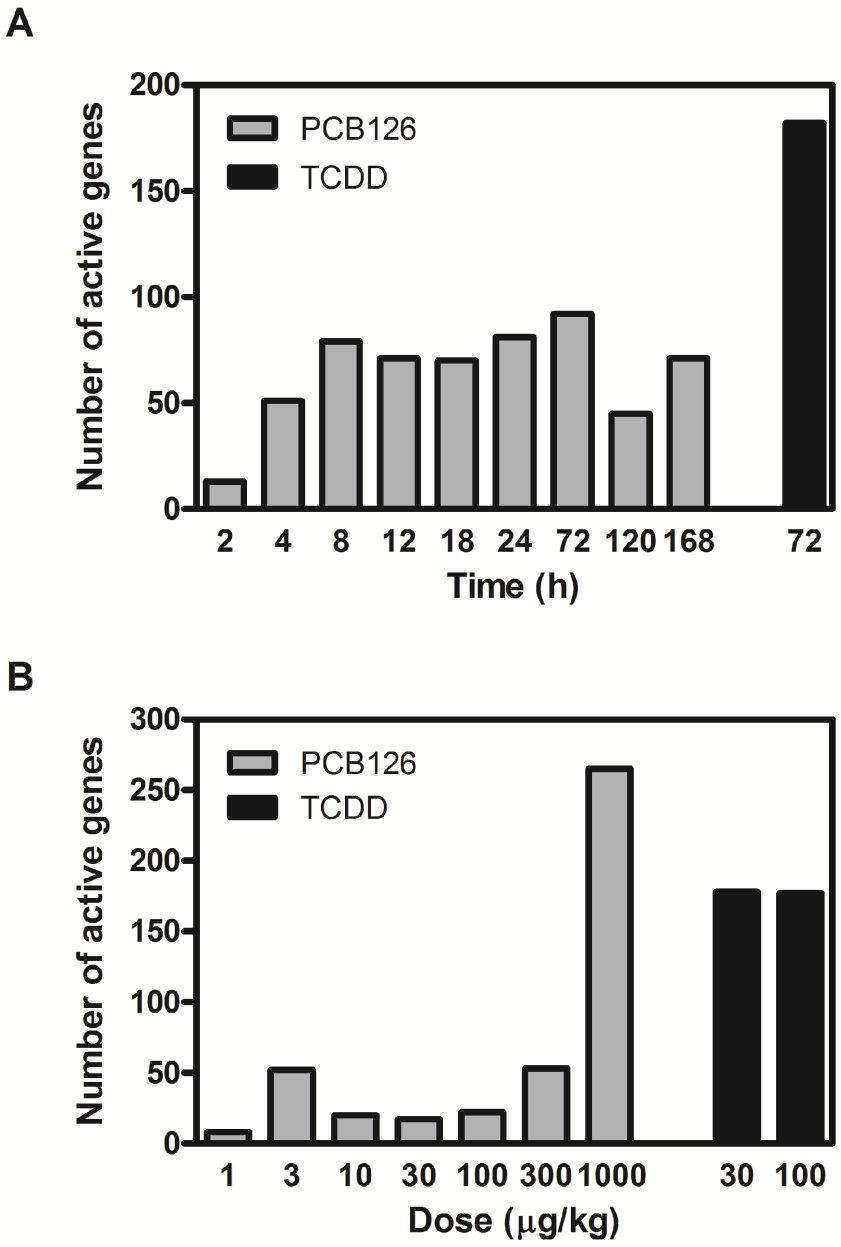

Figure 7. Number of PCB126 differentially expressed genes.
Number of PCB126 differentially expressed genes in (A) time course and (B) dose-response studies. The microarray data were filtered using a P1(t)≥0.9999 and |fold change|≥1.5 to identify differentially expressed genes. The number of gene expression changes induced by 300 μg/kg PCB126 increased over the course of the study, but did not exhibit the level of activity reported for 30 μg/kg TCDD when compared to internal TCDD treatments and in a comparable TCDD study [17]. Genes identified from the dose-response study were further analyzed to identify dose-dependent changes in gene expression using a Java application to identify the best-fit dose-response model.

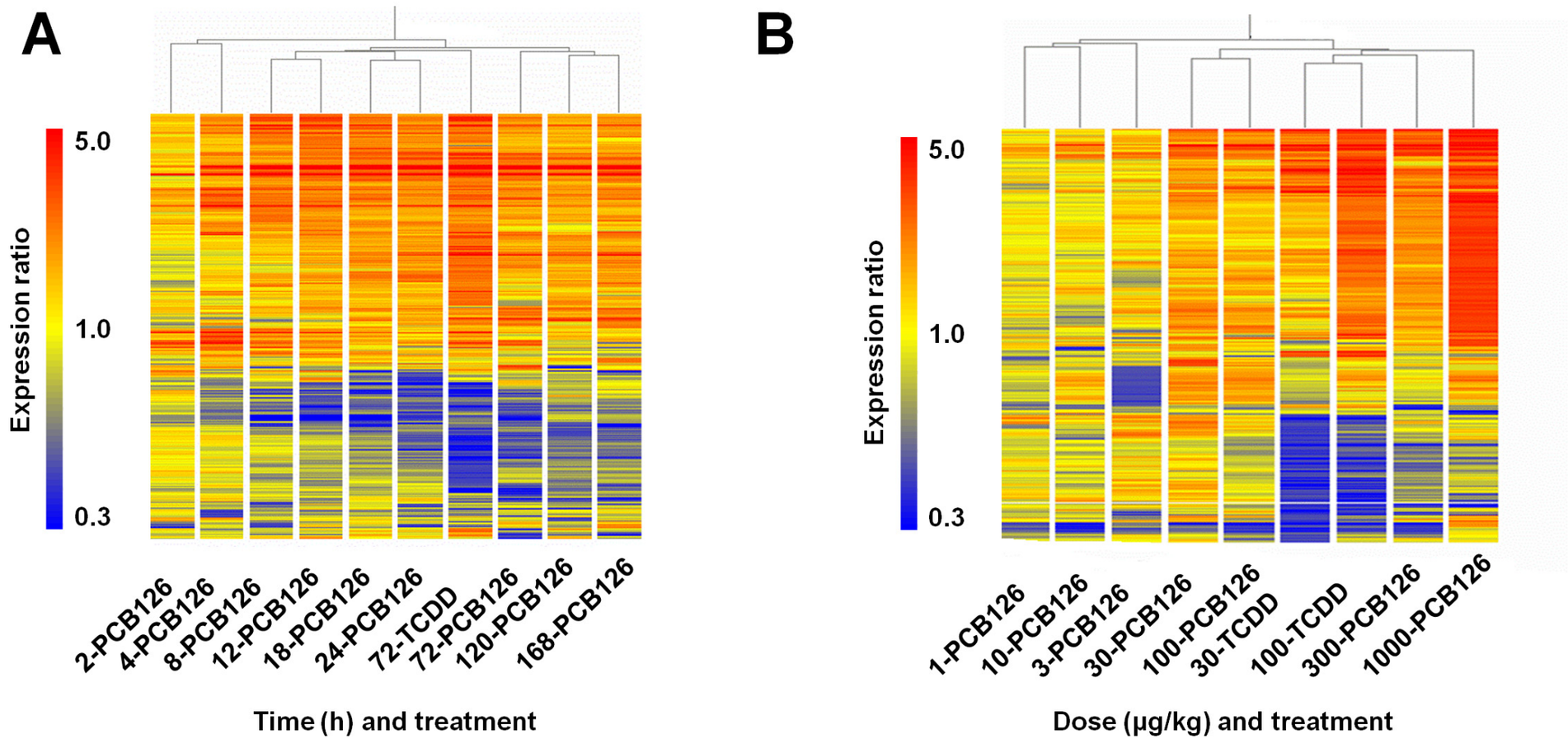

Figure 8. Agglomerative hierarchical clustering of PCB126 gene expression data.
Agglomerative hierarchical clustering of PCB126 gene expression data in the (A) time course and (B) dose-response studies. Temporal microarray data clustered into early (2-4 h), middle (8-24 h) and late (72-168 h) time point branches. 72 h TCDD gene expression data clustered with the 18 and 24 h PCB126 profiles. The PCB126 dose-response data followed a positive correlation between gene expression and the administered dose, forming low, medium and high dose clusters. 30 and 100 µg/kg TCDD gene expression data clustered with the 1000 µg/kg PCB126 gene expression profile.

response data for each gene using sigmoidal, exponential, linear, Gaussian, parametric classes to identify the best-fit dose-response model (i.e. the model with the parameter set that best fits the experimental data). The algorithm then chooses the model that best fits the data and calculates the ED_{50}.

ED_{50} values for differential gene expression ranged from 2.21 to 513 μg/kg dose of PCB126. Because the PCB126 and Boverhof *et al*. TCDD dose-response studies were done at different time points (72 h vs. 24 h, respectively), comprehensive comparisons between the ED_{50s} are not possible. In general, PCB126 exhibited higher ED_{50} values for Cyp1a1 (24.5 vs. 0.3 μg/kg), Nqo1 (301.4 vs. 8.8 μg/kg), and Pck1 (144.1 vs. 0.4 μg/kg) when compared with TCDD.

Hierarchical clustering of the dose-response gene expression data clustered according to lower (1, 3 and 10 μg/kg), intermediate (30 and 100 μg/kg) and high (300 and 1000 μg/kg) PCB126 doses with 30 and 100 μg/kg TCDD clustering with the high PCB126 group (Figure 8B).

FUNCTIONAL ANNOTATION OF DIFFERENTIALLY EXPRESSED GENES

Functional annotation of the 251 PCB126 elicited temporal gene expression changes was associated with metabolizing enzymes, lipid metabolism, gluconeogenesis/glucose metabolism, development and differentiation, necrosis, and immune signaling (Table 7). Metabolism functions included the catalytic action of monooxygenases, oxidoreductases and xenobiotic metabolizing enzymes such as the classical TCDD-inducible "AhR gene battery" members Cyp1a1, Tiparp and Nqo1. Others included P450 oxidoreductase (Por), epoxide hydrolase 1, microsomal (Ephx1), dehydrogenase/reductase (sdr family) member 3 (Dhrs3), glutaredoxin (Glrx) and xanthine dehydrogenase (Xdh). A majority of the glutathione S-transferase family (Gsta2, Gsta4, Gstm3, Gstt2) were also differentially regulated by PCB126. Genes associated

Table 7. Functional categorization and regulation of select hepatic genes identified as differentially regulated in response to PCB126 and TCDD [17].

Functional category	Entrez Gene ID	Gene name	Gene symbol	Fold change[a]	TCDD internal controls	TCDD time course [17]	DRE[b]
Metabolizing enzymes	11671	Aldehyde dehydrogenase family 3, subfamily A2	Aldh3a2	1.5	No	No	No
	13076	Cytochrome P450, family 1, subfamily a, polypeptide 1	Cyp1a1	92	Yes	Yes	Yes
	13119	Cytochrome P450, family 4, subfamily a, polypeptide 14	Cyp4a14	-1.9	Yes	Yes	No
	20148	Dehydrogenase/reductase (sdr family) member 3	Dhrs3	1.8	Yes	Yes	Yes
	13849	Epoxide hydrolase 1, microsomal	Ephx1	1.8	No	Yes	Yes
	14629	Glutamate-cysteine ligase, catalytic subunit	Gclc	1.7	No	Yes	Yes
	93692	Glutaredoxin	Glrx	1.6	No	No	Yes
	14860	Glutathione S-transferase, alpha 4	Gsta4	1.7	Yes	Yes	Yes
	14864	Glutathione S-transferase, mu 3	Gstm3	1.8	Yes	No	No
	14870	Glutathione S-transferase, pi 1	Gstp1	4.4	Yes	Yes	Yes
	14872	Glutathione S-transferase, theta 2	Gstt2	1.7	No	Yes	Yes
	18104	NAD(P)H dehydrogenase, quinone 1	Nqo1	2.1	Yes	Yes	Yes
	18984	P450 (cytochrome) oxidoreductase	Por	2.2	Yes	No	Yes
	99929	TCDD-inducible poly(ADP-ribose) polymerase	Tiparp	14	Yes	Yes	Yes
	53376	Ubiquitin specific protease 2	Usp2	2.1	No	No	Yes
	22235	UDP-glucose dehydrogenase	Ugdh	2.7	Yes	Yes	Yes
	22436	Xanthine dehydrogenase	Xdh	2	Yes	Yes	No

Table 7 (cont'd).

Functional category	Entrez Gene ID	Gene name	Gene symbol	Fold change[a]	TCDD internal controls	TCDD time course [17]	DRE[b]
Lipid metabolism	11806	Apolipoprotein A-I	Apoa1	-1.9	Yes	Yes	No
	23801	Arachidonate lipoxygenase 3	Aloxe3	-1.6	Yes	Yes	Yes
	64436	Inositol polyposphate-5-phosphatase e	Inpp5e	1.5	No	No	No
	16956	Lipoprotein lipase	Lpl	2.5	Yes	Yes	No
	12401	Serine (or cysteine) proteinase inhibitor, clade A, member 6	Serpina6	2.1	Yes	No	Yes
	26458	Solute carrier family 27 (fatty acid transporter), member 2	Slc27a2	2.1	Yes	Yes	Yes
	20249	stearoyl-coenzyme a desaturase 1	Scd1	2.1	No	No	No
	20787	Sterol regulatory element binding factor 1	Srebf1	-2.1	Yes	Yes	No
	22359	Very low density lipoprotein receptor	Vldlr	1.6	Yes	Yes	Yes
Development/ differentiation	27494	Angiomotin	Amot	1.7	No	Yes	Yes
	56484	Forkhead box o3a	Foxo3a	1.8	No	Yes	Yes
	15251	Hypoxia inducible factor 1, alpha subunit	Hif1a	1.7	Yes	Yes	Yes
	18128	Notch gene homolog 1 (Drosophila)	Notch1	2.4	Yes	Yes	Yes
	21928	Tumor necrosis factor, alpha-induced protein 2	Tnfaip2	3.6	Yes	Yes	Yes

Table 7 (cont'd).

Functional category	Entrez Gene ID	Gene name	Gene symbol	Fold change[a]	TCDD internal controls	TCDD time course [17]	DRE[b]
Glucose metabolism/ gluconeogenesis	26384	Glucosamine-6-phosphate deaminase 1	Gnpda1	-1.6	No	Yes	Yes
	14381	Glucose-6-phosphate dehydrogenase x-linked	G6pdx	-1.5	No	No	No
	14718	Glutamate oxaloacetate transaminase 1, soluble	Got1	-1.7	Yes	Yes	Yes
	14571	Glycerol phosphate dehydrogenase 2, mitochondrial	Gpd2	-1.7	Yes	Yes	Yes
	18534	Phosphoenolpyruvate carboxykinase 1, cytosolic	Pck1	-2.2	Yes	Yes	Yes
Necrosis/ apoptosis	12176	Bcl2/adenovirus e1b interacting protein 1, nip3	Bnip3	1.8	No	No	Yes
	215114	Huntingtin interacting protein 1	Hip1	1.8	Yes	Yes	Yes
	17869	Myelocytomatosis oncogene	Myc	1.7	Yes	Yes	Yes
Immune response	12500	CD3 antigen, delta polypeptide	Cd3d	-1.7	No	Yes	Yes
	20299	Chemokine (c-c motif) ligand 22	Ccl22	1.7	Yes	No	Yes
	15439	Haptoglobin	Hp	-2	Yes	No	Yes

[a]Maximum expression (|fold change| $\geq$1.5, P1(t) $\geq$ 0.9999).

[b]DRE identified in -1500 to + 1500 of the transcriptional start site (TSS) [29].

with metabolism exhibited the highest fold change across the time course study. For example, Cyp1a1 was induced 92-fold at the 18 h time point in the PCB126 time course, whereas Tiparp was induced 14-fold at 4 h. PCB126 treatment also induced glutathione S-transferases by 1.7- to 4.4-fold at late time points.

Lipid metabolism genes like very low density lipoprotein receptor (Vldlr), lipoprotein lipase (Lpl), apolipoprotein (Apoa1), stearoyl-Coenzyme A desaturase 1 (Scd1), arachidonate lipoxygenase 3 (Aloxe3), and sterol regulatory element binding factor 1 (Srebf1) were either induced or repressed by PCB126 treatment. For example, Srebf1 was repressed between 8-24 h, whereas Aloxe3 and Apoa1 were repressed at later time points. In contrast, Vldlr, Lpl, and Scd1 were induced at least 1.6-fold at mid and late time points.

PCB126 and TCDD [17] elicited gene expression changes associated with development and differentiation, including Notch gene homolog 1 (Drosophila) (Notch1), tumor necrosis factor, alpha-induced protein 2 (Tnfaip2) and hypoxia inducible factor 1, and alpha subunit (Hif1a). Apart from Notch1, which was continuously up-regulated, both Tnfaip2 and Hif1a were induced at early and mid time points with fold changes ranging from 1.7- to 3.6-fold.

Overall, PCB126 differentially regulated the same gene functions as TCDD except for changes associated with immune cell infiltration and hepatocellular necrosis, in agreement with the histopathology observations. A more thorough discussion of the association between differential gene expression and pathology has been previously published [17, 30]. Moreover, the number of PCB126-elicited gene expression changes was approximately five times lower than that of TCDD (Figure 9A) when compared with a TCDD study using the same experimental design [17]. After relaxing the filtering criteria (Figure 9A), the number of TCDD regulated

Figure 9. Gene expression comparisons and correlation analysis.
(A) Differentially regulated genes sets for 300 μg/kg PCB126 and 30 μg/kg TCDD were compared at 2, 4, 8, 12, 18, 24, 72 and 168 h with stringent filtering criteria (P1(t)≥0.9999 and |fold change|≥1.5) and using relaxed criteria (P1(t)≥0.99 and |fold change|≥1.2) to further examine ligand specific gene expression changes. Numbers in the Venn diagram represent unique genes. (B) Toxicogenomic correlation plot of genes regulated by PCB126 and TCDD at relaxed filtering criteria. Correlation analysis was used to visualize significance and expression profiles comparisons to identify similarities and differences between PCB126 and TCDD [17] temporal data sets. A vast majority of genes was found within the upper right hand quadrant and exhibited profiles that were positively correlated in both gene expression and significance. Overall, PCB126-elicited gene expression responses were a subset of TCDD regulated genes, suggesting PCB126 does not elicit the full spectrum of responses induced by TCDD as indicated in the histopathology and clinical chemistry results.

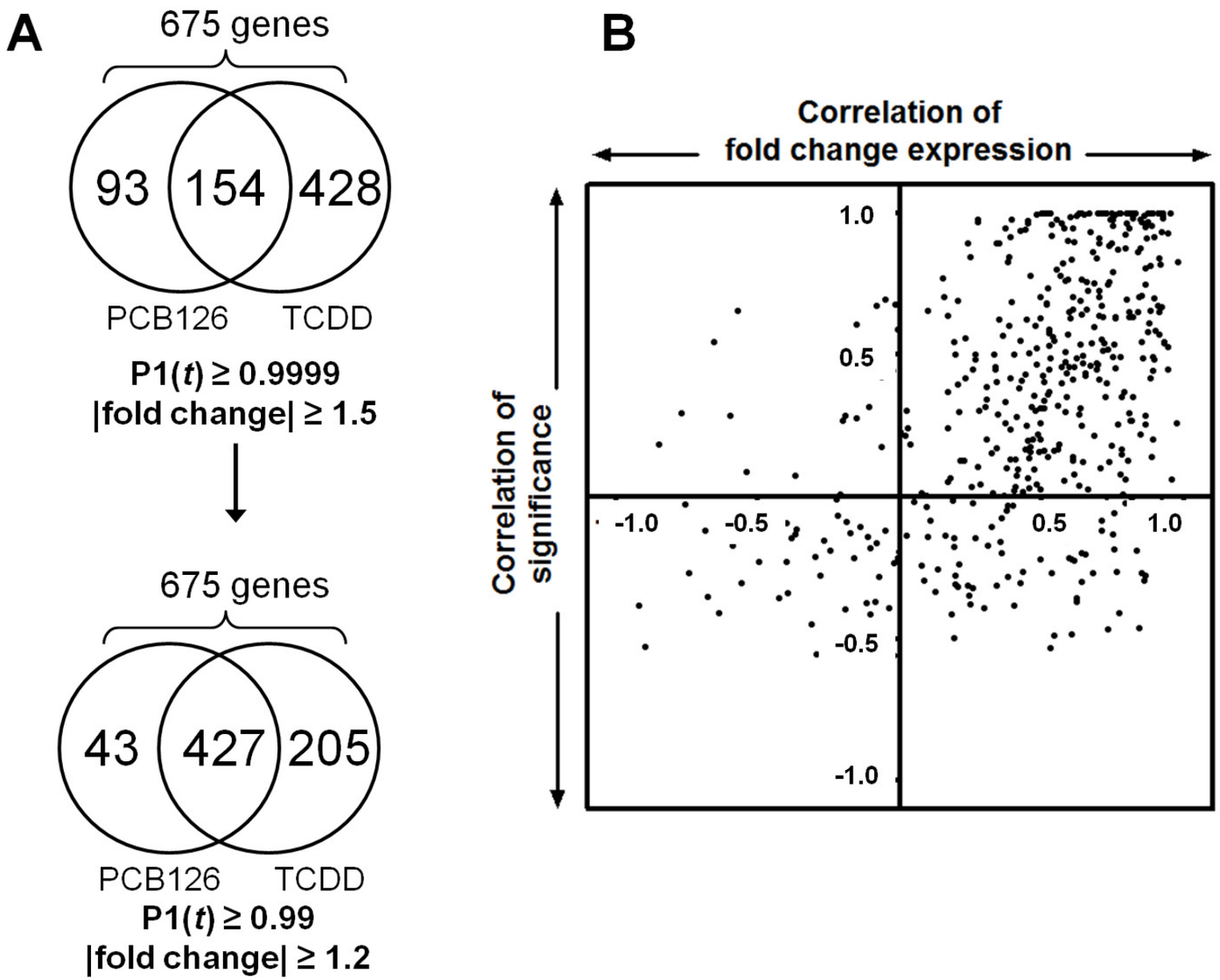
A
675 genes
93
154
428
PCB126
TCDD
P1(t) ≥ 0.9999
|fold change| ≥ 1.5
675 genes
43
427
205
PCB126
TCDD
P1(t) ≥ 0.99
|fold change| ≥ 1.2
B
Correlation of
fold change expression
Correlation of
significance
1.0
0.5
-0.5
-1.0
-1.0
-0.5
0.5
1.0

genes was significantly greater, with a majority of the common differentially expressed genes having the same temporal expression pattern (Figure 9B). Nevertheless, at equipotent doses, based on the TEF of 0.1, 300 μg/kg PCB126 was less effective in eliciting gene expression responses when compared with 30 μg/kg TCDD.

VERIFICATION OF MICROARRAY RESPONSES

QRTPCR verified the temporal and dose-dependent changes in transcript levels for a selected subset of differentially regulated genes identified by microarray analysis (Figure 10A and 10B, respectively). However, data compression was evident for Cyp1a1 due in part to the limited dynamic fluorescence intensity range (0-65,535) of microarrays, which resulted in signal saturation and compression of the true level of induction.

DISCUSSION

The present study compared the hepatic effects of 300 μg/kg PCB126 to 30 μg/kg TCDD using a comprehensive time course and dose-response toxicogenomic approach with complementary histopathology, tissue-level analysis, and clinical chemistry. In order to use a published report examining the hepatic effects of 30 μg/kg TCDD using the same experimental design [17] as a comparator for this study, an equipotent dose of 300 μg/kg PCB126 was used in this study based on the WHO TEF of 0.1. Given the conserved AhR mediated mechanism of action, as well as the use of "equipotent" doses, we examined the hypothesis that 300 μg/kg PCB126 would quantitatively and qualitatively elicit comparable effects when compared with 30 μg/kg TCDD. In general, the similar elicited effects were consistent with the AhR mediated mechanism of action. However, there were also notable qualitative and quantitative differential gene expression, pathology, and clinical chemistry differences suggesting that 30 μg/kg PCB126 does not elicit comparable responses compared with 30 μg/kg TCDD.

Figure 10. QRTPCR verification of microarray responses.
QRTPCR verification of selected PCB126 (A) temporal and (B) dose-dependent microarray gene expression responses. The same RNA that was used for cDNA microarrays was examined by QRTPCR. All fold changes were calculated relative to time-matched vehicle controls. Bars (left y-axis) and lines (right y-axis) represent QRTPCR and microarray data respectively with the x-axis representing the time points or dose. The genes are represented by their official gene symbols. The error bars represent the standard error of the mean of five independent replicates. Asterisks (*) indicate a significant change ($p<0.05$) for QRTPCR.

A

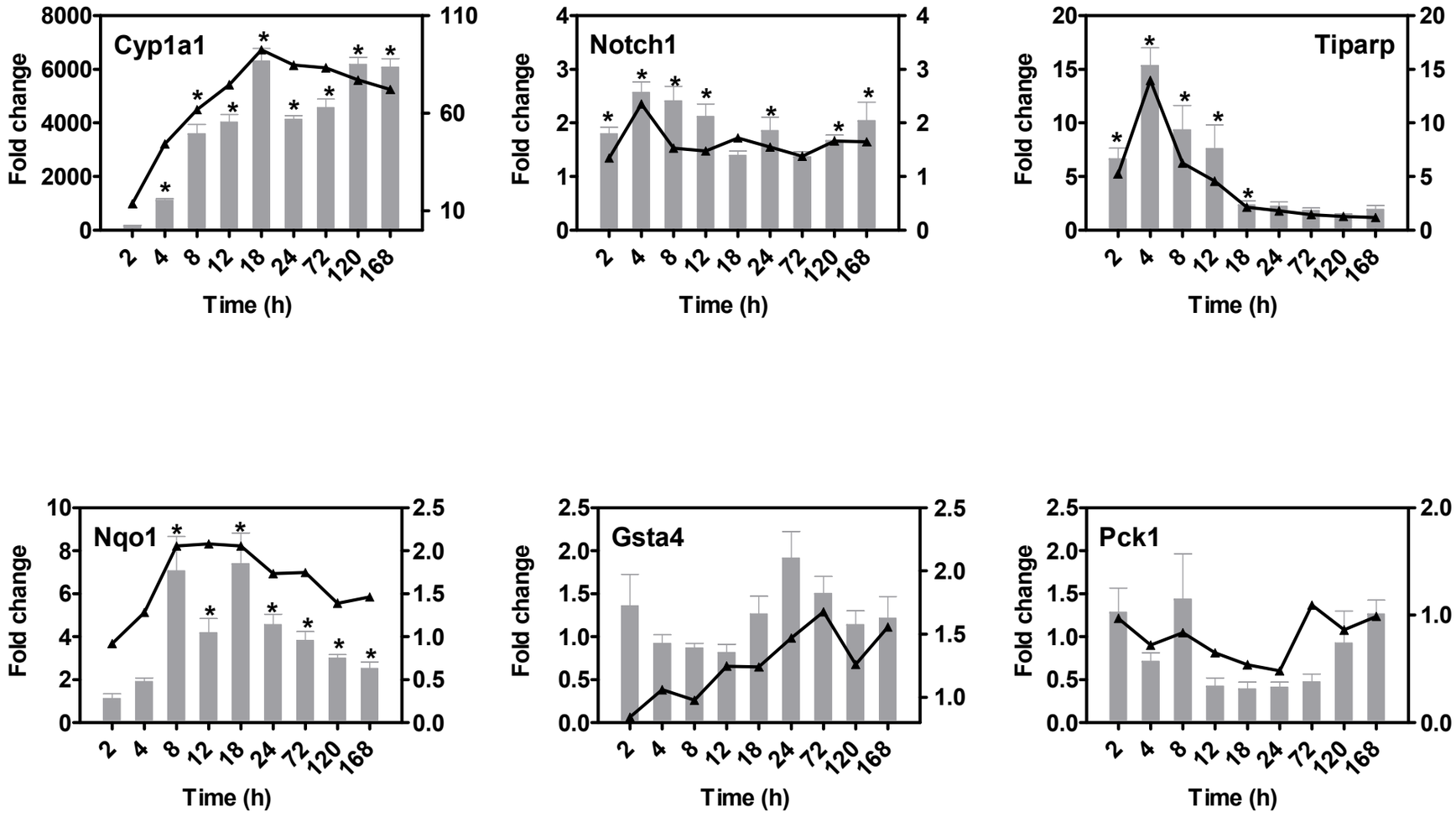
Cyp1a1
Notch1
Tiparp
Nqo1
Gsta4
Pck1
Fold change
Time (h)
2
4
8
12
18
24
72
120
168

Figure 10 (cont'd).

B

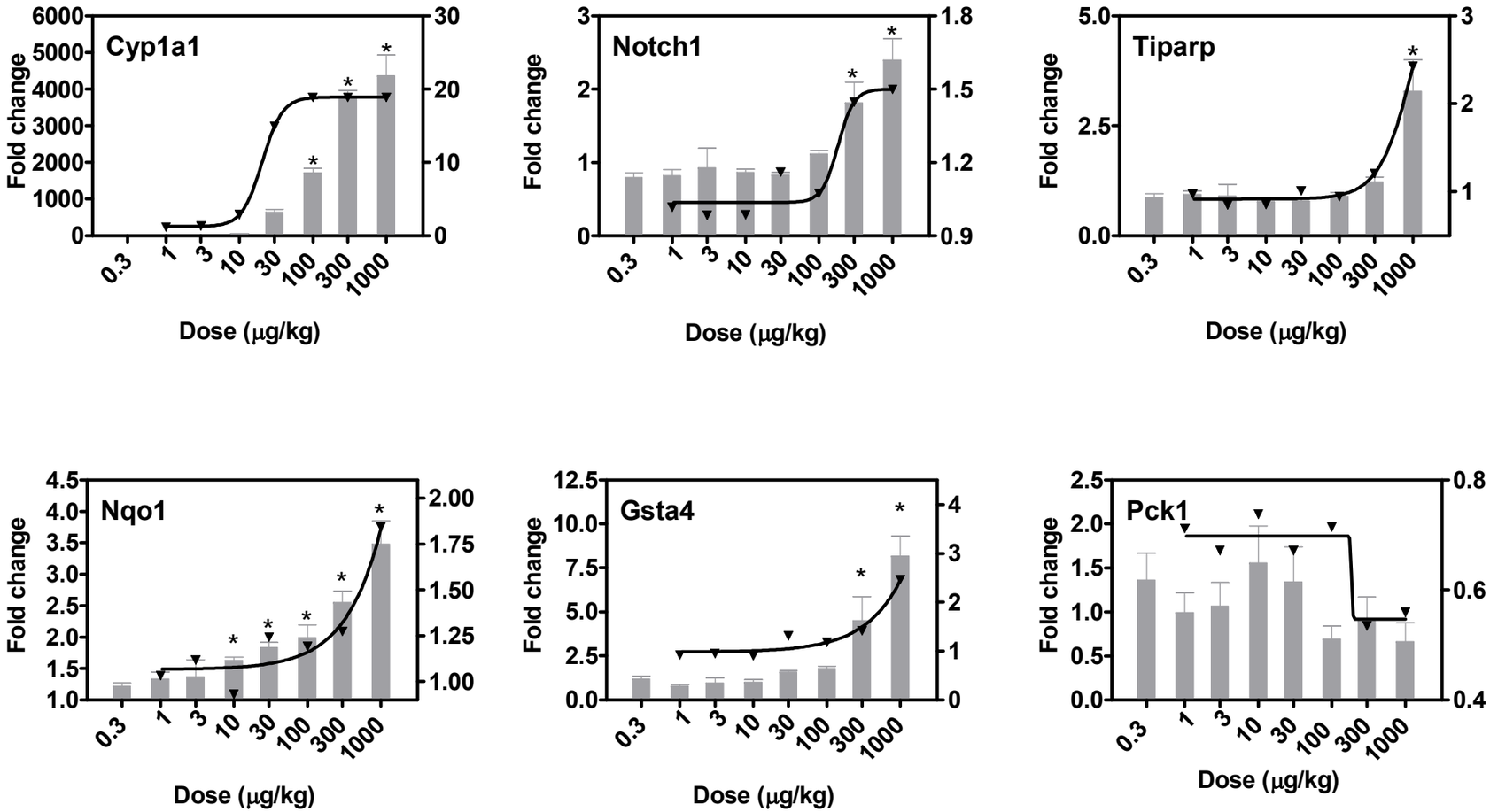

For example, PCB126, like TCDD, significantly increased RLW. Complementary microarray, clinical chemistry, and histopathology data suggest the increased RLW was due to fatty accumulation resulting from the disruption of hepatic lipid uptake and metabolism. PCB126-induced lipoprotein lipase (Lpl) expression may involve the hydrolysis of lipids from chylomicrons and very low density lipoproteins, enabling free fatty acid accumulation [17]. PCB126 and TCDD also induced very low density lipoprotein receptor (Vldlr), which is required for Lpl regulation. A decrease of Vldlr may result in hypertriglyceridemia associated with decreased Lpl activity [31]. In addition, apolipoprotein A-1 was inhibited by PCB126 and TCDD, consistent with reported decreases in transcript and activity levels after hepatic fatty acid accumulation [32]. PCB126 and TCDD also induced solute carrier family 27 (fatty acid transporter), member 2 (Slc27a2), which supports hepatocellular vacuolization through transport of fatty acids into hepatocytes [33]. Direct comparison of hematoxylin and eosin stained slides indicates that 300 μg/kg PCB126 is less effective in inducing hepatocellular vacuolization than 30 μg/kg TCDD [17] (Table 4) at later time points (18-168 h). This may also be attributed to the TCDD-elicited differential expression of fatty acid synthase (Fasn), lipin 2 (Lpin2), low density lipoprotein receptor-related protein 2 (Lrp2), CD36 antigen (Cd36), and fatty acid binding protein 5, epidermal (Fabp5) [17], which were not induced by PCB126.

The presence of mixed cell infiltrates at later time points has been associated with the expression of immune signaling genes [17]. Minimal PCB126-mediated inflammation was observed at 168 h and was not observed in the 72 h dose-response study. It was coincident with (C-C motif) ligand 22 (Ccl22) induction, which is produced in response to activated murine B lymphocytes and dendritic cells [34]. Significant down-regulation of CD3 antigen, delta polypeptide (Cd3d) and haptoglobin (Hp) at earlier time points preceded histological

inflammation. CD antigens are important in select immune signaling functions, including rolling and migration, as well as T-cell activation [35], whereas inhibition of haptoglobin is involved in hepatic acute-phase response [36]. Although Ccl22 and Cd3d were comparably regulated by PCB126 and TCDD, haptoglobin showed more significant repression only in response to PCB126. In contrast, TCDD-induced mixed cell infiltration was observed at 72 and 168 h in the time course study and in the dose-response study at 100 μg/kg [17]. Lymphocyte antigen 6 complex, locus A (Ly6a), CD44 antigen (Cd44) involved in T-cell activation [37], as well as the major histocompatibility complex (MHC) class II genes, H2-Ab1 and H2-Eb1, involved in mediating antigen presentation and processing [38] were differentially regulated by TCDD. However, none of these genes was regulated in response to PCB126, suggesting that they are key players in eliciting TCDD-induced hepatic inflammation. The mixed cell infiltrates are likely a response to tissue damage and therefore, the late regulation of immune signaling genes is not directly mediated by the AhR. The attenuated immune signaling gene responses relative to 30 μg/kg TCDD are further evidence of a weaker hepatic response to 300 μg/kg PCB126.

A common hallmark of TCDD exposure is feed refusal, BW loss and depletion of energy stores commonly referred to as "wasting syndrome" [5]. However, because pair-fed animals still experience wasting, feed refusal alone is not sufficient to account for the effect. Like TCDD, PCB126 repressed several gluconeogenesis genes including phosphoenolpyruvate carboxykinase 1 (Pck1), glycerol phosphate dehydrogenase 2, mitochondrial (Gpd2), as well as glutamate oxaloacetate transaminase 1, soluble (Got1), albeit at lower efficacy. For the genes involved in gluconeogenesis, 30 μg/kg TCDD caused more significant repression than 300 μg/kg PCB126. Even though there were no significant changes in BW or BW gain at the doses used, the

inhibition of gluconeogenesis may still contribute to hepatotoxicity and an eventual wasting effect [39].

TCDD also induced minimal to slight necrotic changes at 72 h in this study and in published study at 72 and 168 h. Although, there was no evidence of necrosis in the PCB126 time course and dose-response sections, a number of genes involved in necrosis and apoptosis, including BCL2/adenovirus E1B interacting protein 1, NIP3 (Bnip3), huntingtin interacting protein 1 (Hip1), and myelocytomatosis oncogene (Myc) were regulated by PCB126. Even though upregulation of Hip1 activates apoptosis [40] and Bnip3 mediates apoptosis and oncosis in rodent models [41], 300 μg/kg and higher doses of PCB126 were not sufficient to cause necrosis further indicating that 300 μg/kg PCB126 does not elicit comparable effects when compared with 30 μg/kg TCDD.

Other genes of interest also exhibited lower induction by PCB126 when compared with TCDD treatment. For example, members of the "AhR gene battery" were induced by PCB126 and TCDD including Cyp1a1, Nqo1, and Xdh. Their induction serves an important role in detoxification, but may also contribute to reactive oxygen species formation, leading to cellular oxidative stress and DNA fragmentation [17, 42, 43]. The induction of reactive oxygen species-generating enzymes was accompanied by increases in glutathione transferases (Gsta1, Gsta4, Gstp1, Gstt2, Gstm3). This contributes to the biotransformation of xenobiotics by catalyzing the conjugation of reduced glutathione to electrophiles and products of oxidative stress to facilitate their excretion [44]. In addition, Notch1 and Tnfaip2 were induced by PCB126 and TCDD. Both exhibit specific patterns of expression in the developing liver and have been implicated in tissue development [45]. Their role in hepatotoxicity is unknown, but they may be important in normal AhR signaling during hepatic development because AhR null mice have reduced liver size and

distorted hepatic vasculature [46]. Although these genes were differentially expressed by both compounds with similar profiles, in general, PCB126-elicited differential gene expression was lower and for a shorter duration, again suggesting that 300 μg/kg PCB126 does not elicit responses comparable to 30 μg/kg TCDD.

In summary, there were significant qualitative and quantitative differences in the effects elicited by PCB126 when compared with TCDD. This included differences in gene expression, histopathology, and clinical chemistry. Overall, 30 μg/kg TCDD elicited greater fold changes in gene expression compared with 300 μg/kg PCB126. In addition, vacuolization, necrosis, and mixed cell infiltration were less pronounced in mice treated with 300 μg/kg PCB126 compared to 30 μg/kg TCDD. Furthermore, unlike TCDD, PCB126 did not alter circulating NEFA, TG, CHOL or GLU levels. These differences cannot be attributed to metabolism because PCB126 tissue levels were comparable and even exceeded TCDD levels at later time points according to HRGC-HRMS tissue analysis.

The data collectively and consistently indicate that 300 μg/kg PCB126 does not elicit responses comparable to 30 μg/kg TCDD, suggesting that the 0.1 TEF for PCB126 is an over estimate of its hepatotoxicity in immature, ovariectomized C57BL/6 mice. However, other studies have found that the mammalian TEF of 0.1 for PCB126 accurately reflects its toxicity [2]. Therefore, outside the context of other studies and given that the TEF is a point estimate that may vary by a half-log unit, additional research is needed to warrant adjusting the PCB126 TEF of 0.1. There are significant species differences in toxicity [47], and sensitivity [48], as well as pharmacokinetic differences between congeners [10, 26], that must also be considered. Other factors, including the lack of positionally conserved DREs [29], and non-additive (antagonistic) interactions [10, 26], also confound the establishment of appropriate TEFs for human and

wildlife risk assessment. Consequently, there continue to be significant gaps in knowledge regarding the validity of the PCB126 TEF and the accuracy of the 0.1 point estimate [16]. In order to determine a more accurate TEF for the hepatotoxicity of PCB126, more comprehensive dose-response studies at multiple times optimal for each specific endpoint are required. Ideally, these would be comparative and include multiple species to account for species-specific differences that may not be relevant to human or wildlife toxicity [29, 30].

REFERENCES

REFERENCES

1. Mullin, M.D., et al., *High-resolution PCB analysis: synthesis and chromatographic properties of all 209 PCB congeners.* Environ. Set Technol., 1984. **18**: p. 468-476.

2. NTP, *NTP toxicology and carcinogenesis studies of 3,3',4,4',5-pentachlorobiphenyl (PCB 126) (CAS No. 57465-28-8) in female Harlan Sprague-Dawley rats (Gavage Studies).* NTP Technical Report, 2006(520): p. 4-246.

3. Ganey, P.E. and S.A. Boyd, *An approach to evaluation of the effect of bioremediation on biological activity of environmental contaminants: dechlorination of polychlorinated biphenyls.* Environ Health Perspect, 2005. **113**(2): p. 180-5.

4. Wu, Q., K.R. Sowers, and H.D. May, *Microbial Reductive Dechlorination of Aroclor 1260 in Anaerobic Slurries of Estuarine Sediments.* Appl Environ Microbiol, 1998. **64**(3): p. 1052-1058.

5. Denison, M.S. and S. Heath-Pagliuso, *The Ah receptor: a regulator of the biochemical and toxicological actions of structurally diverse chemicals.* Bull Environ Contam Toxicol, 1998. **61**(5): p. 557-68.

6. Safe, S., *Molecular biology of the Ah receptor and its role in carcinogenesis.* Toxicol Lett, 2001. **120**(1-3): p. 1-7.

7. Hankinson, O., *The aryl hydrocarbon receptor complex.* Annu Rev Pharmacol Toxicol, 1995. **35**: p. 307-40.

8. Nebert, D.W., et al., *Role of the aromatic hydrocarbon receptor and [Ah] gene battery in the oxidative stress response, cell cycle control, and apoptosis.* Biochem Pharmacol, 2000. **59**(1): p. 65-85.

9. Okey, A.B., L.M. Vella, and P.A. Harper, *Detection and characterization of a low affinity form of cytosolic Ah receptor in livers of mice nonresponsive to induction of cytochrome P1-450 by 3-methylcholanthrene.* Mol Pharmacol, 1989. **35**(6): p. 823-30.

10. Safe, S., *Limitations of the toxic equivalency factor approach for risk assessment of TCDD and related compounds.* Teratog Carcinog Mutagen, 1997. **17**(4-5): p. 285-304.

11. Schmidt, J.V., et al., *Characterization of a murine Ahr null allele: involvement of the Ah receptor in hepatic growth and development.* Proc Natl Acad Sci U S A, 1996. **93**(13): p. 6731-6.

12. Van den Berg, M., et al., *Toxic equivalency factors (TEFs) for PCBs, PCDDs, PCDFs for humans and wildlife.* Environ Health Perspect, 1998. **106**(12): p. 775-92.

13. Poland, A. and J.C. Knutson, *2,3,7,8-tetrachlorodibenzo-p-dioxin and related halogenated aromatic hydrocarbons: examination of the mechanism of toxicity.* Annu Rev Pharmacol Toxicol, 1982. **22**: p. 517-54.

14. Safe, S., *Polychlorinated biphenyls (PCBs), dibenzo-p-dioxins (PCDDs), dibenzofurans (PCDFs), and related compounds: environmental and mechanistic considerations which support the development of toxic equivalency factors (TEFs).* Crit Rev Toxicol, 1990. **21**(1): p. 51-88.

15. Haws, L.C., et al., *Development of a refined database of mammalian relative potency estimates for dioxin-like compounds.* Toxicol Sci, 2006. **89**(1): p. 4-30.

16. Van den Berg, M., et al., *The 2005 World Health Organization reevaluation of human and Mammalian toxic equivalency factors for dioxins and dioxin-like compounds.* Toxicol Sci, 2006. **93**(2): p. 223-41.

17. Boverhof, D.R., et al., *Temporal and dose-dependent hepatic gene expression patterns in mice provide new insights into TCDD-Mediated hepatotoxicity.* Toxicol Sci, 2005. **85**(2): p. 1048-63.

18. Yang, Y.H. and T. Speed, *Design issues for cDNA microarray experiments.* Nat Rev Genet, 2002. **3**(8): p. 579-88.

19. Burgoon, L.D., et al., *Protocols for the assurance of microarray data quality and process control.* Nucleic Acids Res, 2005. **33**(19): p. e172.

20. Eckel, J.E., et al., *Normalization of two-channel microarray experiments: a semiparametric approach.* Bioinformatics, 2005. **21**(7): p. 1078-83.

21. Eckel, J.E., et al., *Empirical bayes gene screening tool for time-course or dose-response microarray data.* J Biopharm Stat, 2004. **14**(3): p. 647-70.

22. Vandesompele, J., et al., *Accurate normalization of real-time quantitative RT-PCR data by geometric averaging of multiple internal control genes.* Genome Biol, 2002. **3**(7): p. RESEARCH0034.

23. Shokooh-Saremi, M. and R. Magnusson, *Particle swarm optimization and its application to the design of diffraction grating filters.* Opt Lett, 2007. **32**(8): p. 894-6.

24. Dennis, G., Jr., et al., *DAVID: Database for Annotation, Visualization, and Integrated Discovery.* Genome Biol, 2003. **4**(5): p. P3.

25. Fisher, J.W., et al., *Effect of PCB 126 on hepatic metabolism of thyroxine and perturbations in the hypothalamic-pituitary-thyroid axis in the rat.* Toxicol Sci, 2006. **90**(1): p. 87-95.

26. DeVito, M.J., et al., *Dose-response relationships for disposition and hepatic sequestration of polyhalogenated dibenzo-p-dioxins, dibenzofurans, and biphenyls following subchronic treatment in mice.* Toxicol Sci, 1998. **46**(2): p. 223-34.

27. *NTP toxicology and carcinogenesis studies of 2,3,7,8-tetrachlorodibezno-p-dioxin (TCDD) (CAS No. 1746-01-6) in female Harlan Sprague-Dawley rats (Gavage Studies).* Natl Toxicol Program Tech Rep Ser, 2006(521).

28. *NTP toxicology and carcinogenesis studies of 3,3',4,4',5-pentachlorobiphenyl (PCB 126) (CAS No. 57465-28-8) in female Harlan Sprague-Dawley rats (Gavage Studies)*, in *Natl Toxicol Program Tech Rep Ser*. 2006. p. 4-246.

29. Sun, Y.V., et al., *Comparative analysis of dioxin response elements in human, mouse and rat genomic sequences.* Nucleic Acids Res, 2004. **32**(15): p. 4512-23.

30. Boverhof, D.R., et al., *Comparative toxicogenomic analysis of the hepatotoxic effects of TCDD in Sprague Dawley rats and C57BL/6 mice.* Toxicol Sci, 2006. **94**(2): p. 398-416.

31. Yagyu, H., et al., *Very low density lipoprotein (VLDL) receptor-deficient mice have reduced lipoprotein lipase activity. Possible causes of hypertriglyceridemia and reduced body mass with VLDL receptor deficiency.* J Biol Chem, 2002. **277**(12): p. 10037-43.

32. Duplus, E., M. Glorian, and C. Forest, *Fatty acid regulation of gene transcription.* J Biol Chem, 2000. **275**(40): p. 30749-52.

33. Hirsch, D., A. Stahl, and H.F. Lodish, *A family of fatty acid transporters conserved from mycobacterium to man.* Proc Natl Acad Sci U S A, 1998. **95**(15): p. 8625-9.

34. Schaniel, C., et al., *Activated murine B lymphocytes and dendritic cells produce a novel CC chemokine which acts selectively on activated T cells.* J Exp Med, 1998. **188**(3): p. 451-63.

35. Lai, L., et al., *Mouse cell surface antigens: nomenclature and immunophenotyping.* J Immunol, 1998. **160**(8): p. 3861-8.

36. Venteclef, N., et al., *Liver receptor homolog 1 is a negative regulator of the hepatic acute-phase response.* Mol Cell Biol, 2006. **26**(18): p. 6799-807.

37. Sumoza-Toledo, A. and L. Santos-Argumedo, *The spreading of B lymphocytes induced by CD44 cross-linking requires actin, tubulin, and vimentin rearrangements.* J Leukoc Biol, 2004. **75**(2): p. 233-9.

38. Alfonso, C., et al., *The impact of H2-DM on humoral immune responses.* J Immunol, 2001. **167**(11): p. 6348-55.

39. Viluksela, M., B.U. Stahl, and K.K. Rozman, *Tissue-specific effects of 2,3,7,8-Tetrachlorodibenzo-p-dioxin (TCDD) on the activity of phosphoenolpyruvate carboxykinase (PEPCK) in rats.* Toxicol Appl Pharmacol, 1995. **135**(2): p. 308-15.

40. Gervais, F.G., et al., *Recruitment and activation of caspase-8 by the Huntingtin-interacting protein Hip-1 and a novel partner Hippi.* Nat Cell Biol, 2002. **4**(2): p. 95-105.

41. Copple, B.L., et al., *Modes of cell death in rat liver after monocrotaline exposure.* Toxicol Sci, 2004. **77**(1): p. 172-82.

42. Barouki, R. and Y. Morel, *Repression of cytochrome P450 1A1 gene expression by oxidative stress: mechanisms and biological implications.* Biochem Pharmacol, 2001. **61**(5): p. 511-6.

43. Zimmerman, B.J. and D.N. Granger, *Mechanisms of reperfusion injury.* Am J Med Sci, 1994. **307**(4): p. 284-92.

44. Raza, H., et al., *Multiple isoforms of mitochondrial glutathione S-transferases and their differential induction under oxidative stress.* Biochem J, 2002. **366**(Pt 1): p. 45-55.

45. Harper, J.A., et al., *Notch signaling in development and disease.* Clin Genet, 2003. **64**(6): p. 461-72.

46. Lahvis, G.P., et al., *Portosystemic shunting and persistent fetal vascular structures in aryl hydrocarbon receptor-deficient mice.* Proc Natl Acad Sci U S A, 2000. **97**(19): p. 10442-7.

47. Huang, S. and G.G. Gibson, *Species and congener specific induction of hepatic cytochrome P4504A by polychlorinated biphenyls.* Biochem Pharmacol, 1992. **43**(3): p. 637-9.

48. Silkworth, J.B., et al., *Comparison of TCDD and PCB CYP1A induction sensitivities in fresh hepatocytes from human donors, sprague-dawley rats, and rhesus monkeys and HepG2 cells.* Toxicol Sci, 2005. **87**(2): p. 508-19.

CHAPTER 4

Kopec AK, Burgoon LD, Ibrahim-Aibo D, Burg AR, Lee AW, Tashiro C, Potter D, Sharratt B, Harkema JR, Rowlands JC, Budinsky RA, Zacharewski TR: **Automated Dose-Response Analysis and Comparative Toxicogenomic Evaluation of the Hepatic Effects Elicited by TCDD, TCDF, and PCB126 in C57BL/6 Mice**. *Toxicol Sci* 2010, 118:286-297.

CHAPTER 4

AUTOMATED DOSE-RESPONSE ANALYSIS AND COMPARATIVE TOXICOGENOMIC EVALUATION OF THE HEPATIC EFFECTS ELICITED BY TCDD, TCDF, AND PCB126 IN C57BL/6 MICE

ABSTRACT

The toxic equivalency factor (TEF) approach recommended by the World Health Organization is used to quantify dioxin-like exposure concentrations for mixtures of polychlorinated dibenzo-dioxins, -furans, and polychlorinated biphenyls (PCBs), including 2,3,7,8-tetrachlorodibenzofuran (TCDF) and 3,3',4,4',5-pentachlorobiphenyl (PCB126) relative to 2,3,7,8-tetrachlorodibenzo-*p*-dioxin (TCDD). Whole-genome microarrays were used to evaluate the hepatic gene expression potency of TCDF and PCB126, relative to TCDD with complementary histopathology, tissue level analysis, and ethoxyresorufin-O-deethylase (EROD) assay results. Immature ovariectomized C57BL/6 mice were gavaged with 0.001, 0.01, 0.03, 0.1, 0.3, 1, 3, 10, 30, 100, and 300 μg/kg TCDD and TEF-adjusted doses (TEF for TCDF and PCB126 is 0.1) of TCDF or PCB126 (1, 3, 10, 30, 100, 300, 1000, and 3000 μg/kg of TCDF or PCB126), or sesame oil vehicle and sacrificed 24 h post dose. In general, TCDD, TCDF and PCB126 tissue levels, as well as histopathological effects, were comparable when comparing TEF-adjusted doses. Automated dose-response modeling (ToxResponse Modeler) of the microarray data identified 210 TCDF and 40 PCB126 genes that exhibited sigmoidal dose-response curves with comparable slopes when compared to TCDD. These similar responses were

used to calculate a median TCDF gene expression REP of 0.06 and a median PCB126 gene expression REP of 0.02. REPs of 0.02 were also calculated for EROD induction for both compounds. Collectively, these data suggest that differences in the ability of the liganded aryl hydrocarbon receptor:AhR nuclear translocator complex to elicit differential hepatic gene expression, in addition to pharmacokinetic differences between ligands, influence their potency in immature ovariectomized C57BL/6 mice.

INTRODUCTION

Polychlorinated aromatic hydrocarbons (PCAHs), including 2,3,7,8-tetrachlorodibenzo-*p*-dioxin (TCDD) and related chemicals, such as 2,3,7,8-tetrachlorodibenzofuran (TCDF) and 3,3',4,4',5-pentachlorobiphenyl (PCB126) are ubiquitous environmental contaminants that elicit a broad spectrum of species-specific biochemical and toxic effects. Polychlorinated dibenzo-*p*-dioxins (PCDDs) and dibenzofurans (PCDFs) are by-products of waste combustion, herbicide production, and other industrial processes [1-4]. In contrast, polychlorinated biphenyls (PCBs) were manufactured between 1930 and 1977 as mixtures that included PCB126, as well as other congeners [5]. PCBs were used as coolants, lubricants and dielectric insulating fluids for transformers and capacitors [4, 6, 7]. Even though their production has ceased, they continue to be released into the environment through the mishandling of PCB-containing products [8].

Although there are 75, 135, and 209 possible PCDD, PCDF and PCB congeners, respectively, only 7, 10, and 12 are considered dioxin-like based on their ability to bind and activate the aryl hydrocarbon receptor (AhR) [9]. The AhR is a cytosolic ligand-activated basic helix-loop-helix Per-Arnt-Sim domain containing transcription factor [10-13]. Following ligand binding, chaperone proteins that maintain the AhR in an inactive state dissociate from the AhR allowing translocation to the nucleus and heterodimerization with AhR nuclear translocator

(ARNT). The AhR:ARNT heterodimer complex then interacts with dioxin response elements in the regulatory regions of target genes followed by recruitment of co-regulatory proteins, leading to changes in gene expression [12, 14].

Environmental exposure to PCDDs, PCDFs, and PCBs typically occurs as a complex mixture. In order to estimate the risk associated with a mixture, the concentration and potency of each toxic PCDD, PCDF, and PCB congeners is taken into account based on its toxic equivalency factor (TEF) relative to TCDD, the most toxic congener [9, 15-19]. TEFs are single point potency estimates that were developed from relative potency (REP) values calculated by comparing the effective dose (ED_{50}) value of a single response elicited by TCDD and dividing it by the ED_{50} for the same response elicited by the congener of interest [9, 19]. Consequently, the uncertainty of a TEF point estimate can extend over orders of magnitude, reflecting the range of relative potency values available for a particular congener in various model systems [7, 9, 11, 18, 20-22]. TEFs are independent of dose, time point, and tissue and largely reflect biochemical effects such as enzyme induction. Although results from cancer bioassays or developmental-reproductive studies have been considered and are the critical human health risk assessment endpoints for PCDDs and PCDFs, no TEF value is based exclusively on these endpoints. Furthermore, it is assumed that at submaximal doses, the contribution of each congener is additive. There are also pharmacokinetic and distributional differences between congeners that may affect their REPs [23-27].

The TEFs for TCDF and PCB126 are currently set at 0.1, indicating that they are 10 times less potent than TCDD. However, our recent studies suggest that the TEF of 0.1 does not accurately reflect the hepatic potency of TCDF and PCB126 relative to TCDD in C57BL/6 mice [28-30]. Although pharmacokinetic differences are an important factor, temporal and dose-

dependent microarray data suggest that TCDF- and PCB126-elicited gene expression responses are also not equivalent, in terms of potency and efficacy, relative to TCDD at TEF-adjusted equivalent doses. To further investigate this hypothesis, parallel TCDD, TCDF and PCB126 dose-response studies were conducted at 24 h to minimize the pharmacokinetic and distributional differences between these compounds. In addition to using the same species, comparable study designs and analysis methods were also used as previously reported [28-30]. Moreover, complementary histopathology, tissue level analysis, and ethoxyresorufin-O-deethylase (EROD) activities were assessed. Results from this study not only expand the available REP data in C57BL/6 mice but also suggest that TCDF- and PCB126-elicited differential gene expression responses are not comparable to TCDD at TEF-adjusted equivalent doses at 24 h when pharmacokinetic and distributional differences are minimized.

MATERIALS & METHODS

ANIMAL HUSBANDRY

Female C57BL/6 mice, ovariectomized by the supplier on postnatal day (PND) 20, with body weights (BW) within 10% of the average, were obtained from Charles Rivers Laboratories (Kingston, NY) on PND 25. Animals were housed in polycarbonate cages containing cellulose fiber chips (Aspen Chip Laboratory Bedding, Northeastern Products, Warrensberg, NY) with 30-40% humidity and a 12-h light/dark cycle (0700 h – 1900 h). Mice had free access to deionized water and Harlan Teklad 22/5 Rodent Diet 8640 (Madison, WI). Animals were dosed on PND 28 following acclimatization for 3 days. Immature mice were used because they are more responsive to AhR ligands and to facilitate comparisons with other data sets obtained using the same model, study design and analysis methods [29-31]. Animals were ovariectomized to negate potential interactions with estrogens produced by the developing ovaries because some animals

are approaching reproductive maturity. All procedures were carried out with the approval of the Michigan State University Institutional Animal Care and Use Committee.

DOSE-RESPONSE STUDY

A stock solution of PCB126 (99.7% purity, AccuStandard, New Haven, CT) was dissolved in acetone (J.T. Baker), followed by dilution in sesame oil (Sigma, St. Louis, MO), and evaporation of the acetone using a mild stream of nitrogen gas. The PCB126 stock was further diluted in sesame oil to achieve the desired doses. TCDD and TCDF were gifts from The Dow Chemical Company (Midland, MI). Animals were orally gavaged using 1.5-inch feeding needle with a 2.25-mm ball end (Cadence Science, Lake Success, NY). Mice received 0.1 ml of a single dose of 0.001, 0.01, 0.03, 0.1, 0.3, 1, 3, 10, 30, 100, and 300 μg/kg of TCDD or 1, 3, 10, 30, 100, 300, 1000, and 3000 μg/kg of PCB126 or TCDF or 0.1 ml sesame oil vehicle and sacrificed 24 h post dose. PCB126 and TCDF doses were TEF adjusted to be equivalent to the TCDD doses [9] (Table 8). Mice were sacrificed by cervical dislocation and tissue samples were removed, weighed, flash frozen in liquid nitrogen, and stored at –80°C. The right lobe of the liver was fixed in 10% neutral buffered formalin (Sigma) for histological analysis.

HISTOLOGICAL ANALYSIS

Fixed liver tissues were sectioned and processed in ethanol, xylene, and paraffin using a Thermo Electron Excelsior tissue processor (Waltham, MA). Tissues were embedded in paraffin with Miles Tissue Tek II embedding center, after which paraffin blocks were sectioned at 5 μm with a rotary microtome. Liver sections were placed on glass microscope slides, washed twice in xylene for 5 min, followed by four quick washes in ethanol and rinsed in water. Slides were placed in Gill 2 hematoxylin (Thermo Fisher Scientific, Waltham, MA) for 1.5 min followed by two to three quick dips in 1% glacial acetic acid water and rinsed with running water for 2-3 min.

Table 8. The 24 h dose-response study design.

Dose (µg/kg)	Number of animals			
	TCDD	PCB126	TCDF	Vehicle (sesame oil)
0	-	-	-	7
0.001	4	-	-	-
0.01	4	-	-	-
0.03	4	-	-	-
0.1	4	-	-	-
0.3	4	-	-	-
1	4	4	4	-
3	4	4	4	-
10	4	4	4	-
30	4	4	4	-
100	4	4	4	-
300	4	4	4	-
1000	-	4	4	-
3000	-	4	4	-

Slides were then rinsed in ethanol and counterstained with 1% eosin Y-phloxine B solution (Sigma) followed by multiple rinses in ethanol and xylene. Coverslips were attached using aqueous mounting media. All the histological processing was performed at Michigan State University Investigative HistoPathology Laboratory, Division of Human Pathology, using a modified version of previously published procedures [32].

QUANTIFICATION OF HEPATIC TCDD, PCB126, AND TCDF LEVELS

Liver samples were processed in parallel with laboratory blanks and a reference or background sample at Wellington Laboratories Inc. (Guelph, ON, Canada). The samples (100-500 mg) were transferred to a tared screw cap culture tube and weights were recorded. Samples were then spiked with a mixture of $^{13}C_{12}$-2,3,7,8-TCDD, $^{13}C_{12}$-PCB126, and $^{13}C_{12}$-2,3,7,8-TCDF surrogates and digested with HCl. Each digest was split between two screw cap tubes and 3-4 ml hexane was added to each tube followed by vigorous mixing. The tubes were centrifuged, and the organic layer was removed. The hexane extraction was performed three times per tube with the six hexane fractions combined. The hexane fraction was then split and one fraction was archived. The other fraction was processed further using a small multilayer (acid/base/neutral) silica gel column eluted with 20-25 ml of hexane. The eluate was concentrated and transferred to a conical microvial with pentane and dichloromethane rinses and allowed to dry. Immediately prior to injection on the high-resolution gas chromatograph/high-resolution mass spectrometer (HRGC-HRMS) system, a mixture of $^{13}C_{12}$-1,2,3,4-TCDD, $^{13}C_{12}$-PCB111, and $^{13}C_{12}$-1,2,3,4-TCDF injection standards were added to the conical microvial. TCDD, PCB126, and TCDF analyses were performed using an Agilent (Santa Clara, CA, USA) 6890 series HRGC with direct capillary interface to a Waters (Milford, MA, USA) Autospec Ultima HRMS. Chromatographic separations were carried out on a 60-m DB5 (0.25 mm ID, 0.25 μm film

thickness) column in constant flow mode (Helium, 1 ml /min). All injections were 1 µl using splitless injection. The mass spectrometer was operated in positive electron ionization selective ion recording mode at a mass resolving power of 10,000 or greater.

EROD ASSAY

Microsomes were extracted from ~100 mg samples by differential centrifugation [33]. Tissue was minced and homogenized using Tri-R Stir-R homogenizer (*Tri-R* Instruments, Inc., Rockville Centre, NY) in 0.05 M Tris (Invitrogen), 1.15% KCl (JT Baker, Phillipsburg NJ), pH 7.5, and then centrifuged at 4°C, 10,000 × g for 10 min. The supernatant was centrifuged at 4°C, 100,000 × g for 30 min. The microsomal pellets were re-suspended in 0.01 M EDTA (Invitrogen), and 1.15% KCl, pH 7.4, and re-centrifuged at 100,000 × g for 60 min. Final pellets were resuspended in a stabilizing buffer (20% glycerol [J.T. Baker], 0.1 M KH_2PO_4 [J.T. Baker], and 1 mM EDTA and 1 mM DTT [Roche Applied Science, Indianapolis IN], pH 7.25) and stored at –80°C. Extracted hepatic microsomes from vehicle, TCDD-, PCB126-, and TCDF-treated mice were assayed for EROD activity by monitoring the production of resorufin measured at 590 nm in a 96-well plate (Costar, Corning, NY) using a Fluoroskan Ascent fluorometer (Thermo Fisher Scientific, Waltham, MA) and corresponding software (version 2.6). The assay was performed in 0.05 M HEPES (Sigma), pH 7.8, and 3.35 mM 7-ethoxyresorufin (Molecular Probes, Eugene OR). Catalytic activity was initiated by addition of 0.3 mM NADPH (Sigma), and fluorescence was measured every 2 min. After 30 min, the assay was terminated by addition of 36 µg fluorescamine (Sigma) in acetonitrile. Protein concentrations were measured at 460 nm using bovine serum albumin (Roche) as a protein standard. Linear portions of each kinetic profile analysis were used to determine picomoles of resorufin produced per minute and standardized to the total protein (mg).

RNA ISOLATION

Frozen liver samples (left lobe, ~100 mg stored at –80°C) were immediately transferred to 1 ml TRIzol (Invitrogen, Carlsbad, CA) and homogenized using a Mixer Mill 300 tissue homogenizer (Retsch, Germany). Total RNA was isolated according to the manufacturer's protocol with an additional acid phenol:chloroform extraction. Isolated RNA was resuspended in RNA storage solution (Ambion Inc., Austin, TX) and quantified (A_{260}). RNA quality was assessed by determining the A_{260}/A_{280} ratio and visual inspection of 2 μg on a denaturing gel.

MICROARRAY EXPERIMENTAL DESIGN

Treated and vehicle RNA samples were individually hybridized to 4 × 44 K Agilent oligonucleotide microarrays (Agilent Technologies, Inc., Santa Clara, CA). Three biological replicates were performed using one-color labeling (Cy3) for each dose according to the manufacturer's protocol (Agilent Manual: G4140-90040 v. 5.7). Microarray slides were scanned at 532 nm (Cy3) on a GenePix 4000B scanner (Molecular Devices, Union City, CA). Images were analyzed for feature and background intensities using GenePix Pro 6.0 (Molecular Devices). All data were archived in TIMS dbZach data management system [34].

MICROARRAY ANALYSIS

All microarray data in this study passed our laboratory quality assurance protocol [35]. TCDD, PCB126, and TCDF data sets were independently normalized due to the overall size of the files using a semiparametric approach [36]. Posterior probabilities were then calculated using an empirical Bayes method on a per-gene and dose basis using model-based *t* values [37]. Gene expression data were then ranked and prioritized (P1(*t*) values >0.99 or >0.90 and |fold change|>1.5) to identify differentially expressed genes.

QUANTITATIVE REAL-TIME PCR

Quantitative real-time PCR (QRTPCR) was performed as previously described [31]. Briefly, 1 μg of total RNA was reverse transcribed by SuperScript II (Invitrogen) using an anchored oligo-dT primer. The complementary DNA (cDNA) (1 μl) was used as a template in a 30-μl reaction containing 0.1 μM of forward and reverse gene-specific primers, 3 mM $MgCl_2$, 1 mM dNTPs, 0.025 IU AmpliTaq Gold, and 1× SYBR Green PCR buffer (Applied Biosystems, Foster City, CA). Amplification was conducted on an Applied Biosystems PRISM 7500 Sequence Detection System. The cDNAs were quantified using a standard curve approach, and the copy number of each sample was standardized to 3 housekeeping genes (Actb, Gapdh, Hprt) [38]. For graphing purposes (GraphPad Prism 5.0), the relative expression levels were scaled such that the expression level of the time-matched control group was equal to one.

DOSE-RESPONSE MODELING

Dose-response modeling was performed using the ToxResponse Modeler [39]. ToxResponse Modeler performs automated dose-response modeling by identifying the best fit model among five different mathematical models (linear, exponential, Gaussian, sigmoidal, and quadratic). The algorithm then chooses the best-fit of the five best in-class models. The overall best-fit model is then used to calculate the ED_{50} values. Microarray dose-response data were first filtered using a $P1(t)>0.90$ cut-off and filtered to identify genes exhibiting a sigmoidal dose-response profile. REP values were calculated on a per-feature/per-gene basis using model-based ED_{50} values:

$$\mathrm{REP} = \frac{\mathrm{TCDD\ ED_{50}}}{\mathrm{TCDF\ or\ PCB126\ ED_{50}}}$$

STATISTICAL ANALYSIS

All statistical analyses were performed with SAS 9.1 (SAS Institute, Cary, NC). All data (with the exception of microarray data) were analyzed by ANOVA followed by Dunnett's or Tukey's *post hoc* tests. Differences between treatment groups were considered significant when $p<0.05$.

RESULTS

LIVER AND BWS

Rodents exposed to PCAHs including dioxins, PCBs, and furans exhibit temporal and dose-dependent hepatic changes characterized by increases in liver weight [8, 12, 40]. PCB126 and TCDF have TEFs of 0.1 [9], indicating that 10 times more chemical is required to elicit similar effects compared to an equivalent dose of TCDD. In our study, PCB126 and TCDF doses were TEF-adjusted to theoretically match the potency of TCDD. Significant ($p<0.05$) increases in relative liver weight (RLW) were observed with 300 μg/kg TCDD, 300 μg/kg PCB126, and 1000 and 3000 μg/kg TCDF in agreement with previous reports using the same compounds, animal models and study designs (Figure 11) [29-31, 41]. No changes in BW or BW gain relative to vehicle controls were observed within 24 h, indicating no systemic toxicity or wasting syndrome response at the doses used.

HEPATIC TCDD, PCB126, AND TCDF LEVELS

TCDD, PCB126, and TCDF levels per liver wet weight (in pg/g) were measured in three individual samples per dose using HRGC-HRMS. A dose-dependent increase in the hepatic concentration of all three compounds was observed (Figure 12A-C and Table 9). The tissue levels of TCDD, PCB126, and TCDF were significantly ($p<0.05$) higher compared to vehicle controls, except for the lowest doses of TCDD (0.001-0.1 μg/kg), because of the presence of low

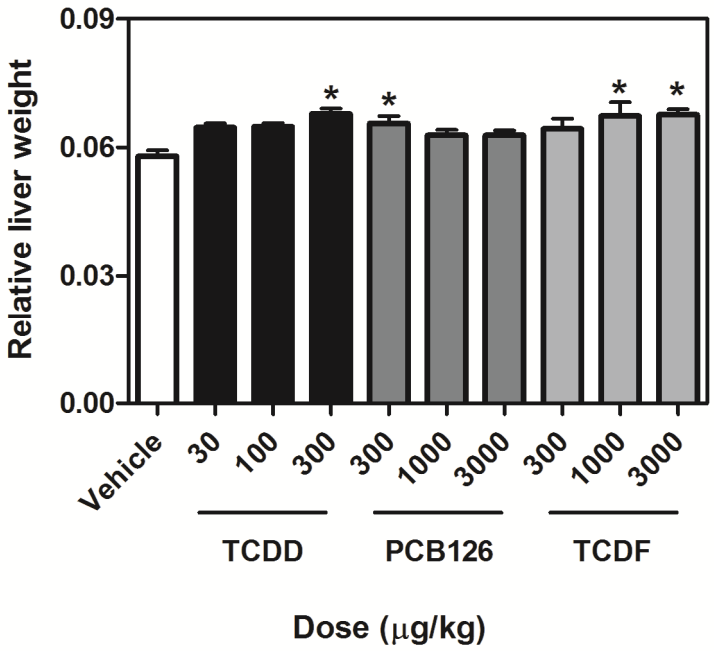

Figure 11. Dose-dependent changes in the RLWs.
Dose-dependent changes in the relative liver weights 24 h post dose for TCDD, PCB126, and TCDF. Results are displayed as mean ± SE of at least 4 independent replicates. Data were analyzed by ANOVA followed by Dunnett's *post hoc* test. Asterisk (*) indicates $p<0.05$ for vehicle vs. treated samples. No additional significant treatment-related alterations in liver or organ weights were noted in the dose-response study.

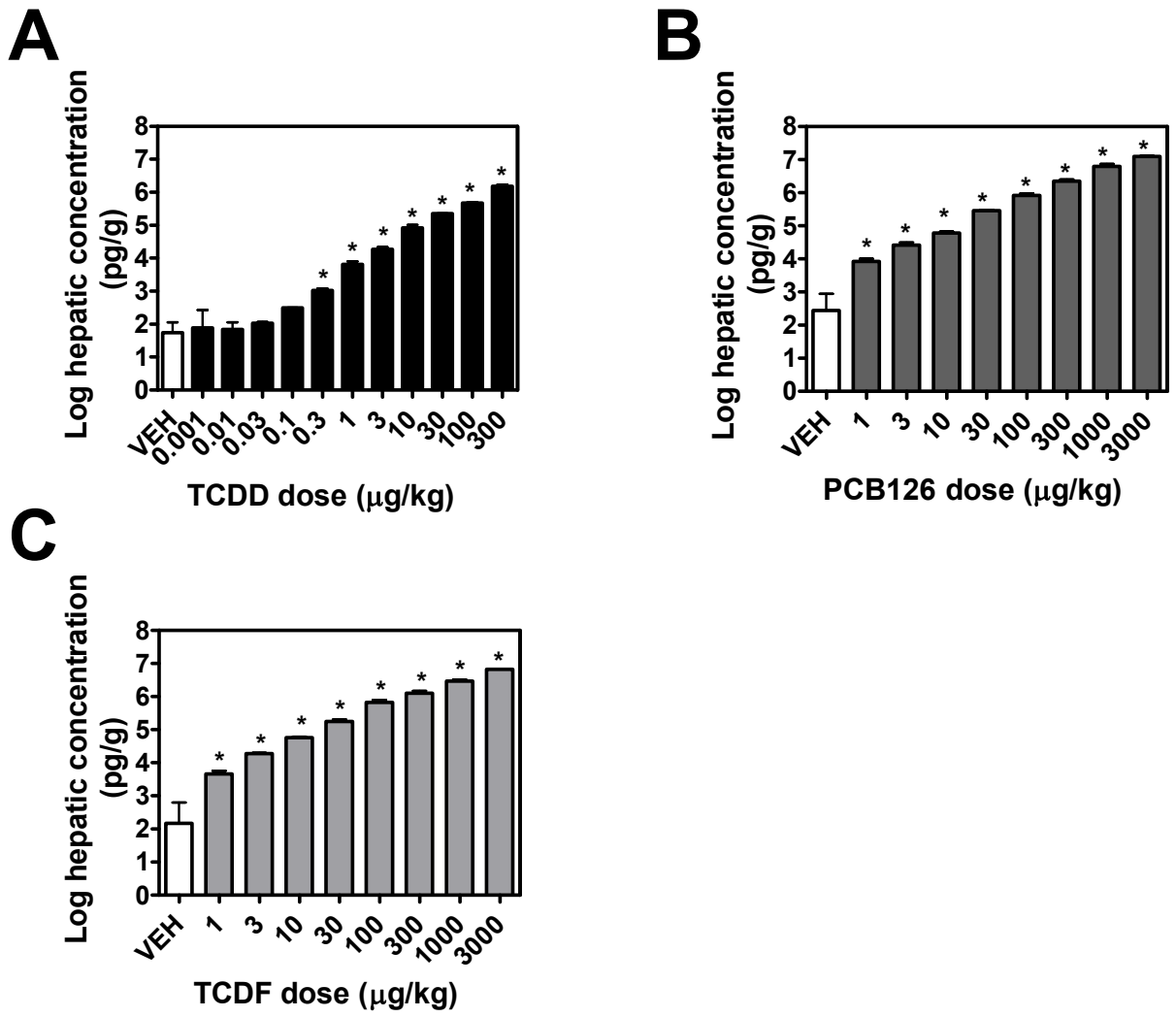

Figure 12. Hepatic tissue level quantification.
Hepatic (A) TCDD, (B) PCB126 and (C) TCDF levels per g liver wet weight measured 24 h post dose using HRGC-HRMS. The data are displayed on a log scale to visualize tissue concentrations at all doses. The results are displayed as mean ± SE of at least three independent samples. Data were analyzed by ANOVA followed by Dunnett's *post hoc* test: *$p<0.05$ for vehicle vs. treated samples.

Table 9. Absolute hepatic tissue levels (in pg/g or ppt per wet weight) for TCDD-, PCB126-, and TCDF-treated samples and vehicle controls measured by HRGC-HRMS.

	Absolute hepatic tissue levels (in pg/g or ppt per wet weight)		
Dose (µg/kg)	**TCDD**	**PCB126**	**TCDF**
Vehicle (sesame oil)	$1.00\times10^{2} \pm 9.84\times10^{1}$	$1.22\times10^{3} \pm 1.98\times10^{3}$	$1.05\times10^{3} \pm 1.68\times10^{3}$
0.001	$2.07\times10^{2} \pm 2.39\times10^{2}$	-	-
0.01	$8.83\times10^{1} \pm 7.12\times10^{1}$	-	-
0.03	$1.09\times10^{2} \pm 1.29\times10^{1}$	-	-
0.1	$3.10\times10^{2} \pm 2.06\times10^{1}$	-	-
0.3	$1.08\times10^{3} \pm 2.21\times10^{2}$	-	-
1	$6.73\times10^{3} \pm 2.21\times10^{3}$	$8.66\times10^{3} \pm 2.58\times10^{3}$	$4.79\times10^{3} \pm 1.56\times10^{3}$
3	$1.90\times10^{4} \pm 4.85\times10^{3}$	$2.72\times10^{4} \pm 9.24\times10^{3}$	$1.88\times10^{4} \pm 1.70\times10^{3}$
10	$8.70\times10^{4} \pm 2.78\times10^{4}$	$6.08\times10^{4} \pm 1.23\times10^{4}$	$5.81\times10^{4} \pm 6.36\times10^{3}$
30	$2.25\times10^{5} \pm 1.06\times10^{4}$	$2.89\times10^{5} \pm 2.72\times10^{4}$	$1.80\times10^{5} \pm 3.81\times10^{5}$
100	$4.75\times10^{5} \pm 5.08\times10^{4}$	$8.39\times10^{5} \pm 2.06\times10^{5}$	$6.81\times10^{5} \pm 2.24\times10^{5}$
300	$1.52\times10^{6} \pm 3.07\times10^{5}$	$2.29\times10^{6} \pm 4.92\times10^{5}$	$1.29\times10^{6} \pm 3.52\times10^{5}$
1000	-	$6.41\times10^{6} \pm 1.95\times10^{6}$	$2.96\times10^{6} \pm 4.66\times10^{5}$
3000	-	$1.25\times10^{7} \pm 1.01\times10^{6}$	$6.63\times10^{6} \pm 4.05\times10^{5}$

Note. The values represent mean ± SD of at least 3 independent replicates.

background levels of TCDD. At TEF-equivalent doses, the levels of all three compounds were comparable, except for statistical differences at 0.1, 0.3, 100, and 300 μg/kg. The use of TEF values for determining tissue concentrations increases the uncertainty and reliability of potency estimates [9]. Despite this limitation, the use of TEF-adjusted tissue level data suggests that the potencies of TCDD, TCDF, and PCB126 should be comparable because there were minimal differences in hepatic absorption, distribution and metabolism between compounds at 24 h. This is significant because pharmacokinetic differences between these ligands have been reported to contribute to substantial differences in potencies at later time points [29, 30, 42, 43].

HISTOPATHOLOGY

Hematoxylin and eosin staining was examined on the three highest TEF-equivalent doses (30, 100, and 300 μg/kg TCDD; 300, 1000, and 3000 μg/kg PCB126 and TCDF). TCDD, PCB126, and TCDF elicited dose-dependent increases in periportal hepatocellular vacuolization and multifocal mixed inflammatory infiltration (Table 10, Figure 13). TCDD and the equivalent TEF-matched TCDF doses elicited comparable hepatic vacuolization, while TEF-equivalent PCB126 doses exhibited slightly less vacuolization (Table 10). Hepatocellular single cell necrosis was present only in the highest dosed groups for all three compounds with the most pronounced necrosis occurring with 3000 μg/kg TCDF (Table 10, Figure 13). Comparable levels of dose-dependent mixed inflammatory cell foci (lymphocytes, monocytes and neutrophils) were observed. Qualitatively, these results suggest that TEF-matched doses of TCDD, PCB126, and TCDF elicit comparable histopathological effects at 24 h.

EROD ACTIVITY

Hepatic EROD activity was assessed to anchor our results to data within the World Health Organization (WHO) REP database [18]. TCDD induced a dose-dependent, sigmoidal

Table 10. Dose-dependent incidence and severity of hepatic histopathological responses in the vehicle, TCDD, PCB126 and TCDF treated mice at 24 h.

	Treatment and dose (µg/kg)									
	Vehicle	TCDD			PCB126			TCDF		
	0	30	100	300	300	1000	3000	300	1000	3000
Hepatocellular vacuolization										
Average severity:	0	1	1.75	2.5	1	1.5	2	1.25	1.75	2.5
Hepatocellular single cell necrosis										
Average severity:	0	0	0	0.5	0	0	0.5	0	0	1.25
Mixed cell infiltration										
Average severity:	0	0.25	0.25	0.5	0	0.5	0.5	0	0.25	0.75

Note. The average severity scores are reported as a weighted average based on the following scoring scheme: minimal (grade of 1), slight (grade of 2), moderate (grade of 3), and/or marked (grade of 4) responses divided by the total number of examined animals.

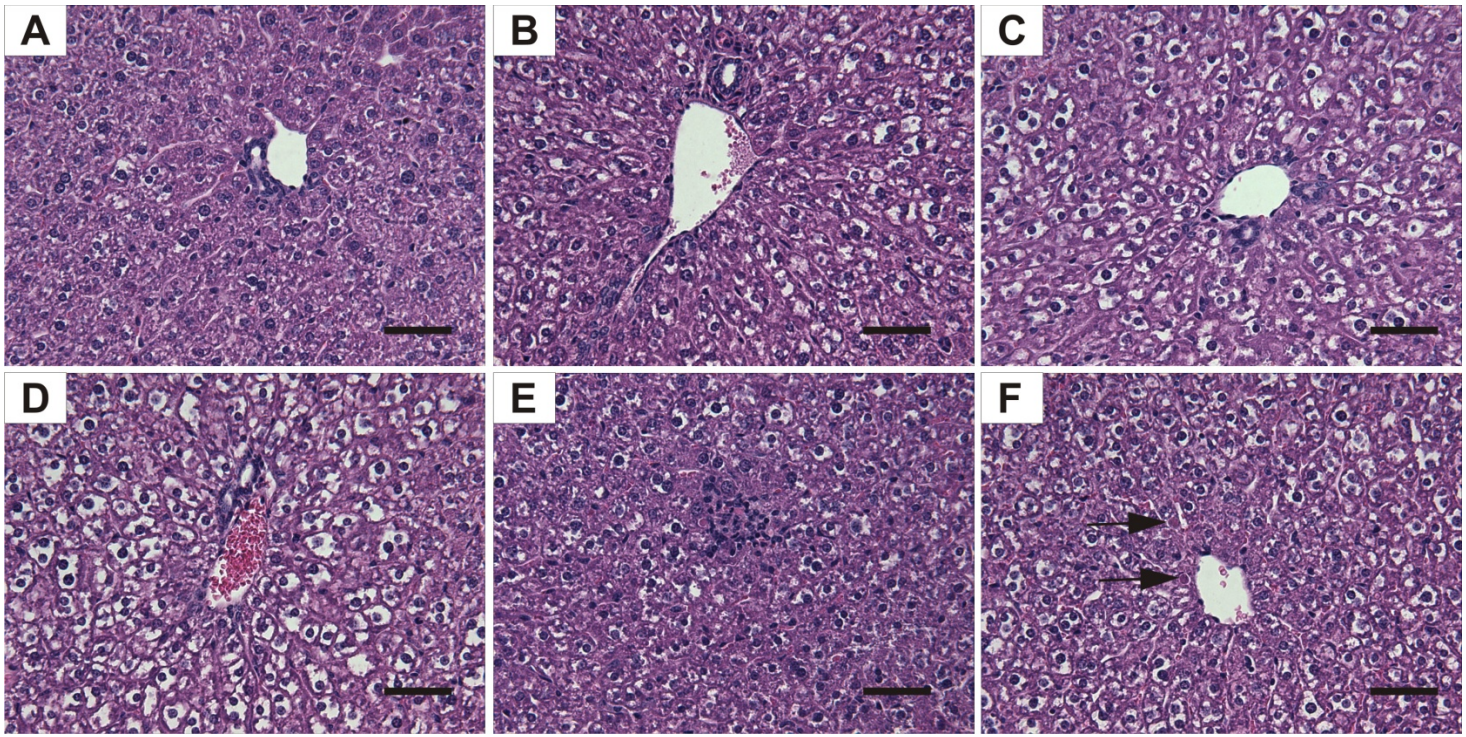

Figure 13. Representative hematoxylin and eosin stained liver sections 24 h post exposure to PCB126, TCDF, or TCDD. Selected doses resulted in vacuolization, single cell necrosis and/or immune cell infiltration. (A) Vehicle treatment resulted in no visible hepatic alterations. (B) 300 μg/kg PCB126 elicited minimal vacuolization, compared to (C) 1000 μg/kg TCDF and (D) 300 μg/kg TCDD which exhibited more pronounced vacuolization. (E) 3000 μg/kg TCDF resulted in immune cell infiltration, as well as (F) instances of necrosis (arrow). Bars = 50 μm.

increase in EROD activity with an ED_{50} of 1.1 μg/kg, calculated using the ToxResponse Modeler [39] (Figure 14). TEF-matched doses of PCB126 and TCDF elicited comparable EROD induction (Figure 14), but were less potent than TCDD (PCB126 ED_{50}=53.6 μg/kg, TCDF ED_{50}=54.2 μg/kg). These EROD activity REPs (0.02 for PCB126 and TCDF) are consistent with values reported in the WHO REP database [18]. Moreover, in our published study examining TEF-equivalent doses of TCDD and TCDF at 72 h, the ToxResponse Modeler identified a comparable EROD REP value (TCDF EROD REP_{72h} of 0.04) [28].

HEPATIC TCDF AND PCB126 GENE EXPRESSION REPS

TCDF and PCB126 microarray data were analyzed to determine both per-gene and aggregate gene expression REP values using set theory and our ToxResponse Modeler (Figure 15A-C). The analysis abides by assumptions underlying the TEF concept (e.g., same mechanism of action, parallel dose-response curves). TCDD, TCDF, and PCB126 microarray data sets were individually normalized [36] and analyzed using an Empirical Bayes approach to identify differentially expressed features. Compared to previously published microarray studies [29-31], a more relaxed P1(t) cut-off was used (P1(t)>0.90) to be more inclusive, yielding higher statistical power at the risk of including more false-positives at this early stage in the dose-response analysis.

TCDD elicited ~1.6 times more differentially expressed features when compared to TCDF (13,476 vs. 8655, respectively) (Figure 15A) at comparable hepatic levels. This trend is similar to the 72 h dose-response analysis, where TCDD elicited the differential expression of almost twice as many features compared to TCDF, but at lower hepatic TCDF levels due to

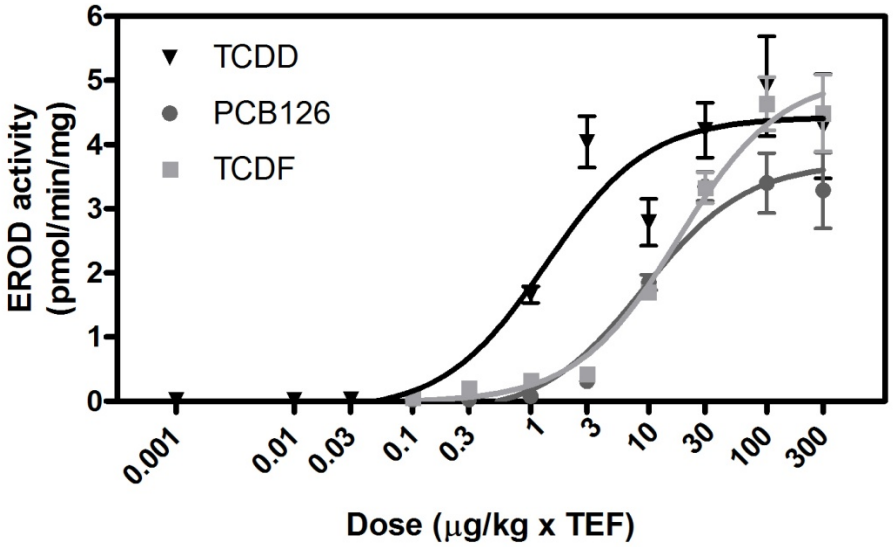

Figure 14. EROD activity.
Dose-dependent induction of EROD activity following exposure to TEF-equivalent doses of TCDD, PCB126 and TCDF. The ToxResponse Modeler calculated ED_{50} values of 1.1 μg/kg, 53.6 μg/kg and 54.2 μg/kg for TCDD, PCB126, and TCDF, respectively, yielding PCB126 and TCDF EROD REPs of 0.02. Symbols represent the mean ± SE of four independent samples. Sigmoidal dose-response curve fitting was done using GraphPad Prism 5.0.

ligand-specific pharmacokinetics [26, 28, 42-45]. Likewise, TCDD differentially expressed ~1.3 times more features compared to PCB126 (13,476 vs. 10,983, respectively) (Figure 15A). It should be noted that TCDD consistently elicited the greatest number of differentially expressed features (and genes in subsequent analysis) compared to either TCDF or PCB126.

Unions of the TCDD plus TCDF (16,227 features) and TCDD plus PCB126 (17,053 features) data sets were taken to include all differentially regulated features for further dose-response and REP analysis. Features missing data at one or more doses, as well as the Agilent included controls were removed and not considered further. Features were then mapped back to genes to investigate dose-dependent changes in expression (Figure 15A).

Genes with a P1(t) > 0.90 were also filtered for a >1.5-fold change in expression for at least one dose, relative to time-matched controls. This resulted in 5191 TCDD and 3919 TCDF genes that exhibited an expression change greater than 1.5-fold for at least one dose with a corresponding P1(t)>0.90 and an ED_{50} value within the experimental dose range (Figure 15B). This means that of the 5191 genes differentially expressed by TCDD for at least one dose, 3120 genes were not represented in the TCDF data set, and of the 3919 TCDF genes, 1848 were not represented in the TCDD set (Figure 15B). Compared with the 72 h dose-response analysis [28], approximately five times more TCDD and TCDF genes were identified at 24 h (5191 TCDD and 3919 TCDF genes at 24 h compared with 1027 TCDD and 837 TCDF genes at 72 h).

The ToxResponse Modeler then identified the best linear, exponential, Gaussian, sigmoidal, and quadratic models for each dose-responsive differentially expressed gene (e.g., best in class). The model that best fit the data among the different classes (e.g., best in show) was then used to calculate an ED_{50} for each dose-responsive gene. Only those genes with an ED_{50} within the experimental dose-response range were retained for subsequent REP analysis.

Figure 15. Comprehensive TCDD, TCDF, and PCB126 dose-response analysis.
(A) Differentially regulated features were identified using a relaxed P1(*t*) cut-off of 0.90 to maximize the number of differentially expressed genes under consideration. TCDD elicited ~1.6 times more differentially expressed features compared to TCDF (13,476 vs. 8655) and ~1.3 times more differentially expressed features compared to PCB126 (13,476 vs. 10,983). Unions were taken to identify all differentially regulated features. Features missing data at any dose, as well as Agilent controls, were removed and not considered further. Features were mapped to specific genes for further analysis.
(B) Differentially expressed genes were analyzed further if the change in expression was greater than 1.5-fold for at least one dose. Genes exhibiting a sigmoidal dose-response were identified and intersected to identify genes responsive to both TCDD and TCDF and to TCDD and PCB126 at 24 h. Genes were examined further if the model-based ED_{50} value, calculated by ToxResponse Modeler, was within the experimental dose range. Genes exhibiting a sigmoidal dose-response curve for both TCDD and TCDF were intersected to identify 1506 genes that exhibited an expression change greater than 1.5-fold for at least one dose, a P1(*t*)>0.90, a sigmoidal profile and an ED_{50} value within the experimental range. Identical analysis yielded only 388 sigmoidal genes for TCDD and PCB126. PCB126 lost a majority of differentially expressed, dose-responsive genes from further consideration because the ED_{50s} were not within the experimental dose range.
(C) In the final analysis, assumptions regarding similarities in the slopes and shapes of corresponding TCDD and TCDF as well as TCDD and PCB126 sigmoidal dose-response curves were assessed by calculating the correlation coefficients of the elicited dose-response curves. The correlation analysis identified 210 genes from TCDD vs. TCDF comparisons, and only 40 genes from TCDD and PCB126 comparisons with correlation coefficients greater than 0.60. The distribution of individual gene expression REPs is provided. The median REP for hepatic gene expression in the immature, ovariectomized C57BL/6 mouse at 24 h was calculated to be 0.06 and 0.02 for TCDF and PCB126, respectively.

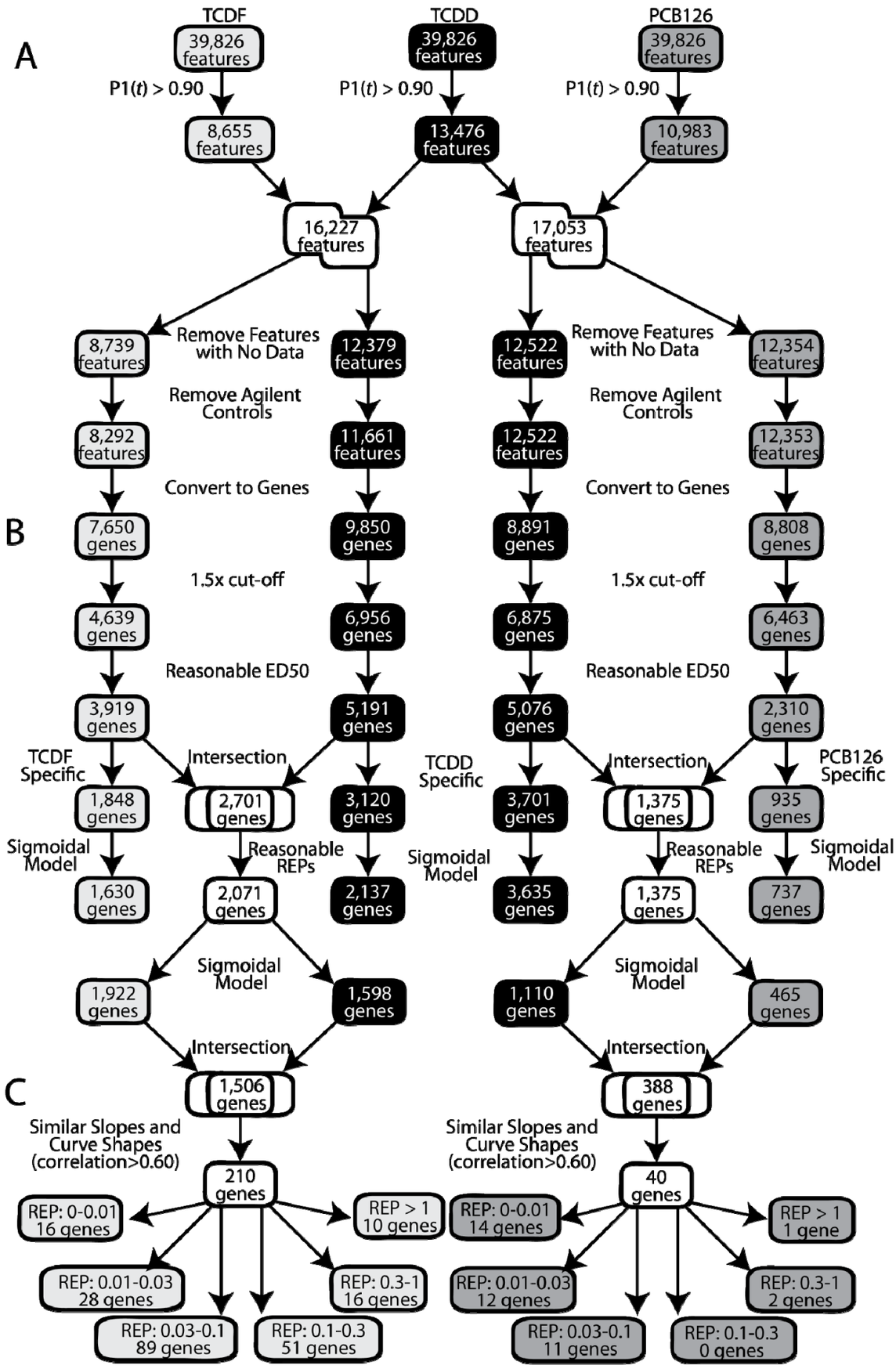
A
TCDF
39,826 features
P1(t) > 0.90
8,655 features
TCDD
39,826 features
P1(t) > 0.90
13,476 features
PCB126
39,826 features
P1(t) > 0.90
10,983 features
16,227 features
17,053 features
B
8,739 features
Remove Features with No Data
12,379 features
12,522 features
Remove Features with No Data
12,354 features
Remove Agilent Controls
8,292 features
11,661 features
12,522 features
Remove Agilent Controls
12,353 features
Convert to Genes
7,650 genes
9,850 genes
8,891 genes
Convert to Genes
8,808 genes
1.5x cut-off
4,639 genes
6,956 genes
6,875 genes
1.5x cut-off
6,463 genes
Reasonable ED50
3,919 genes
5,191 genes
5,076 genes
Reasonable ED50
2,310 genes
TCDF Specific
1,848 genes
Intersection
2,701 genes
3,120 genes
TCDD Specific
3,701 genes
Intersection
1,375 genes
PCB126 Specific
935 genes
Sigmoidal Model
1,630 genes
Reasonable REPs
2,071 genes
2,137 genes
Sigmoidal Model
3,635 genes
Reasonable REPs
1,375 genes
Sigmoidal Model
737 genes
Sigmoidal Model
1,922 genes
1,598 genes
Sigmoidal Model
1,110 genes
465 genes
Intersection
1,506 genes
Intersection
388 genes
C
Similar Slopes and Curve Shapes (correlation>0.60)
210 genes
REP: 0-0.01 16 genes
REP > 1 10 genes
REP: 0.01-0.03 28 genes
REP: 0.3-1 16 genes
REP: 0.03-0.1 89 genes
REP: 0.1-0.3 51 genes
Similar Slopes and Curve Shapes (correlation>0.60)
40 genes
REP: 0-0.01 14 genes
REP > 1 1 gene
REP: 0.01-0.03 12 genes
REP: 0.3-1 2 genes
REP: 0.03-0.1 11 genes
REP: 0.1-0.3 0 genes

The intersection of 5191 TCDD and 3919 TCDF genes identified 2071 genes that were used to calculate gene-specific REPs. Furthermore, 3120 and 1848 genes were TCDD- and TCDF-specific, respectively. Of those, 2137 TCDD and 1630 TCDF genes exhibited sigmoidal dose-response curves. The intersection of 2071 genes in common between TCDD and TCDF with reasonable ED_{50} values identified 1506 genes with sigmoidal dose-response curves (Figure 15B).

In order to comply with WHO TEF assumptions regarding similar slopes and curve shapes, only those genes that exhibited correlation coefficient greater than 60% were considered further for gene-specific REP analysis. In this study, the coefficient was lowered compared to the 72 h TCDF dose-response analysis (correlation coefficient> 80%) [28] to include more genes and to account for the smaller overlap between TCDD and PCB126 data sets, thus facilitating comparisons between PCB126 and TCDF at 24 h. Correlation analysis identified 210 genes with similar slopes and curve shapes elicited by TCDD and TCDF (Figure 15C). Sixteen of these genes had gene specific REP values between 0 and 0.01, 28 between 0.01 and 0.03, 89 between 0.03 and 0.1, 51 between 0.1 and 0.3, 16 between 0.3 and 1, and 10 genes had REPs greater than 10. The median REP for all 210 genes was 0.06, lower than the 72 h median REP of 0.1 (0.096) calculated using 83 genes with similar slopes and curves for TCDD and TCDF [28]. Relaxing the correlation coefficient used for the 72 h dose-response study [28] to 60% resulted in an almost identical median gene expression REP of 0.1 (0.112).

An identical approach was used to determine PCB126 gene-specific REPs and a median REP (Figure 15C). In summary, only 40 genes exhibited similar slope and sigmoidal curves, of which 14 genes had REPs between 0 and 0.01, 12 between 0.01 and 0.03, 11 between 0.03 and 0.1, 2 between 0.3 and 1, and only 1 gene had a REP greater than 1. The median PCB126 gene

expression REP for the 40 sigmoidal genes was 0.02. The PCB126 data set lost a majority of genes from further consideration because the ED_{50s} were not within the experimental dose range. The low number of dose-responsive genes considered for the PCB126 REP analysis can be attributed to the lower number of differentially expressed genes with sufficient potency when compared to TCDF and TCDD.

REPs based on tissue levels were also calculated for a subset of responsive genes used to determine REPs based on administered dose. However, a vast majority of tissue level-based REPs could not be calculated due to differences in curve shapes and slopes. Overall, the median tissue level gene expression REPs for TCDF and PCB126 were comparable to administered dose-based REPs for the limited number of genes considered (TCDF $REP_{administered\ dose}$ = 0.06, TCDF $REP_{tissue\ level}$ = 0.04, and PCB126 $REPs_{administered\ dose\ and\ tissue\ level}$ = 0.02). Note that approximately 60% of the tissue level-based REPs were within an order of magnitude of the administered dose-based REPs.

Microarray analysis suggests there were a number of TCDF- and PCB126-specific responses. Three-way Venn analysis of the 3280, 2343, and 1411 gene expression changes elicited by TCDD, TCDF, and PCB126 (P1(*t*)>0.99 and |fold change|>1.5), respectively, identified only 202 genes differentially expressed by all 3 compounds (Figure 16A). However, after relaxing the statistical cut-off (P1(*t*)>0.90 and |fold change|>1.5) (Figure 16B), almost all PCB126- and TCDF-elicited gene expression changes overlapped, consistent with the conserved AhR-mediated mechanism of action. Overlaps between TCDD versus TCDF and TCDD versus PCB126 also significantly increased. The high number of TCDD-specific genes could be attributed to a wider range of doses used in the study (11 doses of TCDD vs. 8 doses of PCB126

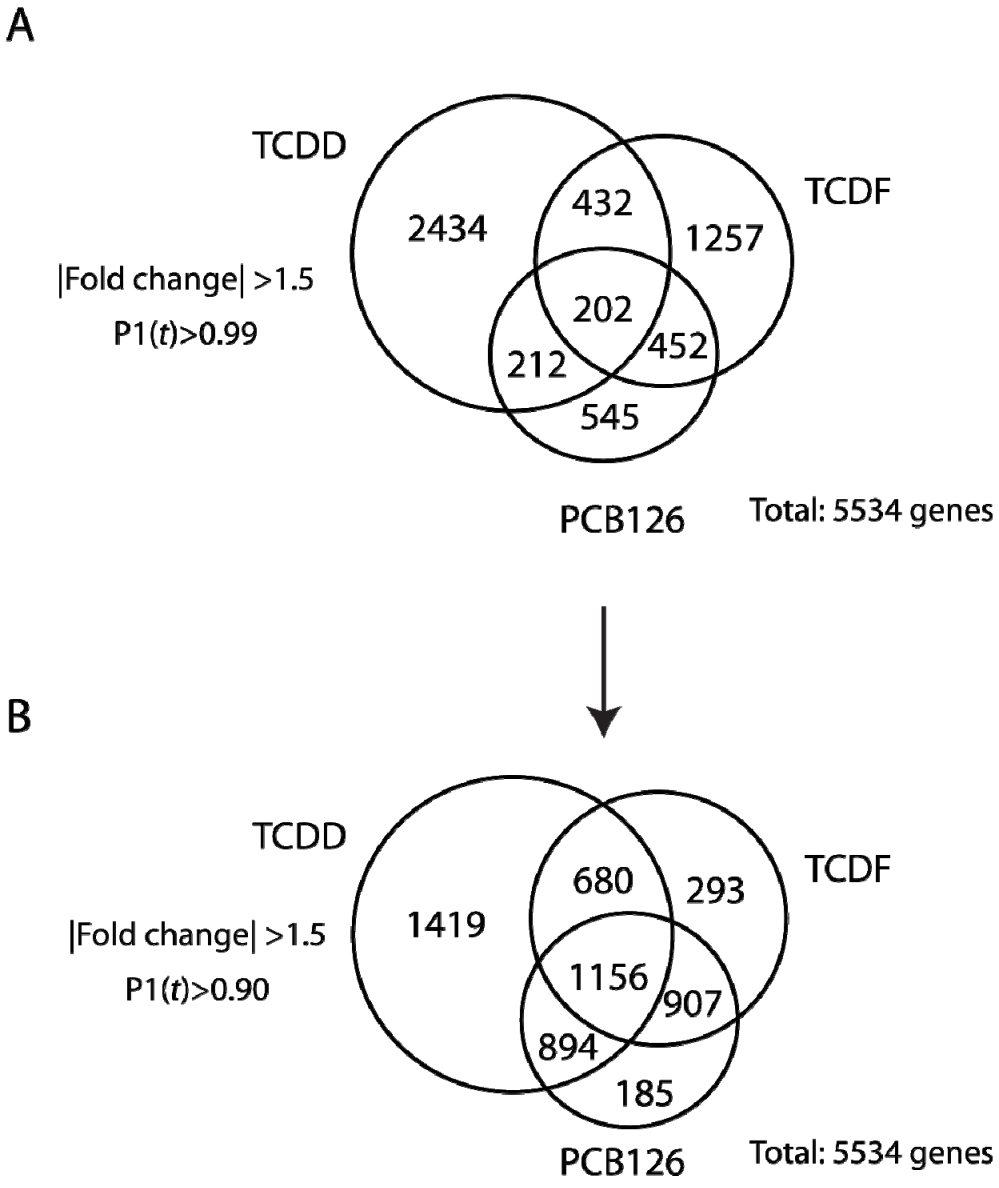

Figure 16. Three-way Venn analysis.
Three-Way Venn analysis of TCDD, PCB126 and TCDF elicited differentially expressed genes at (A) stringent (|fold change|>1.5, P1(*t*)>0.99) and (B) relaxed statistical criteria (|fold change|>1.5, P1(*t*)>0.90).

and TCDF), and the greater potency and efficacy of TCDD even at TEF-adjusted doses of TCDF and PCB126.

These results are in agreement with reports suggesting that TCDF- and PCB126-elicited responses are a subset of TCDD regulated genes and consistent with a common AhR-mediated mode of action [29, 30]. At later time points, TCDD elicits more pronounced histopathological responses and changes in serum clinical chemistry compared with TCDF and PCB126. A more thorough discussion of the association between differential gene expression and pathology was previously reported [29-31, 41]. QRTPCR confirmed the dose-dependent changes in expression for a subset of AhR-regulated genes (Figure 17). The classic members of the "AhR gene battery" involved in phase I and phase II metabolism including Cyp1a1, Cyp1a2, and Nqo1 [46] were induced. In addition, Tiparp previously reported to exhibit robust AhR-dependent expression [47, 48], and Notch1, implicated in cell differentiation and suggested to have a role in normal AhR signaling during liver development [31, 49], were also significantly expressed. The results from QRTPCR analysis were in good agreement with the microarray data.

DISCUSSION

In this study, the dose-dependent hepatic gene expression effects of TEF-adjusted, equipotent doses of TCDF and PCB126 (WHO TEF = 0.1) relative to TCDD (WHO TEF = 1) were examined at 24 h. In addition, complementary histopathology and EROD activity were assessed to associate dose-dependent changes in gene expression to higher order effects, at comparable TEF-adjusted TCDD, TCDF, and PCB126 tissue levels. Unlike comparable studies at later time points, the TEF-adjusted tissue levels for TCDD, TCDF, and PCB126 were comparable at 24 h, except for slight statistical differences at 0.1, 0.3, 100 and 300 μg/kg (dose × TEF). Therefore, differences in pharmacokinetics cannot be used to explain the weaker responses

elicited by equipotent, TEF-adjusted doses of TCDF and PCB126. By minimizing the differences in TEF-adjusted levels of TCDD, TCDF, and PCB126 in the liver, we further investigated qualitative and quantitative gene expression differences that may contribute to the weaker responses elicited by TCDF and PCB126.

Overall, the results of this 24 h study are consistent with our previous 72 h studies using a similar model, the same oligonucleotide microarrays, and the same analysis methods [28-30]. At the highest doses, 3000 μg/kg TCDF, 3000 μg/kg PCB126, and 300 μg/kg TCDD elicited comparable increases in RLW accompanied by similar levels of hepatocellular vacuolization, and minimal evidence of necrosis and immune cell infiltration at 24 h. Consequently, TEF-adjusted, equipotent doses of TCDF and PCB126 elicited comparable phenotypic level effects when compared to TCDD. However, at later time points (72 and 168 h), with more apparent differences in tissue levels, TCDD, TCDF, and PCB126 elicited different levels of vacuolization, necrosis, and immune cell infiltration [28-31], consistent with reported ligand-specific pharmacokinetics [25].

Despite comparable levels of vacuolization, necrosis, and immune cell infiltration at 24 h, there were significant differences in EROD activity induced by TCDF, PCB126, and TCDD. TCDF and PCB126 induced comparable EROD activity levels, resulting in ED_{50} values of 53.6 and 54.2 μg/kg, respectively. The EROD ED_{50} for TCDD was 1.1 μg/kg, comparable to the ED_{50} of 2.5 μg/kg in B6 mice at 24 h [50] and 1.6 μg/kg in C57BL/6 mice at 7 days [51]. This is also in agreement with the TCDF EROD ED_{50} at 72 h in terms of maximum EROD induction, as well as the ED_{50} values and REPs [28]. In addition, ED_{50} values for TCDD, TCDF, and PCB126 induction of Cyp1a1 mRNA levels (0.09, 2.5, and 3.9 μg/kg, respectively) were

Figure 17. QRTPCR verification of microarray responses.
QRTPCR verification of selected AhR-regulated genes: Cyp1a1, Cyp1a2, Nqo1, Tiparp and Notch1 for (A) TCDD, (B) PCB126, and (C) TCDF at 24 h. The same RNA samples used in the dose-response microarray studies were also used for QRTPCR analysis. All fold changes were calculated relative to vehicle controls. Bars (left y-axis) and lines (right y-axis) represent QRTPCR and microarray data, respectively. The genes are represented by their official gene symbols. Bars represent the mean ± SE of four independent QRTPCR samples. QRTPCR data were analyzed by ANOVA followed by Dunnett's *post hoc* test: *$p<0.05$ for vehicle vs. treated samples.

A

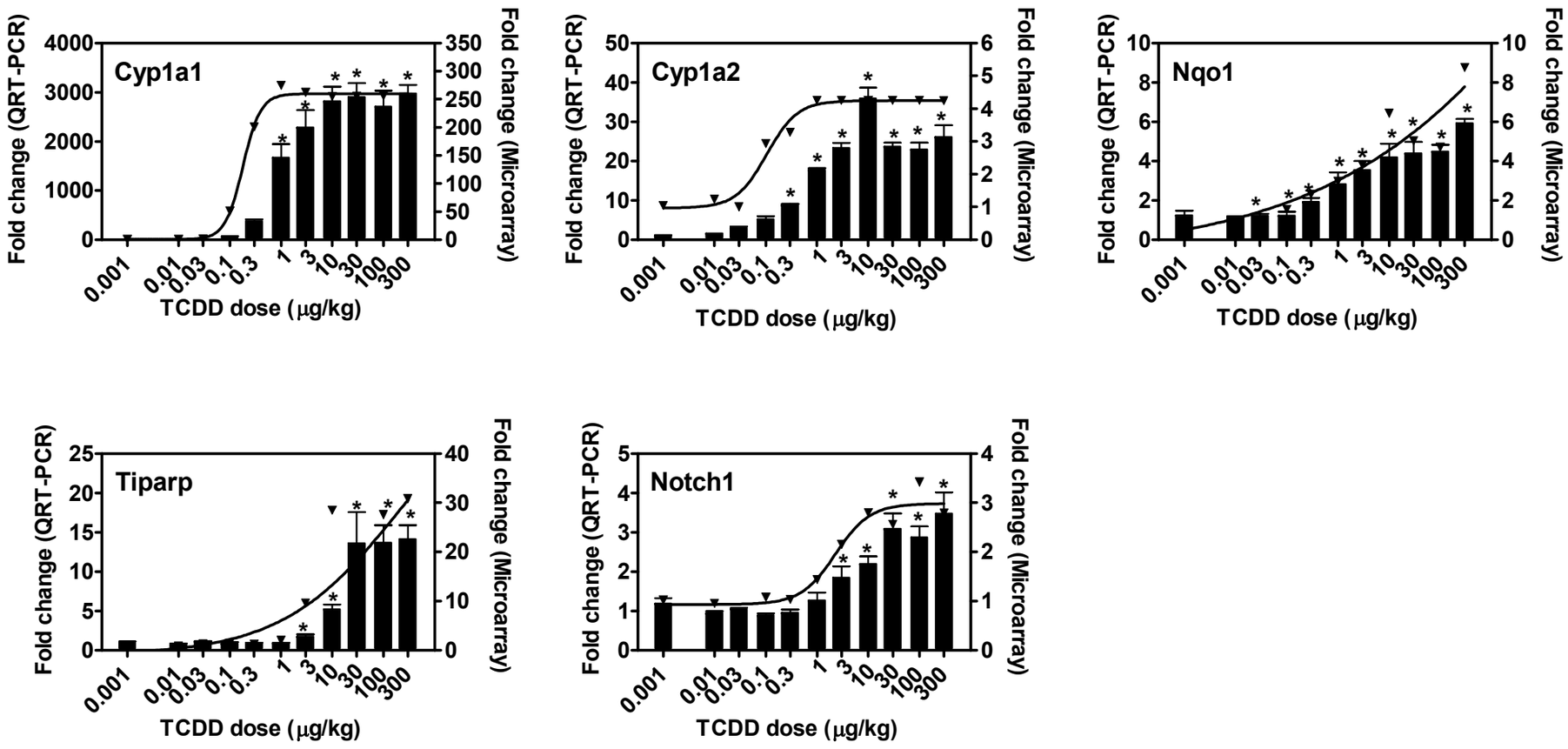
Cyp1a1
Cyp1a2
Nqo1
Tiparp
Notch1
Fold change (QRT-PCR)
Fold change (Microarray)
TCDD dose (μg/kg)
0.001
0.01
0.03
0.1
0.3
1
3
10
30
100
300

Figure 17 (cont'd).

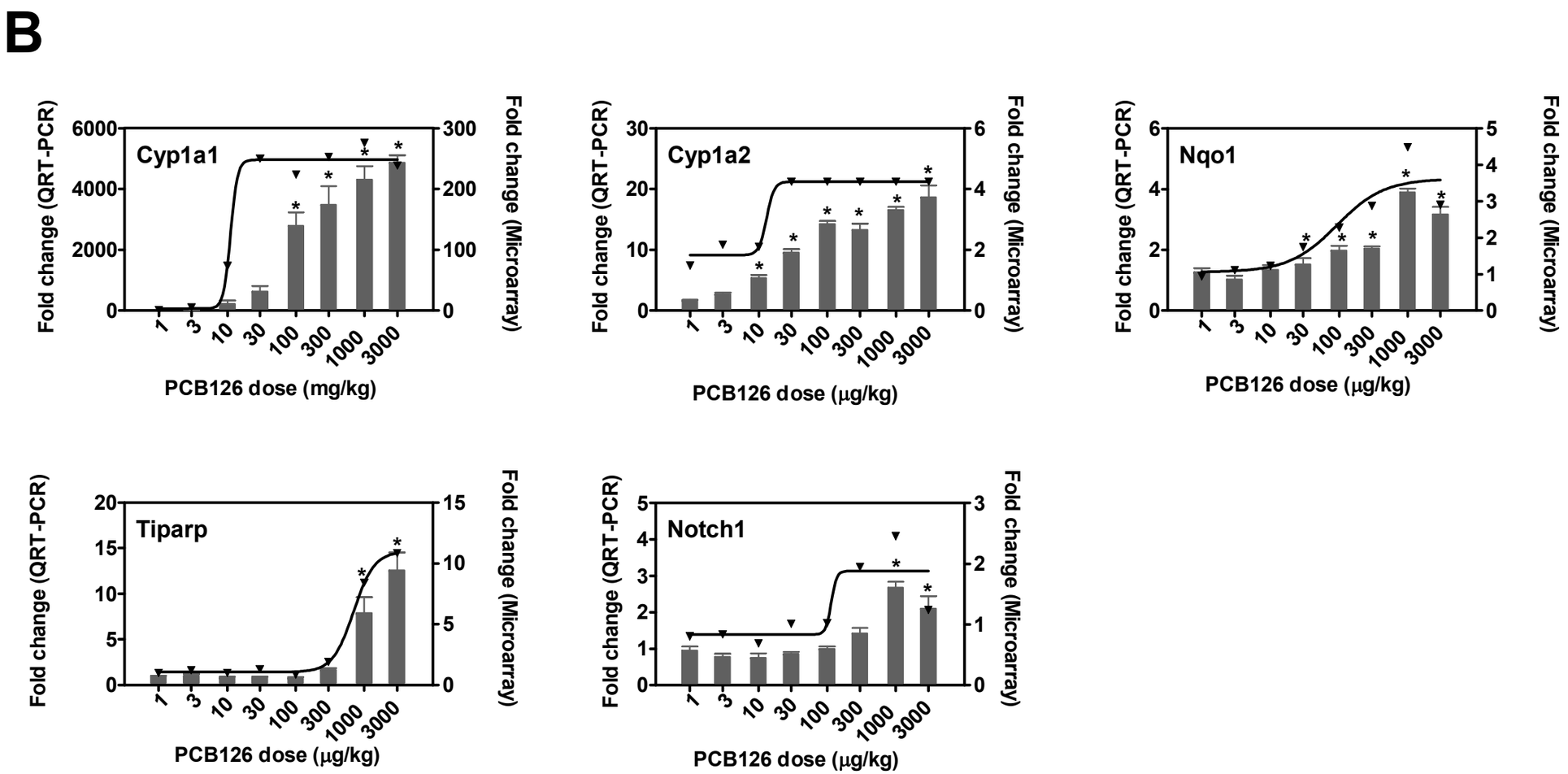

Figure 17 (cont'd).

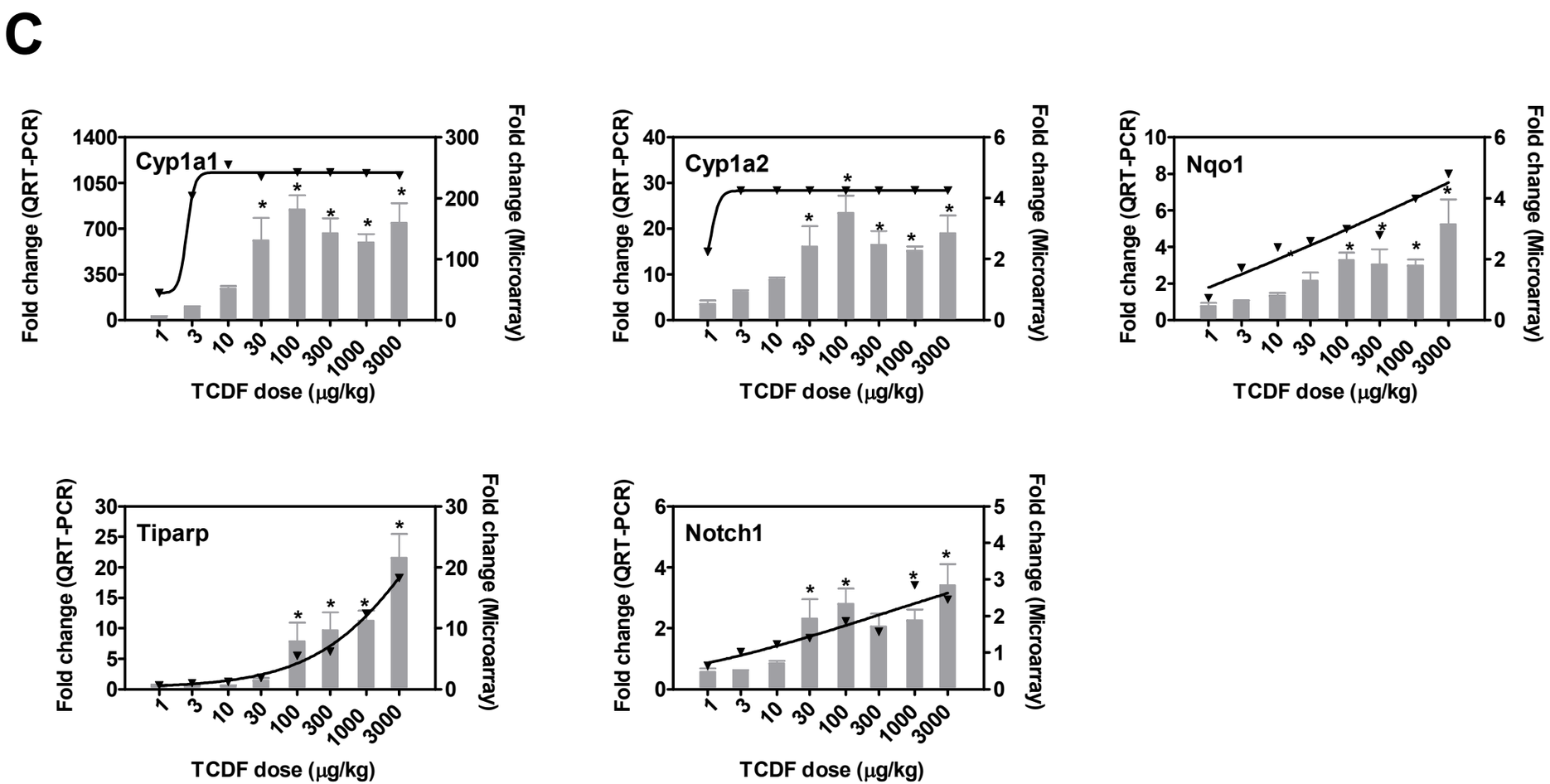

consistently lower compared with the corresponding EROD values (1.1, 53.6, and 54.2 μg/kg, respectively). The 0.09 μg/kg TCDD Cyp1a1 mRNA ED_{50} from this study is almost identical to that reported by Abel *et al*. in C57BL/6 mice at 24 h (0.08 μg/kg) [52]. Others have also reported lower ED_{50s} values for Cyp1a1 mRNA compared with EROD activity in B6C3F1 at the same time point (mRNA ED_{50} of 1.6 μg/kg and EROD ED_{50} of 5.3 μg/kg) [53]. Therefore, dose-dependent changes in gene expression may provide a more sensitive indicator of exposure, and possibly toxicity, provided an association can be established between gene function and the etiology of an adverse effect, assuming that a change in gene expression correlates with protein expression and activity.

TEF-adjusted, equipotent doses of TCDD, TCDF, and PCB126 did not elicit comparable gene expression changes. TCDD elicited the greatest number of differentially expressed genes in comparison to TCDF and PCB126 at TEF-adjusted equipotent doses. Furthermore, TCDF- and PCB126-elicited changes in gene expression were a subset of the genes differentially expressed by TCDD. Suggestions of TCDF- and PCB126-specific gene expression responses have been previously shown to be a statistical artifact. When hard cut-off values (P1(t)>0.99 and |fold change|>1.5) are relaxed (P1(t) >0.90 and |fold change|>1.5), almost all PCB126- and TCDF-elicited genes become a subset of genes differentially expressed by TCDD [29, 30] (Figure 16). However, the quantitatively lower number of TCDF- and PCB126-elicited differentially expressed genes cannot be fully attributed to differences in ligand pharmacokinetics. HRGC-HRMS analysis indicates the hepatic levels of TCDD, TCDF, and PCB126 at 24 h were essentially equipotent when TEF-adjusted. Consequently, the ability of the liganded AhR:ARNT complex to efficiently recruit the same complement of coactivators may also be an important

factor for overall congener potency. For example, gene transactivation is reported to be congener structure-, coactivator-, and cell context dependent [54].

In order to calculate gene-specific REP values, TCDD-, TCDF-, and PCB126-elicited gene expression changes with a P1(t) >0.90 and |fold change|>1.5 were analyzed using our automated dose-response modeler [39]. REPs for only 210 TCDF versus TCDD genes and 40 PCB126 versus TCDD genes were calculated to comply with WHO guidelines requiring sigmoidal dose-response curves with similar slopes and shapes [9, 18]. Overall, the TCDF median REP values at 24 (0.06) and 72 h (0.1) are similar. This difference may be attributed, in part, to the use of a wider dose range and higher doses of TCDF and TCDD in the 24 h study, and the use of intact mice in the 72 h study. In contrast, the PCB126 REP of 0.02 reflects its weaker potency even at TEF-adjusted doses. PCB126 treatment also resulted in a lower number of differentially regulated genes exhibiting a sigmoidal dose-response when compared to TCDD. Many PCB126-elicited gene expression changes were excluded due to poor induction (<1.5-fold) or because they did not exhibit a sigmoidal dose-response curve. Alternatively, REPs based on points of departure [39], lowest observable adverse effect level, and/or no observable adverse effect level could be also considered [9].

In summary, this study expands the available hepatic REP data for TCDF and PCB126 using immature ovariectomized C57BL/6 mice. It further suggests that at TEF-adjusted doses and at equipotent TEQ hepatic tissue levels, TCDF and PCB126 elicit weaker responses compared to TCDD. Therefore, in addition to pharmacokinetic differences, congener structure also plays an important role in gene expression potency and efficacy. Further associations of specific dose-responsive genes to toxic events are compromised by limited gene annotation and

an incomplete understanding of the mechanisms involved in the etiology of the toxic responses elicited by TCDD and related compounds.

REFERENCES

REFERENCES

1. Mason, G. and S. Safe, *Synthesis, biologic and toxic effects of the major 2,3,7,8-tetrachlorodibenzo-p-dioxin metabolites in the rat.* Toxicology, 1986. **41**(2): p. 153-9.

2. Poland, A. and E. Glover, *Studies on the mechanism of toxicity of the chlorinated dibenzo-p-dioxins.* Environ Health Perspect, 1973. **5**: p. 245-51.

3. Commoner, B., K. Shapiro, and T. Webster, *The Origin and Health Risks of PCDD and PCDF.* Waste Management & Research, 1987. **5**: p. 327-346.

4. Safe, S., et al., *Halogenated biphenyls: molecular toxicology.* Can J Physiol Pharmacol, 1982. **60**(7): p. 1057-64.

5. Mayes, B.A., et al., *Comparative carcinogenicity in Sprague-Dawley rats of the polychlorinated biphenyl mixtures Aroclors 1016, 1242, 1254, and 1260.* Toxicol Sci, 1998. **41**(1): p. 62-76.

6. Mullin, M.D., et al., *High-resolution PCB analysis: synthesis and chromatographic properties of all 209 PCB congeners.* Environ. Set Technol., 1984. **18**: p. 468-476.

7. Safe, S., *Polychlorinated biphenyls (PCBs), dibenzo-p-dioxins (PCDDs), dibenzofurans (PCDFs), and related compounds: environmental and mechanistic considerations which support the development of toxic equivalency factors (TEFs).* Crit Rev Toxicol, 1990. **21**(1): p. 51-88.

8. NTP, *NTP toxicology and carcinogenesis studies of 3,3',4,4',5-pentachlorobiphenyl (PCB 126) (CAS No. 57465-28-8) in female Harlan Sprague-Dawley rats (Gavage Studies).* NTP Technical Report, 2006(520): p. 4-246.

9. Van den Berg, M., et al., *The 2005 World Health Organization reevaluation of human and Mammalian toxic equivalency factors for dioxins and dioxin-like compounds.* Toxicol Sci, 2006. **93**(2): p. 223-41.

10. Safe, S., *Molecular biology of the Ah receptor and its role in carcinogenesis.* Toxicol Lett, 2001. **120**(1-3): p. 1-7.

11. Poland, A. and J.C. Knutson, *2,3,7,8-tetrachlorodibenzo-p-dioxin and related halogenated aromatic hydrocarbons: examination of the mechanism of toxicity.* Annu Rev Pharmacol Toxicol, 1982. **22**: p. 517-54.

12. Denison, M.S. and S. Heath-Pagliuso, *The Ah receptor: a regulator of the biochemical and toxicological actions of structurally diverse chemicals.* Bull Environ Contam Toxicol, 1998. **61**(5): p. 557-68.

13. Denison, M.S., et al., *Ligand binding and activation of the Ah receptor.* Chem Biol Interact, 2002. **141**(1-2): p. 3-24.

14. Nebert, D.W., et al., *Role of the aromatic hydrocarbon receptor and [Ah] gene battery in the oxidative stress response, cell cycle control, and apoptosis.* Biochem Pharmacol, 2000. **59**(1): p. 65-85.

15. Ahlborg, U.G., *Human health risk assessment and risk perception related to the Baltic Sea.* Arch Toxicol Suppl, 1994. **16**: p. 53-9.

16. Barnes, D.G., *Toxicity equivalents and EPA's risk assessment of 2,3,7,8-TCDD.* Sci Total Environ, 1991. **104**(1-2): p. 73-86.

17. Birnbaum, L.S. and M.J. DeVito, *Use of toxic equivalency factors for risk assessment for dioxins and related compounds.* Toxicology, 1995. **105**(2-3): p. 391-401.

18. Haws, L.C., et al., *Development of a refined database of mammalian relative potency estimates for dioxin-like compounds.* Toxicol Sci, 2006. **89**(1): p. 4-30.

19. Van den Berg, M., et al., *Toxic equivalency factors (TEFs) for PCBs, PCDDs, PCDFs for humans and wildlife.* Environ Health Perspect, 1998. **106**(12): p. 775-92.

20. Starr, T.B., et al., *The trouble with TEFs.* Environ Health Perspect, 1999. **107**(10): p. A492-3.

21. Safe, S., *Limitations of the toxic equivalency factor approach for risk assessment of TCDD and related compounds.* Teratog Carcinog Mutagen, 1997. **17**(4-5): p. 285-304.

22. Harris, M., T. Zacharewski, and S. Safe, *Comparative potencies of Aroclors 1232, 1242, 1248, 1254, and 1260 in male Wistar rats--assessment of the toxic equivalency factor (TEF) approach for polychlorinated biphenyls (PCBs).* Fundam Appl Toxicol, 1993. **20**(4): p. 456-63.

23. Budinsky, R.A., et al., *Recommended relative potency factors for 2,3,4,7,8-pentachlorodibenzofuran: the impact of different dose metrics.* Toxicol Sci, 2006. **91**(1): p. 275-85.

24. DeVito, M.J., et al., *Dose-response relationships for polyhalogenated dioxins and dibenzofurans following subchronic treatment in mice. I. CYP1A1 and CYP1A2 enzyme activity in liver, lung, and skin.* Toxicol Appl Pharmacol, 1997. **147**(2): p. 267-80.

25. DeVito, M.J., et al., *Dose-response relationships for disposition and hepatic sequestration of polyhalogenated dibenzo-p-dioxins, dibenzofurans, and biphenyls following subchronic treatment in mice.* Toxicol Sci, 1998. **46**(2): p. 223-34.

26. Diliberto, J.J., et al., *Subchronic Exposure of [3H]- 2,3,7,8-tetrachlorodibenzo-p-dioxin (TCDD) in female B6C3F1 mice: relationship of steady-state levels to disposition and metabolism.* Toxicol Sci, 2001. **61**(2): p. 241-55.

27. Safe, S.H., *Modulation of gene expression and endocrine response pathways by 2,3,7,8-tetrachlorodibenzo-p-dioxin and related compounds.* Pharmacol Ther, 1995. **67**(2): p. 247-81.

28. Burgoon, L.D., et al., *Automated Dose-Response Analysis of the Relative Hepatic Gene Expression Potency of TCDF in C57BL/6 Mice.* Toxicol Sci, 2009. **112**(1): p. 221-228.

29. Kopec, A.K., et al., *Comparative Toxicogenomic Examination of the Hepatic Effects of PCB126 and TCDD in Immature, Ovariectomized C57BL/6 Mice.* Toxicol Sci, 2008. **102**(1): p. 61-75.

30. N'Jai, A., et al., *Comparative temporal toxicogenomic analysis of TCDD- and TCDF-mediated hepatic effects in immature female C57BL/6 mice.* Toxicol Sci, 2008. **103**(2): p. 285-97.

31. Boverhof, D.R., et al., *Temporal and dose-dependent hepatic gene expression patterns in mice provide new insights into TCDD-Mediated hepatotoxicity.* Toxicol Sci, 2005. **85**(2): p. 1048-63.

32. Sheehan, D.C. and B.B. Hrapchak, *Theory and Practice of Histotechnology*. second ed ed. 1980, St. Louis: Mosby.

33. Moore, J.N., et al., *Hepatic P450 enzyme activity, tissue morphology and histology of mink (Mustela vison) exposed to polychlorinated dibenzofurans.* Arch Environ Contam Toxicol, 2009. **57**(2): p. 416-25.

34. Burgoon, L.D. and T.R. Zacharewski, *dbZach toxicogenomic information management system.* Pharmacogenomics, 2007. **8**(3): p. 287-91.

35. Burgoon, L.D., et al., *Protocols for the assurance of microarray data quality and process control.* Nucleic Acids Res, 2005. **33**(19): p. e172.

36. Eckel, J.E., et al., *Normalization of two-channel microarray experiments: a semiparametric approach.* Bioinformatics, 2005. **21**(7): p. 1078-83.

37. Eckel, J.E., et al., *Empirical bayes gene screening tool for time-course or dose-response microarray data.* J Biopharm Stat, 2004. **14**(3): p. 647-70.

38. Vandesompele, J., et al., *Accurate normalization of real-time quantitative RT-PCR data by geometric averaging of multiple internal control genes.* Genome Biol, 2002. **3**(7): p. RESEARCH0034.

39. Burgoon, L.D. and T.R. Zacharewski, *Automated quantitative dose-response modeling and point of departure determination for large toxicogenomic and high-throughput screening data sets.* Toxicol Sci, 2008. **104**(2): p. 412-8.

40. NTP, *NTP technical report on the toxicology and carcinogenesis studies of 2,3,7,8-tetrachlorodibenzo-p-dioxin (TCDD) (CAS No. 1746-01-6) in female Harlan Sprague-Dawley rats (Gavage Studies).* Natl Toxicol Program Tech Rep Ser, 2006(521): p. 4-232.

41. Boverhof, D.R., et al., *Comparative toxicogenomic analysis of the hepatotoxic effects of TCDD in Sprague Dawley rats and C57BL/6 mice.* Toxicol Sci, 2006. **94**(2): p. 398-416.

42. DeVito, M.J. and L.S. Birnbaum, *The importance of pharmacokinetics in determining the relative potency of 2,3,7,8-tetrachlorodibenzo-p-dioxin and 2,3,7,8-tetrachlorodibenzofuran.* Fundam Appl Toxicol, 1995. **24**(1): p. 145-8.

43. Budinsky, R.A., et al., *A pilot study of oral bioavailability of dioxins and furans from contaminated soils: Impact of differential hepatic enzyme activity and species differences.* Chemosphere, 2008. **70**(10): p. 1774-86.

44. Hamm, J.T., C.Y. Chen, and L.S. Birnbaum, *A mixture of dioxins, furans, and non-ortho PCBs based upon consensus toxic equivalency factors produces dioxin-like reproductive effects.* Toxicol Sci, 2003. **74**(1): p. 182-91.

45. Diliberto, J.J., et al., *Dose-response relationships of tissue distribution and induction of CYP1A1 and CYP1A2 enzymatic activities following acute exposure to 2,3,7,8-tetrachlorodibenzo-p-dioxin (TCDD) in mice.* Toxicol Appl Pharmacol, 1995. **130**(2): p. 197-208.

46. Nebert, D.W., D.D. Petersen, and A.J. Fornace, Jr., *Cellular responses to oxidative stress: the [Ah] gene battery as a paradigm.* Environ Health Perspect, 1990. **88**: p. 13-25.

47. Ma, Q., et al., *TCDD-inducible poly(ADP-ribose) polymerase: a novel response to 2,3,7,8-tetrachlorodibenzo-p-dioxin.* Biochem Biophys Res Commun, 2001. **289**(2): p. 499-506.

48. Tijet, N., et al., *Aryl hydrocarbon receptor regulates distinct dioxin-dependent and dioxin-independent gene batteries.* Mol Pharmacol, 2006. **69**(1): p. 140-53.

49. Harper, J.A., et al., *Notch signaling in development and disease.* Clin Genet, 2003. **64**(6): p. 461-72.

50. Ma, X., N.A. Mufti, and J.G. Babish, *Protein tyrosine phosphorylation as an indicator of 2,3,7,8-tetrachloro-p-dioxin exposure in vivo and in vitro.* Biochem Biophys Res Commun, 1992. **189**(1): p. 59-65.

51. Lin, F.H., et al., *The effects of 2,3,7,8-tetrachlorodibenzo-p-dioxin (TCDD) on the hepatic estrogen and glucocorticoid receptors in congenic strains of Ah responsive and Ah nonresponsive C57BL/6J mice.* Toxicol Appl Pharmacol, 1991. **108**(1): p. 129-39.

52. Abel, J., et al., *Dose-response relationship of cytochrome P4501b1 mRNA induction by 2,3,7,8-tetrachlorodibenzo-p-dioxin in livers of C57BL/6J and DBA/2J mice.* Arch Toxicol, 1996. **70**(8): p. 510-3.

53. Narasimhan, T.R., et al., *Relative sensitivities of 2,3,7,8-tetrachlorodibenzo-p-dioxin-induced Cyp1a-1 and Cyp1a-2 gene expression and immunotoxicity in female B6C3F1 mice.* Fundam Appl Toxicol, 1994. **23**(4): p. 598-607.

54. Zhang, S., C. Rowlands, and S. Safe, *Ligand-dependent interactions of the Ah receptor with coactivators in a mammalian two-hybrid assay.* Toxicol Appl Pharmacol, 2008. **227**(2): p. 196-206.

CHAPTER 5

Kopec AK, Burgoon LD, Ibrahim-Aibo D, Mets BM, Tashiro C, Potter D, Sharratt B, Harkema JR, Zacharewski TR: **PCB153-Elicited Hepatic Responses in the Immature, Ovariectomized C57BL/6 Mice: Comparative Toxicogenomic Effects of Dioxin and Non-dioxin-like Ligands**. *Toxicol Appl Pharmacol* 2010, 243:359-371.

CHAPTER 5

PCB153-ELICITED HEPATIC RESPONSES IN THE IMMATURE, OVARIECTOMIZED C57BL/6 MICE: COMPARATIVE TOXICOGENOMIC EFFECTS OF DIOXIN AND NON-DIOXIN-LIKE LIGANDS

ABSTRACT

Polychlorinated biphenyls (PCBs) are ubiquitous contaminants found as complex mixtures of coplanar and non-coplanar congeners. The hepatic temporal and dose-dependent effects of the most abundant non-dioxin-like congener, 2,2',4,4',5,5'-hexachlorobiphenyl (PCB153), were examined in immature, ovariectomized C57BL/6 mice, and compared to 2,3,7,8-tetrachlorodibenzo-*p*-dioxin (TCDD), the prototypical aryl hydrocarbon receptor (AhR) ligand. Animals were gavaged once with 300 mg/kg PCB153 or sesame oil vehicle and sacrificed 4, 12, 24, 72 or 168 h post dose. In the dose-response study, mice were gavaged with 1, 3, 10, 30, 100 or 300 mg/kg PCB153 or sesame oil for 24 h. Significant increases in relative liver weights were induced with 300 mg/kg PCB153 between 24 and 168 h, accompanied by slight vacuolization and hepatocellular hypertrophy. The hepatic differential expression of 186 and 177 genes was detected using Agilent 4 × 44 K microarrays in the time course (|fold change|≥1.5, P1(*t*)≥0.999) and dose-response (|fold change|≥1.5, P1(*t*)≥0.985) studies, respectively. Comparative analysis with TCDD suggests that the differential gene expression elicited by PCB153 was not mediated by the AhR. Furthermore, constitutive androstane and pregnane X receptor (CAR/PXR) regulated genes including Cyp2b10, Cyp3a11, Ces2, Insig2,

and Abcc3 were dose-dependently induced by PCB153. Collectively, these results suggest that the hepatocellular effects elicited by PCB153 are qualitatively and quantitatively different from TCDD and suggestive of CAR/PXR regulation.

INTRODUCTION

Polychlorinated biphenyls (PCBs), manufactured in the United States from 1929 to 1977, had various applications as coolants, insulating fluids for transformers and capacitors, plasticizers in paints and cements, pesticide extenders, lubricating oils, and sealants [1, 2]. Their chemical stability and lipophilic properties facilitated their distribution, persistence, and biomagnification in the food chain, particularly in fatty tissues [3].

PCBs and related compounds elicit tissue- and species-specific effects including hepatotoxicity, immune suppression, reproductive toxicity, endocrine disruption, developmental toxicity, and carcinogenicity [4, 5]. They are classified as coplanar, designated dioxin-like based on their structural similarity to 2,3,7,8-tetrachlorodibenzo-*p*-dioxin (TCDD), and non-coplanar [1]. The effects of TCDD and dioxin-like PCBs, such as 3,3',4,4',5-pentachlorobiphenyl (PCB126), are mediated by the aryl hydrocarbon receptor (AhR), facilitating the toxicity assessment of dioxin-like PCB mixtures to be expressed as toxic equivalents relative to TCDD [6]. TCDD and related dioxin-like PCBs are more toxic than non-coplanar PCBs, which contain *ortho* chlorine substituents on the biphenyl ring, which significantly reduces their binding affinity for the AhR [7]. Despite their non-dioxin-like characteristics, non-coplanar PCBs account for a majority of the PCBs found in environmental and biological samples.

Non-coplanar 2,2',4,4',5,5'-hexachlorobiphenyl (PCB153) is the congener found at the highest concentrations in human samples on a molar basis [8, 9]. PCB153 bears little structural resemblance to TCDD, has little to no AhR binding affinity, and elicits a unique toxicity profile

relative to TCDD and other coplanar PCBs, and therefore is not assigned a TEF value. Its mode of action has not been fully elucidated, but based on its structural similarity to phenobarbital and limited gene expression activity, it may be mediated via the constitutive androstane receptor (CAR)/ pregnane X receptor (PXR) [10-14].

Previous studies have demonstrated non-additive interactions between PCB153 and dioxin-like compounds [15-18]. PCB153 partially antagonizes TCDD-mediated cleft palate and immunotoxicity, as well as suppresses hepatic microsomal ethoxyresorufin-O-deethylase (EROD) induction in C57BL/6 mice [15]. Immunohistochemistry of rat livers following co-treatment with PCB126 and PCB153 also showed differential induction of Cyp1a1 compared to PCB126 alone [16]. In addition, PCB126 and PCB153 co-treatment synergistically altered hepatocellular foci development and expression of γ-glutamyltranspeptidase [18]. Consequently, a more thorough examination of PCB153 is warranted in order to further elucidate the mechanisms involved in these non-additive activities.

In this report, time course and dose-dependent gene expression studies with complementary histopathology, gas chromatography/mass spectrometry (GC/MS) lipid profiling and high-resolution gas chromatography/high-resolution mass spectrometry (HRGC-HRMS) tissue level analyses were conducted to investigate the hepatic effects elicited by PCB153 in immature, ovariectomized C57BL/6 mice. Comparisons were made to comparable TCDD and PCB126 studies, which used the same model, study design and data analysis strategies [19, 20].

MATERIALS & METHODS

ANIMAL HUSBANDRY

Immature female C57BL/6 mice, ovariectomized by the supplier on postnatal day (PND) 20, with body weights (BW) within 10% of the average, were obtained from Charles Rivers

Laboratories (Portage, MI) on PND 25. Animals were housed in polycarbonate cages (n=5 per cage) containing cellulose fiber chips (Aspen Chip Laboratory Bedding, Northeastern Products, Warrensberg, NY) with 30-40% humidity and a 12 h light/dark cycle (07:00 h – 19:00 h). Mice had free access to deionized water and were fed *ab libitum* with Harlan Teklad 22/5 Rodent Diet 8640 (Madison, WI). Animals were acclimatized for 3 days prior to dosing on PND 28. The immature ovariectomized mouse was used to facilitate comparisons with other data sets obtained using the same model, study design and analysis methods [19, 20]. Immature animals were used because they are more responsive to AhR ligands. The animals were ovariectomized to negate potential interactions with estrogens produced by the developing ovaries, since some animals in our studies are approaching reproductive maturity. All procedures were carried out with the approval of the Michigan State University All-University Committee on Animal Use and Care.

DOSE-RESPONSE AND TIME COURSE STUDIES

A stock solution of PCB153 (99.9% purity, AccuStandard, New Haven, CT) was first dissolved in acetone (J.T. Baker), followed by a dilution with sesame oil (Sigma, St. Louis, MO), and evaporation of the acetone using nitrogen gas. The PCB153 stock solution was further diluted using sesame oil to achieve the desired dose. Animals were orally gavaged using 1.5 inch feeding needle with a 2.25 mm ball end (Cadence Science: formerly Popper and Sons, Lake Success, NY). For the dose-response study, mice (n=5 per group) were administered 0.1 ml of a single dose of 1, 3, 10, 30, 100 or 300 mg/kg of PCB153 or 0.1 ml pure sesame oil vehicle (Sigma) and sacrificed 24 h post-treatment. The 300 mg/kg PCB153 dose was used in a complementary time course study, as it was the highest dose examined that did not alter body weight gain. Animals were gavaged with either 300 mg/kg PCB153 or sesame oil vehicle and sacrificed at 4, 12, 24, 72 or 168 h. For direct comparisons between dioxin-like and non-dioxin-

like responses, additional animals were treated with 30 μg/kg TCDD and sacrificed at the same time points. Furthermore, additional data sets generated using the same animal model, study design and analysis methods for 30 μg/kg TCDD and 300 μg/kg PCB126 [19, 20] served as comparators for this study. Mice were sacrificed by cervical dislocation and tissue samples were removed, weighed, flash frozen in liquid nitrogen, and stored at –80°C. For both the time course and dose-response studies, the section of the right liver lobe was fixed in 10% neutral buffered formalin (Sigma) for histological analysis.

HISTOLOGICAL ANALYSES

Fixed liver tissues were sectioned and processed in ethanol, xylene, and paraffin using a Thermo Electron Excelsior tissue processor (Waltham, MA). Tissues were embedded in paraffin with Miles Tissue Tek II embedding center, after which paraffin blocks were sectioned at 5 μm with a rotary microtome. Liver sections were placed on glass microscope slides, washed twice in xylene for 5 min, followed by four quick washes in ethanol and rinsing in water. Slides were placed in Gill 2 hematoxylin (Thermo Fisher Scientific, Waltham, MA) for 1.5 min followed by 2-3 quick dips in 1% glacial acetic acid water and rinsed with running water for 2-3 min. Slides were then rinsed in ethanol and counterstained with 1% eosin Y-phloxine B solution (Sigma) followed by multiple rinses in ethanol and xylene. For lipid staining, liver sections were frozen in Tissue-Tek O.C.T. compound (Sakura, Torrance, CA) before further processing. Liver samples were sectioned at 6 μm, fixed in 10% neutral buffered formalin for 5 min, rinsed with water and immersed in 100% propylene glycol for 5 min. The slides were stained with Oil Red O solution (Sigma) for 8 min at 60°C. Following staining, slides were placed in 80% propylene glycol for 5 min and rinsed in water for 15 min. Slides were counterstained with Gill 2 hematoxylin for 30 sec and washed with water for 30 min. Coverslips were attached using

aqueous mounting media. All the histological processing was performed at Michigan State University Investigative HistoPathology Laboratory, Division of Human Pathology using a modified version of previously published procedures [21].

LIPID ANALYSIS BY GAS CHROMATOGRAPHY-MASS SPECTROMETRY (GC-MS)

Liver samples (~100 mg) from the 24, 72, 168 h PCB153, TCDD and vehicle control groups were homogenized (Polytron PT2100, Kinematica AG, Luzern, CH) in 40% methanol and acidified with concentrated HCl. Lipids were extracted with chloroform: methanol (2:1) containing 1 mM 2,6-di-tert-butyl-4-methylphenol (BHT; Sigma) and extraction efficiency controls (19:1n9 FFA [free fatty acid] and 19:0 TAG [triacylglycerol]) were added (Nu-Chek Prep, Elysian, MN). Protein and aqueous phases were re-extracted with chloroform and the organic phases were pooled. A derivatization standard (19:2n6 FFA; Nu-Chek Prep) was added and samples were dried under nitrogen, resuspended in 2% non-aqueous methanolic HCl and incubated at 60ºC overnight. Samples were cooled to room temperature (RT) and 0.9% (w/v) NaCl and hexane were added. The organic phase was collected and a loading control (17:1n9 fatty acid methyl ester [FAME]; Nu-Chek Prep) was added. Samples were dried under nitrogen, resuspended in equal volumes of hexane and separated on Agilent 6890N gas chromatograph interfaced to Agilent 5973 mass spectrometer with DB23 column (30 m length, 0.25 mm internal diameter, 0.25 μm film thickness). Samples were run on the following temperature program: 50°C to 150°C at 40°C/ min, to 185°C at 5°C/ min, to 235°C at 3°C/ min, to 250°C at 10°C/ min. Principal component analysis (PCA) of lipid profiles was performed in R 2.6.0, data were extracted and used to generate PCA plots in GraphPad Prism 4.0.

HEPATIC TRIGLYCERIDE MEASUREMENT

Frozen liver samples (~100 mg) were homogenized (Polytron PT2100, Kinematica) in 1 ml of 1.15% KCl. Triglycerides were extracted from 200 µl of hepatic homogenate with 800 µl of isopropyl alcohol by vortex-mixing for 10 min. The samples were centrifuged for 5 min at 800 x g at RT and supernatant was collected into separate vials. The concentration of hepatic triglycerides was determined using a commercial L-Type Triglyceride M kit (Wako Diagnostics, Richmond, VA) with Multi-Calibrator Lipids as a standard (Wako Diagnostics). The measurements were performed according to manufacturer's protocol with 20 µl of the triglyceride extract incubated with 150 µl of Reagent 1 followed by incubation with 50 µl of Reagent 2. Final results were normalized to the starting amount of liver.

QUANTIFICATION OF PCB153 AND TCDD TISSUE LEVELS

Liver samples were processed in parallel with laboratory blanks and a reference or background sample at Wellington Laboratories Inc. (Guelph, ON, Canada). The samples (100 to 500 mg) were transferred to a tared screw cap culture tube and weight recorded. The sample was spiked with $^{13}C_{12}$-PCB153 and $^{13}C_{12}$-2,3,7,8-TCDD surrogates and then digested with hydrochloric acid. Each digested sample was then split between two screw cap tubes and hexane (3-4 ml) was added to each tube followed by vigorous mixing. The tubes were centrifuged, and the organic layer removed. The hexane extraction was performed three times per screw cap tube and the six hexane fractions were combined. The hexane fraction was then split evenly prior to clean-up and one fraction was archived. The other fraction was cleaned-up using a small multilayer (acid/base/neutral) silica gel column eluted with 20-25 ml of hexane. The eluate was concentrated on a rotary evaporator and then transferred to a conical microvial with pentane and dichloromethane rinses and allowed to dry. Immediately prior to injection on the high-resolution

gas chromatograph/high-resolution mass spectrometer (HRGC-HRMS) system, $^{13}C_{12}$-PCB111 and $^{13}C_{12}$-1,2,3,4-TCDD injection standards were added to the conical microvial.

Sesame oil (control) samples (100 to 500 mg) were weighed into tared screw cap tubes, spiked with $^{13}C_{12}$-PCB153 and $^{13}C_{12}$-2,3,7,8-TCDD surrogates, and diluted in 5 ml of hexane. The controls were then mixed and digested with 5 ml of sulfuric acid. The tube was centrifuged and the hexane layer was removed, split evenly with one half subjected to the same clean-up as the liver samples.

Harlan Teklad 22/5 Rodent Diet 8640 feed samples were crushed and weighed (~8 g) into a pre-extracted cellulose thimble. The samples were then spiked with $^{13}C_{12}$-PCB153 and $^{13}C_{12}$-2,3,7,8-TCDD surrogates prior to Soxhlet extraction overnight with dichloromethane. The samples were concentrated on a rotary evaporator and, transferred to a screw cap tube with hexane. The samples were then mixed and digested with 5 ml of sulfuric acid. Following centrifugation, the hexane layer was removed, split evenly, and processed as described above.

The identification and quantification of PCB153 and TCDD was performed using an Agilent (Santa Clara, CA, USA) 6890 series HRGC with direct capillary interface to a Waters (Milford, MA, USA) Autospec Ultima HRMS. Chromatographic separations were carried out on a 60 m DB5 (0.25 mm ID, 0.25 µm film thickness) column in constant flow mode (Helium, 1 ml /min). All injections were 1 µl and a splitless injection was used. The mass spectrometer was operated in EI+ selective ion recording mode (SIR) at a mass resolving power of 10,000 or greater.

RNA ISOLATION

Frozen liver samples (~100 mg, stored at –80°C) were immediately transferred to 1 ml TRIzol (Invitrogen, Carlsbad, CA) and homogenized using a Mixer Mill 300 tissue homogenizer (Retsch, Germany). Total RNA was isolated according to the manufacturer's protocol with an additional acid phenol:chloroform extraction. Isolated RNA was resuspended in RNA storage solution (Ambion Inc., Austin, TX), quantified (A_{260}), and quality was assessed by determining the A_{260}/A_{280} ratio and by visual inspection of 2 μg on a denaturing gel.

MICROARRAY EXPERIMENTAL DESIGN

PCB153-, TCDD-treated and vehicle samples were individually hybridized to 4 × 44K whole mouse genome oligo microarrays (Agilent Technologies, Inc., Santa Clara, CA). Hybridizations were performed with three biological replicates using one-color labeling (Cy3) for each time point and dose, according to the manufacturer's protocol (Agilent Manual: G4140-90040 v. 5.7). Published reports suggest that one- and two-color microarrays provide comparable data, with no significant differences detected when compared to studies utilizing Cy3 and Cy5 labeling [22]. Microarray slides were scanned at 532 nm (Cy3) on a GenePix 4000B scanner (Molecular Devices, Union City, CA). Images were analyzed for feature and background intensities using GenePix Pro 6.0 (Molecular Devices). All data were managed in TIMS dbZach data management system [23].

MICROARRAY ANALYSIS

All microarray data in this study passed our laboratory quality assurance protocol [24]. Microarray data were normalized using a semiparametric approach [25] and the posterior probabilities were calculated using an empirical Bayes method based on a per gene and time point or dose basis using model-based *t* values [26]. Gene expression data were ranked and

prioritized using a |fold change|≥1.5 and P1(t) values ≥0.999 for the temporal PCB153 and TCDD data sets. However, relaxed P1(t) values (≥0.985) were also used for the PCB153 dose-response data to identify differentially expressed genes that approached the selection cut-offs to ensure the identification of ligand-specific regulation. In addition, the different statistical cut-offs were used to obtain a comparable number of differentially expressed genes between the temporal and dose-dependent microarray data sets and to account for studies being performed at two different times.

DOSE-RESPONSE MODELING

Dose-response modeling was performed using a grid-enabled version of the ToxResponse Modeler [27]. ToxResponse Modeler performs automated dose-response modeling by identifying the best fit model amongst five different mathematical model families (linear, exponential, Gaussian, sigmoidal, quadratic). The algorithm then chooses the best-fit of the five best in-class models. The overall best-fit model is then used to calculate the ED_{50} values. The microarray dose-response PCB153 data set was first filtered using a P1(t)>0.90 cut-off and the filtered data were analyzed to identify genes exhibiting a sigmoidal dose-response profile.

DNA RESPONSE ELEMENT ANALYSIS MODELING

Dioxin response elements (DREs) [28], constitutive androstane receptor response elements (CAREs) [29] and pregnane X receptor response elements (PXREs) were identified computationally using position weight matrices (PWMs) specific to each site. The PXRE PWM was generated using seven published response elements that were aligned to the genome [30-35]. Gene regulatory regions (-10,000 relative to the transcriptional start site [TSS] together with 5'-untranslated region [UTR]) were obtained from the University of California, Santa Cruz, Genome Browser for mouse (build 37), computationally searched, and each DRE, CARE and

PXRE was scored. Matrix similarity scores (MSS) >0.80 are considered to be putative functional response elements.

QUANTITATIVE REAL-TIME PCR (QRTPCR)

QRTPCR verification of selected microarray data was performed as described previously [19]. Briefly, 1 μg of total RNA was reverse transcribed by SuperScript II (Invitrogen) using an anchored oligo-dT primer as described by the manufacturer. The cDNA (1.0 μl) was used as a template in a 30 μl PCR reaction containing 0.1 μM of forward and reverse gene-specific primers, 3 mM $MgCl_2$, 1 mM dNTPs, 0.025 IU AmpliTaq Gold, and 1× SYBR Green PCR buffer (Applied Biosystems, Foster City, CA). PCR amplification was conducted on an Applied Biosystems PRISM 7500 Sequence Detection System. cDNAs were quantified using a standard curve approach and the copy number of each sample was standardized to 3 housekeeping genes (ActB, Gapdh, Hprt) to control for the differences in RNA loading, quality, and cDNA synthesis [36] . For graphing purposes, the relative expression levels were scaled such that the expression level of the time-matched control group was equal to one.

FUNCTIONAL GENE ANNOTATION AND STATISTICAL ANALYSIS

Annotation and functional categorization of differentially regulated genes were performed using Database for Annotation, Visualization and Integrated Discovery (DAVID) [37]. All statistical analyses were performed with SAS 9.1 (SAS Institute, Cary, NC). All data were analyzed by analysis of variance (ANOVA) followed by Tukey's or Dunnett's *post hoc* tests. Differences between treatment groups were considered significant when $p<0.05$.

RESULTS

ORGAN AND BODY WEIGHTS

In the time course study, 300 mg/kg PCB153 increased ($p<0.05$) relative liver weight (RLW) at 72 and 168 h (Table 11), comparable to other reports using lower doses [9, 10]. In the dose-response study, 300 mg/kg significantly increased RLW at 24 h (Table 12), similarly to 30 μg/kg TCDD and 300 μg/kg PCB126, which also increased RLW at later time points (Table 11) [19, 20]. No significant decreases in body weight gain were observed at any of the PCB153 doses or time points, in agreement with other reports with doses as high as 360 mg/kg [10, 15].

HEPATIC TISSUE LEVEL QUANTIFICATION

HRGC-HRMS analysis of liver samples at 24 and 168 h time points indicate that PCB153 levels (in pg/g) exhibited different hepatic accumulation kinetics relative to TCDD (Figure 18A). PCB153 levels dramatically decreased (~3.3 fold) after 7 days, compared to TCDD which exhibited modest reductions (~1.4 fold), and in contrast to PCB126 which continued to increase throughout the study, reaching the highest concentration at 7 days [20]. These differences may be partially due to the induction of Cyp1a2 (~30 fold), which sequesters TCDD and dioxin-like compounds in the liver [38] (Figure 23A). PCB153 only marginally induced Cyp1a2 (~1.8 fold) (Figure 23B), which may account for the time dependent decrease of hepatic PCB153 levels.

PCB153 exhibited a dose-dependent increase in hepatic levels that was significantly different from controls (Figure 18B). Interestingly, hepatic PCB153 levels for sesame oil treated controls (Figure 18B) were ~500 times higher than the corresponding PCB126 or TCDD levels [20]. High levels in vehicle animals have been attributed to the ingestion of PCB153 found in rodent chow [39, 40]. However, only 62.1 pg/g of PCB153 was detected in Harlan Teklad 22/5 Rodent Diet 8640 using HRGC-HRMS, while levels in sesame oil were below the limits of

Table 11. Temporal effects of 300 mg/kg PCB153 and 30 µg/kg TCDD on terminal body, body weight gain, absolute liver weight. and relative liver weight.

Sacrifice time (h)	Treatment	Terminal body weight (g)	Body weight gain	Liver weight (g)	Relative liver weight
4	Vehicle	12.5 ± 0.5	1.0 ± 0.0	0.666 ± 0.028	0.053 ± 0.002
	PCB153	12.5 ± 0.8	1.0 ± 0.0	0.712 ± 0.048	0.057 ± 0.001
	TCDD	13.6 ± 0.8	1.0 ± 0.0	0.733 ± 0.044	0.054 ± 0.003
12	Vehicle	14.0 ± 0.7	1.0 ± 0.0	0.766 ± 0.048	0.055 ± 0.001
	PCB153	13.0 ± 0.6	1.0 ± 0.0	0.730 ± 0.075	0.056 ± 0.003
	TCDD	12.8 ± 0.7	1.1 ± 0.0	0.724 ± 0.025	0.056 ± 0.001
24	Vehicle	14.4 ± 0.9	1.1 ± 0.0	0.814 ± 0.070	0.056 ± 0.003
	PCB153	13.3 ± 0.9	1.1 ± 0.0	0.813 ± 0.137	0.061 ± 0.009
	TCDD	14.2 ± 0.9	1.1 ± 0.0	0.973 ± 0.088	0.068 ± 0.003*
72	Vehicle	15.6 ± 1.5	1.2 ± 0.0	0.918 ± 0.055	0.059 ± 0.005
	PCB153	15.7 ± 0.7	1.1 ± 0.0	1.086 ± 0.135	0.069 ± 0.007*
	TCDD	15.1 ± 0.7	1.2 ± 0.1	1.068 ± 0.060	0.071 ± 0.003*
168	Vehicle	17.6 ± 0.4	1.4 ± 0.1	1.017 ± 0.082	0.058 ± 0.004
	PCB153	17.9 ± 1.2	1.4 ± 0.1	1.280 ± 0.074	0.072 ± 0.002*
	TCDD	17.5 ± 0.4	1.3 ± 0.0	1.263 ± 0.080	0.072 ± 0.003*

Note. Values represent mean ± SD of five independent replicates. Body weight gain is represented as terminal body weight divided by body weight prior to dosing. An asterisk (*) indicates $p<0.05$ vs. vehicle.

Table 12. Dose-dependent effects of PCB153 on terminal body, body weight gain, absolute liver weight and relative liver weight at 24 h.

Dose (mg/kg)	Treatment	Terminal body weight (g)	Body weight gain	Liver weight (g)	Relative liver weight
0	Vehicle	11.8 ± 1.9	1.1 ± 0.0	0.694 ± 0.085	0.059 ± 0.006
1	PCB153	14.3 ± 1.8	1.1 ± 0.0	0.850 ± 0.121	0.059 ± 0.002
3	PCB153	14.4 ± 1.7	1.1 ± 0.0	0.865 ± 0.119	0.060 ± 0.002
10	PCB153	12.7 ± 1.1	1.1 ± 0.1	0.721 ± 0.073	0.056 ± 0.004
30	PCB153	13.4 ± 1.0	1.1 ± 0.0	0.836 ± 0.066	0.062 ± 0.001
100	PCB153	13.8 ± 1.1	1.1 ± 0.0	0.829 ± 0.071	0.060 ± 0.002
300	PCB153	12.7 ± 1.9	1.1 ± 0.0	0.855 ± 0.152	0.067 ± 0.003*

Note. Values represent mean ± SD of five independent replicates. Body weight gain is represented as terminal body weight divided by body weight prior to dosing. An asterisk (*) indicates $p<0.05$ vs. vehicle.

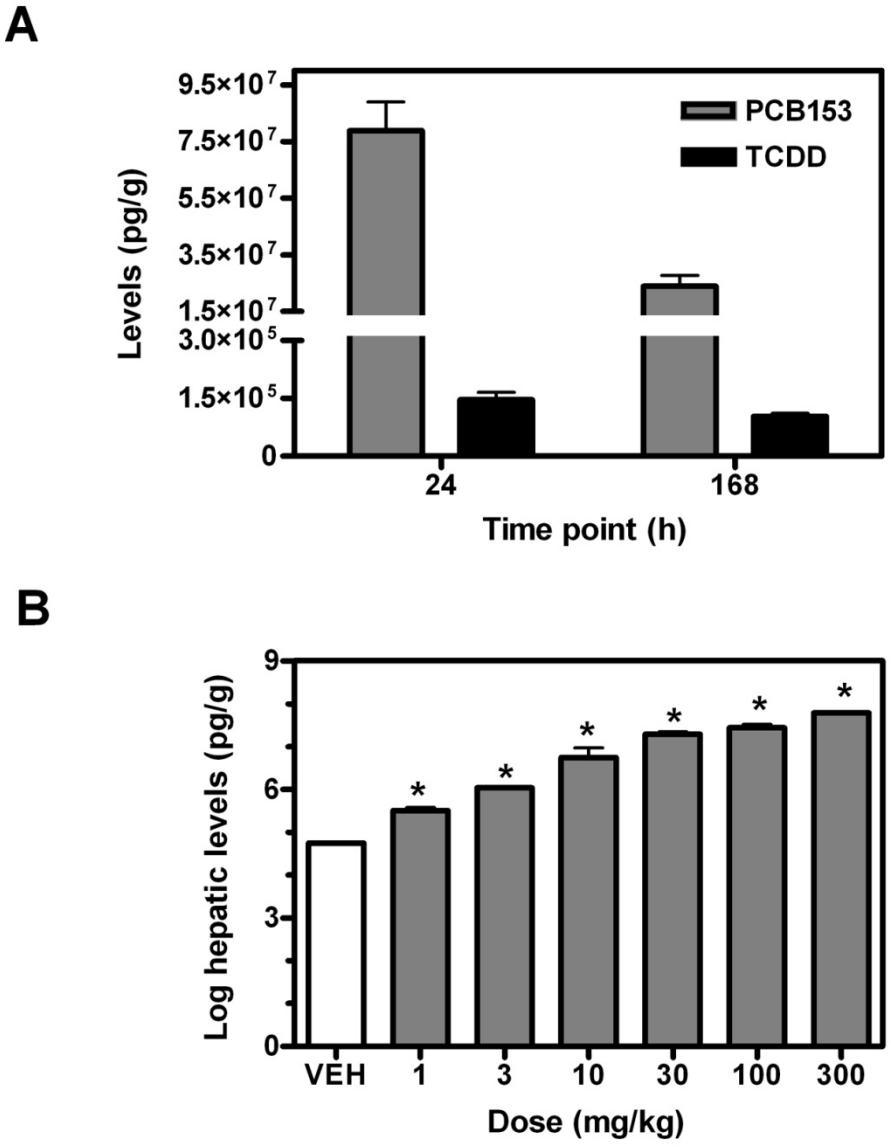

Figure 18. Hepatic PCB153 and TCDD levels per g liver wet weight measured using HRGC-HRMS.

(A) Mice were gavaged with 300 mg/kg PCB153 or 30 µg/kg TCDD. Hepatic levels of PCB153 showed a dramatic decrease (~3.3 fold) after 7 days, compared to TCDD, which exhibited more modest decreases (~1.4 fold). (B) PCB153 levels attained in the 24 h dose-response study. The results are displayed as the mean ± standard error (SE) of at least three independent samples. Dose-response data are displayed on a log scale to visualize tissue levels at all doses. An asterisk (*) indicates a significant ($p<0.05$) difference between the treated samples and vehicle (VEH) controls.

detection (data not shown). Others suggest that non-dioxin-like PCBs may also accumulate in animals via lactational transfer [41].

HISTOPATHOLOGY

PCB153 induced minimal hepatocellular vacuolization (Figure 19C), comparable to the levels observed in vehicle controls (Figure 19A). In contrast, TCDD-elicited vacuolization was more severe and localized to the periportal regions and extended to the midzonal and centrilobular regions in more severely affected mice. TCDD treatment also resulted in moderate multifocal inflammation (Figure 19B, arrow), which was almost absent in the PCB153-treated mice. However, PCB153 elicited increasing hypertrophic responses between 24 and 168 h. Furthermore, Oil Red O staining (ORO) identified significant lipid accumulation only in the TCDD-treated animals, while PCB153 livers showed no fatty accumulation.

In the dose-response study, 300 mg/kg PCB153 induced the highest levels of hepatocellular vacuolization; however incidences of hypertrophy were not observed. Compared to our previous studies [19, 42], 30 μg/kg TCDD elicited more dramatic vacuolization and necrosis, as well as mixed cell infiltration that was absent in PCB153 treatment.

LIPID PROFILING

Total lipids were extracted from control, TCDD and PCB153-treated livers at 24, 72 and 168 h, derivatized to fatty acid methyl esters (FAMEs) and analyzed by GC-MS. The temporal and treatment-dependent separation of FAME profiles (as fold changes) is summarized in Figure 20. The cumulative proportion of variance for principal component (PC) 1 and PC2 is 99%, indicating that the PCA plot accurately represents the separation of the data. Comparison of PCB153- and TCDD-elicited FAME profiles identified separation around PC1 and PC2 indicating differences due to treatment and time, respectively (Figure 20). In agreement with

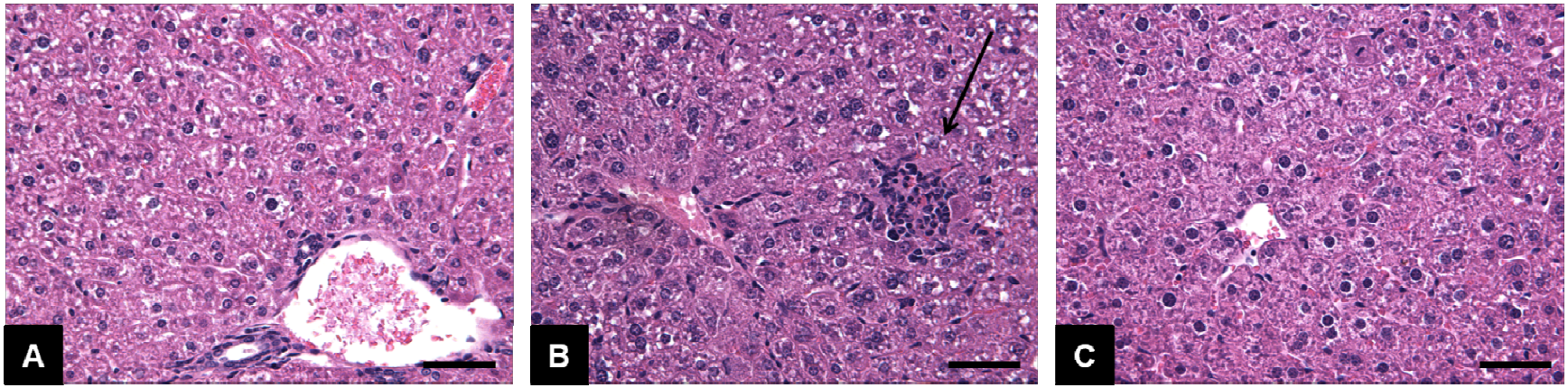

Figure 19. Representative histopathology results from vehicle, 30 µg/kg TCDD and 300 mg/kg PCB153-treated mice at 168 h. Liver sections from (**A**) vehicle showed an overall lack of vacuolization, (**B**) 30 µg/kg TCDD-treated animal exhibited slight to moderate vacuolization and instances of multifocal inflammation (arrow), and (**C**) an animal treated with 300 mg/kg PCB153 exhibited minimal vacuolization and hepatocellular hypertrophy. PCB153 did not elicit immune cell infiltration or necrosis. PV – Portal Vein; CV – Central Vein. Bars = 50 µm.

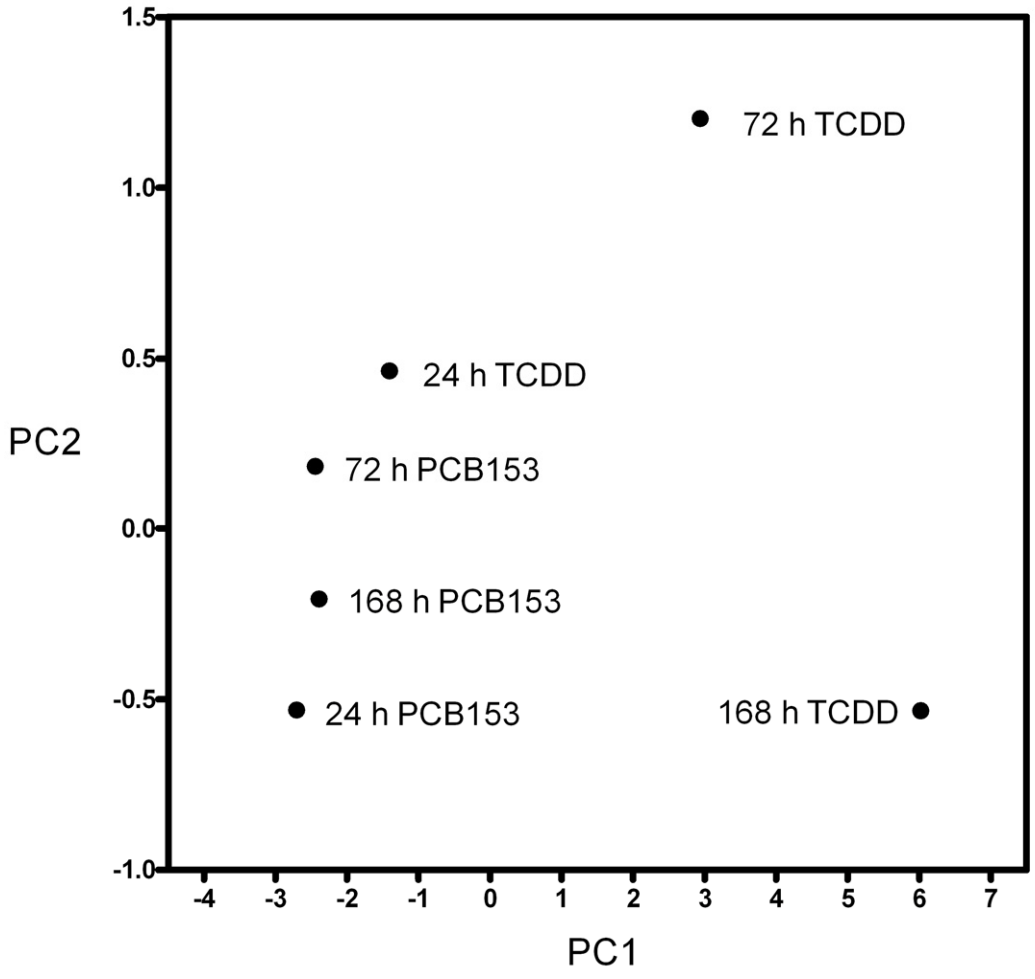

Figure 20. GC-MS lipid profile analysis at 24, 72 and 168 h.
Principal component analysis indicated temporal and treatment-dependent separation of PCB153 and TCDD fatty acid methyl ester profiles (fold change ratios) relative to their respective time-matched controls.

ORO staining, TCDD exhibited a time-dependent induction in the level of several individual FAMEs that was the highest at 168 h (Figure 21) and led to hepatic lipid accumulation [20, 42] that was not detected in PCB153-treated animals (Figure 21).

Hepatic triglyceride measurement identified a time-dependent increase in triglycerides in the TCDD group. In contrast, there was no difference in triglyceride levels between vehicle and PCB153-exposed mice, consistent with ORO and GC-MS FAME analysis.

TEMPORAL AND DOSE-DEPENDENT PCB153 GENE EXPRESSION CHANGES

Hepatic gene expression was assessed using 4 × 44K Agilent oligonucleotide microarrays, containing ~21,000 unique annotated genes. PCB153 elicited the differential expression of 186 unique, annotated genes at one or more time points ($P1(t) \geq 0.999$ and |fold change|≥1.5) relative to vehicle controls with 72 h exhibiting the most changes (127 unique genes). In the 24 h dose-response study, PCB153 differentially regulated 177 unique genes at one or more doses ($P1(t) \geq 0.985$ and |fold change|≥1.5).

Functional annotation of PCB153-elicited differential gene expression was associated with xenobiotic metabolism and oxidoreductase activity, lipid metabolism, cell cycle and cell death, and transport (Table 13). Position weight matrices (PWMs) were used to computationally identify putative dioxin, PXR/CAR response elements [28-35] in the promoter region (-10,000 bp relative to the [TSS] together with the 5' UTR) of responsive genes identified from the microarray analysis (Table 13).

Xenobiotic and oxidoreductase activity functions were the most highly induced among all functional clusters and almost exclusively included cytochrome P450s (e.g. Cyp2b9, Cyp2b10, Cyp2c54, Cyp3a25) and glutathione S-transferases (e.g. Gsta2, Gstt3, Gstm4), with Cyp2c55

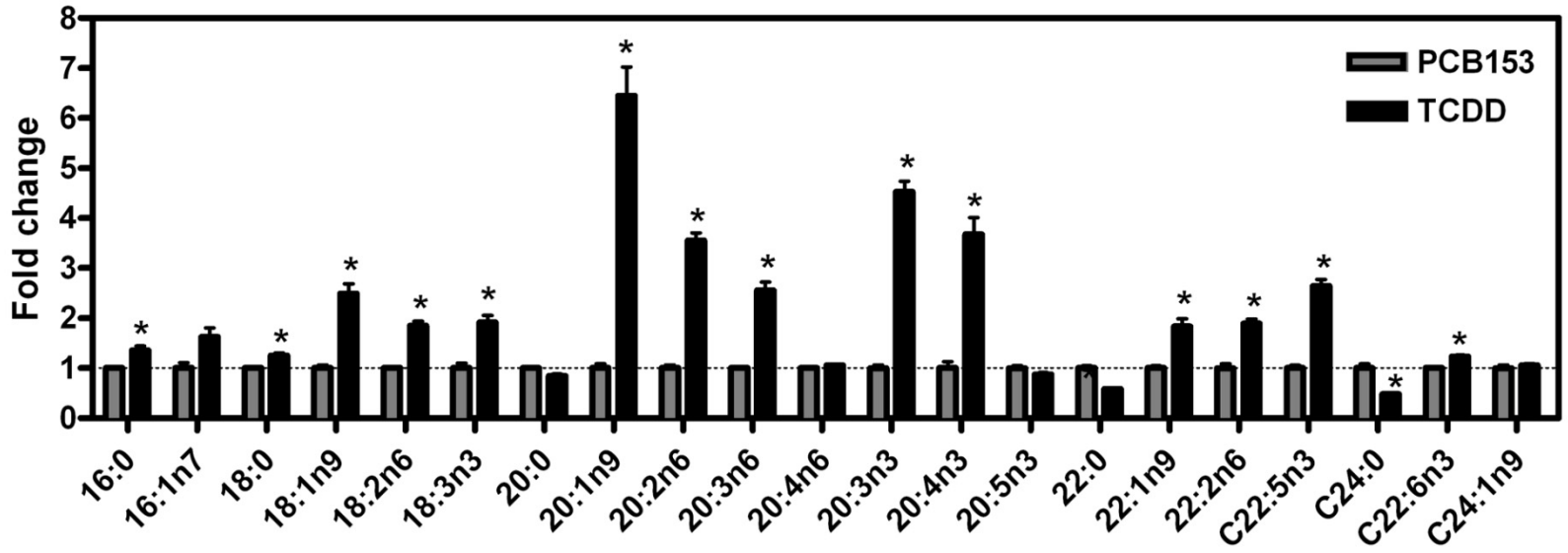

Figure 21. Fatty acid methyl ester (FAME) GC-MS analysis of PCB153- and TCDD-treated mouse livers at 168 h.
Treatment with 30 μg/kg TCDD induced a variety of individual FAMEs compared to 300 mg/kg PCB153 which did not affect FAME composition relative to control animals. An asterisk (*) indicates a significant ($p<0.05$) difference between the treated samples and vehicle controls.

Table 13. Functional categorization and regulation of select hepatic genes identified as differentially regulated in response to 300 mg/kg PCB153 and 30 µg/kg TCDD [19].

Functional category	Gene name	Gene symbol	Entrez Gene ID	PCB153 fold change[a]	TCDD *	TCDD [19]	DREs [b]	PXREs [c]	CAREs [d]
Metabolizing enzymes/ oxidoreductase activity	Aldehyde oxidase 1	Aox1	11761	2.9	2.2	N/A	4	5	2
	Aldo-keto reductase family 1, member B7	Akr1b7	11997	22.1	NC	NC	4	6	2
	Aldo-keto reductase family 1, member C20	Akr1c20	116852	-2.3	-1.7	N/A	–	1	–
	Carboxylesterase	Ces2	234671	5.8	2.5	1.6	1	4	1
	Cytochrome P450, family 2, subfamily b, polypeptide 10	Cyp2b10	13088	27.5	2.3	NC	5	5	1
	Cytochrome P450, family 2, subfamily b, polypeptide 23	Cyp2b23	243881	19.7	NC	N/A	2	5	–
	Cytochrome P450, family 2, subfamily b, polypeptide 9	Cyp2b9	13094	7.6	NC	N/A	–	4	1
	Cytochrome P450, family 2, subfamily c, polypeptide 54	Cyp2c54	404195	2.4	NC	N/A	–	5	1
	Cytochrome P450, family 2, subfamily c, polypeptide 55	Cyp2c55	72082	48.4	1.8	N/A	4	3	1
	Cytochrome P450, family 3, subfamily a, polypeptide 25	Cyp3a25	56388	3.8	NC	N/A	–	5	–

Table 13 (cont'd).

Functional category	Gene name	Gene symbol	Entrez Gene ID	PCB153 fold change[a]	TCDD *	TCDD [19]	DREs b	PXREs c	CAREs d
Metabolizing enzymes/ oxidoreductase activity	Dihydrofolate reductase	Dhfr	13361	-2.1	NC	-1.5	5	5	1
	Flavin containing monooxygenase 5	Fmo5	14263	3.0	NC	NC	2	5	1
	Glutathione peroxidase 2	Gpx2	14776	1.7	NC	NC	8	9	3
	Glutathione S-transferase, alpha 2 (Yc2)	Gsta2	14858	4.1	5.9	7.2	4	10	2
	Glutathione S-transferase, mu 4	Gstm4	14865	4.0	2.4	N/A	2	5	1
	Glutathione S-transferase, theta 3	Gstt3	103140	1.7	1.5	NC	3	10	3
	UDP-glucose dehydrogenase	Ugdh	22235	2.5	2.7	3.1	6	2	2
Lipid metabolism	Acyl-CoA synthetase long-chain family member 3	Acsl3	74205	-3.1	-2.3	N/A	2	4	-
	1-Acylglycerol-3-phosphate O-acyltransferase 4 (lysophosphatidic acid acyltransferase, delta)	Agpat4	68262	-1.9	NC	NC	7	4	1
	3-Hydroxy-3-methylglutaryl-Coenzyme A reductase	Hmgcr	15357	-5.3	-2.6	N/A	4	5	1
	CDP-diacylglycerol synthase (phosphatidate cytidylyltransferase) 2	Cds2	110911	1.7	NC	NC	5	4	3

Table 13 (cont'd).

Functional category	Gene name	Gene symbol	Entrez Gene ID	PCB153 fold change[a]	TCDD *	TCDD [19]	DREs[b]	PXREs[c]	CAREs[d]
Lipid metabolism	ELOVL family member 6, elongation of long chain fatty acids (yeast)	Elovl6	170439	-3.8	-4.3	-1.8	3	5	1
	Fatty acid synthase	Fasn	14104	-3.9	-4.3	-1.9	4	7	1
	Hydroxysteroid (17-beta) dehydrogenase 2	Hsd17b2	15486	-2.0	2.2	N/A	6	6	–
	Insulin induced gene 2	Insig2	72999	5.9	-1.7	NC	1	4	1
	Phospholipase A2, group XIIA	Pla2g12a	66350	1.7	3.1	N/A	14	9	1
	Sterol regulatory element binding factor 2	Srebf2	20788	-2.1	-1.7	1.5	8	6	4
	Sterol regulatory element binding transcription factor 1	Srebf1	20787	-2.4	-2.3	-2.1	4	16	1
Cell cycle/ cell death	Mitotic arrest deficient 1-like 1	Mad1l1	17120	2.4	NC	N/A	8	8	1
	Cell division cycle associated 2	Cdca2	108912	2.8	NC	N/A	2	3	1
	Growth arrest and DNA-damage-inducible 45 alpha	Gadd45a	13197	2.0	-3.6	N/A	3	–	2
	Growth arrest and DNA-damage-inducible 45 beta	Gadd45b	17873	10.7	3.2	4.6	4	14	4

Table 13 (cont'd).

Functional category	Gene name	Gene symbol	Entrez Gene ID	PCB153 fold change[a]	TCDD *	TCDD [19]	DREs [b]	PXREs [c]	CAREs [d]
Cell cycle/ cell death	Myelocytomatosis oncogene	Myc	17869	2.9	3.0	3.7	9	2	1
	Nucleolar protein 3 (apoptosis repressor with CARD domain)	Nol3	78688	4.9	NC	NC	12	6	–
	Sphingomyelin phosphodiesterase 3, neutral	Smpd3	58994	10.8	-2.6	N/A	4	6	1
	ZW10 interactor	Zwint	52696	1.8	NC	N/A	2	5	–
Transport	ATP-binding cassette, sub-family C (CFTR/MRP), member 3	Abcc3	76408	1.9	1.7	1.5	2	9	5
	Solute carrier family 1 (glutamate/neutral amino acid transporter), member 4	Slc1a4	55963	-2.5	NC	NC	6	10	–
	Solute carrier family 23 (nucleobase transporters), member 1	Slc23a1	20522	2.3	-1.7	N/A	3	2	1

[a]Maximum expression (|fold change| ≥1.5, P1(t) ≥ 0.985).
*Maximum expression (|fold change| ≥1.5, P1(t) ≥ 0.90).
[b,c,d]Putative DREs, PXREs, and CAREs identified by computational searches (Materials & Methods).
N/A – not available on cDNA microarray.
NC – no change (not meeting the |fold change| ≥1.5, P1(t) ≥ 0.90 cut-off).

showing the highest (48-fold) induction in both the time course and dose-response study. PCB153 modestly induced the typical "AhR-battery" genes such as Cyp1a1, Cyp1a2 and Tiparp compared to TCDD (Figure 23A-B), while TCDD induction of PCB153-responsive genes was reciprocally modest (Table 13 and Figure 22C).

PCB153 down-regulated the lipid metabolism acyl-CoA synthetase long-chain family member 3, Acsl3, and sterol regulatory element binding factors (Srebf1 and Srebf2) genes, -2.1 to -3.1-fold, respectively. Moreover, PCB153 repressed Elovl5 -1.9-fold, while it was induced 2.2-fold by TCDD, suggesting divergent regulation (Figure 23A-B). The down-regulation of many lipid biosynthesis and metabolism genes by PCB153 is consistent with GS-MS FAMEs and triglyceride analysis, all indicating a lack of lipid accumulation compared to TCDD.

Genes involved in cell cycle and DNA replication, including Mad1l1 and Zwint, were up-regulated 2.4- and 2.0-fold, respectively, by PCB153. However, in contrast to TCDD, PCB153 did not induce necrosis or immune cell infiltration, even though genes involved in cell death and immune response were differentially regulated. A number of transport genes were also differentially expressed by PCB153, including ATP-binding cassette and solute carrier family members, such as Abcc3, Slc1a4, and Slc23a1.

COMPUTATIONAL DOSE-RESPONSE MODELING

Dose-response microarray data were filtered using P1(t)>0.90 cut-off and identified 846 unique annotated genes exhibiting a sigmoidal dose-response profile with reasonable ED_{50} values (i.e. between 1 and 300 mg/kg) (Figure 24). 315 genes exhibited ED_{50s} between 1 and 10 mg/kg, 124 genes were between 10 and 30 mg/kg, 140 genes between 30 and 100 mg/kg and 267 genes had ED_{50s} between 100 and 300 mg/kg. The CAR/PXR regulated genes, Cyp2b10, Cyp2c55, Nol3, Entpd5 and Abcc3 exhibited ED_{50s} of 38.1, 31.7, 33.9, 34.2 and 2.9 mg/kg, respectively.

Figure 22. QRTPCR verification of selected PCB153-induced genes.
The same RNA samples used in the time course and dose-response microarray studies were also used for QRTPCR analysis. PCB153 induced CAR/PXR regulated genes, Cyp2b10, Cyp3a11, Cyp2c55 and Gadd45b, in (A) time course and (B) dose-response studies. (C) TCDD elicited minimal differential expression of CAR/PXR responsive genes. All fold changes were calculated relative to vehicle controls. Bars (left y-axis) and lines (right y-axis) represent QRTPCR and microarray data, respectively. The genes are represented by their official gene symbols. Bars represent the mean ± SE of at least four independent samples. Data were analyzed by ANOVA followed by Tukey's and Dunnett's *post hoc* tests. The asterisk (*) indicates $p<0.05$.

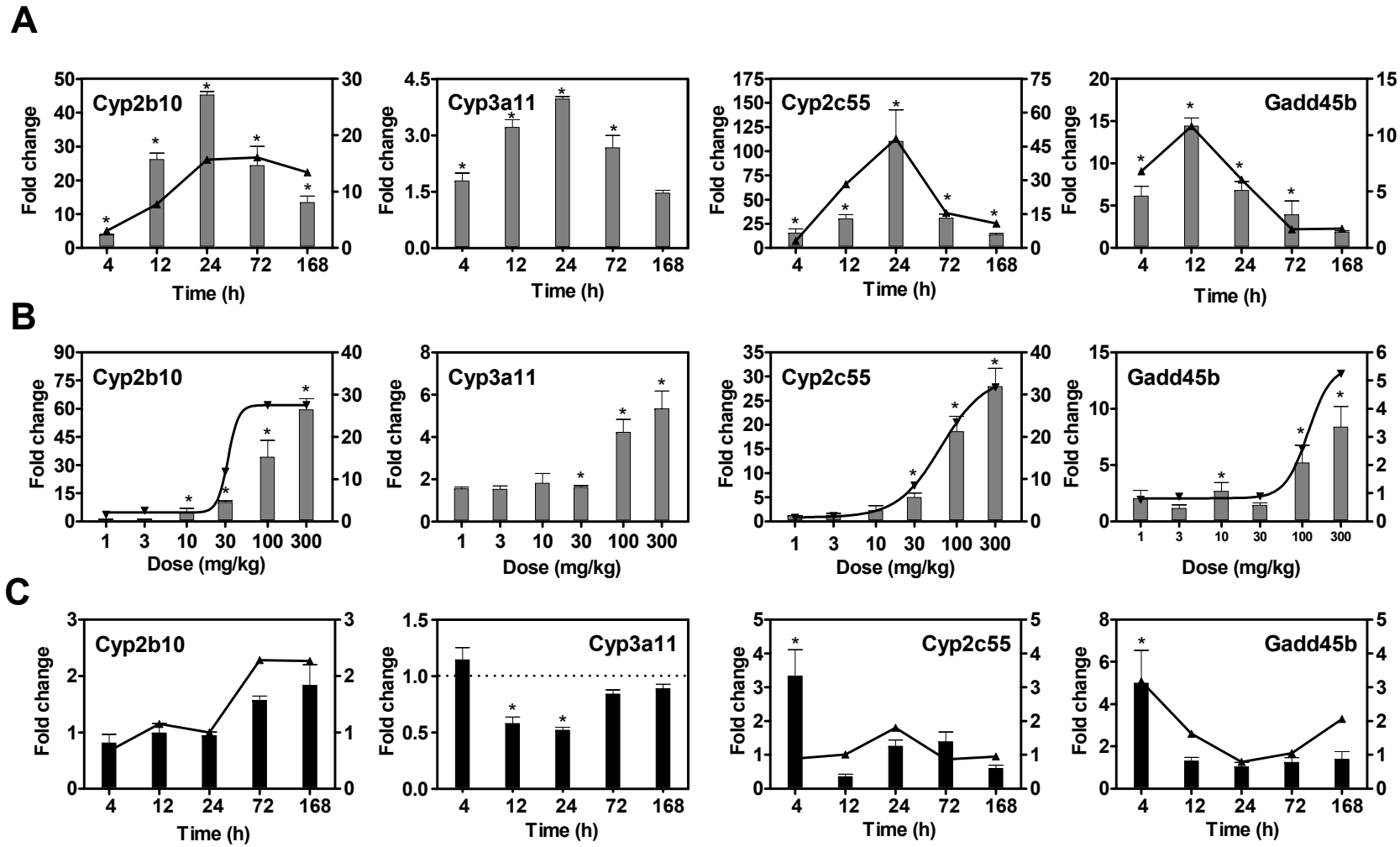
A
Cyp2b10
Cyp3a11
Cyp2c55
Gadd45b
Fold change
Time (h)
4 12 24 72 168
B
Dose (mg/kg)
1 3 10 30 100 300
C

Figure 23. QRTPCR verification of selected TCDD-regulated genes.
The same RNA samples used in the time course microarray studies were also used for QRTPCR analysis. (A) TCDD-induced AhR-responsive genes, Cyp1a1, Cyp1a2, Tiparp, as well as Elovl5. (B) PCB153 elicited modest regulation of AhR-responsive genes, but down-regulation of Elovl5. All fold changes were calculated relative to vehicle controls. Bars (left y-axis) and lines (right y-axis) represent QRTPCR and microarray data, respectively. The genes are represented by their official gene symbols. Bars represent the mean ± SE of at least four independent samples. Data were analyzed by ANOVA followed by Tukey's *post hoc* test. The asterisk (*) indicates $p<0.05$.

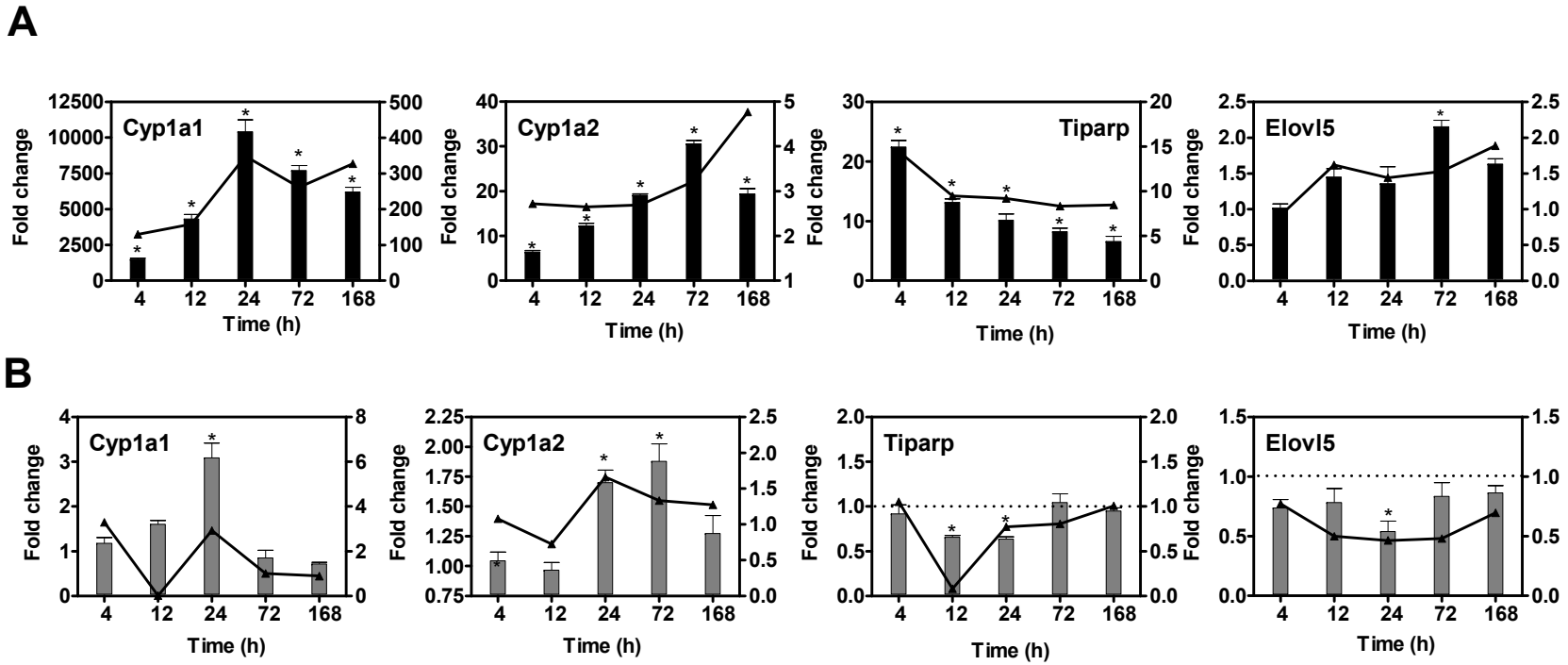
A
Cyp1a1
Cyp1a2
Tiparp
Elovl5
Fold change
Time (h)
4
12
24
72
168
B
Cyp1a1
Cyp1a2
Tiparp
Elovl5
Fold change
Time (h)

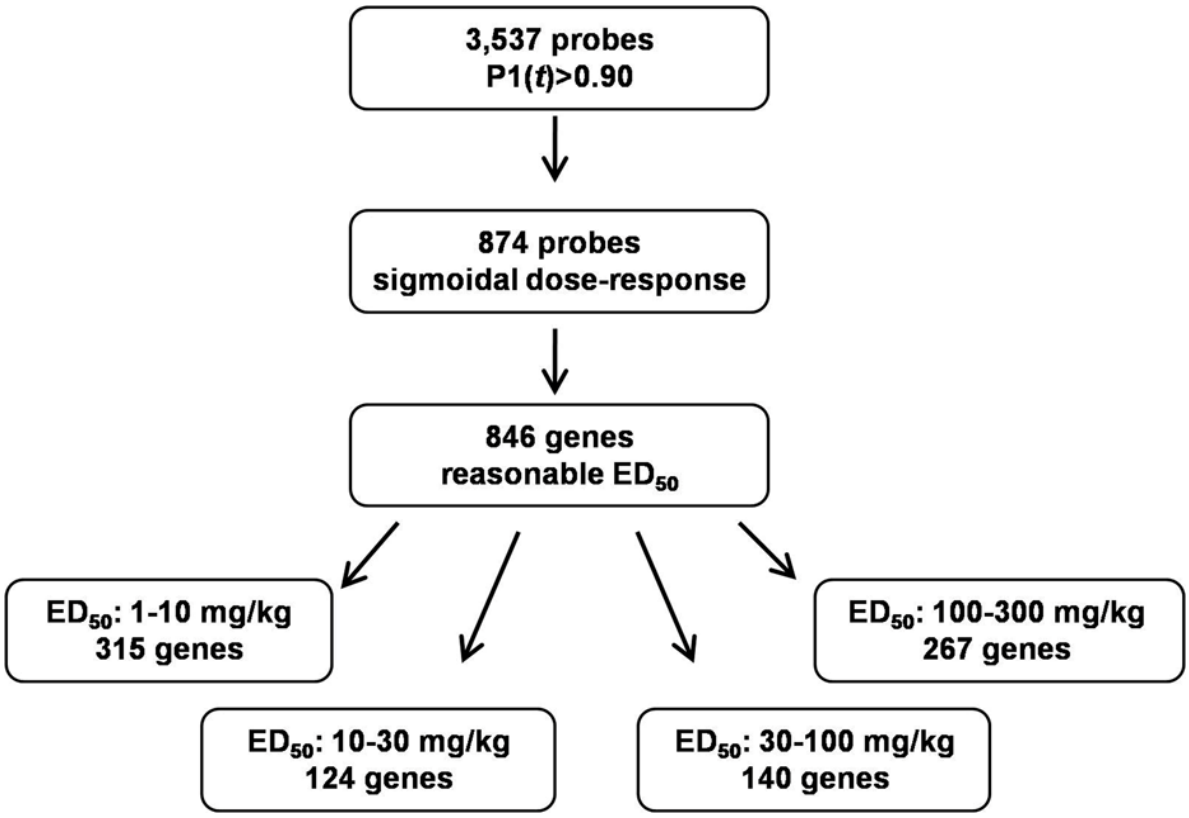

Figure 24. Dose-response modeling.
846 genes exhibited a dose-response profile and were categorized according to their ED_{50} value.

VERIFICATION OF MICROARRAY RESPONSES

QRTPCR was used to verify the temporal and dose-dependent changes in expression for a subset of genes. In total, 20 differentially regulated genes where confirmed, including Cyp3a11, which did not satisfy the Agilent microarray data selection criteria. The differential expression of CAR/PXR-regulated genes Cyp2b10, Cyp3a11 and Gadd45b [11, 43, 44], as well as Cyp2c55 (48-fold) by PCB153 and TCDD was also confirmed (Figure 22A-C). In addition, AhR-responsive genes (Cyp1a1, Cyp1a2 and Tiparp) were included as a positive control for TCDD and a negative control for PCB153 (Figure 23A-B). Elovl5 was included as an example of divergent regulation (Figure 23A-B). Overall, there was a good agreement in temporal and dose-dependent expression patterns between QRTPCR and microarray analysis.

COMPARISON OF TCDD AND PCB153 ELICITED DIFFERENTIAL GENE EXPRESSION

Overall, when compared to TCDD and PCB126, PCB153 elicited a significantly different gene expression profile that did not include "AhR battery genes", but CAR/PXR regulated genes, such as Ces2, Cyp2b10, Fmo5, Fasn, Insig2, Abcc3 and Gsta2 (Table 13). To further investigate these differences, a comprehensive comparison of the Agilent 300 mg/kg PCB153 and 30 μg/kg TCDD temporal microarray data between 4 and 168 h was performed (Figure 25A). Using the same filtering criteria ($P1(t)\geq 0.999$ and |fold change|≥ 1.5), 170 and 186 differentially expressed genes elicited by TCDD and PCB153, respectively, were identified, of which only 14 were regulated by both compounds. Relaxing the statistical cut-off to $P1(t)\geq 0.985$ increased the overlap to 74 genes (Figure 25A). A correlation plot of expression ratios compared to significance was then used to identify conserved and divergent responses between TCDD and PCB153 (Figure 25B). Overall, only 54% of the commonly regulated genes were positively correlated in terms of fold change and significance, suggesting that TCDD and PCB153 elicit

Figure 25. Gene expression comparisons.
(A) Microarray data sets for 30 μg/kg TCDD and 300 mPCB153 were compared at 4, 12, 24, 72 and 168 h with stringent (|fold change|≥1.5, P1(*t*)≥0.999) and relaxed (|fold change|≥1.5, P1(*t*)≥0.985) selection criteria. Numbers in the Venn diagram represent unique genes. (B) The correlation plot illustrates that the 74 genes regulated by TCDD and PCB153 are poorly correlated, indicating that many of the genes exhibited divergent regulation. The x-axis represents the correlation of gene expression, while the y-axis represents the correlation between significance values. Genes (dots) located within the upper right quadrant exhibit good correlation across their gene expression profiles and significance values indicating that their expression patterns are similar. Genes in the lower left quadrant are poorly correlated with respect to fold induction and significant values indicating that the TCDD and PCB153-elicited expression patterns are different, suggesting different mechanisms of regulation. Approximately 54% of the genes (40/74) were located within the upper right hand quadrant, indicating that 34 of the 74 common genes were poorly correlated. In contrast, when PCB126 and 2,3,7,8-tetrachlorodibenzofuran (TCDF) were compared to TCDD in the same model, 68% and 82% of the genes were located in the upper right hand quadrant [20, 45], further illustrating the differences between PCB153 and TCDD, PCB126 and TCDF.

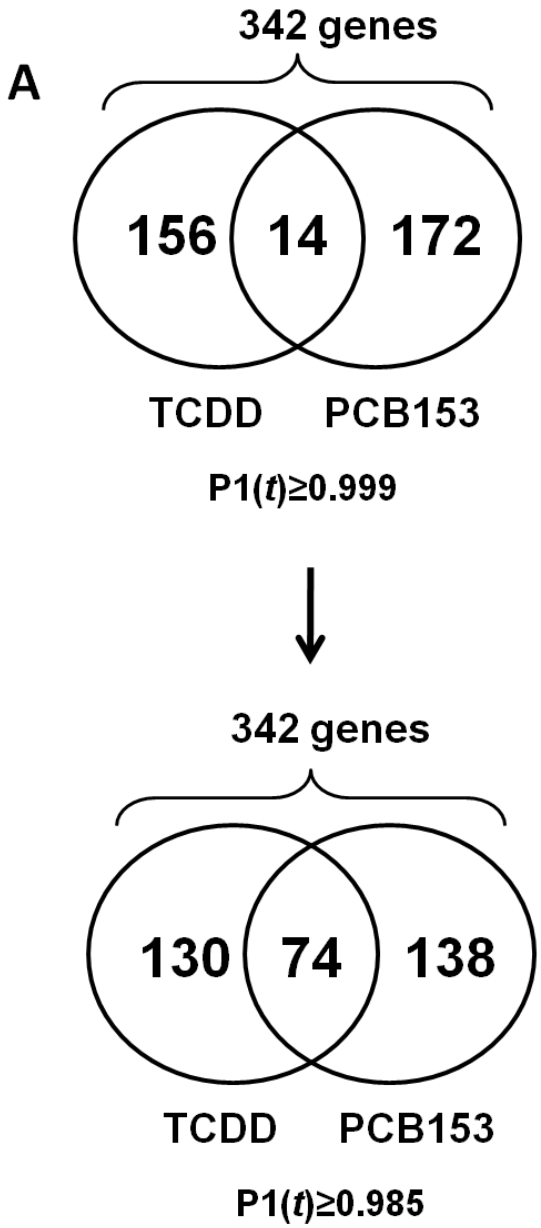
A
342 genes
156
14
172
TCDD
PCB153
P1(t)≥0.999
342 genes
130
74
138
TCDD
PCB153
P1(t)≥0.985

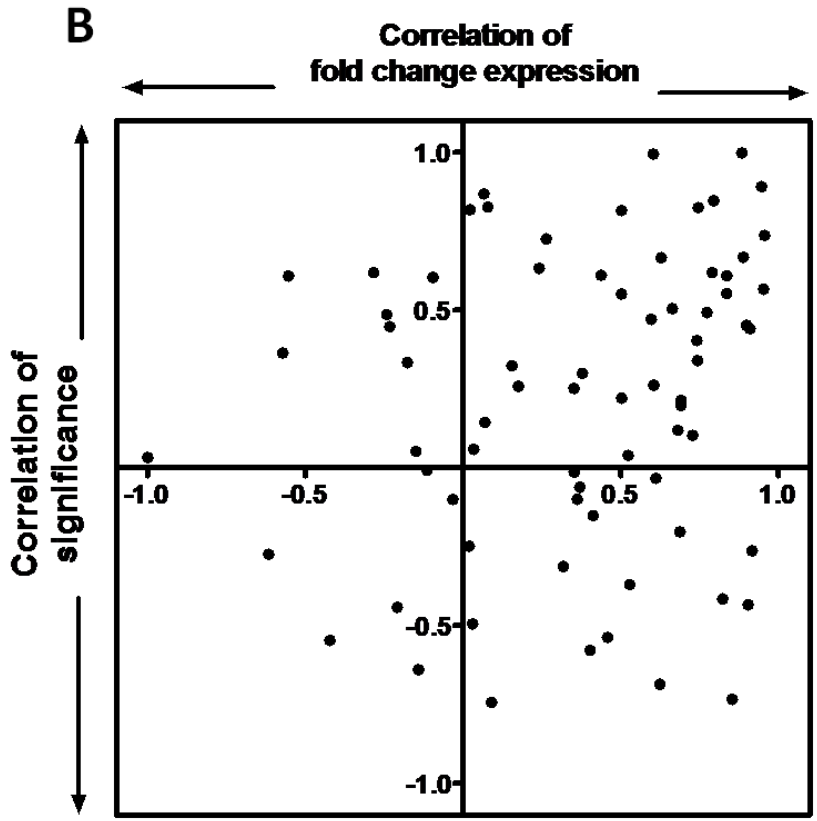
B
Correlation of
fold change expression
Correlation of
significance
1.0
0.5
-0.5
-1.0
-1.0
-0.5
0.5
1.0

different expression patterns via different mechanisms of regulation.

DISCUSSION

Hepatic gene expression, histopathology and lipid profiling analysis quantitatively and qualitatively indicate that the temporal and dose-dependent effects elicited by PCB153 are mechanistically different when compared to TCDD and PCB126. These data are consistent with the effects elicited by PCB153 being regulated by CAR/PXR.

PCB153 elicited a gene expression profile that included the induction of xenobiotic metabolism genes such as Cyp2c55, Cyp2b10, Cyp3a11, Ces2, Fmo5 and Gsta2 [11, 43, 44] in the absence of "AhR gene battery" induction. PWM analysis computationally identified putative CAREs and PXREs within the regulatory region of numerous genes that exhibited differential expression following PCB153 treatment, further suggesting CAR/PXR regulation. This is also consistent with the *in vivo* induction of Cyp3a23 by highly chlorinated non co-planar PCBs [46], and more specifically, the induction of Gal4-PXR-regulated reporter gene activity [14]. In addition, Sprague-Dawley rat studies concluded PCB153 did not activate AhR and may be associated with the induction of phenobarbital-responsive genes [9, 47, 48].

Hepatic responses induced by PCB153 are also in agreement with reported CAR/PXR-mediated hepatic hypertrophy [49-51]. In contrast, hepatocyte cell size and number are not affected by TCDD and PCB126 [19, 20]. PCB153 induced hepatocellular hypertrophy between 24 and 168 h compared to controls, in agreement with the NTP Technical Report that identified pronounced and persistent increase in cell size elicited by PCB153 [9]. In addition, liver hypertrophic responses to known CAR inducers (TCPOBOP or phenobarbital) are abolished in mice lacking the CAR gene [11, 52].

TCDD, PCB126 and PCB153 all induced RLW in the time course and dose-response studies [19, 20]. However, PCB153 elicited minimal vacuolization which completely subsided by 168 h. Histopathology and lipid profiling also suggest that PCB153 did not induce hepatic steatosis [19, 20], and microarray analysis indicated that PCB153 down-regulated many lipid metabolism genes. For example, Elovl5 was repressed by PCB153 but induced by TCDD, suggesting divergent regulation that may partially explain the histopathology differences. Interestingly, Elovl5 null mice (*Elovl5* $^{-/-}$) have higher SREBP1 protein levels that increase fatty acid synthesis and the development of steatosis [53]. However, PCB153 did not affect Srebf1 expression and did not promote lipid synthesis. Other studies have shown that the CAR/PXR-mediated insulin induced genes (Insig1 and Insig2) also repress Srebf1, thereby lowering hepatic fatty acids [44, 54]. The PCB153 induction of Insig2 by 5.9-fold and repression of Srebf1 by -2.4-fold suggests that Elovl5 repression does fully explain the observed lipid changes. In contrast, Insig2 was down-regulated -1.7-fold and Srebf1 was repressed -2.3-fold by TCDD suggesting that this down-regulation was not sufficient to affect lipid biosynthesis.

Histopathology revealed a lack of PCB153-elicited hepatocellular necrosis/apoptosis, when compared to TCDD [19], consistent with other studies suggesting PCB153 reduces apoptosis in mouse hepatocytes [55, 56]. PCB153 induced Gadd45b ~11 fold, a known inhibitor of c-Jun N-terminal kinase (JNK)-mediated apoptosis [57]. In addition, Gadd45b null mice have attenuated Cyp2b10 expression, linking Gadd45b with direct co-activation of CAR-mediated transcription [58]. PCB153 also regulated the expression of genes involved in cell death, although there was no evidence of necrosis. For example, Myc induction following chronic PCB153 exposure has been associated with increased apoptosis in HepG2 cells [59]. However,

the single dose of PCB153 used in the current study may not be sufficient to induce cell death within 168 h.

Furthermore, there was a lack of significant immune cell accumulation associated with PCB153 treatment, unlike TCDD, which increased mixed cell infiltration, primarily in the centrilobular regions [19]. Nevertheless, PCB153 induced expression of chemokine (C-C motif) ligand 9 (Ccl9), in agreement with the increased incidence of liver inflammation in chronically treated rats [9]. This suggests that a single dose of PCB153 may not be sufficient to increase mixed cell infiltration within a week.

In summary, PCB153 and possibly other non-coplanar congeners elicit responses that are qualitatively and quantitatively different than TCDD and other planar PCBs. PCB153 elicited no instances of inflammation or necrosis/apoptosis and did not lead to hepatic lipid accumulation. These effects are consistent with the differential gene expression responses and suggestive of CAR/PXR-mediated regulation. However, the relevance of these effects in risk assessment warrants further investigation due to significant species-specific differences in ligand preference, binding, and receptor activation when comparing human and rodent CAR/PXR orthologs [14, 43, 60, 61].

REFERENCES

REFERENCES

1. Mullin, M.D., et al., *High-resolution PCB analysis: synthesis and chromatographic properties of all 209 PCB congeners.* Environ. Set Technol., 1984. **18**: p. 468-476.

2. NTP, *NTP toxicology and carcinogenesis studies of 3,3',4,4',5-pentachlorobiphenyl (PCB 126) (CAS No. 57465-28-8) in female Harlan Sprague-Dawley rats (Gavage Studies).* NTP Technical Report, 2006(520): p. 4-246.

3. Kimbrough, R.D., *Polychlorinated biphenyls (PCBs) and human health: an update.* Crit Rev Toxicol, 1995. **25**(2): p. 133-63.

4. Poland, A. and J.C. Knutson, *2,3,7,8-tetrachlorodibenzo-p-dioxin and related halogenated aromatic hydrocarbons: examination of the mechanism of toxicity.* Annu Rev Pharmacol Toxicol, 1982. **22**: p. 517-54.

5. Knerr, S. and D. Schrenk, *Carcinogenicity of "non-dioxinlike" polychlorinated biphenyls.* Crit Rev Toxicol, 2006. **36**(9): p. 663-94.

6. Van den Berg, M., et al., *The 2005 World Health Organization reevaluation of human and Mammalian toxic equivalency factors for dioxins and dioxin-like compounds.* Toxicol Sci, 2006. **93**(2): p. 223-41.

7. Giesy, J.P. and K. Kannan, *Dioxin-like and non-dioxin-like toxic effects of polychlorinated biphenyls (PCBs): implications for risk assessment.* Crit Rev Toxicol, 1998. **28**(6): p. 511-69.

8. Schecter, A., et al., *Polychlorinated biphenyl levels in the tissues of exposed and nonexposed humans.* Environ Health Perspect, 1994. **102 Suppl 1**: p. 149-58.

9. NTP, *NTP technical report on the toxicology and carcinogenesis studies of 2,2',4,4',5,5'-hexachlorobiphenyl (PCB 153) (CAS No. 35065-27-1) in female Harlan Sprague-Dawley rats (Gavage studies).* Natl Toxicol Program Tech Rep Ser, 2006(529): p. 4-168.

10. Craft, E.S., M.J. DeVito, and K.M. Crofton, *Comparative responsiveness of hypothyroxinemia and hepatic enzyme induction in Long-Evans rats versus C57BL/6J mice exposed to TCDD-like and phenobarbital-like polychlorinated biphenyl congeners.* Toxicol Sci, 2002. **68**(2): p. 372-80.

11. Honkakoski, P., T. Sueyoshi, and M. Negishi, *Drug-activated nuclear receptors CAR and PXR.* Ann Med, 2003. **35**(3): p. 172-82.

12. Pascussi, J.M., et al., *The Tangle of Nuclear Receptors that Controls Xenobiotic Metabolism and Transport: Crosstalk and Consequences.* Annu Rev Pharmacol Toxicol, 2007.

13. Strathmann, J., et al., *PCB 153, a non-dioxin-like tumor promoter, selects for beta-catenin (Catnb)-mutated mouse liver tumors.* Toxicol Sci, 2006. **93**(1): p. 34-40.

14. Tabb, M.M., et al., *Highly chlorinated PCBs inhibit the human xenobiotic response mediated by the steroid and xenobiotic receptor (SXR).* Environ Health Perspect, 2004. **112**(2): p. 163-9.

15. Biegel, L., et al., *2,2',4,4',5,5'-hexachlorobiphenyl as a 2,3,7,8-tetrachlorodibenzo-p-dioxin antagonist in C57BL/6J mice.* Toxicol Appl Pharmacol, 1989. **97**(3): p. 561-71.

16. Chubb, L.S., et al., *Regional induction of CYP1A1 in rat liver following treatment with mixtures of PCB 126 and PCB 153.* Toxicol Pathol, 2004. **32**(4): p. 467-73.

17. Suh, J., et al., *Antagonism of aryl hydrocarbon receptor-dependent induction of CYP1A1 and inhibition of IgM expression by di-ortho-substituted polychlorinated biphenyls.* Toxicol Appl Pharmacol, 2003. **187**(1): p. 11-21.

18. Bager, Y., et al., *Interaction of 3,4,5,3',4'-pentachlorobiphenyl and 2,4,5,2',4',5'-hexachlorobiphenyl in promotion of altered hepatic foci in rats.* Pharmacol Toxicol, 1995. **77**(2): p. 149-54.

19. Boverhof, D.R., et al., *Temporal and dose-dependent hepatic gene expression patterns in mice provide new insights into TCDD-Mediated hepatotoxicity.* Toxicol Sci, 2005. **85**(2): p. 1048-63.

20. Kopec, A.K., et al., *Comparative Toxicogenomic Examination of the Hepatic Effects of PCB126 and TCDD in Immature, Ovariectomized C57BL/6 Mice.* Toxicol Sci, 2008. **102**(1): p. 61-75.

21. Sheehan, D.C. and B.B. Hrapchak, *Theory and Practice of Histotechnology*. second ed ed. 1980, St. Louis: Mosby.

22. Patterson, T.A., et al., *Performance comparison of one-color and two-color platforms within the MicroArray Quality Control (MAQC) project.* Nat Biotechnol, 2006. **24**(9): p. 1140-50.

23. Burgoon, L.D. and T.R. Zacharewski, *dbZach toxicogenomic information management system.* Pharmacogenomics, 2007. **8**(3): p. 287-91.

24. Burgoon, L.D., et al., *Protocols for the assurance of microarray data quality and process control.* Nucleic Acids Res, 2005. **33**(19): p. e172.

25. Eckel, J.E., et al., *Normalization of two-channel microarray experiments: a semiparametric approach.* Bioinformatics, 2005. **21**(7): p. 1078-83.

26. Eckel, J.E., et al., *Empirical bayes gene screening tool for time-course or dose-response microarray data.* J Biopharm Stat, 2004. **14**(3): p. 647-70.

27. Burgoon, L.D. and T.R. Zacharewski, *Automated quantitative dose-response modeling and point of departure determination for large toxicogenomic and high-throughput screening data sets.* Toxicol Sci, 2008. **104**(2): p. 412-8.

28. Sun, Y.V., et al., *Comparative analysis of dioxin response elements in human, mouse and rat genomic sequences.* Nucleic Acids Res, 2004. **32**(15): p. 4512-23.

29. Phillips, J.M., L.D. Burgoon, and J.I. Goodman, *Phenobarbital (PB) Elicits Unique, Early Changes in the Expression of Hepatic Genes That Affect Critical Pathways in Tumor-Prone B6C3F1 Mice.* Toxicol Sci, 2009.

30. Vyhlidal, C.A., P.K. Rogan, and J.S. Leeder, *Development and refinement of pregnane X receptor (PXR) DNA binding site model using information theory: insights into PXR-mediated gene regulation.* J Biol Chem, 2004. **279**(45): p. 46779-86.

31. Zhou, J., et al., *A novel pregnane X receptor-mediated and sterol regulatory element-binding protein-independent lipogenic pathway.* J Biol Chem, 2006. **281**(21): p. 15013-20.

32. Pascussi, J.M., et al., *Possible involvement of pregnane X receptor-enhanced CYP24 expression in drug-induced osteomalacia.* J Clin Invest, 2005. **115**(1): p. 177-86.

33. Echchgadda, I., et al., *Gene regulation for the senescence marker protein DHEA-sulfotransferase by the xenobiotic-activated nuclear pregnane X receptor (PXR).* Mech Ageing Dev, 2004. **125**(10-11): p. 733-45.

34. Igarashi, M., et al., *Vitamin K induces osteoblast differentiation through pregnane X receptor-mediated transcriptional control of the Msx2 gene.* Mol Cell Biol, 2007. **27**(22): p. 7947-54.

35. Wang, H., et al., *A novel distal enhancer module regulated by pregnane X receptor/constitutive androstane receptor is essential for the maximal induction of CYP2B6 gene expression.* J Biol Chem, 2003. **278**(16): p. 14146-52.

36. Vandesompele, J., et al., *Accurate normalization of real-time quantitative RT-PCR data by geometric averaging of multiple internal control genes.* Genome Biol, 2002. **3**(7): p. RESEARCH0034.

37. Dennis, G., Jr., et al., *DAVID: Database for Annotation, Visualization, and Integrated Discovery.* Genome Biol, 2003. **4**(5): p. P3.

38. DeVito, M.J., et al., *Dose-response relationships for disposition and hepatic sequestration of polyhalogenated dibenzo-p-dioxins, dibenzofurans, and biphenyls following subchronic treatment in mice.* Toxicol Sci, 1998. **46**(2): p. 223-34.

39. Jordan, S.A. and M.M. Feeley, *PCB congener patterns in rats consuming diets containing Great Lakes salmon: analysis of fish, diets, and adipose tissue.* Environ Res, 1999. **80**(2 Pt 2): p. S207-S212.

40. Luotamo, M., J. Jarvisalo, and A. Aitio, *Assessment of exposure to polychlorinated biphenyls: analysis of selected isomers in blood and adipose tissue.* Environ Res, 1991. **54**(2): p. 121-34.

41. Vodicnik, M.J. and J.J. Lech, *The transfer of 2,4,5,2',4',5'-hexachlorobiphenyl to fetuses and nursing offspring. I. Disposition in pregnant and lactating mice and accumulation in young.* Toxicol Appl Pharmacol, 1980. **54**(2): p. 293-300.

42. Boverhof, D.R., et al., *Comparative toxicogenomic analysis of the hepatotoxic effects of TCDD in Sprague Dawley rats and C57BL/6 mice.* Toxicol Sci, 2006. **94**(2): p. 398-416.

43. Maglich, J.M., et al., *Nuclear pregnane x receptor and constitutive androstane receptor regulate overlapping but distinct sets of genes involved in xenobiotic detoxification.* Mol Pharmacol, 2002. **62**(3): p. 638-46.

44. Rosenfeld, J.M., et al., *Genetic profiling defines the xenobiotic gene network controlled by the nuclear receptor pregnane X receptor.* Mol Endocrinol, 2003. **17**(7): p. 1268-82.

45. N'Jai, A., et al., *Comparative temporal toxicogenomic analysis of TCDD- and TCDF-mediated hepatic effects in immature female C57BL/6 mice.* Toxicol Sci, 2008. **103**(2): p. 285-97.

46. Schuetz, E.G., C. Brimer, and J.D. Schuetz, *Environmental xenobiotics and the antihormones cyproterone acetate and spironolactone use the nuclear hormone pregnenolone X receptor to activate the CYP3A23 hormone response element.* Mol Pharmacol, 1998. **54**(6): p. 1113-7.

47. Connor, K., et al., *Structure-dependent induction of CYP2B by polychlorinated biphenyl congeners in female Sprague-Dawley rats.* Biochem Pharmacol, 1995. **50**(11): p. 1913-20.

48. Vezina, C.M., N.J. Walker, and J.R. Olson, *Subchronic exposure to TCDD, PeCDF, PCB126, and PCB153: effect on hepatic gene expression.* Environ Health Perspect, 2004. **112**(16): p. 1636-44.

49. Blanco-Bose, W.E., et al., *C-Myc and its target FoxM1 are critical downstream effectors of constitutive androstane receptor (CAR) mediated direct liver hyperplasia.* Hepatology, 2008. **48**(4): p. 1302-11.

50. Staudinger, J.L., et al., *Regulation of drug transporter gene expression by nuclear receptors.* Drug Metab Dispos, 2003. **31**(5): p. 523-7.

51. Wei, P., et al., *The nuclear receptor CAR mediates specific xenobiotic induction of drug metabolism.* Nature, 2000. **407**(6806): p. 920-3.

52. Wei, P., et al., *Specific and overlapping functions of the nuclear hormone receptors CAR and PXR in xenobiotic response.* Pharmacogenomics J, 2002. **2**(2): p. 117-26.

53. Moon, Y.A., R.E. Hammer, and J.D. Horton, *Deletion of ELOVL5 leads to fatty liver through activation of SREBP-1c in mice.* J Lipid Res, 2008.

54. Roth, A., et al., *Regulatory cross-talk between drug metabolism and lipid homeostasis: constitutive androstane receptor and pregnane X receptor increase Insig-1 expression.* Mol Pharmacol, 2008. **73**(4): p. 1282-9.

55. Tharappel, J.C., et al., *Regulation of cell proliferation, apoptosis, and transcription factor activities during the promotion of liver carcinogenesis by polychlorinated biphenyls.* Toxicol Appl Pharmacol, 2002. **179**(3): p. 172-84.

56. Lu, Z., et al., *Effect of 2,2',4,4',5,5'-hexachlorobiphenyl (PCB-153) on hepatocyte proliferation and apoptosis in mice deficient in the p50 subunit of the transcription factor NF-kappaB.* Toxicol Sci, 2004. **81**(1): p. 35-42.

57. Papa, S., et al., *Gadd45 beta mediates the NF-kappa B suppression of JNK signalling by targeting MKK7/JNKK2.* Nat Cell Biol, 2004. **6**(2): p. 146-53.

58. Yamamoto, Y. and M. Negishi, *The antiapoptotic factor growth arrest and DNA-damage-inducible 45 beta regulates the nuclear receptor constitutive active/androstane receptor-mediated transcription.* Drug Metab Dispos, 2008. **36**(7): p. 1189-93.

59. Ghosh, S., S. De, and S.K. Dutta, *Altered Protein Expressions in Chronic PCB-153-Induced Human Liver (HepG2) Cells.* Int J Toxicol, 2007. **26**(3): p. 203-12.

60. Blumberg, B. and R.M. Evans, *Orphan nuclear receptors--new ligands and new possibilities.* Genes Dev, 1998. **12**(20): p. 3149-55.

61. Jones, S.A., et al., *The pregnane X receptor: a promiscuous xenobiotic receptor that has diverged during evolution.* Mol Endocrinol, 2000. **14**(1): p. 27-39.

CHAPTER 6

Kopec AK, D'Souza ML, Mets BM, Burgoon LD, Reese SE, Archer KJ, Potter D, Tashiro C, Sharratt B, Harkema JR, Zacharewski TR: **Non-Additive Hepatic Gene Expression Effects Elicited by 2,3,7,8-Tetrachlorodibenzo-*p*-dioxin and 2,2',4,4',5,5'-Hexachlorobiphenyl in C57BL/6 Mice**

CHAPTER 6

NON-ADDITIVE HEPATIC GENE EXPRESSION EFFECTS ELICITED BY 2,3,7,8-TETRACHLORODIBENZO-*P*-DIOXIN AND 2,2',4,4',5,5'-HEXACHLOROBIPHENYL IN C57BL/6 MICE

ABSTRACT

Interactions between environmental contaminants can lead to non-additive effects that may affect toxicity and influence the risk assessment of a mixture. Comprehensive time course and dose-response studies with 2,3,7,8-tetrachlorodibenzo-*p*-dioxins (TCDD), non-dioxin-like 2,2',4,4',5,5'-hexachlorobiphenyl (PCB153) and their mixture were performed in immature, ovariectomized C57BL/6 mice. Mice were gavaged once with 30 μg/kg TCDD, 300 mg/kg PCB153, a mixture of 30 μg/kg TCDD and 300 mg/kg PCB153 (MIX) or sesame oil vehicle for 4, 12, 24, 72 or 168 h. In the dose-response study, animals were gavaged with TCDD (0.3, 1, 3, 6, 10, 15, 30, 45 μg/kg), PCB153 (3, 10, 30, 60, 100, 150, 300, 450 mg/kg), MIX (0.3+3, 1+10, 3+30, 6+60, 10+100, 15+150, 30+300, 45 μg/kg TCDD + 450 mg/kg PCB153, respectively) or vehicle for 24 h. Relative liver weights (RLW) were significantly increased by all three treatments, but MIX induction was significantly ($p<0.05$) greater compared to TCDD and PCB153 alone. Histologically, MIX induced marked hepatocellular hypertrophy, vacuolization, immune cell infiltration, hyperplasia and necrosis, reflecting a combination of TCDD- and PCB153-elicited responses. Complementary lipid analyses identified significant increases in hepatic triglycerides in MIX- and TCDD-treated samples, while PCB153 had no effect on lipid

accumulation. Hepatic PCB153 levels were also significantly increased with TCDD co-treatment. Microarray analysis identified 568 unique differentially expressed genes, with 167, 185 and 388 differentially expressed in response to TCDD, PCB153 and MIX, respectively (|fold change|>1.5, P1(t)>0.999). Statistical modeling of quantitative real-time PCR analysis of Pla2g12a, Serpinb6a, Nqo1, Srxn1 and Dysf identified non-additive expression following MIX treatment compared to TCDD and PCB153 alone at 24 h. Furthermore, computational searches identified dioxin, constitutive androstane, and pregnane X receptor response elements in the promoter region of genes exhibiting non-additive interactions. This study has identified specific non-additive gene expression responses following co-treatment with TCDD plus PCB153 that are consistent with effects on gross physiology, histopathology, inflammation, and hepatic lipid accumulation.

INTRODUCTION

Polyhalogenated aromatic hydrocarbons (PHAHs), including polychlorinated biphenyls (PCBs) and polychlorinated dibenzo-*p*-dioxins (PCDDs), are persistent environmental contaminants that elicit species- and tissue-specific toxic effects. 2,3,7,8-Tetrachlorodibenzo-*p*-dioxin (TCDD) and other PCDDs are by-products of various activities including municipal solid waste and sewage sludge incineration, herbicide production, pulp and paper bleaching, backyard barrel burning, and other processes [1-4]. Despite the banning of both the production and the use of PCBs in many industrial applications in the late 1970s [4-6], various PCBs are still present in the environment and pose a potential adverse health threat. The chemical stability of PCBs and PCDDs coupled with their lipophilic nature has led to their bioaccumulation and biomagnification in the food chain, particularly in fatty tissues [7, 8].

The broad spectrum of effects elicited by PCBs and PCDDs include hepatotoxicity, immune suppression, reproductive toxicity, endocrine disruption, developmental toxicity, and carcinogenicity [9, 10]. Overall toxicity is determined by the structural similarity of the congener to TCDD and its ability to bind and activate the aryl hydrocarbon receptor (AhR) [11]. PCB congeners containing *meta* and *para* chlorines on the biphenyl ring (coplanar, dioxin-like PCBs) are more toxic than non-coplanar PCBs with *ortho* chlorine substituents reducing their AhR binding affinity [6, 12].

The responses elicited by dioxin and dioxin-like PCBs are mediated through the ligand-activation of AhR, a cytosolic basic helix-loop-helix Per/ARNT/Sim domain containing transcription factor [9, 13-15]. Upon ligand binding, chaperone proteins dissociate from the AhR, allowing its translocation to the nucleus and heterodimerization with AhR nuclear translocator (ARNT). AhR:ARNT heterodimers interact with dioxin response elements (DREs) in the regulatory regions of target genes and recruit transcriptional co-regulators, leading to changes in gene expression [14, 16].

Despite their non-dioxin-like characteristics, non-coplanar PCBs, in particular 2,2',4,4',5,5'-hexachlorobiphenyl (PCB153), account for a majority of the PCBs found in environmental and biological samples [17, 18]. PCB153 does not bind or activate the AhR. In addition, it elicits a unique response profile compared to TCDD and other dioxin-like PCBs that is constitutive androstane receptor (CAR)/pregnane X receptor (PXR) mediated [19-22]. Following ligand binding, CAR/PXR translocates to the nucleus to heterodimerize with the retinoid X receptor. This heterodimer complex can then bind to CAR and PXR response elements in the regulatory regions of target genes, recruiting co-activators and eliciting changes in gene expression [23-25].

Traditionally, risk assessment of environmental chemical exposure has focused on single congener toxicity. However, PCBs and dioxins exist as complex mixtures, and interactions between components can influence the toxicity of a mixture. For example, interactions can lead to additive effects elicited by two chemicals, or result in non-additive responses (i.e., synergistic or antagonistic) [26].

Previous studies have documented non-additive interactions between PCB153 and other dioxin-like chemicals. For example, PCB153 inhibits TCDD- and PCB126-induced cleft palate and immunotoxicity, and suppresses *in vivo* and *in vitro* ethoxyresorufin-O-deethylase (EROD) induction [27-29]. In contrast, others reported synergistic induction in mouse hepatic EROD and aryl hydrocarbon hydroxylase activities compared to TCDD treatment alone [30]. PCB153 and TCDD co-treatment has also been shown to elicit synergistic effects on porphyrin accumulation in Sprague-Dawley rats [31]. However, there have been no studies examining the non-additive effects of PCB153 and TCDD co-treatment on gene expression and associating these effects to a phenotypic response.

In this report, time course and dose-dependent hepatic gene expression studies with complementary computational response element searches, histopathology, lipid profiling and tissue analyses of PCB153 and TCDD levels were performed to evaluate the hepatic effects elicited by a mixture of TCDD and PCB153 in immature, ovariectomized C57BL/6 mice. Dose-response non-linear regression modeling identified non-additive gene expression responses elicited by the mixture that were consistent with the non-additive phenotypic responses observed at later time points.

MATERIALS & METHODS

ANIMAL HUSBANDRY

Female C57BL/6 mice, ovariectomized by the supplier on postnatal day (PND) 20, with body weights (BW) within 10% of the average, were obtained from Charles Rivers Laboratories (Portage, MI) on PND 25. Animals were housed in polycarbonate cages containing cellulose fiber chips (Aspen Chip Laboratory Bedding, Northeastern Products, Warrensberg, NY) with 30-40% humidity and a 12 h light/dark cycle (07:00 h – 19:00 h), had free access to deionized water and were fed *ad libitum* with Harlan Teklad 22/5 Rodent Diet 8640 (Madison, WI). Animals were acclimatized prior to dosing on PND 28. Immature ovariectomized mice were used to facilitate comparisons with other data sets obtained using the same model, study design and analysis methods [22, 32-34]. Immature animals are more responsive to AhR ligands, and ovariectomy negates potential interactions with estrogens produced by the maturing ovaries. All procedures were carried out with the approval of the Michigan State University All-University Committee on Animal Use and Care.

TIME COURSE AND DOSE-RESPONSE STUDIES

A stock solution of PCB153 (99.9% purity, AccuStandard, New Haven, CT) was first dissolved in acetone (J.T. Baker), followed by dilution with sesame oil (Sigma, St. Louis, MO), and evaporation of acetone under nitrogen gas. A stock solution of TCDD was a gift from the Dow Chemical Company (Midland, MI). PCB153 and TCDD stock solutions were diluted using sesame oil to achieve the desired dose. Animals were orally gavaged using 1.5 inch feeding needles with 2.25 mm ball ends (Cadence Science, Lake Success, NY). For the time course study, mice (n=5 per group) were administered 0.1 ml of a single dose of 30 μg/kg TCDD, 300 mg/kg PCB153, a mixture (MIX) of 1:10,000 ratio of TCDD:PCB153 (30 μg/kg TCDD with 300

mg/kg PCB153) or sesame oil vehicle and sacrificed after 4, 12, 24, 72 or 168 h. In the dose-response study, mice (n=5 per group) were gavaged with TCDD (0.3, 1, 3, 6, 10, 15, 30, 45 μg/kg), PCB153 (3, 10, 30, 60, 100, 150, 300, 450 mg/kg), MIX (0.3+3, 1+10, 3+30, 6+60, 10+100, 15+150, 30+300, 45 μg/kg TCDD + 450 mg/kg PCB153, respectively) or vehicle, and sacrificed 24 h post dose by cervical dislocation. Livers were removed, and sections weighed, flash frozen in liquid nitrogen, and stored at –80°C. A section of the right liver lobe was fixed in 10% neutral buffered formalin (Sigma) for histological analysis. For lipid staining, the remaining right lobe of the liver was frozen in Tissue-Tek O.C.T. compound (Sakura, Torrance, CA).

HISTOLOGICAL ANALYSIS

Fixed liver tissues were sectioned and processed in ethanol, xylene, and paraffin using a Thermo Electron Excelsior tissue processor (Waltham, MA). Tissues were embedded in paraffin with Miles Tissue Tek II embedding center, after which paraffin blocks were sectioned at 5 μm with a rotary microtome. Liver sections were placed on glass microscope slides, washed twice in xylene for 5 min, followed by four quick washes in ethanol and rinsing in water. Slides were placed in Gill 2 hematoxylin (Thermo Fisher Scientific, Waltham, MA) for 1.5 min followed by 2-3 quick dips in 1% glacial acetic acid water and rinsed with running water for 2-3 min. Slides were then rinsed in ethanol and counterstained with 1% eosin Y-phloxine B solution (Sigma) followed by multiple rinses in ethanol and xylene.

For lipid staining, liver samples were sectioned at 6 μm, fixed in 10% neutral buffered formalin for 5 min, rinsed with water and immersed in 100% propylene glycol for 5 min. Slides were stained with Oil Red O solution (Sigma) for 8 min at 60°C, placed in 80% propylene glycol for 5 min and rinsed in water for 15 min. Slides were counterstained with Gill 2 hematoxylin for 30 sec and washed with water for 30 min. Coverslips were attached using aqueous mounting

media. All the histological processing was performed at Michigan State University Investigative Histopathology Laboratory, Division of Human Pathology using a modified version of previously published procedures [35].

LIPID ANALYSIS BY GAS CHROMATOGRAPHY-MASS SPECTROMETRY (GC-MS)

TCDD, PCB153, MIX and vehicle control liver samples (~100 mg) from the time course (24, 72, 168 h) and dose-response (24 h) studies were homogenized (Polytron PT2100, Kinematica AG, Luzern, CH) in 40% methanol and acidified with concentrated HCl. Lipids were extracted with chloroform:methanol (2:1) containing 1 mM 2,6-di-tert-butyl-4-methylphenol (BHT; Sigma) and extraction efficiency controls (19:1n9 FFA [free fatty acid] and 19:0 TAG [triacylglycerol]) were added (Nu-Chek Prep, Elysian, MN). Protein and aqueous phases were re-extracted with chloroform and the organic phases were pooled. A derivatization standard (19:2n6 FFA; Nu-Chek Prep) was added and samples were dried under nitrogen, resuspended in 2% non-aqueous methanolic HCl and incubated at 60ºC overnight. Samples were cooled to room temperature and 0.9% (w/v) NaCl and hexane were added. The organic phase was collected and a loading control (17:1n9 fatty acid methyl ester [FAME]; Nu-Chek Prep) was added. Samples were dried under nitrogen, resuspended in equal volumes of hexane and separated on Agilent 6890N gas chromatograph interfaced to Agilent 5973 mass spectrometer with DB23 column (30 m length, 0.25 mm internal diameter, 0.25 μm film thickness). Samples were run on the following temperature program: 50°C to 150°C at 40°C/ min, to 185°C at 5°C/ min, to 235°C at 3°C/ min, to 250°C at 10°C/ min. Peak areas were integrated with MassLynx software (Waters, Milford, MA) and data were normalized to the starting amount of liver and loading controls. Principal component analysis of temporal lipid profiles was performed in R 2.6.0, data were extracted and used to generate PCA plots in GraphPad Prism 5.0 (La Jolla, CA).

HEPATIC TRIGLYCERIDE MEASUREMENT

Frozen liver samples (~100 mg) were homogenized (Polytron PT2100, Kinematica) in 1 ml of 1.15% KCl. Triglycerides were extracted from 200 µl of hepatic homogenate with 800 µl of isopropyl alcohol by vortex-mixing for 10 min. The samples were centrifuged for 5 min at 800 x g at room temperature and supernatant was collected into separate vials. The concentration of hepatic triglycerides was determined using a commercial L-Type Triglyceride M kit (Wako Diagnostics, Richmond, VA) with Multi-Calibrator Lipids as a standard (Wako Diagnostics). The measurements were performed according to the manufacturer's protocol with 20 µl of the triglyceride extract incubated with 150 µl of Reagent 1 followed by incubation with 50 µl of Reagent 2. Final results were normalized to the starting amount of liver.

QUANTIFICATION OF HEPATIC PCB153 AND TCDD LEVELS

Liver samples were processed in parallel with laboratory blanks and a reference or background sample at Wellington Laboratories Inc. (Guelph, ON, Canada). Samples (100 to 500 mg) were transferred to a tared screw cap culture tube and weights were recorded. Samples were spiked with $^{13}C_{12}$-PCB153 and $^{13}C_{12}$-2,3,7,8-TCDD surrogates and digested with hydrochloric acid. Each digested sample was then split between two screw cap tubes and 3-4 ml hexane was added to each tube followed by vigorous mixing. Tubes were centrifuged, and the organic layer was removed. Hexane extraction was repeated three times per screw cap tube and the six hexane fractions were combined. The hexane fraction was then split evenly prior to clean-up and one fraction was archived. The other fraction was cleaned-up using a small multi-layer (acid/base/neutral) silica gel column eluted with 20-25 ml of hexane. The eluate was concentrated on a rotary evaporator and then transferred to a conical microvial with pentane and dichloromethane rinses and allowed to dry. Immediately prior to injection on the high-resolution

gas chromatograph/high-resolution mass spectrometer (HRGC-HRMS) system, $^{13}C_{12}$-PCB111 and $^{13}C_{12}$-1,2,3,4-TCDD injection standards were added to the conical microvial. The identification and quantification of PCB153 and TCDD was performed using an Agilent (Santa Clara, CA, USA) 6890 series HRGC with direct capillary interface to a Waters Autospec Ultima HRMS. Chromatographic separations were carried out on a 60 m DB5 (0.25 mm ID, 0.25 μm film thickness) column in constant flow mode (Helium, 1 ml /min). All injections were 1 μl and a splitless injection was used. The mass spectrometer was operated in EI+ selective ion recording mode at a mass resolving power of 10,000 or greater.

RNA ISOLATION

Liver samples (~100 mg stored at –80°C) were immediately transferred to 1 ml TRIzol (Invitrogen, Carlsbad, CA) and homogenized using a Mixer Mill 300 tissue homogenizer (Retsch, Germany). Total RNA was isolated according to the manufacturer's protocol with an additional acid phenol:chloroform extraction. Isolated RNA was resuspended in RNA storage solution (Ambion Inc., Austin, TX), quantified (A_{260}), and quality was assessed by determining the A_{260}/A_{280} ratio and by visual inspection of 2 μg on a denaturing gel.

MICROARRAY EXPERIMENTAL DESIGN

TCDD, PCB153, MIX and vehicle RNA samples from the time course study were individually hybridized to 4 × 44 K Agilent microarrays (Agilent Technologies, Inc., Santa Clara, CA). Three biological replicates were performed using one-color labeling (Cy3) for each time point and treatment, according to the manufacturer's protocol (Agilent Manual: G4140-90040 v. 5.7). Microarray slides were scanned at 532 nm (Cy3) on a GenePix 4000B scanner (Molecular Devices, Union City, CA). Images were analyzed for feature and background

intensities using GenePix Pro 6.0 (Molecular Devices). All data were managed in TIMS dbZach data management system [36].

MICROARRAY ANALYSIS

All microarray data passed our laboratory quality assurance protocol [37]. Microarray data were normalized using a semi-parametric approach [38] and the posterior probabilities were calculated using an empirical Bayes method based on a per gene and dose basis using model-based *t* values [39]. Gene expression data were ranked and prioritized using a P1(*t*) values >0.999 and |fold change|>1.5 to identify differentially expressed genes. Data obtained from the time course microarray were used as a filter to identify putative non-additive candidates for further verification in the 24 h dose-response study.

QUANTITATIVE REAL-TIME PCR (QRTPCR)

QRTPCR verification of microarray responses was performed as described previously [32]. Briefly, 1 μg of total RNA was reverse transcribed by SuperScript II (Invitrogen) using an anchored oligo-dT primer as described by the manufacturer. The cDNA (1.0 μl) was used as a template in a 30 μl PCR reaction containing 0.1 μM of forward and reverse gene-specific primers, 3 mM $MgCl_2$, 1 mM dNTPs, 0.025 IU AmpliTaq Gold, and 1× SYBR Green PCR buffer (Applied Biosystems, Foster City, CA). PCR amplification was conducted on an Applied Biosystems PRISM 7500 Sequence Detection System. cDNAs were quantified using a standard curve approach and the copy number of each sample was standardized to 3 housekeeping genes (Actb, Gapdh, Hprt) to control for the differences in RNA loading, quality, and cDNA synthesis [40]. For graphing purposes, the relative expression levels were scaled such that the expression level of the time-matched control group was equal to one.

COMPUTATIONAL DNA RESPONSE ELEMENT IDENTIFICATION

Dioxin response elements (DREs) [41, 42], constitutive androstane receptor response elements (CAREs) [43] and pregnane X receptor response elements (PXREs) [22] were computationally identified using position weight matrices specific to each element. Gene regulatory regions (-10,000 bp relative to the transcriptional start site [TSS] together with 5'-untranslated region [UTR]) were obtained from the University of California, Santa Cruz, Genome Browser for mouse (build 37), computationally searched, and each DRE, CARE and PXRE was scored. Matrix similarity scores (MSS) >0.80 are considered to be putative response elements.

DOSE-RESPONSE NON-LINEAR LOGISTIC MODELING

Gene-specific non-linear models were fit to investigate the dose-response relationship for Dysf, Pla2g12a, Serpinb6a, Srxn1, Nqo1, Got1, Elovl5, Dexi, Akr1c20 and Srebf1 identified in the microarray study as putative candidates exhibiting non-additive gene expression and further verified using QRTPCR in the 24 h dose-response study. Specifically, for each gene a non-linear logistic model for the mean was used to estimate the dose-response relationship for TCDD and PCB153, according to:

$$\mu_{add} = \frac{\gamma}{1+\exp(-(\beta_0+\beta_1\chi_1+\beta_2\chi_2))},$$

where β_0 is the unknown intercept parameter, $\beta_i, i = 1,2,3,$ is the unknown slope parameter associated with the *i*th chemical, χ_i is the dose associated with the *i*th chemical, γ is the maximum-effect parameter, and μ_{add} is the expected value of the response under the additive model. Simultaneously, the MIX data were fit with a mixture model:

$$\mu_{mix} = \frac{\gamma}{1+\exp(-(\beta_0+\theta_{\mathrm{mix}}t))},$$

where *t* is the dose associated with MIX data. For a fixed-ratio of TCDD and PCB153 given by $(\alpha_1, \alpha_2$, such that $\alpha_1 + \alpha_2$=1), the slope for the mixture under additivity is $\theta_{\mathrm{mix}} = (\beta_1\alpha_1 + \beta_2\alpha_2)$. Based on preliminary analyses, using the quasi-likelihood estimation criterion, the assumption is made that variance is a function of the mean: $Var\ (y) = \tau\mu$, where τ is the parameter associated with the functional form of the variance and has to be estimated. The quasi-likelihood criterion has assumptions only concerning the first and second moments, and some regularity conditions related to the regression equation: $E(Y) = \mu(\theta)$ and $Var(Y) = \tau V(\mu)$. It is of interest to maximize the quasi-likelihood function given by:

$$Q = \frac{1}{\tau}\int_{\mu}^{y}\frac{y-t}{t}dt = \frac{1}{\tau}(ylog\mu - \mu).$$

Gene-specific plots of the mean versus the variance for TCDD, PCB153, and MIX confirmed the relationship between the mean and the variance. In the study, the additive dose-response model for the fixed-ratio mixture based on TCDD and PCB153 data alone was compared to the mixture model obtained using MIX data. Therefore, the null hypothesis states that $\theta_{\mathrm{mix}} = \theta_{\mathrm{add}}$, where θ_{mix} and θ_{add} are the parameter vectors assuming the mixture and the additive models, respectively. The modeling (PROC NLIN) was performed with SAS 9.2 (SAS Institute, Cary, NC).

FUNCTIONAL GENE ANNOTATION AND STATISTICAL ANALYSIS

Annotation and functional categorization of the differentially regulated genes was performed using Database for Annotation, Visualization and Integrated Discovery (DAVID) [44]

and Ingenuity Pathway Analysis (Ingenuity Systems, Redwood City, CA). All statistical analyses were performed with SAS 9.2. Unless stated otherwise, all data were analyzed by analysis of variance (ANOVA) followed by Dunnett's or Tukey's *post hoc* test. Differences between treatment groups were considered significant when $p<0.05$.

RESULTS

ORGAN AND BODY WEIGHTS

Exposure to environmental contaminants including dioxins and PCBs leads to temporal and dose-dependent increases in liver weight in rodents [14, 18, 19, 22, 45, 46]. In the time course study, significant increases in relative liver weight (RLW) were observed with 300 mg/kg PCB153 (72, 168 h), 30 μg/kg TCDD, and MIX (24, 72, 168 h), relative to time-matched vehicle controls (Figure 26A). TCDD and PCB153 treatment resulted in comparable increases in RLW, while MIX-elicited induction in RLW was significantly greater compared to TCDD and PCB153 at 72 and 168 h (Figure 26A). These results are consistent with reported increases in RLW in C57BL/6 and B6C3F1 mice 3, 7 and 13 days after a single gavage of TCDD and PCB153 mixture [47, 48].

In the 24 h dose-response study, TCDD and MIX elicited comparable significant increases in RLW in all but the lowest dose groups (Figure 26B). MIX-induced RLW increase at 15+150 (μg/kg TCDD + mg/kg PCB153, respectively) was also significantly greater when compared to 150 mg/kg PCB153 (Figure 26B). In contrast, PCB153 increased RLW only at 100 and 300 mg/kg.

Minimal (≤ 10%) decreases in body weight gain were observed with PCB153 (300 and 450 mg/kg) and MIX (three highest dose group combinations) at 24 h, but were not considered indicative of systemic toxicity [49].

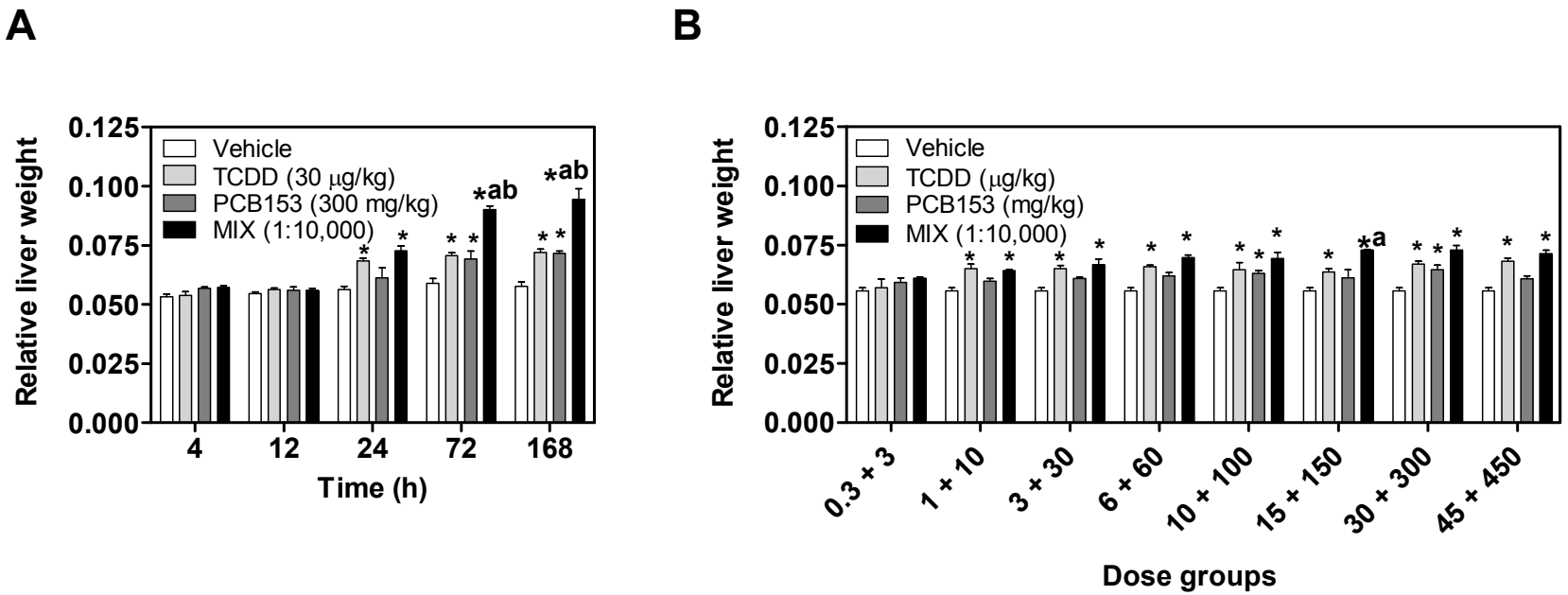

Figure 26.Temporal and dose-dependent changes in the relative liver weights following exposure to TCDD, PCB153, and MIX. (A) In the time course study, 30 μg/kg TCDD + 300 mg/kg PCB153 were co-administered in a MIX group (1:10,000 ratio of TCDD to PCB153, respectively). (B) In the dose-response at 24 h, MIX dose groups (represented as μg/kg TCDD + mg/kg PCB153) were also administered at 1:10,000 ratio of TCDD to PCB153, respectively. Results are displayed as mean ± standard error (SE) of at least 5 independent replicates. Data were analyzed by analysis of variance (ANOVA) followed by Tukey's *post hoc* test: *$p<0.05$ vs. vehicle, [a]$p<0.05$ vs. PCB153 and [b]$p<0.05$ vs. TCDD.

HEPATIC TISSUE LEVEL QUANTIFICATION

HRGC-HRMS analysis of liver samples at 24 and 168 h indicate that the hepatic PCB153 accumulation was potentiated following TCDD co-treatment compared to PCB153 alone (Figure 27B). No changes were detected in the hepatic accumulation of TCDD following co-administration with PCB153 (Figure 27A). In addition, PCB153 levels dramatically decreased at 168 h compared to more modest decreases in TCDD levels after seven days [22].

HISTOPATHOLOGY

In the time course study, TCDD elicited moderate multifocal inflammation and marked hepatocellular vacuolization localized in periportal regions and extending to midzonal and centrilobular regions at later time points. Instances of vacuolization corresponded with significant Oil Red O (ORO) staining indicating neutral lipid accumulation (Figure 28B,F). These changes are consistent with previous reports on the hepatic effects of TCDD in mice [32, 45].

PCB153 elicited levels of vacuolization comparable to those observed in vehicles, as well as mild to moderate centrilobular hypertrophy with cytoplasmic granularity (Figure 28C,G) [22]. In contrast to TCDD, PCB153 did not elicit inflammation. Treatment with MIX exhibited a combination of the TCDD and PCB153 responses. Vacuolization and ORO staining in MIX was the most severe at 24 h, which decreased by 168 h compared to TCDD-exposed mice. MIX-treated livers also had moderate multifocal inflammation and a temporal increase in cellular hypertrophy that was comparable to time-matched TCDD and PCB153-exposed livers, respectively. Furthermore, MIX elicited minimal necrosis and instances of mitotic figures indicative of hyperplasia (Figure 28D,H).

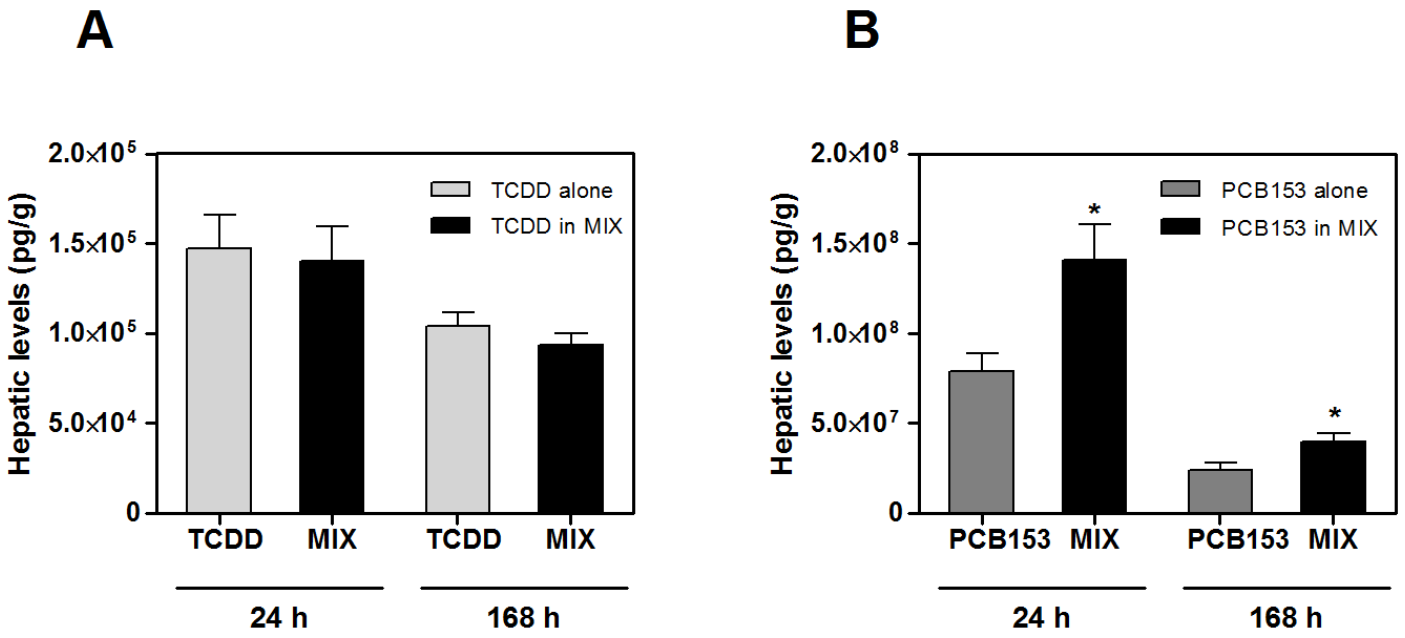

Figure 27. Tissue level quantification.
Hepatic (A) TCDD and (B) PCB153 accumulation levels per g liver wet weight measured by HRGC-HRMS. PCB153 levels were significantly induced following co-administration with TCDD (in MIX) at 24 and 168 h. However no changes were detected in TCDD hepatic accumulation following co-treatment with PCB153 (in MIX). Results are displayed as mean ± SE of 3 independent replicates. Data were analyzed by ANOVA followed by Tukey's *post hoc* test: *$p<0.05$ vs. time-matched PCB153 levels alone.

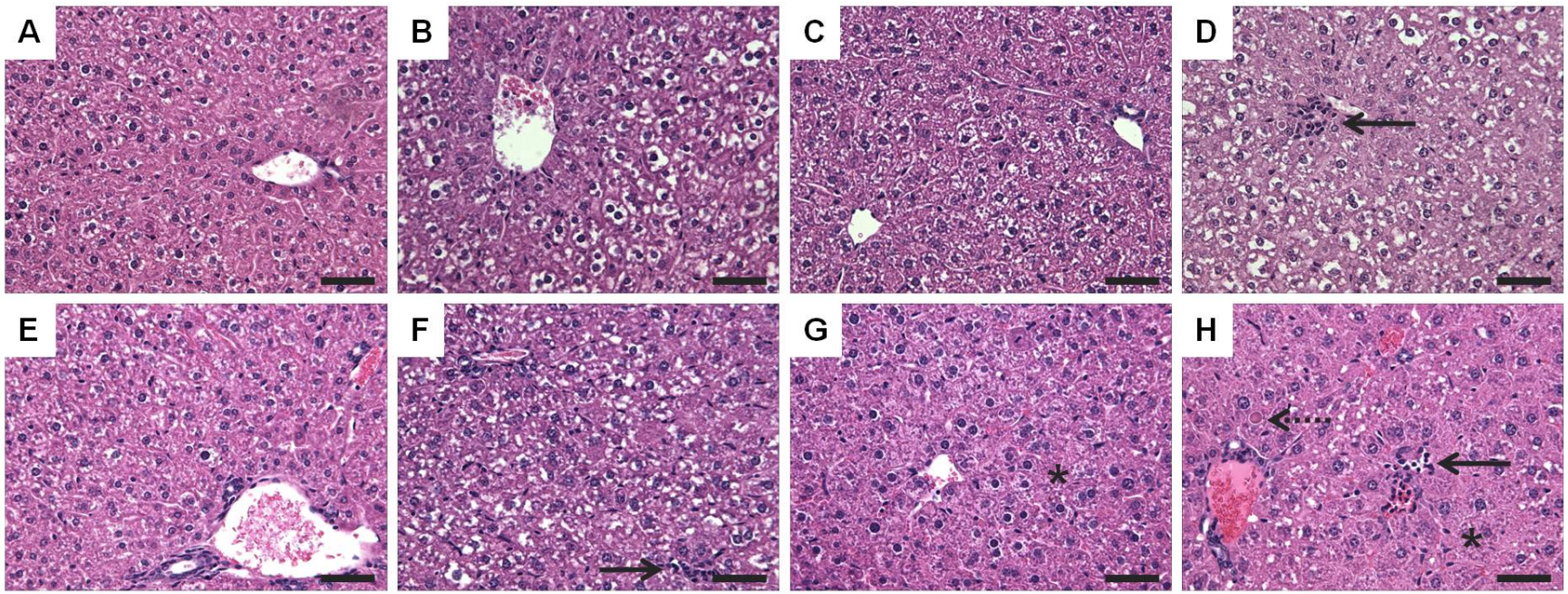

Figure 28. Representative histopathology results.
Standard hematoxylin and eosin staining of liver sections at 24 (top panel: A-D) and 168 h (bottom panel: E-H). (A&E) Sesame oil treatment exhibited minimal vacuolization. (B&F) 30 µg/kg TCDD elicited vacuolization and inflammation (solid arrow). (C&G) 300 mg/kg PCB153 resulted in minimal vacuolization and hypertrophy (star). (D&H) MIX exposure resulted in vacuolization, inflammation (solid arrow), hypertrophy (star) and necrosis (dashed arrow). Bars = 50 µm.

Liver microscopic changes observed in the dose-response study were most severe in the highest dose groups for each treatment. TCDD elicited moderate periportal hepatocellular vacuolization and minimal multifocal inflammation (15, 30, 45 μg/kg), while PCB153 elicited mild to moderate centrilobular hypertrophy (300 and 450 mg/kg) and minimal to mild hepatocellular vacuolization. MIX treatment resulted in moderate to marked periportal hepatocellular vacuolization and centrilobular hypertrophy and minimal mixed cell infiltration (15+15, 30+300, 45 μg/kg TCDD + 450 mg/kg PCB153, respectively).

LIPID PROFILING

Total lipids extracted from TCDD, PCB153, MIX and control livers from the time course (24, 72 and 168 h) and dose-response studies were derivatized to fatty acid methyl esters. The levels of twenty one individual fatty acid species were measured and analyzed using GC-MS. Principal component (PC) analysis (Figure 29) identified a time- and treatment-dependent separation of fatty acid (FA) profiles (as fold changes) around PC1 and PC2, respectively. Treatment and time-dependent induction in individual fatty acids is represented in Figure 30A-C.

Compared to all treatments, TCDD induced the most pronounced changes in total FAs that increased in a time-dependent fashion, with significant inductions at 72 and 168 h ($p<0.05$ vs. vehicle and PCB153) (Table 14), consistent with the most pronounced ORO staining at 168 h. MIX-elicited increases in total FAs were comparable across time, with significant changes at 24 and 168 h ($p<0.05$ vs. vehicle and PCB153) (Table 14).

Comparison of saturated (SFA), monounsaturated (MUFA), and n3 and n6 polyunsaturated fatty acids (PUFA) revealed significant differences in MIX inductions compared to individual chemical exposure (Table 14). In agreement with the lack of ORO staining,

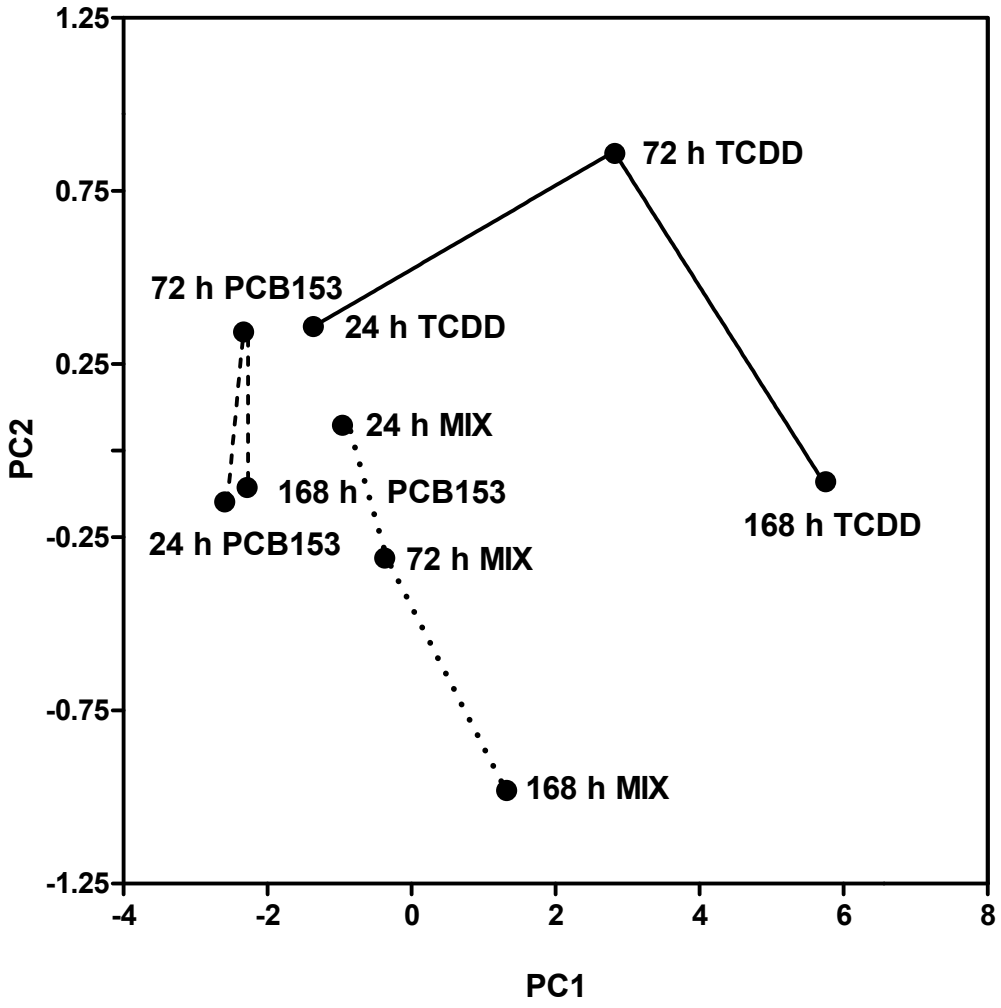

Figure 29. Principal component analysis of lipid profiles.
GC-MS lipid profile for TCDD (solid line), PCB153 (dashed line), and MIX (dotted line) at 24, 72 and 168 h. PCA was performed in R as described in the Materials and Methods. The cumulative proportion of variance for PC1 and PC2 is 95%, indicating that the PCA plot accurately represents the separation of the data. PCA indicated treatment- and time-dependent separation of fatty acid species (represented as fold changes).

Table 14. GC-MS analysis of fatty acid composition.

Time (h)	Treatment	SFA	MUFA	n3 PUFA	n6 PUFA	Total FA
24	Vehicle	472.71 ± 64.53	170.21 ± 41.37	103.94 ± 9.56	349.80 ± 42.12	1096.65 ± 152.52
	TCDD	504.19 ± 57.39	197.54 ± 54.99	106.95 ± 10.60	363.20 ± 32.40	1171.89 ± 148.03
	PCB153	422.49 ± 45.64	134.35 ± 31.72	103.70 ± 11.67	331.29 ± 26.02	991.84 ± 97.90
	MIX	590.06 ± 37.85*[a]	264.58 ± 27.06*[a]	114.20 ± 6.99	447.42 ± 29.96*[ab]	1416.26 ± 96.05*[a]
72	Vehicle	470.31 ± 39.09	184.24 ± 33.04	93.26 ± 10.15	317.51 ± 22.72	1065.32 ± 72.23
	TCDD	702.20 ± 80.64*[a]	394.28 ± 63.50*[a]	109.14 ± 2.92	432.07 ± 40.07*	1637.68 ± 180.72*[a]
	PCB153	513.23 ± 125.56	213.53 ± 100.64	98.27 ± 15.94	326.28 ± 64.06	1151.31 ± 270.82
	MIX	558.24 ± 80.12[b]	257.33 ± 67.52	104.47 ± 5.89	394.45 ± 23.05	1314.50 ± 174.81
168	Vehicle	455.12 ± 15.19	178.44 ± 24.29	97.07 ± 7.28	333.55 ± 14.33	1064.17 ± 51.85
	TCDD	778.11 ± 105.98*[a]	432.65 ± 75.20*[a]	130.39 ± 6.76*[a]	526.26 ± 46.53*[a]	1867.40 ± 226.62*[a]
	PCB153	492.70 ± 59.68	184.20 ± 19.16	104.39 ± 8.46	342.23 ± 26.61	1123.52 ± 110.42
	MIX	628.25 ± 60.38*[ab]	272.31 ± 62.84*[ab]	121.32 ± 11.21*[a]	461.61 ± 41.32*[a]	1483.49 ± 159.37*[a]

Note. Hepatic fatty acids were measured by GC-MS and peak areas were integrated using MassLynx software. The results are displayed in arbitrary units and reported as mean ± SD of 5 independent replicates. Data were analyzed by ANOVA followed by Tukey's *post hoc* test: *$p<0.05$ vs. vehicle, [a]$p<0.05$ vs. PCB153 and [b]$p<0.05$ vs. TCDD.

Figure 30. GC-MS fatty acid profiles.
Fatty acid profiles measured by GC-MS for TCDD, PCB153, and MIX-treated mouse livers at (A) 24 (B) 72 and (C) 168 h relative to vehicle controls. TCDD elicited time-dependent induction of multiple fatty acid species compared to PCB153 which did not alter fatty acid composition. At later time points, the induction of 20:1n9, 20:2n6 and 20:3n3 by TCDD was significantly repressed following co-treatment with PCB153 (in MIX). Results are displayed as mean ± SE of 5 independent replicates. Data were analyzed by ANOVA followed by Tukey's *post hoc* test: *$p<0.05$ vs. vehicle, $^{a}p<0.05$ vs. PCB153 and $^{b}p<0.05$ vs. TCDD.

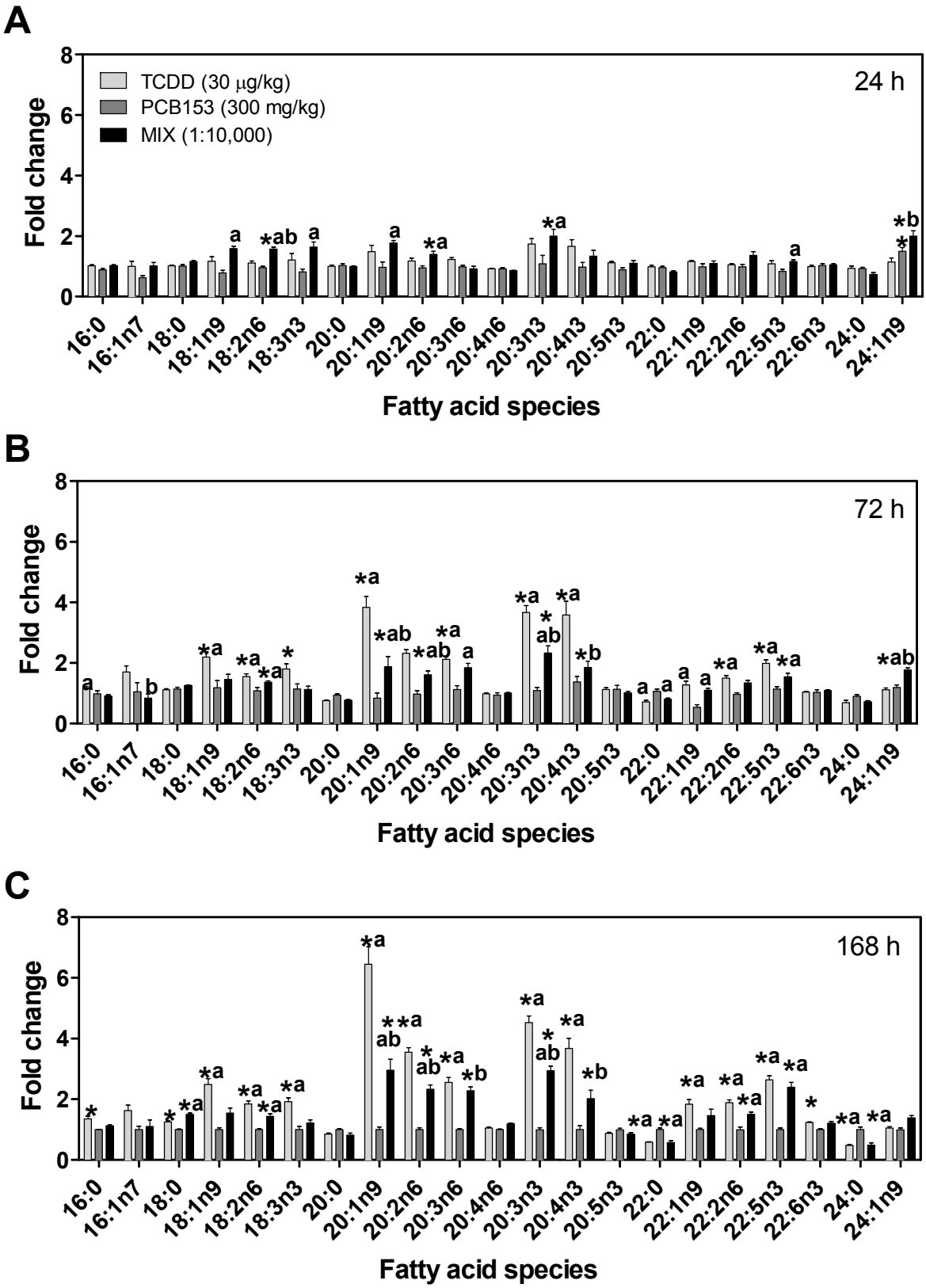
A
TCDD (30 μg/kg)
PCB153 (300 mg/kg)
MIX (1:10,000)
24 h
Fold change
Fatty acid species
B
72 h
Fold change
Fatty acid species
C
168 h
Fold change
Fatty acid species
16:0
16:1n7
18:0
18:1n9
18:2n6
18:3n3
20:0
20:1n9
20:2n6
20:3n6
20:4n6
20:3n3
20:4n3
20:5n3
22:0
22:1n9
22:2n6
22:5n3
22:6n3
24:0
24:1n9

PCB153 did not change total FAs or any of the FA classes at any time point (Table 14), in agreement with CAR-mediated inhibition of lipogenesis (Zhai *et al.*, 2010).

Overall, TCDD significantly induced SFAs, MUFAs and PUFAs in a time-dependent fashion, although changes in n3 PUFAs were modest. Interestingly, MIX significantly repressed SFAs and MUFAs but increased n6 PUFA levels compared to TCDD at 168 and 24 h, respectively (Table 14). These non-additive effects on fatty acids are consistent with MIX inductions in triglyceride levels and ORO staining at 24 h that decreased by 168 h compared to TCDD at the same time points. GC-MS analysis of FA profiles in the dose-response study revealed slightly higher increases in MIX compared to TCDD groups, but the differences were not statistically significant.

TEMPORAL MICROARRAY GENE EXPRESSION

Hepatic gene expression was evaluated using whole genome 4x44K Agilent oligonucleotide microarrays containing ~21,000 unique annotated genes. Statistical analysis of the time course study data identified 568 unique gene expression changes, with 167, 185 and 388 genes differentially regulated in response to TCDD, PCB153 and MIX, respectively (|fold change|>1.5, P1(t)>0.999) at one or more time points. MIX elicited the highest number of differentially expressed genes at each time point.

Comparative analysis identified 68 TCDD-, 111 PCB153-, and 230 MIX-specific responses (|fold change|>1.5, P1(t)>0.999). Only 13 genes were differentially expressed by all three treatments (Figure 31A). When the statistical criteria were relaxed for more inclusive analysis (|fold change|>1.5, P1(t)>0.95) (Figure 31B), the number of overlapping genes significantly increased, including the overlaps between MIX and TCDD, and MIX and PCB153.

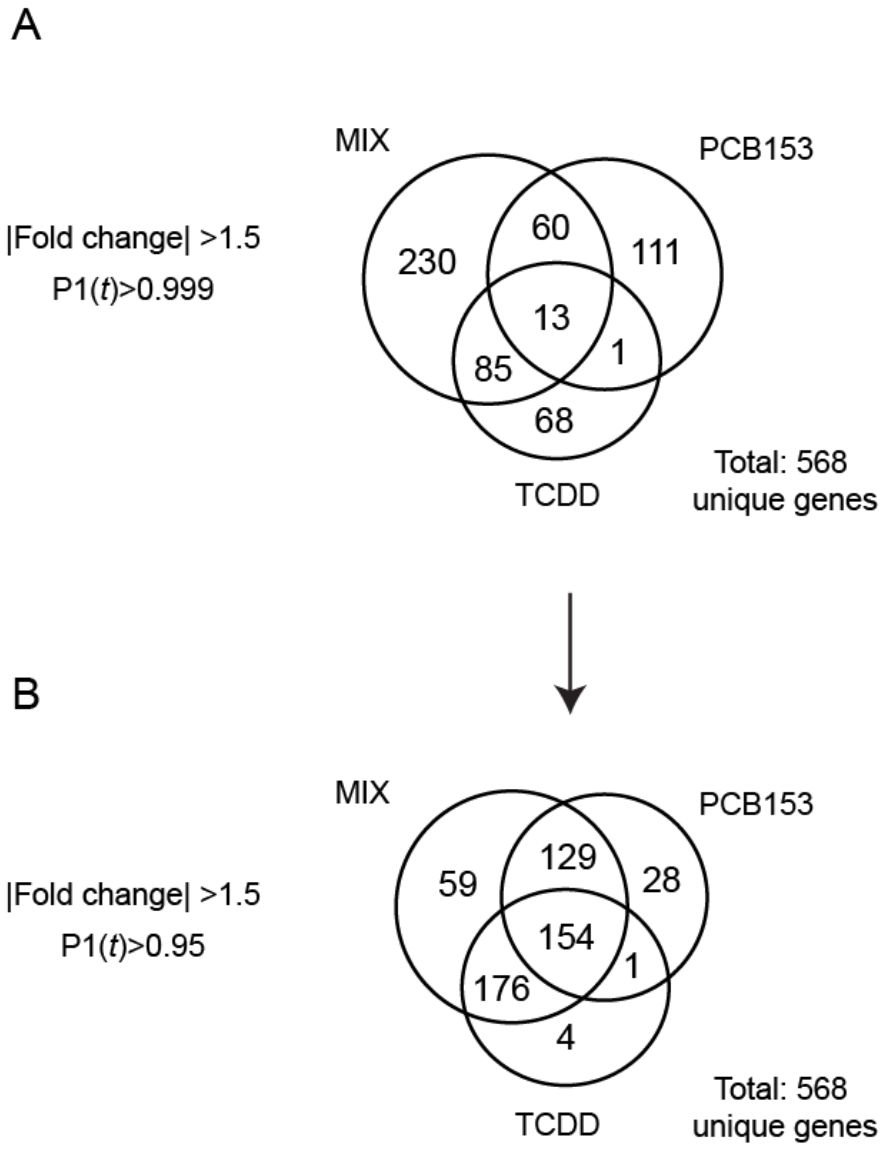

Figure 31. Three-way Venn analysis.
Temporal microarray data sets for 30 µg/kg TCDD, 300 mg/kg PCB153, and MIX (1:10,000 TCDD:PCB153, respectively) groups were compared at (A) stringent (|fold change|>1.5, P1(*t*)>0.999) and (B) relaxed (|fold change|>1.5, P1(*t*)>0.95) selection criteria. Numbers in the Venn diagram represent unique genes.

Functional annotation of the 568 differentially regulated genes was associated with xenobiotic metabolism, oxidoreduction/oxidative stress, lipid metabolism, immune response, cell division and differentiation, cell death, and transport. Many of these over-represented functions (Table 15) could be phenotypically anchored to the changes in RLW, histopathology, and lipid profiles. For example, the differential expression of genes involved in lipid metabolism and transport was consistent with the hepatic fatty accumulation, increased hepatic triglyceride levels, and changes in specific FAMEs. TCDD and MIX induced significant fatty vacuolization between 24-168 h consistent with the induction of Cd36 (~6 fold) or Fabp12 (~54-34 fold), which were not induced by PCB153. Down-regulation of Elovl5 (-2 fold) and up-regulation of Insig2 (~6 fold) by PCB153, in contrast to TCDD, was also consistent with GC-MS fatty acid profiling indicating lack of lipid accumulation in PCB153-exposed livers.

Histopathology also revealed alterations in cell size (hypertrophy), as well as cell division and cell death (hyperplasia and necrosis) (Figure 28). TCDD and MIX significantly induced genes that promote cell death including Bcl2l11 (~2-4 fold), Tnfaip2 (~7 fold), Tnfaip8l1 (~3-4 fold), Traf5 (~2 fold), and Htatip2 (~4 fold), which were not regulated by PCB153, in agreement with observed lack of cell death.

Furthermore, TCDD significantly induced genes involved in the immune response (~2-8 fold; Clec7a, Fcgr1, H2-Eb1, H2-DMa, H2-DMb1, Irf8, Ltb, Mfg28 and Saa2-3), consistent with the marked multifocal inflammation at later time points. In contrast, PCB153 did not alter the expression of these genes, while MIX elicited significant inflammation, reflected by comparable induction of immune related genes relative to TCDD.

Table 15. Functional categorization and potential response element regulation of select hepatic genes differentially expressed by 30 µg/kg TCDD, 300 mg/kg PCB153. and MIX.

Functional category	Entrez Gene ID	Gene name	Gene symbol	TCDD *	PCB153 *	MIX *	DREs [a]	PXREs [a]	CAREs [a]
Xenobiotic metabolism/ oxidoreductase activity/ oxidative stress	11761	Aldehyde oxidase 1	Aox1	2.2	2.9	4.8	yes	yes	yes
	11997	Aldo-keto reductase family 1, member B7	Akr1b7	NC	22.1	16.8	yes	yes	yes
	432720	Aldo-keto reductase family 1, member C19	Akr1c19	NC	1.7	2.0	yes	yes	no
	116852	Aldo-keto reductase family 1, member C20	Akr1c20	-1.7	-1.6	-3.0	no	yes	no
	13076	Cytochrome P450, family 1, subfamily a, polypeptide 1	Cyp1a1	348.1	NC	348.2	yes	yes	yes
	13077	Cytochrome P450, family 1, subfamily a, polypeptide 2	Cyp1a2	2.4	1.7	2.4	yes	yes	yes
	13088	Cytochrome P450, family 2, subfamily b, polypeptide 10	Cyp2b10	NC	16.1	24.2	yes	yes	yes
	13089	Cytochrome P450, family 2, subfamily b, polypeptide 13	Cyp2b13	NC	1.9	1.9	yes	yes	yes
	13094	Cytochrome P450, family 2, subfamily b, polypeptide 9	Cyp2b9	NC	7.6	6.2	no	yes	yes
	72082	Cytochrome P450, family 2, subfamily c, polypeptide 55	Cyp2c55	NC	48.4	48.4	yes	yes	yes
	13113	Cytochrome P450, family 3, subfamily a, polypeptide 13	Cyp3a13	-1.9	2.5	NC	no	yes	no

Table 15 (cont'd).

Functional category	Entrez Gene ID	Gene name	Gene symbol	TCDD *	PCB153 *	MIX *	DREs a	PXREs a	CAREs a
Xenobiotic metabolism/ oxidoreductase activity/ oxidative stress	56388	Cytochrome P450, family 3, subfamily a, polypeptide 25	Cyp3a25	NC	3.8	3.0	no	yes	yes
	56050	Cytochrome P450, family 39, subfamily a, polypeptide 1	Cyp39a1	NC	2.5	2.0	yes	yes	no
	14776	Glutathione peroxidase 2	Gpx2	NC	4.3	8.9	yes	yes	yes
	14858	Glutathione S-transferase, alpha 2 (Yc2)	Gsta2	5.8	4.1	11.3	yes	yes	yes
	14863	Glutathione S-transferase, mu 2	Gstm2	2.0	2.0	2.2	yes	yes	yes
	14865	Glutathione S-transferase, mu 4	Gstm4	2.4	4.0	5.6	yes	yes	yes
	14872	Glutathione S-transferase, theta 2	Gstt2	2.0	2.0	2.2	yes	yes	yes
	18104	NAD(P)H dehydrogenase, quinone 1	Nqo1[s]	4.6	2.8	12.6	yes	yes	yes
	76650	Sulfiredoxin 1 homolog (S. cerevisiae)	Srxn1[s]	2.6	2.3	3.9	yes	yes	yes
	394435	UDP glucuronosyltransferase 1 family, polypeptide A6B	Ugt1a6b	5.6	NC	6.4	yes	yes	no
	22235	UDP-glucose dehydrogenase	Ugdh	2.7	2.5	2.7	yes	yes	yes

Table 15 (cont'd).

Functional category	Entrez Gene ID	Gene name	Gene symbol	TCDD *	PCB153 *	MIX *	DREs a	PXREs a	CAREs a
Lipid and glucose metabolism	12491	CD36 antigen	Cd36	5.7	NC	6.1	yes	yes	yes
	26903	Dysferlin	Dysf[S]	3.3	1.5	14.9	yes	yes	yes
	170439	ELOVL family member 6, elongation of long chain fatty acids (yeast)	Elovl6	-4.3	-3.8	-5.2	yes	yes	yes
	75497	Fatty acid binding protein 12	Fabp12	53.7	-1.5	34.4	yes	yes	yes
	14104	Fatty acid synthase	Fasn	-4.3	-3.9	-6.4	yes	yes	yes
	14718	Glutamate oxaloacetate transaminase 1, soluble	Got1	-2.6	NC	-4.3	yes	yes	yes
	14571	Glycerol phosphate dehydrogenase 2, mitochondrial	Gpd2	-3.0	1.5	-3.3	yes	yes	yes
	72999	Insulin induced gene 2	Insig2	NC	5.9	4.0	yes	yes	yes
	53357	Phospholipase A2, group VI	Pla2g6	NC	2.5	1.8	yes	yes	yes
	66350	Phospholipase A2, group XIIA	Pla2g12a[S]	3.7	2.7	7.7	yes	yes	yes
	228026	Pyruvate dehydrogenase kinase, isoenzyme 1	Pdk1	-1.6	NC	1.6	yes	yes	no
	20250	Stearoyl-Coenzyme A desaturase 2	Scd2	2.0	NC	NC	yes	yes	yes
	20788	Sterol regulatory element binding factor 2	Srebf2	-1.7	-2.1	-1.6	yes	yes	yes
	20787	Sterol regulatory element binding transcription factor 1	Srebf1	-2.3	-2.4	-4.6	yes	yes	yes

Table 15 (cont'd).

Functional category	Entrez Gene ID	Gene name	Gene symbol	TCDD *	PCB153 *	MIX *	DREs a	PXREs a	CAREs a
Cell cycle/ cell death	12125	BCL2-like 11 (apoptosis facilitator)	Bcl2l11	1.9	NC	4.2	yes	yes	no
	13197	Growth arrest and DNA-damage-inducible 45 alpha	Gadd45a	-3.6	9.4	3.1	yes	no	yes
	17873	Growth arrest and DNA-damage-inducible 45 beta	Gadd45b	5.7	10.8	29.2	yes	yes	yes
	53415	HIV-1 tat interactive protein 2, homolog (human)	Htatip2	3.5	NC	4.4	yes	yes	no
	15937	Immediate early response 3	Ier3	3.5	NC	3.8	yes	yes	yes
	17869	Myelocytomatosis oncogene	Myc	3.0	4.2	7.2	yes	yes	yes
	211323	Neuregulin 1	Nrg1	2.8	NC	6.7	yes	yes	yes
	78688	Nucleolar protein 3	Nol3	NC	4.8	4.7	yes	yes	no
	22033	Tnf receptor-associated factor 5	Traf5	2.1	NC	2.3	yes	yes	yes
	21813	Transforming growth factor, beta receptor II	Tgfbr2	1.6	1.8	2.4	yes	yes	yes
	29820	Tumor necrosis factor receptor superfamily, member 19	Tnfrsf19	3.9	2.6	7.7	yes	yes	yes
	21928	Tumor necrosis factor, alpha-induced protein 2	Tnfaip2	6.7	NC	6.9	yes	yes	yes
	66443	Tumor necrosis factor, alpha-induced protein 8-like 1	Tnfaip8l1	3.0	NC	4.1	yes	yes	yes

Table 15 (cont'd).

Functional category	Entrez Gene ID	Gene name	Gene symbol	TCDD *	PCB153 *	MIX *	DREs a	PXREs a	CAREs a
Immune response	12774	Chemokine (C-C motif) receptor 5	Ccr5	2.4	-1.6	NC	no	yes	yes
	56644	C-type lectin domain family 7, member a	Clec7a	3.9	NC	2.9	yes	yes	yes
	58239	Dexamethasone-induced transcript	Dexi	-1.9	-1.9	-4.3	yes	yes	no
	14129	Fc receptor, IgG, high affinity I	Fcgr1	2.4	NC	1.9	yes	yes	no
	14969	Histocompatibility 2, class II antigen E beta	H2-Eb1	7.8	NC	5.0	yes	yes	yes
	14998	Histocompatibility 2, class II, locus DMa	H2-DMa	4.0	NC	2.7	yes	yes	yes
	14999	Histocompatibility 2, class II, locus Mb1	H2-DMb1	4.9	NC	3.2	yes	yes	yes
	15900	Interferon regulatory factor 8	Irf8	3.1	NC	2.0	yes	yes	yes
	16994	Lymphotoxin B	Ltb	2.9	NC	2.3	yes	yes	yes
	17304	Milk fat globule-EGF factor 8 protein	Mfge8	4.6	NC	5.0	yes	yes	yes
	20719	Serine (or cysteine) peptidase inhibitor, clade B, member 6a	Serpinb6a[s]	5.1	NC	11.0	yes	yes	yes
	20209	Serum amyloid A 2	Saa2	3.2	NC	3.2	yes	yes	yes
	20210	Serum amyloid A 3	Saa3	7.8	NC	3.5	yes	yes	no

*Maximum fold change in the microarray (|fold change| >1.5, P1(t) > 0.90).

[a]Putative DNA response elements identified by computational searches (Materials & Methods).

[s]Non-additive, synergistic responses were verified by statistical modeling (Materials & Methods).

NC – no change (not meeting the |fold change| >1.5, P1(t) > 0.90 cut-off).

Genes involved in xenobiotic metabolism and oxidoreductase activities exhibited the highest induction in all three treatment groups. This included cytochrome P450s (e.g. Cyp1a1, Cyp1a2, Cyp2b10, Cyp2b13, Cyp2b9, Cyp2c55, Cyp23a25, Cyp39a1) and glutathione S-transferases (e.g. Gsta2, Gstm2, Gstt2, Gstm4), as well as Nqo1, Ugdh, and Aox1. For example, Cyp1a1 was induced ~348 fold by TCDD and MIX. Unlike treatment-specific induction of Cyp1a (TCDD) and Cyp2b/2c/23a/39a (PCB153) families, MIX elicited the differential expression of the above listed cytochrome P450s, suggesting activation of both AhR and CAR/PXR pathways. Computational analysis identified putative dioxin, CAR and PXR response elements in the promoter regions (-10,000 bp relative to the TSS together with the 5' UTR) of the differentially regulated genes (Table 15) [22, 42].

QRTPCR VERIFICATION OF MICROARRAY RESPONSES

In addition to functional categorization of the gene expression responses, the temporal microarray dataset with corresponding statistics was used to identify genes displaying putative non-additive expression in MIX compared to TCDD and PCB153 treatments.

QRTPCR was used to verify the temporal and dose-dependent changes in expression of 13 genes. The differential expression of Cyp1a1, Cyp2b10, and Cyp3a11 (Figure 32) was confirmed in the time course and dose-response study as a positive control for AhR, CAR, and PXR-mediated responses, respectively [20, 51, 52]. TCDD significantly induced Cyp1a1, while PCB153 significantly up-regulated Cyp2b10 and Cyp3a11. The induction of CYp1a1, Cyp2b10, and Cyp3a11 by MIX was comparable to TCDD and PCB153 alone and therefore was not further considered for non-additive modeling.

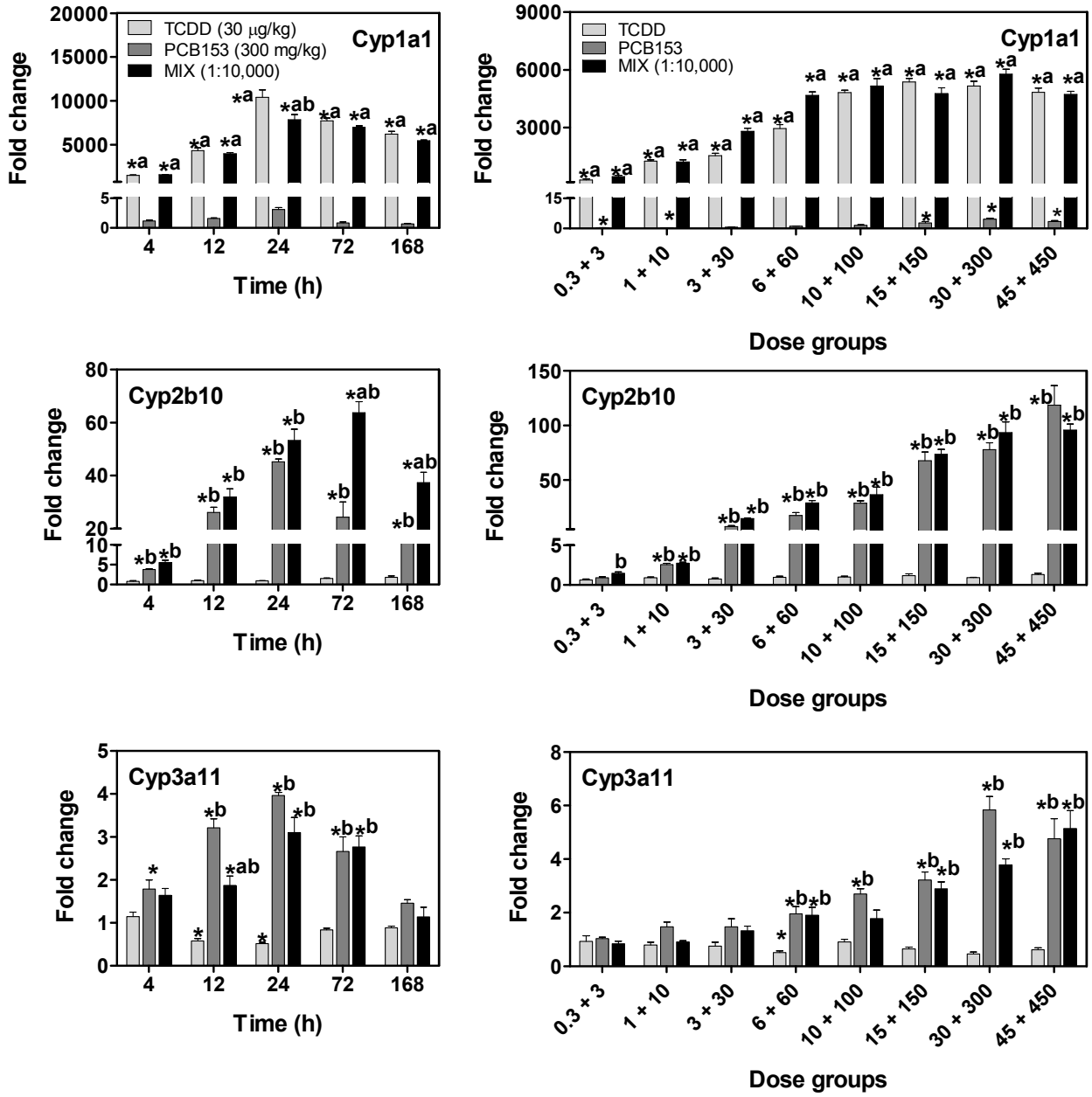

Figure 32. QRTPCR verification of AhR, CAR, and PXR-regulated genes.
TCDD significantly induced Cyp1a1 (AhR), while PCB153 significantly induced Cyp2b10 and Cyp3a11 (CAR/PXR). MIX significantly up-regulated all three genes. All fold changes were calculated relative to time-matched vehicle controls. The genes are represented by their official gene symbols. Doses are μg/kg for TCDD and mg/kg for PCB153. Results are displayed as mean ± SE of 5 independent replicates. Data were analyzed by ANOVA followed by Tukey's *post hoc* test: *$p<0.05$ vs. time-matched vehicle, $^{a}p<0.05$ vs. PCB153 and $^{b}p<0.05$ vs. TCDD.

STATISTICAL VERIFICATION OF NON-ADDITIVE GENE EXPRESSION

Analysis of gene expression time course data suggested that Nqo1, Dysf, Pla2g12a, Serpinb6a, Srxn1 (Figure 33) and Elovl5, Srebf1, Dexi, Got1, Akr1c20 exhibited potential non-additive interactions. The time course and dose-response profiles elicited by TCDD, PCB153, and MIX were verified using QRTPCR and gene-specific non-linear models were fit to statistically define the interactions as synergistic, antagonistic, or additive. Initial analysis confirmed that the variance is proportional to the mean: $Var(Y) = \tau V(\mu)$. Linear regression provided parameter estimates used as initial values for β_i's and maximum fold expression for each gene was used as the initial value for γ. The final model fit for the expected value for each gene was:

$$\mu = \frac{\gamma}{1+\exp(-(\beta_0+\beta_1 x_1 I_1+\beta_2 x_2 I_2+\theta_{mix} t I_3))},$$

where β_0 is the unknown intercept, β_1 is the unknown slope parameter associated with TCDD doses, β_2 is the unknown parameter associated with PCB153 doses, θ_{mix} is the parameter associated with doses of the mixture TCDD+PCB153, and I_i are indicator functions for the chemical groups, where:

$$I_i = \begin{cases} 1 & \text{if chemical } i \\ 0 & \text{if not chemical } i \end{cases} \quad \text{for } i = \{1,2,3\},$$

where $i = 1$, $i = 2$, and $i = 3$ represent TCDD, PCB153, and MIX, respectively. The intercept parameter α is assumed to be zero. Plots of the residuals against the predicted values were assessed for goodness of fit of the models, and no abnormalities were found.

Figure 33. Temporal and dose-dependent QRTPCR verification of putative non-additive genes.

Genes exhibiting putative non-additive interactions were initially identified in the time course study. Putative non-additive interactions were verified by QRTPCR in the time course study and the 24 h dose-response study. The genes are represented by their official gene symbols. The dose groups are represented as μg/kg TCDD + mg/kg PCB153. Results are displayed as mean ± SE of 5 independent replicates. Data were analyzed by ANOVA followed by Tukey's *post hoc* test: *$p<0.05$ vs. time-matched vehicle, $^{a}p<0.05$ vs. PCB153 and $^{b}p<0.05$ vs. TCDD.

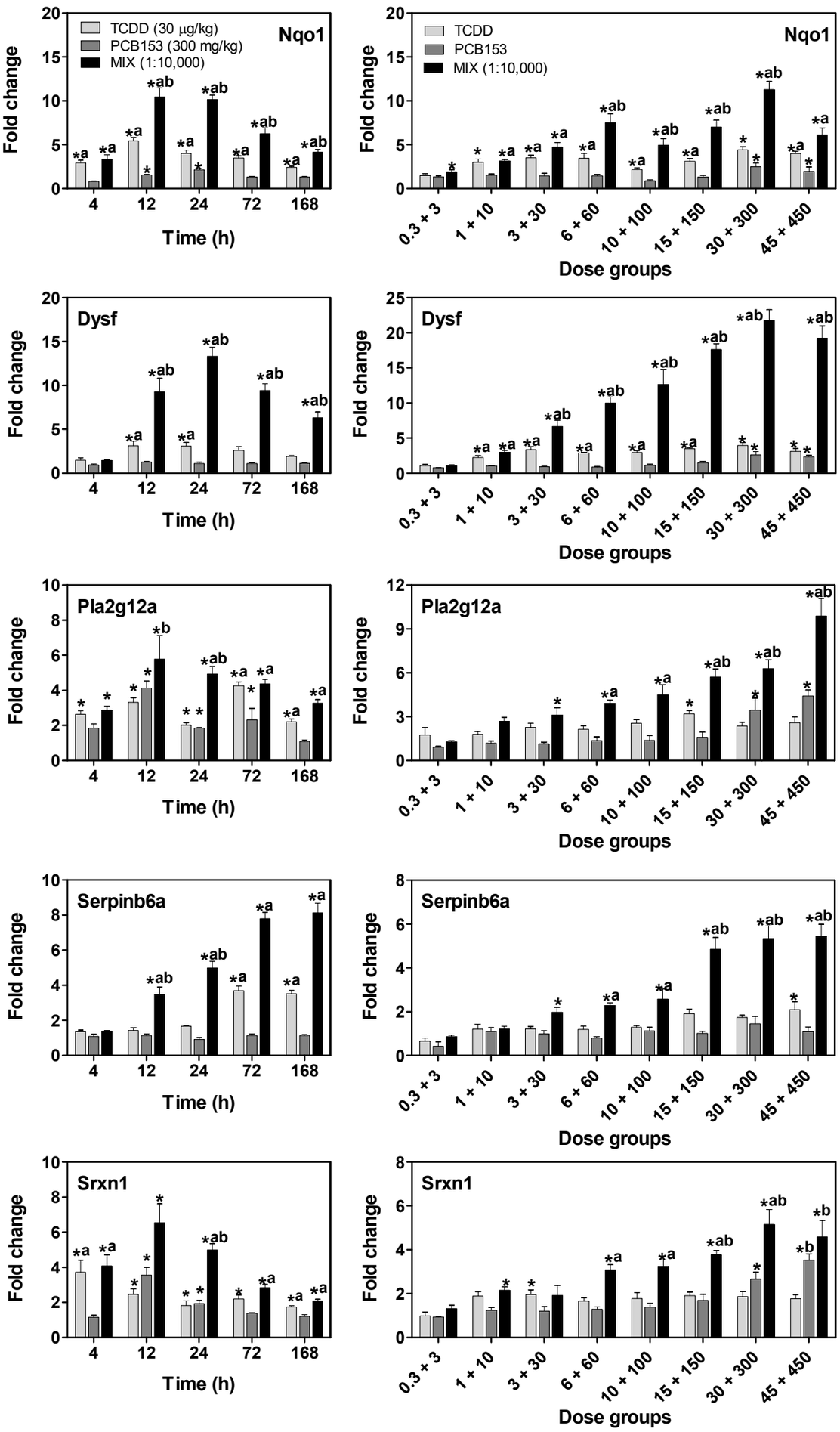
Nqo1
TCDD (30 μg/kg)
PCB153 (300 mg/kg)
MIX (1:10,000)
Fold change
Time (h)
4
12
24
72
168
Nqo1
TCDD
PCB153
MIX (1:10,000)
Fold change
Dose groups
0.3 + 3
1 + 10
3 + 30
6 + 60
10 + 100
15 + 150
30 + 300
45 + 450
Dysf
Pla2g12a
Serpinb6a
Srxn1

To determine statistically significant deviation from additivity, the quasi-likelihood ratio test was used to compare the empirical mixture model with the reduced additivity model based on the F-distribution [53]:

$$\mu = \frac{\gamma}{1+\exp(-(\beta_0+\beta_1 x_1 I_1+\beta_2 x_2 I_2+\theta_{add} t I_3))},$$

where $\theta_{add} = (\beta_1 a_1 + \beta_2 a_2)$, where a_1 and a_2 are the 'mix ratios' for TCDD and PCB153 respectively. The 'mix ratios' were obtained by dividing the dose by the total dose. For example, when the TCDD dose is 1 μg/kg, the PCB153 dose is 10000 μg/kg (10 mg/kg), so the 'mix ratios' are $a_1 = \frac{1}{10000+1} = 0.0001$ and $a_2 = \frac{10000}{10000+1} = 0.9999$ such that $\sum_i a_i = 1$.

Each graph in Figure 34 illustrates the overlay between the additive model generated using TCDD and PCB153 data alone and the mixture model fitted using MIX data for each gene. The quasi-likelihood ratio test determined that the mixture model was significantly ($p<0.0001$) different from the additive model for Nqo1, Dysf, Pla2g12a, Serpinb6a and Srxn1, indicating that co-administration of TCDD plus PCB153 resulted in synergistic gene expression changes.

MIX expression of Srebf1, Akr1c20, and Dexi approached significant non-additive expression ($p=0.0619$, $p=0.0615$, $p=0.0806$, respectively), while Elovl5 ($p=0.5164$) and Got1 ($p=0.9181$) expression was not significantly different from additivity.

Figure 34. Dose-response non-linear logistic modeling of the dose-response QRTPCR results from Figure 33.
Graphs depict the additive model (dashed line) generated using TCDD and PCB153 data and the mixture model (solid line) fitted using MIX data (black dots). For Nqo1, Dysf, Pla2g12a, Serpinb6a and Srxn1, the mixture model fit the MIX data significantly better than the additive model, indicating a synergistic interaction ($p<0.0001$).

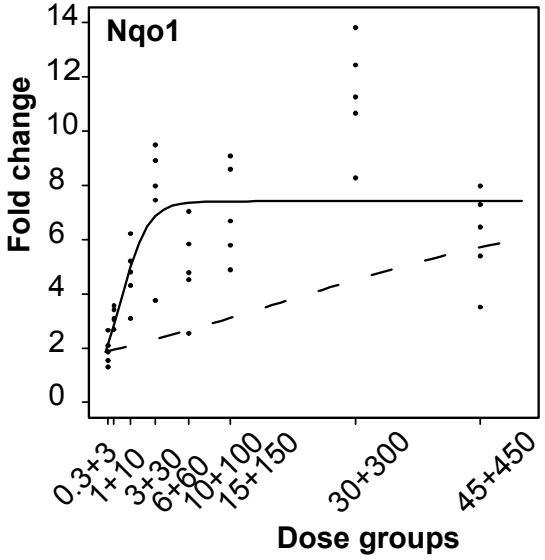
Nqo1
Fold change
0
2
4
6
8
10
12
14
0.3+3
1+10
3+30
6+60
10+100
15+150
30+300
45+450
Dose groups

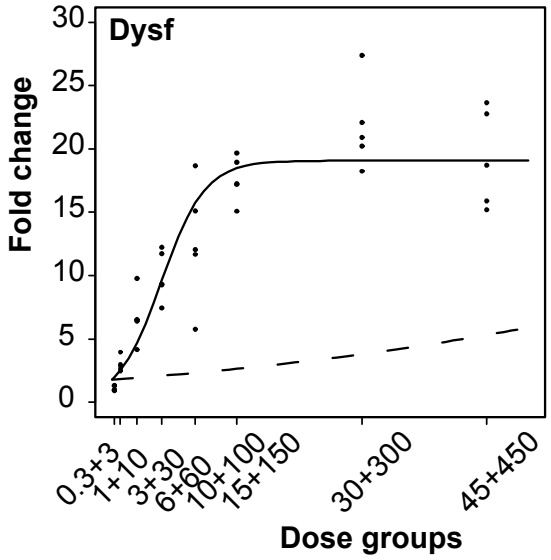
Dysf
Fold change
0
5
10
15
20
25
30
0.3+3
1+10
3+30
6+60
10+100
15+150
30+300
45+450
Dose groups

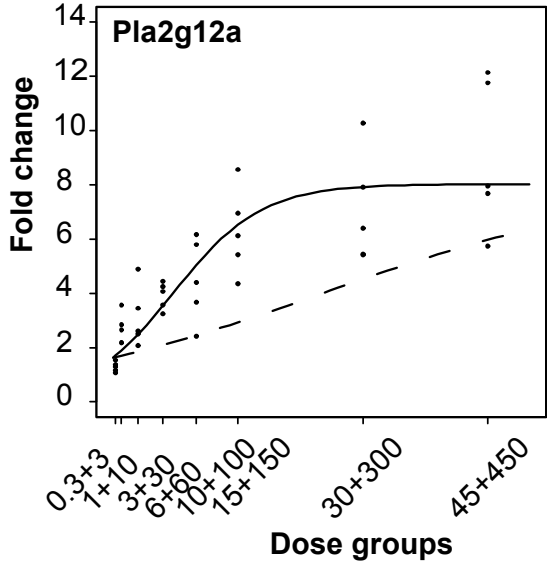
Pla2g12a
Fold change
0
2
4
6
8
10
12
14
0.3+3
1+10
3+30
6+60
10+100
15+150
30+300
45+450
Dose groups

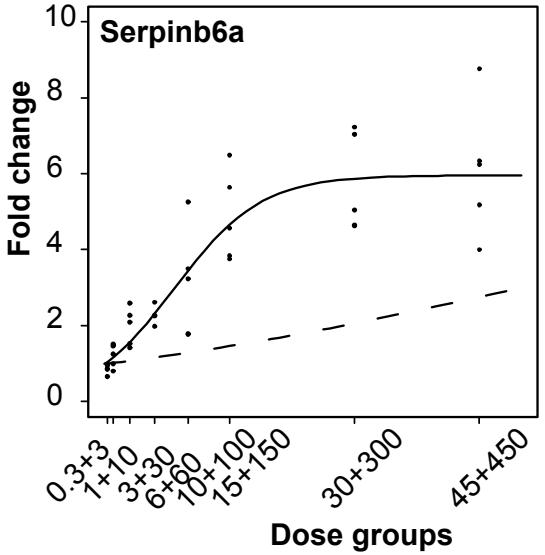
Serpinb6a
Fold change
0
2
4
6
8
10
0.3+3
1+10
3+30
6+60
10+100
15+150
30+300
45+450
Dose groups

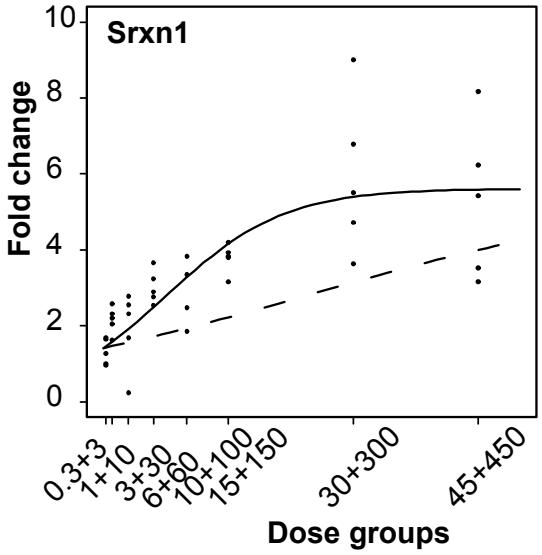
Srxn1
Fold change
0
2
4
6
8
10
0.3+3
1+10
3+30
6+60
10+100
15+150
30+300
45+450
Dose groups

DISCUSSION

In the current study, comprehensive time course and dose-dependent hepatic gene expression changes elicited by a mixture of TCDD and PCB153 were anchored to changes in gross physiology, histopathology, tissue concentrations, and hepatic lipid composition, and these were compared to effects elicited by TCDD and PCB153 alone. Statistical modeling confirmed dose- additive and synergistic effects in a subset of differentially expressed genes that could be associated with specific phenotypic changes.

Exposure to mixtures of dioxin and non-dioxin-like chemicals has been reported to increase hepatic disposition of these chemicals when compared to single chemical administration [48]. In the current study, hepatic PCB153 levels were significantly increased following co-administration with TCDD at 24 and 168 h. However the levels of TCDD did not change when co-administered with PCB153, as previously reported [47, 48]. These results are consistent with rat studies that also reported TCDD co-treatment increased PCB153 levels [54]. Co-administration of PCB153 with dioxin-like PCB156 also led to significant hepatic retention of PCB153 after 7 and 14 days in C57BL/6J mice [55]. In B6C3F1 mice, TCDD-elicited increases in PCB153 levels were specific to the liver and not observed in other tissues [47].

Hepatic sequestration of TCDD and other dioxin-like PCBs is mediated by binding to Cyp1a2 protein [56]. Cyp1a2 null mice exhibit 10-fold lower hepatic TCDD accumulation compared to wild type animals [57]. PCB153 has a higher affinity for adipose compared to hepatic tissue [47] and unlike TCDD and dioxin-like PCBs, it is not sequestered by Cyp1a2 protein. However, exposure to TCDD leads to fatty accumulation in the liver [32], increasing hepatic lipophilicity, which may contribute to hepatic accumulation of PCB153 following co-administration with TCDD [47, 54].

MIX induced xenobiotic metabolism gene expression, comparable to levels elicited by individual treatments. Cytochrome P450 induction was the highest among all functional categories, and included typical AhR (Cyp1a1, Cyp1a2) and CAR/PXR (Cyp2b9, Cyp2b10, Cyp2b13, Cyp23a25, Cyp3a11) induced genes [20, 51, 52]. Differential expression of Nqo1, a known AhR- and Nrf2- (nuclear factor erythroid 2-related factor 2) inducible gene [58], displayed synergistic induction following co-administration of TCDD with PCB153. Synergistically elevated expression of Nqo1 may be cytoprotective against chemical toxicity [59, 60]. MIX also synergistically induced Srxn1, sulfiredoxin 1 homolog, an Nrf2-dependent oxidoreductase, which has been reported to protect from smoke-induced oxidative injury in the lung [61, 62]. Synergistic induction of Nqo1 and Srxn1 may support hepatic defense mechanisms following the increased load of xenobiotic stress induced by MIX.

Among oxidoreductase and xenobiotic metabolism genes, aldo-keto reductase (AKR) superfamily members were also differentially expressed including the induction of Akr1b7, Akr1c19 and repression of Akr1c20. AKRs are involved in NAD(P)H-dependent oxidoreductions of a variety of natural and foreign substrates and have been implicated in alleviating toxicity associated with lipid peroxidation [63]. Expression of Akr1b7 is abolished in CAR and PXR null mice [63], in agreement with PCB153 and MIX-mediated Akr1b7 induction and putative CAREs and PXREs identification. Statistical modeling approached significant ($p=0.0615$) synergistic repression of Akr1c20 levels following MIX treatment. Akr1c20 expression is liver-specific, but its function is unknown [64]. Based on structural similarity to 17β-hydroxysteroid dehydrogenase type 5 and enzymatic properties, it may be involved in steroid metabolism and reduction of non-steroidal α-dicarbonyl compounds [64].

Integrating histopathology, ORO staining, GC-MS fatty acid and triglyceride analyses suggests that TCDD- and MIX-elicited increases in RLW can be partially attributed to hepatic lipid accumulation. The AhR-mediated fatty accumulation (steatosis) by TCDD can be directly associated with the differential expression of lipid transport and metabolism genes. For example, TCDD induces the expression of the fatty acid transporter, Cd36 [65], which was also induced by MIX. Cd36 facilitates hepatic uptake of free fatty acids and was found up-regulated in non-alcoholic fatty liver disease patients [66]. TCDD and MIX also induced fatty acid binding protein 12 (Fabp12) [67]. In contrast, PCB153 did not alter Cd36 or Fabp12 expression, consistent with no steatosis. Instead PCB153 down-regulated a number of lipid metabolism genes, including Elovl5 was induced by TCDD, suggesting divergent regulation. Deletion of Elovl5 in mice leads to steatosis through activation of SREBP-1c protein [68]. MIX approached significant ($p=0.0619$) synergistic repression of Srebf1 consistent with less fat accumulation at 168 h compared to TCDD which did not affect Srebf1 expression. PCB153 minimally repressed Srebf1 expression (at 12 h and at 450 mg/kg at 24 h), but did not promote lipid accumulation. In addition, repression of SREBP-mediated lipogenesis in Zucker diabetic fatty rats is associated with CAR/PXR-mediated over-expression of insulin induced genes (Insig1/2) [69, 70]. PCB153 and MIX induced Insig2, while TCDD down-regulated Insig2 at 4 h, consistent with the observed hepatic phenotypes.

MIX also synergistically induced Pla2g12a, a novel secretory phospholipase, which is involved in the digestion of dietary phospholipids and the production of molecules that induce inflammatory responses [71]. Although MIX induction of Pla2g12a may be linked to elevated free fatty acids, previous reports suggest Pla2g12a has very weak catalytic activity and contributes little to increase cellular fatty acid release [71, 72].

TCDD and dioxin-like chemical are associated with feed refusal, body weight loss and exhaustion of energy sources, collectively referred to as “wasting syndrome” [73]. PCB153 is linked to increased glucose consumption in MCF-10A human non-tumorigenic mammary epithelial cells [74]. TCDD and MIX repression of the glucose metabolism genes, including glutamate oxaloacetate soluble 1, (Got1), glycerol-phosphate dehydrogenase 2, mitochondrial (Gpd2), and pyruvate dehydrogenase kinase, isoenzyme 1 (Pdk1), was consistent with dioxin-mediated repression of gluconeogenesis in chick embryo hepatocytes [75]. MIX also repressed Got1 expression but statistical modeling did not confirm non-additive expression.

There was a lack of hepatocellular necrosis in PCB153-treated mice compared to TCDD and MIX, consistent with reports of PCB153-mediated decreases in cell death in mouse hepatocytes [76, 77]. PCB153 and MIX increased hepatic cell size, in agreement with reported CAR/PXR-mediated liver hypertrophy [18, 78-80]. In contrast to PCB153, which did not regulate cell death related genes, TCDD and MIX induced Tnfaip2 and Tnfaip8l1, members of the tumor necrosis factor (TNF)-signaling pathway, which mediate cell death, proliferation, differentiation, and inflammation [81]. In addition, TCDD and MIX, but not PCB153, induced Bcl2l11and Htatip2 [82, 83]. MIX also induced hyperplasia at 168 h, in agreement with Myc induction [84]. Myc, a transcription factor associated with cell proliferation, growth and metabolism, regulates early response 3 (Ier3), which was induced by TCDD and MIX, and not affected by PCB153. Transgenic mice studies indicate that Ier3 is anti-apoptotic and may stimulate cell proliferation [85].

Histopathology also revealed a lack of inflammatory cells associated with PCB153 treatment, unlike TCDD and MIX, which increased mixed cell infiltration. A number of immune related genes were induced by TCDD and MIX, including major histocompatibility complex

molecules H2-Eb1, H2-DMa, H2-DMb1, also expressed in mice exposed to hepatic parasites [86]. PCB153 did not alter expression of immune response related genes.

MIX synergistically induced Serpinb6a, a member of a serine protease inhibitors involved in diverse processes, such as inflammation and cell death [87]. Serpinb6a is highly expressed by mast cells in all organs and may regulate the activity of endogenous β-tryptase in the cytoplasm, a biomarker of mast cell activation and mastocytosis immune response [88]. PCB153 did not affect Serpinb6a expression, in contrast to TCDD induction at later time points and synergistic induction by MIX, consistent with comparable extent of immune cell infiltration elicited by TCDD and MIX.

Dexamethasone-induced transcript (Dexi) is regulated by the glucocorticoid analogue dexamethasone, a very potent PXR ligand [89, 90]. Dexi was down-regulated in this study by all treatments. Expression of glucocorticoids is linked to suppressed inflammatory response, partially by regulated expression of TNF [91]. MIX synergistically ($p=0.0806$) suppressed Dexi transcript at 24 h and at later time points, concomitant with histopathological findings indicating significant immune cell infiltration.

The most dramatic synergistic induction was observed in dysferlin (Dysf), following exposure to MIX. Dysf was only minimally induced by TCDD and was not differentially expressed following PCB153 treatment. Dysf is a transmembrane protein implicated in calcium-dependent sarcolemmal membrane repair. Dysf-deficient skeletal muscles induce and activate key inflammasome adaptor components, including NACHT, LRR and PYD-containing proteins [92]. The C2 domains of dysferlin exhibit lipid binding specificity, facilitating interactions with lipid bilayer components including phosphatidylserine (PtdS), phosphatidylinositol 4-phosphate (PtdIns[4]P) and phosphatidylinositol 4,5-bisphosphate (PtdIns[4,5]P_2) in a calcium-dependent

fashion [93-95]. MIX elicited the most significant changes in hepatic architecture that may be linked to cellular membrane stress. Dysf induction by MIX during membrane injury may lead to calcium-dependent interactions with PtdS and PtdIns to patch and repair membrane damage [93]. Deficiencies in phosphatidylcholine synthesis, another major membrane component, are linked to muscular dystrophy [96].

In summary, co-administration of TCDD with PCB153 elicits non-additive, synergistic AhR/CAR/PXR-mediated gene expression responses that can be associated with changes in RLW, hepatic cell size and number, immune response and lipid accumulation in ovariectomized C57BL/6 mice. Non-additive interactions may confound the risk assessment of mixtures, and therefore require special considerations [97]. For example, dose-response curves for mixture components should be adequately characterized, the "no-interaction" hypothesis should be explicitly stated and used as the basis for assessing synergy and antagonism, combinations of mixture components should be assessed across a sufficient range, statistical tests should be used to determine departure from additivity, and interactions should be assessed at relevant levels of biological organization to assure meaningful interpretation of the results. Development of predictive models integrating *in vitro*, pharmacokinetic and pharmacodynamic components will enable a better understanding of the influence of mixture composition on elicited toxic effects.

REFERENCES

REFERENCES

1. Mason, G. and S. Safe, *Synthesis, biologic and toxic effects of the major 2,3,7,8-tetrachlorodibenzo-p-dioxin metabolites in the rat.* Toxicology, 1986. **41**(2): p. 153-9.

2. Poland, A. and E. Glover, *Studies on the mechanism of toxicity of the chlorinated dibenzo-p-dioxins.* Environ Health Perspect, 1973. **5**: p. 245-51.

3. Commoner, B., K. Shapiro, and T. Webster, *The Origin and Health Risks of PCDD and PCDF.* Waste Management & Research, 1987. **5**: p. 327-346.

4. Safe, S., et al., *Halogenated biphenyls: molecular toxicology.* Can J Physiol Pharmacol, 1982. **60**(7): p. 1057-64.

5. Mullin, M.D., et al., *High-resolution PCB analysis: synthesis and chromatographic properties of all 209 PCB congeners.* Environ. Set Technol., 1984. **18**: p. 468-476.

6. Safe, S., *Polychlorinated biphenyls (PCBs), dibenzo-p-dioxins (PCDDs), dibenzofurans (PCDFs), and related compounds: environmental and mechanistic considerations which support the development of toxic equivalency factors (TEFs).* Crit Rev Toxicol, 1990. **21**(1): p. 51-88.

7. Kimbrough, R.D., *Polychlorinated biphenyls (PCBs) and human health: an update.* Crit Rev Toxicol, 1995. **25**(2): p. 133-63.

8. Safe, S., *Limitations of the toxic equivalency factor approach for risk assessment of TCDD and related compounds.* Teratog Carcinog Mutagen, 1997. **17**(4-5): p. 285-304.

9. Poland, A. and J.C. Knutson, *2,3,7,8-tetrachlorodibenzo-p-dioxin and related halogenated aromatic hydrocarbons: examination of the mechanism of toxicity.* Annu Rev Pharmacol Toxicol, 1982. **22**: p. 517-54.

10. Knerr, S. and D. Schrenk, *Carcinogenicity of "non-dioxinlike" polychlorinated biphenyls.* Crit Rev Toxicol, 2006. **36**(9): p. 663-94.

11. Van den Berg, M., et al., *The 2005 World Health Organization reevaluation of human and Mammalian toxic equivalency factors for dioxins and dioxin-like compounds.* Toxicol Sci, 2006. **93**(2): p. 223-41.

12. Safe, S.H., *Polychlorinated biphenyls (PCBs): environmental impact, biochemical and toxic responses, and implications for risk assessment.* Crit Rev Toxicol, 1994. **24**(2): p. 87-149.

13. Safe, S., *Molecular biology of the Ah receptor and its role in carcinogenesis.* Toxicol Lett, 2001. **120**(1-3): p. 1-7.

14. Denison, M.S. and S. Heath-Pagliuso, *The Ah receptor: a regulator of the biochemical and toxicological actions of structurally diverse chemicals.* Bull Environ Contam Toxicol, 1998. **61**(5): p. 557-68.

15. Denison, M.S., et al., *Ligand binding and activation of the Ah receptor.* Chem Biol Interact, 2002. **141**(1-2): p. 3-24.

16. Nebert, D.W., et al., *Role of the aromatic hydrocarbon receptor and [Ah] gene battery in the oxidative stress response, cell cycle control, and apoptosis.* Biochem Pharmacol, 2000. **59**(1): p. 65-85.

17. Schecter, A., et al., *Polychlorinated biphenyl levels in the tissues of exposed and nonexposed humans.* Environ Health Perspect, 1994. **102 Suppl 1**: p. 149-58.

18. NTP, *NTP technical report on the toxicology and carcinogenesis studies of 2,2',4,4',5,5'-hexachlorobiphenyl (PCB 153) (CAS No. 35065-27-1) in female Harlan Sprague-Dawley rats (Gavage studies).* Natl Toxicol Program Tech Rep Ser, 2006(529): p. 4-168.

19. Craft, E.S., M.J. DeVito, and K.M. Crofton, *Comparative responsiveness of hypothyroxinemia and hepatic enzyme induction in Long-Evans rats versus C57BL/6J mice exposed to TCDD-like and phenobarbital-like polychlorinated biphenyl congeners.* Toxicol Sci, 2002. **68**(2): p. 372-80.

20. Honkakoski, P., T. Sueyoshi, and M. Negishi, *Drug-activated nuclear receptors CAR and PXR.* Ann Med, 2003. **35**(3): p. 172-82.

21. Tabb, M.M., et al., *Highly chlorinated PCBs inhibit the human xenobiotic response mediated by the steroid and xenobiotic receptor (SXR).* Environ Health Perspect, 2004. **112**(2): p. 163-9.

22. Kopec, A.K., et al., *PCB153-elicited hepatic responses in the immature, ovariectomized C57BL/6 mice: Comparative toxicogenomic effects of dioxin and non-dioxin-like ligands.* Toxicol Appl Pharmacol, 2010. **243**: p. 359-71.

23. Lemaire, G., et al., *Discovery of a highly active ligand of human pregnane x receptor: a case study from pharmacophore modeling and virtual screening to "in vivo" biological activity.* Mol Pharmacol, 2007. **72**(3): p. 572-81.

24. Blumberg, B. and R.M. Evans, *Orphan nuclear receptors--new ligands and new possibilities.* Genes Dev, 1998. **12**(20): p. 3149-55.

25. Masahiko, N. and P. Honkakoski, *Induction of drug metabolism by nuclear receptor CAR: molecular mechanisms and implications for drug research.* Eur J Pharm Sci, 2000. **11**(4): p. 259-64.

26. Staal, Y.C., et al., *Binary PAH mixtures cause additive or antagonistic effects on gene expression but synergistic effects on DNA adduct formation.* Carcinogenesis, 2007. **28**(12): p. 2632-40.

27. Biegel, L., et al., *2,2',4,4',5,5'-hexachlorobiphenyl as a 2,3,7,8-tetrachlorodibenzo-p-dioxin antagonist in C57BL/6J mice.* Toxicol Appl Pharmacol, 1989. **97**(3): p. 561-71.

28. Zhao, F., et al., *Inhibition of 3,3',4,4',5-pentachlorobiphenyl-induced fetal cleft palate and immunotoxicity in C57BL/6 mice by 2,2',4,4',5,5'-hexachlorobiphenyl.* Chemosphere, 1997. **34**(5-7): p. 1605-13.

29. Suh, J., et al., *Antagonism of aryl hydrocarbon receptor-dependent induction of CYP1A1 and inhibition of IgM expression by di-ortho-substituted polychlorinated biphenyls.* Toxicol Appl Pharmacol, 2003. **187**(1): p. 11-21.

30. Bannister, R. and S. Safe, *Synergistic interactions of 2,3,7,8-TCDD and 2,2',4,4',5,5'-hexachlorobiphenyl in C57BL/6J and DBA/2J mice: role of the Ah receptor.* Toxicology, 1987. **44**(2): p. 159-69.

31. van Birgelen, A.P., et al., *Synergistic effect of 2,2',4,4',5,5'-hexachlorobiphenyl and 2,3,7,8-tetrachlorodibenzo-p-dioxin on hepatic porphyrin levels in the rat.* Environ Health Perspect, 1996. **104**(5): p. 550-7.

32. Boverhof, D.R., et al., *Temporal and dose-dependent hepatic gene expression patterns in mice provide new insights into TCDD-Mediated hepatotoxicity.* Toxicol Sci, 2005. **85**(2): p. 1048-63.

33. Kopec, A.K., et al., *Comparative Toxicogenomic Examination of the Hepatic Effects of PCB126 and TCDD in Immature, Ovariectomized C57BL/6 Mice.* Toxicol Sci, 2008. **102**(1): p. 61-75.

34. Kopec, A.K., et al., *Automated Dose-Response Analysis and Comparative Toxicogenomic Evaluation of the Hepatic Effects Elicited by TCDD, TCDF and PCB126 in C57BL/6 Mice.* Toxicol Sci, 2010. **118**: p. 286-97.

35. Sheehan, D.C. and B.B. Hrapchak, *Theory and Practice of Histotechnology*. second ed ed. 1980, St. Louis: Mosby.

36. Burgoon, L.D. and T.R. Zacharewski, *dbZach toxicogenomic information management system.* Pharmacogenomics, 2007. **8**(3): p. 287-91.

37. Burgoon, L.D., et al., *Protocols for the assurance of microarray data quality and process control.* Nucleic Acids Res, 2005. **33**(19): p. e172.

38. Eckel, J.E., et al., *Normalization of two-channel microarray experiments: a semiparametric approach.* Bioinformatics, 2005. **21**(7): p. 1078-83.

39. Eckel, J.E., et al., *Empirical bayes gene screening tool for time-course or dose-response microarray data.* J Biopharm Stat, 2004. **14**(3): p. 647-70.

40. Vandesompele, J., et al., *Accurate normalization of real-time quantitative RT-PCR data by geometric averaging of multiple internal control genes.* Genome Biol, 2002. **3**(7): p. RESEARCH0034.

41. Sun, Y.V., et al., *Comparative analysis of dioxin response elements in human, mouse and rat genomic sequences.* Nucleic Acids Res, 2004. **32**(15): p. 4512-23.

42. Dere, E., et al., *Genome-Wide Computational Analysis of Dioxin Response Element Location and Distribution in the Human, Mouse and Rat Genomes.* submitted manuscript.

43. Phillips, J.M., L.D. Burgoon, and J.I. Goodman, *Phenobarbital (PB) Elicits Unique, Early Changes in the Expression of Hepatic Genes That Affect Critical Pathways in Tumor-Prone B6C3F1 Mice.* Toxicol Sci, 2009.

44. Dennis, G., Jr., et al., *DAVID: Database for Annotation, Visualization, and Integrated Discovery.* Genome Biol, 2003. **4**(5): p. P3.

45. Boverhof, D.R., et al., *Comparative toxicogenomic analysis of the hepatotoxic effects of TCDD in Sprague Dawley rats and C57BL/6 mice.* Toxicol Sci, 2006. **94**(2): p. 398-416.

46. NTP, *NTP technical report on the toxicology and carcinogenesis studies of 2,3,7,8-tetrachlorodibenzo-p-dioxin (TCDD) (CAS No. 1746-01-6) in female Harlan Sprague-Dawley rats (Gavage Studies).* Natl Toxicol Program Tech Rep Ser, 2006(521): p. 4-232.

47. van Birgelen, A.P., et al., *Interactive effects between 2,3,7,8-tetrachlorodibenzo-p-dioxin and 2,2',4,4',5,5'-hexachlorobiphenyl in female B6C3F1 mice: tissue distribution and tissue-specific enzyme induction.* Fundam Appl Toxicol, 1996. **34**(1): p. 118-31.

48. De Jongh, J., et al., *The effects of 2,2',4,4',5,5'-hexachlorobiphenyl cotreatment on the disposition of 2,3,7,8-tetrachlorodibenzo-p-dioxin in mice.* Toxicol Lett, 1995. **80**(1-3): p. 131-7.

49. FDA, *Dose Selection for Carcinogenicity Studies*, U.S.D.o.H.a.H. Services, Editor. 2008. p. 1-10.

50. Zhai, Y., et al., *A Functional Crosstalk Between LXRalpha and CAR Links Lipogenesis and Xenobiotic Responses.* Mol Pharm, 2010.

51. Maglich, J.M., et al., *Nuclear pregnane x receptor and constitutive androstane receptor regulate overlapping but distinct sets of genes involved in xenobiotic detoxification.* Mol Pharmacol, 2002. **62**(3): p. 638-46.

52. Nebert, D.W., D.D. Petersen, and A.J. Fornace, Jr., *Cellular responses to oxidative stress: the [Ah] gene battery as a paradigm.* Environ Health Perspect, 1990. **88**: p. 13-25.

53. Gennings, C., et al., *Statistical analysis of interactive cytotoxicity in human epidermal keratinocytes following exposure to a mixture of four metals.* Journal of Agricultural Biological and Environmental Statistics, 2002. **7**(1): p. 58-73.

54. Van der Kolk, J., et al., *Interactions of 2,2',4,4',5,5'-hexachlorobiphenyl and 2,3,7,8-tetrachlorodibenzo-p-dioxin in a subchronic feeding study in the rat.* Chemosphere, 1992. **25**(12): p. 2023-2027.

55. De Jongh, J., et al., *Toxicokinetic interactions in the liver of the C57BL/6J mouse after administration of a single oral dose of a binary mixture of some PCBs.* Chemosphere, 1992. **25**: p. 1165-1170.

56. DeVito, M.J., et al., *Dose-response relationships for disposition and hepatic sequestration of polyhalogenated dibenzo-p-dioxins, dibenzofurans, and biphenyls following subchronic treatment in mice.* Toxicol Sci, 1998. **46**(2): p. 223-34.

57. Diliberto, J.J., D.E. Burgin, and L.S. Birnbaum, *Effects of CYP1A2 on disposition of 2,3,7, 8-tetrachlorodibenzo-p-dioxin, 2,3,4,7,8-pentachlorodibenzofuran, and 2,2',4,4',5,5'-hexachlorobiphenyl in CYP1A2 knockout and parental (C57BL/6N and 129/Sv) strains of mice.* Toxicol Appl Pharmacol, 1999. **159**(1): p. 52-64.

58. Yeager, R.L., et al., *Introducing the "TCDD-inducible AhR-Nrf2 gene battery".* Toxicol Sci, 2009. **111**(2): p. 238-46.

59. Klaassen, C.D. and S.A. Reisman, *Nrf2 the rescue: effects of the antioxidative/electrophilic response on the liver.* Toxicol Appl Pharmacol, 2010. **244**(1): p. 57-65.

60. Ma, Q., et al., *Induction of murine NAD(P)H:quinone oxidoreductase by 2,3,7,8-tetrachlorodibenzo-p-dioxin requires the CNC (cap 'n' collar) basic leucine zipper transcription factor Nrf2 (nuclear factor erythroid 2-related factor 2): cross-interaction between AhR (aryl hydrocarbon receptor) and Nrf2 signal transduction.* Biochem J, 2004. **377**(Pt 1): p. 205-13.

61. Park, J.W., et al., *Deglutathionylation of 2-Cys peroxiredoxin is specifically catalyzed by sulfiredoxin.* J Biol Chem, 2009. **284**(35): p. 23364-74.

62. Singh, A., et al., *Nrf2-dependent sulfiredoxin-1 expression protects against cigarette smoke-induced oxidative stress in lungs.* Free Radic Biol Med, 2009. **46**(3): p. 376-86.

63. Liu, M.J., et al., *The aldo-keto reductase Akr1b7 gene is a common transcriptional target of xenobiotic receptors pregnane X receptor and constitutive androstane receptor.* Mol Pharmacol, 2009. **76**(3): p. 604-11.

64. Matsumoto, K., et al., *Enzymatic properties of a member (AKR1C20) of the aldo-keto reductase family.* Biol Pharm Bull, 2006. **29**(3): p. 539-42.

65. Lee, J.H., et al., *A Novel Role for the Dioxin Receptor in Fatty Acid Metabolism and Hepatic Steatosis.* Gastroenterology, 2010. **139**(2): p. 653-63.

66. Greco, D., et al., *Gene expression in human NAFLD.* Am J Physiol Gastrointest Liver Physiol, 2008. **294**(5): p. G1281-7.

67. Tijet, N., et al., *Aryl hydrocarbon receptor regulates distinct dioxin-dependent and dioxin-independent gene batteries.* Mol Pharmacol, 2006. **69**(1): p. 140-53.

68. Moon, Y.A., R.E. Hammer, and J.D. Horton, *Deletion of ELOVL5 leads to fatty liver through activation of SREBP-1c in mice.* J Lipid Res, 2008.

69. Takaishi, K., et al., *Hepatic insig-1 or -2 overexpression reduces lipogenesis in obese Zucker diabetic fatty rats and in fasted/refed normal rats.* Proc Natl Acad Sci U S A, 2004. **101**(18): p. 7106-11.

70. Roth, A., et al., *Regulatory cross-talk between drug metabolism and lipid homeostasis: constitutive androstane receptor and pregnane X receptor increase Insig-1 expression.* Mol Pharmacol, 2008. **73**(4): p. 1282-9.

71. Gelb, M.H., et al., *Cloning and recombinant expression of a structurally novel human secreted phospholipase A2.* J Biol Chem, 2000. **275**(51): p. 39823-6.

72. Murakami, M., et al., *Cellular arachidonate-releasing function of novel classes of secretory phospholipase A2s (groups III and XII).* J Biol Chem, 2003. **278**(12): p. 10657-67.

73. Viluksela, M., B.U. Stahl, and K.K. Rozman, *Tissue-specific effects of 2,3,7,8-Tetrachlorodibenzo-p-dioxin (TCDD) on the activity of phosphoenolpyruvate carboxykinase (PEPCK) in rats.* Toxicol Appl Pharmacol, 1995. **135**(2): p. 308-15.

74. Venkatesha, V.A., et al., *PCB-153 exposure coordinates cell cycle progression and cellular metabolism in human mammary epithelial cells.* Toxicol Lett, 2010. **196**: p. 110-116.

75. Diani-Moore, S., et al., *Identification of the aryl hydrocarbon receptor target gene Tiparp as a mediator of suppression of hepatic gluconeogenesis by 2,3,7,8-tetrachlorodibenzo-p-dioxin and of nicotinamide as a corrective agent for this effect.* J Biol Chem, 2010.

76. Tharappel, J.C., et al., *Regulation of cell proliferation, apoptosis, and transcription factor activities during the promotion of liver carcinogenesis by polychlorinated biphenyls.* Toxicol Appl Pharmacol, 2002. **179**(3): p. 172-84.

77. Lu, Z., et al., *Effect of 2,2',4,4',5,5'-hexachlorobiphenyl (PCB-153) on hepatocyte proliferation and apoptosis in mice deficient in the p50 subunit of the transcription factor NF-kappaB.* Toxicol Sci, 2004. **81**(1): p. 35-42.

78. Blanco-Bose, W.E., et al., *C-Myc and its target FoxM1 are critical downstream effectors of constitutive androstane receptor (CAR) mediated direct liver hyperplasia.* Hepatology, 2008. **48**(4): p. 1302-11.

79. Staudinger, J.L., et al., *Regulation of drug transporter gene expression by nuclear receptors.* Drug Metab Dispos, 2003. **31**(5): p. 523-7.

80. Wei, P., et al., *The nuclear receptor CAR mediates specific xenobiotic induction of drug metabolism.* Nature, 2000. **407**(6806): p. 920-3.

81. Tracey, K.J. and A. Cerami, *Tumor necrosis factor: a pleiotropic cytokine and therapeutic target.* Annu Rev Med, 1994. **45**: p. 491-503.

82. Shi, M., et al., *Tip30-induced apoptosis requires translocation of Bax and involves mitochondrial release of cytochrome c and Smac/DIABLO in hepatocellular carcinoma cells.* Biochim Biophys Acta, 2008. **1783**(2): p. 263-74.

83. Seitz, S.J., et al., *Chemotherapy-induced apoptosis in hepatocellular carcinoma involves the p53 family and is mediated via the extrinsic and the intrinsic pathway.* Int J Cancer, 2010. **126**(9): p. 2049-66.

84. Dang, C.V., *c-Myc target genes involved in cell growth, apoptosis, and metabolism.* Mol Cell Biol, 1999. **19**(1): p. 1-11.

85. Wu, M.X., *Roles of the stress-induced gene IEX-1 in regulation of cell death and oncogenesis.* Apoptosis, 2003. **8**(1): p. 11-8.

86. Gottstein, B., et al., *Hepatic gene expression profile in mice perorally infected with Echinococcus multilocularis eggs.* PLoS One, 2010. **5**(4): p. e9779.

87. Scott, F.L., et al., *SerpinB6 is an inhibitor of kallikrein-8 in keratinocytes.* J Biochem, 2007. **142**(4): p. 435-42.

88. Strik, M.C., et al., *Intracellular serpin SERPINB6 (PI6) is abundantly expressed by human mast cells and forms complexes with beta-tryptase monomers.* Blood, 2004. **103**(7): p. 2710-7.

89. Huss, J.M. and C.B. Kasper, *Two-stage glucocorticoid induction of CYP3A23 through both the glucocorticoid and pregnane X receptors.* Mol Pharmacol, 2000. **58**(1): p. 48-57.

90. Edgar, A.J., et al., *Cloning of dexamethasone-induced transcript: a novel glucocorticoid-induced gene that is upregulated in emphysema.* Am J Respir Cell Mol Biol, 2001. **25**(1): p. 119-24.

91. Noti, M., et al., *TNF suppresses acute intestinal inflammation by inducing local glucocorticoid synthesis.* J Exp Med, 2010. **207**(5): p. 1057-66.

92. Rawat, R., et al., *Inflammasome up-regulation and activation in dysferlin-deficient skeletal muscle.* Am J Pathol, 2010. **176**(6): p. 2891-900.

93. Therrien, C., et al., *Characterization of lipid binding specificities of dysferlin C2 domains reveals novel interactions with phosphoinositides.* Biochemistry, 2009. **48**(11): p. 2377-84.

94. Di Paolo, G. and P. De Camilli, *Phosphoinositides in cell regulation and membrane dynamics.* Nature, 2006. **443**(7112): p. 651-7.

95. Boesze-Battaglia, K. and R. Schimmel, *Cell membrane lipid composition and distribution: implications for cell function and lessons learned from photoreceptors and platelets.* J Exp Biol, 1997. **200**(Pt 23): p. 2927-36.

96. Li, Z., L.B. Agellon, and D.E. Vance, *Phosphatidylcholine homeostasis and liver failure.* J Biol Chem, 2005. **280**(45): p. 37798-802.

97. Borgert, C.J., et al., *Evaluating chemical interaction studies for mixture risk assessment.* Human and Ecological Risk Assessment, 2001. **7**(2): p. 259-305.

CHAPTER 7

CHAPTER 7

CONCLUSIONS AND FUTURE RESEARCH

The preceding studies utilized comprehensive gene expression analyses with phenotypic anchoring to characterize non-additive interactions between dioxin-like and non-dioxin-like chemicals on hepatic toxicity in C57BL/6 mice. Comprehensive assessment of hepatic responses elicited by dioxin-like PCB126 (Chapter 3 and 4) and non-dioxin-like PCB153 (Chapter 5) was first performed independently to obtain a quantitative baseline of toxicity. Thorough evaluation of PCB126 hepatic effects confirmed its dioxin-like toxicity, albeit at lower efficacy when compared to equipotent doses of TCDD. Examination of a reconstituted mixture of dioxin and non-dioxin-like PCB153 was therefore performed with TCDD, instead of PCB126, to reflect greater affinity for the AhR and to better illustrate the non-additive effects on the dioxin-like toxicity.

Individually, TCDD and PCB153 elicited unique and complex temporal and dose-dependent gene expression responses, which could be related to physiological outcomes. However, co-administration of both chemicals in a mixture identified a subset of dose-dependent, synergistically induced genes that exhibited greater expression than the sum of TCDD- and PCB153-elicited effects alone. The synergistic gene expression changes at 24 h preceded reported changes in relative liver weights, histopathology, lipid profiles, and pharmacokinetics.

These data have expanded the knowledge on the diversity of gene expression and physiological responses mediated by PCB126, TCDD and PCB153 alone. In addition, the

acquired *in vivo* data can provide insight into the non-additive gene expression underlying non-additive changes at later time points. The data generated in these studies have also opened new research questions, which should be explored to further increase the current understanding of the toxic effects elicited by mixtures of AhR and non-AhR ligands. Future considerations and suggested experiments and approaches are outlined below.

CONSIDERATIONS FOR CROSS-SPECIES COMPARISONS

Multiple reports and previous research from this lab has demonstrated that TCDD mediates its toxic effects in a species-specific manner, which can have significant implications for cross-species mixture evaluation. TCDD exposure in Sprague-Dawley rats has revealed that these rodents are more sensitive to dioxin-mediated toxicity and do not exhibit the same spectrum of toxicological responses when compared to C57BL/6 mice [1]. In addition, important considerations for the evaluation of CAR and PXR-mediated responses have been highlighted in Chapter 5, as species-specific ligand preferences have been reported, particularly for PXR and it is therefore important to investigate species-specific activation by PCB153 [2]. Establishment of permanently transfected cell lines containing human, mouse, and rat CAR and PXR chimeric receptors coupled with luciferase reporter gene systems in collaborations will address the receptor activation by PCB153 across species. Comprehensive assessment of TCDD and PCB153 mixture effects in models other than the one presented in this dissertation may require adjustments in dose spectrum and will require preliminary pilot studies to determine the optimum dose combinations without exerting over toxicity. Future cross-species comparative work utilizing microarray technology should also consider the immaturity of the rat genome annotation compared to either human or mouse that may limit the functional comparisons between the species.

TOXICOGENOMIC EVALUATION OF NON-ADDITIVE GENE EXPRESSION

The major advantage of utilizing toxicogenomics is the ability to simultaneously evaluate thousands of transcripts at the same time. To date, results presented in Chapter 6 are the first to utilize whole-genome mouse microarray analysis to examine non-additive gene expression. Data analysis revealed that hundreds of genes were differentially regulated in response to TCDD, PCB153, and to a mixture of both chemicals at one or more time points, however only a small subset displayed putative non-additive expression that was further investigated in a dose-response study. In addition, all of the identified mixture non-additive responses confirmed dose-dependent synergistic effects compared to TCDD and PCB153 alone. Microarray analysis did not identify candidate genes that displayed antagonistic effects in the mixtures, instead examples of synergistic suppression were observed for some of the down-regulated genes. In addition, the magnitude of gene repression was smaller compared to up-regulation which can further impair statistical modeling and identification of antagonistic responses. Additional dose-response studies at different time points in addition to the 24-h experiments, might reveal time-dependent effects on the non-additive interactions.

Previous studies exploring mixtures of TCDD or tamoxifen with ethynyl estradiol confirmed the lack of "global" non-additive gene expression effects. [3, 4]. These reports further support the findings from this dissertation, suggesting that the majority of genes are not significantly affected by the co-treatment. Instead, mixture gene expression effects are comparable to the gene expression profiles elicited by either of the chemicals alone. Additional studies, with different ratios of the individual chemicals might be required to determine a threshold for non-additive responses. Results from earlier studies investigating mixtures of

TCDD and PCB153 report the lack of consistency of the antagonistic effects, suggesting that a "window of antagonism" exists, which is dependent on the dose and target tissue [5, 6].

Multiple studies have reported PCB153-mediated antagonism of TCDD-induced Cyp1a1 mRNA levels or protein activity (EROD assay), in addition to other changes in physiological endpoints. In contrast to previous reports, the work embodied in this dissertation has focused on non-additive gene expression responses that could be linked to the observable changes in phenotype. Results by Staal *et al.* [7] investigating binary mixtures of polyaromatic hydrocarbons revealed that gene expression changes were generally additive or slightly antagonistic, but DNA adduct formation exhibited synergistic effects in human hepatoma (HepG2) cells, further complicating evaluation of carcinogenic potencies of the mixtures.

IN VITRO CONSIDERATIONS FOR MIXTURE EVALUATION

Studies utilizing *in vivo* designs for mixture evaluation contribute significantly more to risk assessment, however the associated high cost does not permit for factorial evaluation of binary and potentially ternary mixtures, including all possible dose-combinations allowing for the determination of the response surfaces [8]. Utilization of *in vitro* models is favored, as it is expected to reduce, refine and replace the use of animal models in toxicology and can in theory permit the extrapolation of the responses to the whole organism. To further expand the work described in this dissertation, toxicogenomic mixture evaluation could be performed in human, mouse and rat primary hepatocytes and compared to the *in vivo* rodent data to evaluate the non-additive responses in a human model. These cross-model (*in vitro*-*in vivo*) and cross-species (mouse, rat, human) comparisons of mixture effects would significantly expand mixture risk assessment and assess the ability of cost-effective *in vitro* approaches to contribute to risk assessment practices.

REFERENCES

REFERENCES

1. Boverhof, D.R., et al., *Comparative toxicogenomic analysis of the hepatotoxic effects of TCDD in Sprague Dawley rats and C57BL/6 mice.* Toxicol Sci, 2006. **94**(2): p. 398-416.

2. Moore, J.T., et al., *Functional and structural comparison of PXR and CAR.* Biochim Biophys Acta, 2003. **1619**(3): p. 235-8.

3. Boverhof, D.R., et al., *Inhibition of estrogen-mediated uterine gene expression responses by dioxin.* Mol Pharmacol, 2008. **73**(1): p. 82-93.

4. Fong, C.J., et al., *Effects of tamoxifen and ethynylestradiol cotreatment on uterine gene expression in immature, ovariectomized mice.* J Mol Endocrinol, 2010. **45**(3): p. 161-73.

5. Smialowicz, R.J., et al., *Opposite effects of 2,2',4,4',5,5'-hexachlorobiphenyl and 2,3,7,8-tetrachlorodibenzo-p-dioxin on the antibody response to sheep erythrocytes in mice.* Fundam Appl Toxicol, 1997. **37**(2): p. 141-9.

6. Bannister, R. and S. Safe, *Synergistic interactions of 2,3,7,8-TCDD and 2,2',4,4',5,5'-hexachlorobiphenyl in C57BL/6J and DBA/2J mice: role of the Ah receptor.* Toxicology, 1987. **44**(2): p. 159-69.

7. Staal, Y.C., et al., *Binary PAH mixtures cause additive or antagonistic effects on gene expression but synergistic effects on DNA adduct formation.* Carcinogenesis, 2007. **28**(12): p. 2632-40.

8. Bermudez, D.S., L.E. Gray, Jr., and V.S. Wilson, *Modeling the interaction of binary and ternary mixtures of estradiol with bisphenol A and bisphenol A F in an in vitro estrogen mediated transcriptional activation assay (T47D-KBluc).* Toxicol Sci, 2010. **116**(2): p. 447-487.